

RUSSIAN ACADEMY OF SCIENCES
National Geophysical Committee

RUSSIAN NATIONAL REPORT

Meteorology and Atmospheric Sciences

2011–2014

for the XXVI General Assembly
of the International Union of Geodesy and Geophysics
(Prague, Czech Republic, June 22 – July 2, 2015)



Editors: RAS Corresponding Member *I.I. Mokhov* (MASS Chairman); Dr. *A.A. Krivolutsky*
(MASS Scientific Secretary)

Russian National Report: Meteorology and Atmospheric Sciences: 2011– 2014: for the XXVI General Assembly of the International Union of Geodesy and Geophysics (Prague, Czech Republic, June 22 – July 2, 2015). — М.: МАКС Пресс, 2015. — 272 p.

This report of the Meteorology and Atmospheric Sciences Section (MASS) of the Russian National Geophysical Committee presents information on atmospheric research in 2011– 2014 in Russia

Национальный отчет России по метеорологии и атмосферным наукам в 2011–2014 гг.: XXVI Генеральная Ассамблея Международного союза геодезии и геофизики, Прага, Чехия, 22 июня – 2 июля 2015 г. / Ред. И.И. Мохов, А.А. Кривошукский. — М.: МАКС Пресс, 2015. — 272 с. (на англ. яз.).
ISBN 978-5-317-05001-6

Online version of this report is freely accessible at GC RAS server dedicated to *Geoinformatics Research Papers* (<http://ebooks.wdcb.ru>)

DOI: 10.2205/2015IUGG-RU-IAMAS

Citation: Mokhov I. I., A. A. Krivolutsky, Eds. (2015), Russian National Report: Meteorology and Atmospheric Sciences: 2011– 2014, *Geoinf. Res. Papers*, 3, BS3008, doi: 10.2205/2015IUGG-RU-IAMAS

© 2015 National Geophysical Committee RAS

Содержание

Preface	4
Atmospheric Chemistry	5
<i>I. K. Larin</i>	
Atmospheric Electricity	18
<i>E. A. Mareev, V. N. Stasenko, A. A. Bulatov, S. O. Demytyeva, A. A. Evtushenko, N. V. Ilin, F. A. Kuterin, N. N. Slyunyaev, M. V. Shatalina</i>	
Climate	35
<i>I. I. Mokhov</i>	
Clouds and Precipitation	55
<i>N. A. Bezrukova, A. V. Chernokulsky</i>	
Dynamic Meteorology	98
<i>M. V. Kurgansky, V. N. Krupchatnikov</i>	
Middle Atmosphere	142
<i>A. A. Krivolutsky, A. A. Kukoleva</i>	
Ozone	171
<i>N. F. Elansky</i>	
Planetary Atmospheres	199
<i>O. I. Korablev</i>	
Polar Meteorology	222
<i>A. I. Danilov, V. E. Lagun, A. V. Klepikov</i>	
Atmospheric Radiation	240
<i>Yu. M. Timofeyev, E. M. Shulgina</i>	

Preface

This report of the Meteorology and Atmospheric Sciences Section (MASS) of the Russian National Geophysical Committee presents information on atmospheric research in 2011–2014 in Russia. It was prepared for the General Assembly of the International Union of Geodesy and Geophysics (IUGG) which includes the International Association of Meteorology and Atmospheric Sciences (IAMAS). This MASS report is based on reviews of 10 National Commissions:

1. Atmospheric Chemistry (Chairman I. K. Larin, Institute of Energy Problems and Chemical Physics of the Russian Academy of Sciences);
2. Atmospheric Electricity (Chairman V. N. Stasenko, State Research Center “Planeta”);
3. Atmospheric Ozone (Chairman N. F. Elansky, A. M. Obukhov Institute of Atmospheric Physics of the Russian Academy of Sciences);
4. Climate (Chairman I. I. Mokhov, A. M. Obukhov Institute of Atmospheric Physics of the Russian Academy of Sciences);
5. Clouds and Precipitation (Chairman N. A. Bezrukova, Central Aerological Observatory);
6. Dynamic Meteorology (Chairman M. V. Kurgansky, A. M. Obukhov Institute of Atmospheric Physics of the Russian Academy of Sciences);
7. Middle Atmosphere (Chairman A. A. Krivolutsky, Central Aerological Observatory);
8. Planetary Atmospheres (Chairman O. I. Korablev, Space Research Institute of the Russian Academy of Sciences);
9. Polar Meteorology (Chairman A. I. Danilov, Arctic and Antarctic Research Institute);
10. Radiation (Chairman Yu. M. Timofeyev, St. Petersburg State University).

Previous MASS report was published in 2011¹.

Igor I. Mokhov
MASS Chairman

¹ Russian National Report. Meteorology and Atmospheric Sciences. 2007–2010.
Ed. By I. I. Mokhov and A. A. Krivolutsky. National Geophysical Committee RAS, MAKS Press, Moscow, 2011, 213 p.

Atmospheric Chemistry

I. K. Larin

Institute of Energy Problems of Chemical Physics RAS

ilarin@yandex.ru

A brief overview of the work of Russian scientists in the field of atmospheric chemistry in 2011–2014 years, including work on the chemistry of the troposphere, the chemistry of the ozone layer and on the role of chemistry in climate change is presented. Review has been prepared in the Commission on atmospheric chemistry and global pollution meteorology and atmospheric sciences section of the national Geophysics Committee. Key words: chemical processes, the troposphere, the stratosphere, climate.

Note first of all that in 2012 the work “Russian research in atmospheric chemistry in 2007–2010” was presented [1].

1. Chemistry of the troposphere

In the area researches of elementary processes of tropospheric chemistry of compounds of natural and anthropogenic origin has been continued. So, in [2] method of resonance fluorescence in the flowing reactor were used to measure the rate constants of homogeneous reactions of chlorine atoms with C_3F_7I (k_I) and CF_3I (k_{II}): $k_I = (5.2 \pm 0.3) \cdot 10^{-12}$ molecule⁻¹cm³s⁻¹, $k_{II} = (7.4 \pm 0.6) \cdot 10^{-13}$ molecule⁻¹cm³s⁻¹. In [3] the reaction of $Cl + CH_3I$ has been investigated, which, as it turns out, occurs on the walls of the reactor.

“Proceeding on a wall” in a range of temperatures 298–363 K there was also reaction $CO + IO$ [4]. C_3F_7I , CF_3I and CH_3I are used in quality firefighting means and in itself (despite presence of atoms of iodine) do not represent danger to ozone layer owing to the short atmospheric lifetime which is insufficient for achievement of heights of the stratosphere. It is not excluded, however, that as a result of reactions with atoms of chlorine more long-living components which can be dangerous to the ozone layer of the Earth are formed. We will specify also in work [5] in which reaction of atoms of fluorine with pentafluoropropionic acid has been studied by mass spectral methods at temperatures 262–343 at which the basic products are HF , C_2F_5 and CO_2 . In other work of these authors have been similarly studied the mechanism and kinetics reactions of atoms of fluorine with trifluoroacetic acid [6].

Studying of destiny of other chemically active particle of troposphere — radicals OH — has been devoted the work [7] in which interaction of radicals OH with carbonaceous surfaces in the top troposphere has been investigated. It was revealed, that the factor of absorption OH poorly depends on temperature, being

in range from 0,1 to 1, measured in conditions of a flow with use ionizing mass spectrometry. This conclusion has been used for an estimation of the sink of OH on carbonaceous aerosols in conditions of the top troposphere. Calculations of authors have shown, that loss of OH on this channel in the top troposphere can be rather considerable, that can be explained both low diffusion restrictions, and weak temperature dependence of the effect.

Besides laboratory measurements quantum-chemical calculations of rate constants of atmospheric chemical reactions were studied also. So, in [8] quantum-chemical research of a primary stage of joining of ozone to double bond of ethylene, and in [9] — to acetylene has been made. In [10] influence of deformation of double bond in chlorine ethylene on the rate and the mechanism of reaction with ozone, and in [11] — a competition of the co-ordinated and not co-ordinated joining of ozone to double bond has been considered. In [12] reaction of ozone with butene has been studied by methods of quantum chemistry. It has been similarly studied adsorption of ammonia by water clusters [13]. At last, note a work on water clusters, captured molecules of methane [14] that is directly connected with a formation of clathrates of methane huge stocks which are in zones of the permafrost menacing by strengthening the global warming at its thawing.

The important data on the chemical processes proceeding in polluted city air, can be received from data about a chemical composition and acidity of city precipitations. Such data are reported in works of researchers of the Meteorological observatory of Geographical faculty of the Moscow State University [15]–[25]. It is shown, in particular, that in 2005–2013 acidity of precipitations in Moscow has raised in comparison with long-term observations. It is shown also, that last years there is prevalence of chloride-ions over sulphates that can be explained by growing use of containing chlorides anti-icing reagents. Like it in [26] results of long-term investigations (1999–2010) of the ionic and element composition of atmospheric precipitations at stations of monitoring in the Baikal region (Irkutsk, Lisn'vanka, Mondy) are presented. Annual flux of studied components on underlaing surface are calculated. The various factors influencing interannual and intraannual dynamics of a chemical composition of precipitations are considered. It is shown, that in Irkutsk and Lisn'vanka the total content of the basic ions and water-soluble elements in precipitations has increased.

In conclusion of this part we will refer to the works of the general character connected with chemistry of the troposphere. So, in [27] the mechanism of tropospheric oxidation of methane, in [28], [29] the tropospheric chemical processes occurring at night are considered, and in [30] the question of day and night lifetimes of small atmospheric components in troposphere is analyzed.

2. Heterophase processes

The significant amount of works in 2011–2014 has been devoted to studying of heterophase reactions and processes with participation of aerosol particles. We remind, that these processes have played a key role in depletion of the ozone layer in the end of 20th century and in formation of the Antarctic and Arctic ozone holes. As an example we refer to work [31] in which long-term changes of the basic characteristics of spring Antarctic ozone anomaly are considered. It is shown, that since the end of 1980th change of the basic characteristics of ozone anomaly for the first 10 years in appreciable degree have been connected with changes in temperature in the low stratosphere, and the next 10 years of changes in temperature and ozone were not observed. In [32] occurrence of polar stratospheric clouds over Tomsk on January, 10th, 2010 which could be formed over the Scandinavian mountains and over mountain ridges of Polar Urals Mountains and New Land is described. Besides high-altitude processes, aerosol particles make considerable impact on composition of small atmospheric components, including ozone. In this connection we refer to the work [33] in which ozone depletion on a surface of white sand was studied. In the work the parameters characterising initial activity of sand and rate of its deactivation under the influence of 145 ppb of ozone have been defined. In [34] on the basis of the established empirical dependence between a change of concentration of ozone and aerosol at the ground level in Tomsk and a course of solar activity in 21st–3rd eleven-year cycles on literary data about the forecast of solar activity for 24th eleven-year cycle, the forecast of change of mid-annual concentration of ozone and aerosol till 2021 is given. In connection with observable anomalies of concentration of ozone in coastal sea zones in [35] a formation of chemically active haloids in the low troposphere in heterogeneous reactions of NO_3 and ClONO_2 with sea aerosol was studied and the algorithm of extrapolation of laboratory data to real tropospheric conditions for the purpose of including the given class of elementary reactions in modern models to forecast long-term composition of the troposphere over the coastal industrially developed regions has been received. Additional data on this question are reported in [36]. In [37] hydration of negative ions of trichloroacetic acid (TCA) in water solutions was studied. By means of a mass spectrographic method of electrodispersion of solutions of electrolytes (EDSE) the mass spectrum of negative ions of water solution TCA has been studied. In work [38] features of an annual course of concentration of aerosol in the surface air of Moscow suburbs were considered. On materials of daily measurements of characteristics of atmospheric aerosol in Golgoprudny (20 km from the centre of Moscow), executed within 2006–2009, seasonal variations of concentration of particles of the different sizes in the surface layer of atmosphere have been studied. It is established, that steady changes of monthly average

concentration of aerosol are observed in the range of diameters of particles 0,02–1 microns. Other data on monitoring of aerosols are presented in works [39]–[48]. In [49] the distribution of radionuclides in run-off of dry aerosols when they enter the forest ecosystems with the assessment of specific activity of artificial and natural radionuclides studied. In work [50] the chemical composition of aerosols in atmosphere of Mongolia during 2005–2010 is analyzed. It has been shown that in industrial cities (Ulan Bator, Suhe-Bator) local emissions impact the basic influence on composition of aerosols, while in small cities with an underdeveloped industry (Baruun-Urt and Sainshaind) distant carrying polluting substances and a wind mode of district, in particular dusty storms, dominates. In work [51] possibility of an estimation of a dynamic condition of atmosphere through aerosol components is considered. The approach to the analysis of experimental data on measurement of spectra of the sizes and concentration of aerosol particles of atmosphere and meteorological parameters by means of flicker-noise spectroscopy is offered. In [52] possibility of reveal of optical characteristics of the tropospheric aerosols of Western Siberia on the basis of the generalised empirical model taking into account absorption and hygroscopic properties of particles is considered.

At occurrence force majeure ecological circumstances, such as peat and forest fires, atmosphere pollution by harmful substances essentially amplifies, including aerosols. In work [53] numerical calculations were carried out at preset values of emissions of gas impurity and aerosols from the burning centres. In calculations the advanced model free convection taking into account emissions of a thermal fluxes from a burning zone has been used. In [54] for episodes of high pollution of atmosphere in the Moscow region during summer of 2010 a relationship of the short term fluctuations of concentration of aerosol (PM10) and carbonic oxide (CO) with meteorological characteristics has been considered. The assumption is made and arguments are resulted, that high aerosol air pollution observed in the end of June in Moscow has been caused by coming of air masses from areas of a soil drought from the south of Russia.

Other data on the impact of the fires on atmospheric pollution are given in [55]–[61]. In works [62]–[65]) the relationship of volcanic eruptions with atmospheric aerosol is discussed. In this regard, we point out to work [66], which examines the influence of volcanic activities on the Antarctic ozone hole. It is proved, in particular, the increased activity of the volcano mount Erebus in 1976–1984 led to a significant increase in the level of the stratospheric HCl, SO₂ and H₂O in Antarctica, which stimulated the growth of polar stratospheric clouds and ozone hole in the 80's.

In conclusion of this part we shall refer to interesting work [67] which dealt with the experimental results of registration of neutron components and electric field strength thunderstorms during 2009–2011. Short bursts of neutron flux

during the close (5–7 km.) lightning events discharges at sea level (105 m.) has been registered. Spikes were observed during a significant increase of electrical field to -16 kV/m that abruptly changed to $+18$ kV/m at the time of lightning discharge. Increase in the flux of neutrons reaches 10 percent or more from the average level for the minute resolution. It has been found that all the bursts are observed during thunderstorms with the next type of electrical structures: stormy cloud of positive polarity with a compact positive charge at the base.

3. The chemistry of the ozone layer

In this field in 2011–2014 a new set of results have been obtained, as in the theory of the ozone layer, and observation of the evolution of total ozone recovery after its decline in the late 19th century, under influence of the anthropogenic factors.

In addition effect on ozone of the natural factors such as volcanic eruptions has been considered. Thus, [68] analyses the volcanic disturbances of the stratosphere since 1979 to 2008 and their impact on long-term changes in ozonosphere. Authors are trying to prove that the main regulator of ozonosphere in this period was the volcanic aerosol impact on the stratosphere. Note parenthetically that this conclusion contradict to the world science data, according to which the main factor changing the ozonosphere in the period was anthropogenic effects of chlorofluorocarbons on the ozone layer (see, for example, WMO (World Meteorological Organization), *Scientific Assessment of Ozone Depletion: 2014*, Global Ozone Research and Monitoring Project — Report No. 55, 416 pp., Geneva, Switzerland, 2014, CHAPTER2.

At the same time, it is well known that certain powerful volcanic eruptions have significant effects on the ozone layer through the mechanism of the so-called halogen activation of ozone depletion with the participation of sulfates. So, in [69] the effect of the eruption of Mount Pinatubo on stratospheric content of O_3 and NO_2 is evaluated.

In the field of the theory of the ozone layer we point at work [70], [71]–[73] where for the first time processes of the ozone layer chemistry have been considered from the point of view of the theory of unbranched chain processes. Using advanced techniques and two-dimensional model of Socrates for the first time the chain length and the rate of stratospheric ozone depletion in the Ox, HOx, NOx, ClOx and BrOx cycle have been defined. It has been shown that in the middle stratosphere, chlorine and bromine chain length is more than 10^6 , and the greatest contribution to stratospheric ozone depletion is currently due to the nitrogen cycle.

In [74] the influence of solar proton flares on ozonosphere that affect the chemical composition of the upper stratosphere and mesosphere was considered.

In [75] the results of research of the ozone layer over Nizhny Novgorod and over Central Asian region using ground equipment of millimeter range of wavelengths has been considered. In [76] the temperature, humidity and ozone anomalies, registered in March 2011 by TOMS in the Arctic stratosphere have been explored. It is supposed, that the phenomena in Arctic regions is a result of a competition between meridional transfer of ozone from its tropical reservoir during the winter period and the subsequent destruction of ozone as a result of heterogeneous reactions on the surfaces of particles of polar stratospheric clouds, and the phenomena in the middle latitude are caused by drift of the wet Arctic air masses with a depleted ozone.

In conclusion of this part we refer to the book “Chemical Physics of the ozone layer” (published by GEOS, Moscow (2013) [77]), in which for the first time a detailed analysis of stratospheric processes from the point of view of the theory of chain processes has been made.

4. Chemical aspects of climate change

Works in this field were related to the forecasting of climate change, monitoring of greenhouse gases, and geoengineering. Let’s specify the work [78] that using climate model of the Institute of atmospheric physics name A. M. Obukhov RAS the influence of geo-engineering on characteristics of climate and carbon cycle has been evaluated.

Geo-engineering effect in the model is implemented for the period 2020–2070 to decrease the global warming according an aggressive scenarios of anthropogenic effect RCP 8.5. When a homogeneous distribution of stratospheric sulphate horizontally and full compensation of globally averaged anthropogenic warming, developing in the 21st century in this scenario, there is a reduction in rainfall, accompanied by regional temperature anomalies. Geoengineering leads to a decrease in the total primary production of plants and carbon stock in ground vegetation, especially in boreal regions of Siberia. The global total primary production in 2060–2070 compared with the calculations without geoengineering effects decreases by 17 PgC*g⁻¹, and global stock of carbon in the ground vegetation on the 33 PgC. On the other hand, geoengineering leads to the fact that in the 21st century soil does not lose but accumulates carbon. It has been shown that geoengineering slows the accumulation of CO₂ in the atmosphere by anthropogenic emissions by 52 million⁻¹ in the last years of the 21st century But this has no significant effect on the climate performance of geo-engineering.

The use of geoengineering to decrease the global warming also discussed in [79]. In addition to said above let’s note that these techniques would inevitably lead to substantially reduce of ozone through the mechanism of the halogen activation, acting with participation of the sulphate aerosols. Besides, you need to

take into consideration the duration of the application of these methods, which should be not less than 1000 years, which corresponds to atmospheric lifetime of CO_2 .

In [80] the long-term variations of the Earth's upper atmosphere radiation in the line of atomic oxygen at 557.7 nm and fluctuations in the system "atmosphere-ocean" has been analysed. In [81] the mechanism of influence of solar activity on the climate and their contribution to the climatic variations in past centuries and the twenty-first century was discussed. In [82] an overview of the current monitoring data spatio-temporal dynamics of greenhouse gases made on the global network of observations by space, balloon, aircraft and contact sensing was given. The attention focuses on the assessment of the trend of methane. In this regard, we point out to work [83], where the content of the ice clathrates was considered and it was shown that the temperature rise and growth of methane concentration in the atmosphere have gone over glacial-interglacial cycles parallel to each other. Finally, we specify the work [84], which provides estimations of current radiative forcing of aerosol for three areas of the world ocean — the coastal area of Antarctica, the sea of Japan and the "Sea of darkness" (part of the Ocean near the northwest coast of Africa, where the dust is regularly made by the trade winds from the Sahara).

References

1. Larin I. K. Russian investigations in atmospheric chemistry for 2007–2010 // *Izvestiya RAN. Fizika atmosfery i okeana* (2012) V. 48. № 3. P. 272–280. (rus.)
2. Larin I. K., Spasskii A. I., Trofimova E. M. Measurement of the rate constants of the reactions of the chlorine atom with $\text{C}_3\text{F}_7\text{I}$ and CF_3I using the resonance fluorescence of chlorine atoms // *Kinetika i Cataliz* (2012) V. 53. № 1. P. 15–19. (rus.)
3. Larin I. K., Spasskii A. I., Trofimova E. M. Homogeneous and heterogeneous reactions of hydrocarbons that contain an atom of iodine // *Izvestiya RAN. Energetika* (2012) № 3. P. 44–52. (rus.)
4. Larin I. K., Spasskii A. I., Trofimova E. M., Proncheva N. G. Measurement of rate constants of reaction of carbon monoxide with iodine oxide in the temperature range 298–363 K method of resonance fluorescence // *Kinetika i Cataliz* (2014) V. 55. № 3. P. 301–306. (rus.)
5. Vasiliev E. S., Knyazev V. D., Karpov G. V., Morozov I. I. Kinetics and Mechanism of the Reaction of Fluorine Atoms with Pentafluoropropionic Acid // *Journal of Physical Chemistry A* (2014) V. 118. P. 4013–4018.
6. Vasiliev E. S., Knyazev V. D., Morozov I. I. Kinetics and mechanism of the reaction of fluorine atoms with trifluoroacetic acid // *Chemical Physics Letters* (2011) V. 512. P. 172–177.

7. Yong Liu, Ivanov A. V., Zelenov V. V., Molina M. J. Temperature dependence of OH uptake by carbonaceous surfaces of atmospheric importance // *Khimicheskaja fizika* (2012) V. 31. № 2. P. 88–93.
8. Krisyuk B. E., Maiorov A. V. Quantum chemical study of the primary step of ozone addition at the double bond of ethylene // *Kinetica i Catalyz* (2011) V. 52. № 6. P. 819–825. (rus.)
9. Krisyuk B. E., Maiorov A. V., Mamin E. A., Popov A. A. Quantum chemical study of the reaction of attachment of ozone to acetylene // *Kinetica i Cataliz* (2013) V. 54. № 3. P. 303–309. (rus.)
10. Krisyuk B. E., Maiorov A. V., Mamin E. A., Popov A. A. Effect of deformation in the chloroethylene double bond on the speed and reaction mechanism of ozone // *Khemicheskaja Fizika* (2011) V. 30. № 6. P. 23–31. (rus.)
11. Krisyuk B. E., Maiorov A. V. Competition is coordinated and approved ozone's accession to double bond // *Khemicheskaja Fizika* (2011) V. 30, № 9. P. 35–41. (rus.)
12. Krisyuk B. E., Maiorov A. V., Ovchinnikov V. A., Popov A. A. The reaction of ozone with butenom: many configuration calculation // *Khemicheskaja Fizika* (2013) V. 32, № 1. P. 3–8. (rus.)
13. Galashev A. E. Computer study of the adsorption of ammonia water clusters // *Khemicheskaja Fizika* (2013) V. 32, № 7. P. 86–93. (rus.)
14. Galashev A. E. The structure of water clusters, captured methane molecules // *Khemicheskaja Fizika* (2014) V. 33. № 11. P. 32–40. (rus.)
15. Belikov I. B., Gorbarenko E. V., Eremina I. D., Konstantinov P. I., Lokoshenko M. A., Nezval' E. I., Chubarova N. E., Shilovzeva O. A., Shumskij P. A. The chemical composition of precipitation in 2010. In the book: *Ecological and climatic characteristics of the climate in 2010, according to the meteorological observatory of MSU*. Ed. Chubarova N. E. Moscow. MAKS Press (2011) P. 137–141. (rus.)
16. Gorbarenko E. V., Eremina I. D. Variability of aerosol and chemical composition of the air in Moscow // *Vestnik Moskovskogo Universiteta. Seria 5. Geografija* (2011) № 4. P. 31–42. (rus.)
17. Belikov I. B., Gorbarenko E. V., Elovkhov A. S., Eremina I. D., Ivanov V. A., Konstantinov P. I., Lokoshenko M. A., Nezval' E. I., Postjtlakov O. V., Chubarova N. E., Shilovzeva O. A., Shumskij P. A. The chemical composition of precipitation in 2011. In the book: *Ecological characteristics of the atmosphere in 2011, according to the meteorological observatory of the Moscow State University*. Ed. Chubarova N. E. Moscow. MAKS Press (2012) ISBN 978-5-317-04010-9. P. 165–172. (rus.)
18. Belikov I. B., Gorbarenko E. V., Elovkhov A. S., Eremina I. D., Ivanov V. A., Konstantinov P. I., Lokoshenko M. A., Nezval' E. I., Postjtlakov O. V., Chubarova N. E., Shilovzeva O. A., Shumskij P. A. Spatial patterns of chemical composition of snow cover in Moscow and Moscow region. In the book: *Ecological and climatic characteristics of the atmosphere in 2011, according to the meteorological observatory of the Moscow State University*. Ed. Chubarova N. E. Moscow. MAKS Press (2012) ISBN 978-5-317-04010-9. P. 221–230. (rus.)

19. Eremina I.D. 30 years of observations of the chemical composition of precipitation in the meteorological observatory of MSU Materials Intl. scientific conf. "The regional effects of global climate change (causes, effects, projections)". Voronezh, "Nauchnaja kniga" (2012) 576 p. P. 484–487. (rus.)

20. Belikov I.B., Gorbarenko E.V., Eremina I.D., Jdanova E. Ju., Konstantinov P.I., Korneva I.A., Lokoshenko M.A., Nezval' E.I., Skorohod A.I., Chubarova N.E., Shilovzeva O.A., Shumskij P.A., Ahijarova K.I., Remizov A.A. The chemical composition of precipitation in 2012. In the book: Ecological-climate characteristics of the atmosphere in 2012, according to the meteorological observatory of the Moscow State University. Ed. Chubarova N.E. Moscow. MAKS Press (2013) ISBN 978-5-317-04478-7. P. 165–172. (rus.)

21. Gorbarenko E.V., Eremina I.D., Isaev A.A., Gamburtsev A.G. Dynamics of some ecological and climatic characteristics of the atmosphere in Moscow (according to meteorological observatory of MSU). In: Atlas of temporal variations of natural, man-made and social processes. Janus-to Moscow (2013) V. 5. P. 78–93. (rus.)

22. Eremina I.D. Monitoring of the chemical composition of precipitation observed meteorological observatory of MSU // *Alternativnaja energetika i ekologija* (2013) № 6 (Part 2). P. 7–10. (rus.)

23. Eremina I.D. Changes in acidity and chemical composition of precipitation in Moscow within 30 years. In the collection of conference proceedings "Pollution of cities". St. Petersburg, Russia, 1–3 October 2013, St. Petersburg. P. 115–117. (rus.)

24. Belikov I.B., Gorbarenko E.V., Eremina I.D., Jdanova E. Ju., Konstantinov P.I., Korneva I.A., Lokoshenko M.A., Nezval' E.I., Skorohod A.I., Socratov S.A., Chubarova N.E., Shilovzeva O.A., Polukhov A.A., Gorlova I.D., Seliverstov Ju.G., Grebennikov P.B. The chemical composition of precipitation in 2013. In the book: Ecological and climatic characteristics of the atmosphere in 2013, according to the meteorological observatory of the Moscow State University. Edited by N.E. Chubarova. MAKS Press. Moscow (2014) ISBN 978-5-317-04763-4. 168 p. (rus.)

25. Eremina I.D., Chubarova N.E., Alekseeva L.I., Surkova G.V. Acidity and chemical composition of precipitation in the Moscow region in the warm season of the year // *Vestnik MGU. Serija 5. Geographija* (2014) № 5. P. 3–11. (rus.)

26. Netsvetaeva O.G., Onishuk N.A., Ximnik E.A., Sez'ko N.P., Dolja-Lopatina I.N., Hodger T.V. Dynamics of chemical composition of precipitation in the Baikal region // *Optika atmosfery i okeana* (2012) V. 25. № 06. P. 507–512. (rus.)

27. Larin I.K. On the mechanism of methane oxidation in the troposphere // *Ecologicheskaja khimija* (2011) V. 20. № 2. P. 65–73.

28. Larin I.K. Night chemistry of the troposphere. I. Processes involving nitrogen oxides // *Ecologicheskaja khimija* (2011) V. 20. № 3. P. 155–162.

29. Larin I.K. Night chemistry of the troposphere. II. Processes involving organic compounds // *Ecologicheskaja khimija* (2011) V. 20. № 3. P. 163–172. (rus.)

30. Larin I.K., Kuskov M.L. The times of day and night life of small atmospheric constituents in the troposphere // *Khimicheskaja fizika* (2014) V. 33. № 4. P. 85–90. (rus.)

31. Zvjagintsev A. M., Kuznetsova I. N. On the evolution of the spring Antarctic ozone hole // *Optika atmosfery i okeana* (2012) V. 25. № 07. P. 507–512. (rus.)
32. Cheremisin A. A., Marichev V. N., Novikov P. V. Migration of polar stratospheric clouds from the Arctic to the Tomsk city in January, 2010. // *Optika atmosfery i okeana* (2013) V. 26. № 07. P. 507–512. (rus.)
33. Tsjrkina T. B., Obvintseva L. A., Sukhareva I. P., Kaminskii V. A., Avetisov A. K. Ozone decomposition on the white sand. Determination of kinetic and static characteristics // *The composition of the atmosphere. Atmospheric electricity. Climatic effects, Proceedings of the 16th International School-Conference of young scientists* (2012) Zvenigorod. P. 209–211.
34. Anokhin P. N., Arshinov M. Ju., Belan B. D., Skljadneva T. K., Tolmachev G. N. Forecast ozone and aerosol based on predicted the 24th level of solar activity cycle // *Optika atmosfery i okeana* (2012) V. 25. № 09. P. 778–783. (rus.)
35. Zelenov V. V., Aparina E. V. Formation of chemically active haloids in the lower troposphere in heterogeneous reactions of NO_3 and ClNO_3 with sea spray // *Izvestija RAN. Energija* (2012) № 3. P. 26–43.
36. Zelenov V. V., Aparina E. V. // *Heterogeneous source of chlorine in the atmosphere*. Chapter in the book “Chlorine: Properties, Applications and Health Effect”, ISBN 978-1-61470-954-1; Ed.: Roger Mangione and Dana Carlyle, Nova Science Publishers, Inc. 2012, P. 55–124. https://www.novapublishers.com/catalog/product_info.php?products_id=35125.
37. Karpov G. V., Morozov I. I. Negative ion hydration trichloroacetic acid in aqueous solutions // *The composition of the atmosphere. Atmospheric electricity. Climatic effects. Proceedings of the 16th International School-Conference of young scientists* (2012) Zvenigorod. P. 47–51. (rus.)
38. Plaude N. O., Srulov E. A., Parshutkina I. P., Sosnikova E. V., Monakhova N. A., Jakhno V. V. Characteristics of atmospheric aerosol concentrations annual variations in the surface air in the Moscow region // *Meteorologija i gidrologija* (2012) № 1. P. 33–41. (rus.)
39. Samoylova S. V., Balin Ju. S., Kokhanenko G. P., Penner I. E. Study on the vertical distribution of tropospheric aerosol layers according to the dual laser sensing. Part 3. Spectral characteristics of vertical distribution of aerosol optical properties // *Optika atmosfery i okeana* (2012) V. 24. № 03. P. 216–223. (rus.)
40. Pol'kin V. V., Kozlov V. S., Turchinovich Ju. S., Shmargunov V. P. A comparative analysis of the microphysical characteristics of aerosol in the marine and coastal areas of Primorye // *Optika atmosfery i okeana* (2011) V. 24. № 06. P. 538–546. (rus.)
41. Sitnov S. A. Analysis of satellite observations of aerosol optical properties and atmospheric trace gases over the central area of the Russian Federation in the period of abnormally high summer temperatures and widespread fires, 2010 // *Optika atmosfery i okeana* (2011) V. 24. № 07. P. 572–581. (rus.)
42. Pol'kin V. V., Golobokova L. P. Comparative research of chemical composition of aerosol in complex experiments in Primorye // *Optika atmosfery i okeana* (2011) V. 24. № 08. P. 675–683. (rus.)

43. Kutsenozii K. P., Kutsenozii P. K., Levjkin A. I. Simulation of range size of aerosol particles, Nano-and submicron sizes // *Optika atmosfery i okeana* (2011) V. 24. № 09. P. 743–753. (rus.)
44. Vinogradova A. A., Veremeichik A. O. Model estimates of anthropogenic carbon in the atmosphere in the Russian Arctic // *Optika atmosfery i okeana* (2013) V. 26. № 06. P. 443–451. (rus.)
45. Jamsueva G. S., Zajakhanov A. S., Starikov A. V., Tsydyypov V. V. et al. // *Optika atmosfery i okeana* (2013) V. 26. № 06. P. 472–477. (rus.)
46. Antokhin P. N., Arshinova V. G., Arshinov M. Ju. et al. Extensive studies of gas and aerosol composition of air above the Siberian region // *Optika atmosfery i okeana* (2014) V. 27. № 03. P. 232–239. (rus.)
47. Maximova T. A., Maskaeva A. A., Dul'tseva G. G. et al. Biogenic organic compounds as a source of atmospheric aerosol distributed vertically over the forests of Western Siberia // *Optika atmosfery i okeana* (2014) V. 27. № 06. P. 515–519. (rus.)
48. Vinogradova A. A. Anthropogenic emissions of black carbon in the atmosphere: distribution on the territory of Russia // *Optika atmosfery i okeana* (2014) V. 27. № 12. P. 1059–1065. (rus.)
49. Tentjukov M. P. Study of the distribution of radionuclides in run-off dry aerosols when they enter the forest ecosystems // *Meteorologija i gidriologija* (2012) № 3. P. 46–55. (rus.)
50. Jamsueva G. S., Zajakhanov A. S., Starikov A. V. et al. // *Meteorologija i gidriologija* (2012) № 8. P. 59–68. (rus.)
51. Zagainov V. A., Timashov S. F., Birjukov Ju. G. et al. On the evaluation of the dynamic state of the atmosphere in aerosol components // *Khemicheskaja Fizika* (2012) V. 31, № 2. P. 6–17. (rus.)
52. Panchenko M. V., Kozlov V. S., Pol'kin V. V. et al. Restoration of the optical properties of tropospheric aerosol in Western Siberia based on generalized empirical model that takes into account the absorptive and hygroscopic properties of particles // *Optika atmosfery i okeana* (2012) V. 25. № 01. P. 46–54. (rus.)
53. Aloyan A. E., Arutjunjan V. O., Yemakov A. N. // Dynamics of trace gases and aerosols at the forest and peat fires // The composition of the atmosphere. Atmospheric electricity. Climatic effects, "Proceedings of the 16th International School-Conference of young scientists" (2012) Zvenigorod. P. 5–9.
54. Kuznetsova I. N. The influence of meteorological conditions on air pollution Moscow in summer episodes 2010 // *Izvestiya RAN. Fizika atmosfery i okeana* (2012) V. 48. № 5. P. 565–577. (rus.)
55. Konovalov I. B., Bikmann M., Kuznetsova I. N. et al. Assessment of the impact of the fires on air pollution in the region of Moscow city, based on the combined use of chemical transport model and measurement data // *Izvestiya RAN. Fizika atmosfery i okeana* (2011) V. 47. № 4. P. 496–507. (rus.)
56. Gorchakov G. I., Semutnikova, E. G., Isakov A. A. et al. The smoky haze 2010 Moscow city. Extreme aerosol and gaseous air pollution Moscow region // *Optika atmosfery i okeana* (2011) V. 24. № 06. P. 452–458. (rus.)

57. Arshinov M.Ju., and M. Belan B.D. Study of aerosol dispersion during the spring haze and forest fires // *Optika atmosfery i okeana* (2011) V. 24. № 06. P. 468–477. (rus.)
58. Isakov A.A., Anikin P.P., Elohov A.S. et al. On the characteristics of smoke of forest and peat fires in Central Russia in the summer of 2010 // *Optika atmosfery i okeana* (2011) V. 24. № 06. P. 478–482. (rus.)
59. Bisinus M.A., Popova S.A., Čankina O.V. et al. The impact of forest fires on the mass concentration, dispersion and chemical composition of atmospheric aerosol in the regional scale // *Optika atmosfery i okeana* (2013) V. 26. № 06. P. 484–489. (rus.)
60. Surkov G.V., Blinov D.V., Kirsanov A.A. et al. Modeling of air pollution plumes from the pockets of forest fires using chemical-transport model COSMO-Ru7-ART // *Optika atmosfery i okeana* (2014) V. 27. № 01. P. 75–81. (rus.)
61. Rakhimov R.F., Kozlov V.S., Panchenko M.V. et al. Properties of atmospheric aerosol in the plumes of smoke from forest fires, according to the measurement spektrofelometric measurements // *Optika atmosfery i okeana* (2014) V. 27. № 02. P. 126–133. (rus.)
62. Maričev V.N., Samokhalov I.V. Lidar observation of aerosol volcanic layers in the stratosphere of Western Siberia in 2008–2010 // *Optika atmosfery i okeana* (2011) V. 24. № 03. P. 224–231. (rus.)
63. Lysenko S.A., Kuheika M.M. Restoration of optical and microphysical characteristics of stratospheric aerosol postvulkaničeskogo of results three-frequency lidar sensing // *Optika atmosfery i okeana* (2011) V. 24. № 04. P. 308–318. (rus.)
64. Dolgii S.I., Burlakov V.D., Makeev A.P. et al. Aerosol perturbations of the stratosphere after eruption of Grimsvotn Volcano (Iceland, may 2011) the observation stations lidar network CIS CIS-LiNet in Minsk, Tomsk and Vladivostok // *Optika atmosfery i okeana* (2013) V. 26. № 07. P. 547–552. (rus.)
65. Zuev V.V., Zueva N.E., Savelyeva E.S. Temperature and ozone anomalies as indicator of volcanic soot into the stratosphere // *Optika atmosfery i okeana* (2014) V. 27. № 08. P. 698–704. (rus.)
66. Saveleva E.S., Zuev V.V. The influence of volcanic emissions on ozone depletion in the spring over Antarctica // *The composition of the atmosphere. Atmospheric electricity. Climatic effects, “Proceedings of the XVI International School-Conference of young scientists”* (2012) Zvenigorod. P. 169–172.
67. Toropov A.A., Kozlov V.I., Mullarov V.A. et al. Splashes in neutrons connected with a lightning categories a cloud — the earth // *The composition of the atmosphere. Atmospheric electricity. Climatic effects. “Proceedings of the 16th International School-Conference of young scientists”* (2012) Zvenigorod. P. 199–201.
68. Zuev V.V., Zueva N.E. Volcanic perturbations of the stratosphere is the main regulator of the long-term behaviour of ozonosphere in the period from 1979 to 2008 // *Optika atmosfery i okeana* (2011) V. 24. № 01. P. 30–34. (rus.)
69. Gruzdev A.N. Score effects the volcanic eruption of Pinatubo in stratospheric O₃ and NO₂ content, taking into account the level of solar activity variations // *Optika atmosfery i okeana* (2014) V. 27. № 06. P. 506–514. (rus.)

70. Larin I.K. On chain length in major cycles of stratospheric ozone depletion // The composition of the atmosphere. Atmospheric electricity. Climatic effects. "Proceedings of the 16th International School-Conference of young scientists (2012) Zvenyhorod P. 35–39.

71. Larin I. K., and Kuskov M. L., Mechanisms of Stratospheric Ozone Depletion. I. On Chain Processes in the Stratosphere // Russian J. Phys. Chem. B (2013) Vol. 7. No. 4. P. 509–513.

72. Larin I. K., and Kuskov M. L. Mechanisms of Stratospheric Ozone Depletion. II. Chain Length and the Rate of Ozone Depletion in the Main Stratospheric Cycles // Russian J. Phys. Chem. B (2013) Vol. 7. No. 5. P. 580–588.

73. Igor Larin. On the Chain Length and Rate of Ozone Depletion in the Main Stratospheric Cycles // Atmospheric and Climate Sciences (2013) Vol. 3. No. 1. P. 141–149.

74. Lisitsa C.M. The influence of solar proton event on ozonospeer // The composition of the atmosphere. Atmospheric electricity. Climatic effects, "Proceedings of the 16th International School-Conference of young scientists" (2012) Zvenigorod. P. 134–137.

75. Ryskin V.G., Zinchenko I.I., Krasilnikov A.A. et al. About the distribution of ozone in the stratosphere based on simultaneous terrestrial microwave measurements in Nizhny Novgorod, Russia and Kyrgyzstan // Meteorologija i gidriologija (2012) № 10. P. 24–32. (rus.)

76. Bazhenov O.E. Evaluation of influence of humidity and temperature in the stratosphere by ozone anomalies occur in spring 2011 in the Arctic and the northern territory of Russia // Optika atmosfery i okeana (2012) V. 25. № 07. P. 589–593. (rus.)

77. Larin I.K. Chemical physics of the ozone layer. Moscow. GEOS (2013). 159 p.

78. Eliseev A. V. Prevention of climate change through the emission of sulphate in the stratosphere: implications for the global carbon cycle and the terrestrial biosphere // Optika atmosfery i okeana (2012) V. 25. № 06. P. 467–474. (rus.)

79. Volodin E.M., Kostykin S.V., Ryaboshapko A.G. Modeling climate change due to the introduction of sulfur-containing compounds in the stratosphere // Izvestiya RAN. Fizika atmosfery i okeana (2011) V. 47. № 4. P. 467–476. (rus.)

80. Mikhalev A.V. Radiation of Earth's upper atmosphere and fluctuations in the climate system "atmosphere-ocean" // Optika atmosfery i okeana (2012) V. 25. № 01. P. 66–69. (rus.)

81. Eliseev I.I., Mokhov A.V. Influence of solar activity on the climate: possible mechanisms of exposure and the results of simulation // The composition of the atmosphere. Atmospheric electricity. Climatic effects, "Proceedings of the 16th International School-Conference of young scientists" (2012) Zvenigorod. P. 25–28.

82. Belan B.D. Impact of anthropogenic factor on content of greenhouse gases in the troposphere. 1. Methane // Optika atmosfery i okeana (2012) V. 25. № 04. P. 361–373. (rus.)

83. Malakhov V.V. Methanhydrates as a possible source of methane during glacial-intericing cycle // Optika atmosfery i okeana (2011) V. 24. № 01. P. 84–87. (rus.)

84. Nasrtdinov I.M., Zhuravleva T.B., Sakerin S.M. Aerosol forcing in the estimation of radiation for three areas of the oceans // Optika atmosfery i okeana (2013) V. 26. № 07. P. 572–578. (rus.)

Atmospheric Electricity

*E. A. Mareev^{1,2}, V. N. Stasenko³, A. A. Bulatov¹,
S. O. Demytyeva¹, A. A. Evtushenko¹, N. V. Ilin¹,
F. A. Kuterin^{1,2}, N. N. Slyunyaev¹, M. V. Shatalina¹*

¹Institute of Applied Physics of RAS

²Nizhny Novgorod State University

³State research center "Planeta"

Introduction

This publication provides an overview of the results of Russian studies in the field of atmospheric electricity in 2011–2014. Atmospheric electricity remains one of the fundamental problems in the physics of the atmosphere and has attracted attention for many years. Due to the wide application of new techniques and modern computational methods, in the past few years there was a significant development in various fields of investigation: fair weather electricity, thunderstorm electricity, formation of the electrical structure of clouds, lightning detection, the correlation of thunderstorm activity with other dangerous weather events. The analysis of the experimental data obtained in Russian centres of atmospheric electricity research provides a significant contribution to improving theoretical and numerical models of various electrical processes in the atmosphere. A number of important research problems were developed in physics of lightning, discharges in the middle atmosphere, high-energy processes, including X-ray and gamma-ray flashes during thunderstorms. New theoretical approaches were developed to modelling the global electric circuit, lightning activity forecast, the impact of thunderstorm activity on the chemical composition of the atmosphere. In particular, great attention has been given to the construction of systems for lightning flashes ranging and modern nowcasting systems. The main results for each field of study are given in detail in the relevant section of this article.

1. Electricity in the fair weather conditions

In recent years fair weather electricity investigations have been receiving increasing attention in Russia. The processes occurring in the convective atmospheric boundary layer (ABL) are one of the main foci of studies due to the needs of fundamental research of cloud formation and electrical effects associated with industrial and natural aerosols. Numerical models were developed for estimating the electro-aerodynamic parameters of the convective ABL, in particular, the

spatio-temporal distribution of the ion concentration, electric field, current density, conductivity and space charge density in a variety of physical conditions [1–3]. The proposed models are based on field observation databases and laboratory experiments. For horizontally homogeneous approximation with high spatial and temporal resolution the vertical profiles of the atmospheric electric field, space charge density, conductivity and atmospheric electric current density were calculated.

The space charge in the ABL can be estimated numerically on the basis of the results of observations [4]. Using the long-term observatory observations and seasonal field observations at the Borok Geophysical Observatory (58°04'N and 38°14'E), the dynamics of the electric field in the mid-latitude surface atmosphere was analysed in a wide range of time scales. It was found that the diurnal aeroelectric field variation in the middle latitudes closely matches the unitary variation in the winter season. Cross-correlations of the intensity variations of the atmospheric electric field density, vertical electric current density, space charge density and electric conductivity were investigated. The studies of the spectra of the short-period electric field pulsations were continued [5–7]. The formation of the temperature inversion layer was accompanied by a positive trend in the aeroelectric field intensity and by generation of the short-period aeroelectric pulsations. The increase rate of the electric field at the beginning of convection with inversion registered by SODAR amounted to 100 V/(m×h) [8].

Measurements of the atmospheric electric potential gradient were performed near the Earth's surface at two locations in the North Caucasus (in lowland and highland zone). Possible reasons for local electric field variations in the aerosol-free surface layer were analysed on the basis of the real experimental data obtained at Cheget mountain peak. These studies have shown the occurrence of an additional electric field maximum during the period 06–09 UT due to the diurnal variation of the turbulent diffusion coefficient [9, 10].

In recent decades the ideas of seismic events prediction have been further developed on the basis of studying the emanation of radon from the rock mass in the regions of their elastic deformation before an earthquake. According to the research results, radon-222 is one of the most important factors influencing the electricity of the surface layer. Polar conductivities of the atmosphere show particularly close relationship with the concentration of radon. The atmospheric conductivity directly depends on the ion concentration, and by inference on the ion formation factors. Comparative measurements of radon-222 and specific polar air conductivities in the atmospheric surface layer were carried out over a number of years at various locations in the North Caucasus [11]. It was shown that the variations in the concentrations of light atmospheric ions and the space charge density are related with the variations in the radon-222 emanations. Spectral analysis of the space charge density variations was performed [12].

In the fair weather electricity research great attention is given to the electrode effect. In [13] the variability of the electrical parameters under the influence of the electrode effect is investigated, and two extreme cases of the electrode effect, classical and turbulent, are considered. It was found that under the ‘fair weather’ conditions the space electric charge is positive near the ground, and the scale of its distribution is determined by the electrode layer thickness and is equal to several metres. The values of the electric charge density are defined by both the power of the ion formation source and the magnitude of the electric field. On the basis of the research results recommendations for monitoring atmospheric electrical parameters were provided [14].

In [15] a non-stationary electrodynamic model was developed of atmospheric turbulence in the surface layer allowing for multiple-charged aerosol particles. The stability, convergence and conservativeness of the schemes employed were proved. On the basis of experimental observations the conditions for the classical and turbulent electrode effect were established, and the agreement of the obtained model calculations with the experimental data was estimated. The approximate analytical solution was obtained of the boundary value problem for the classical electrode effect in the surface atmosphere. It was shown that the obtained solution is an exact analytical solution for a special case of the problem, which takes place in the real atmosphere. Approximate asymptotic solutions corresponding to low turbulent mixing were found for the cases of stable and neutral atmospheric stratification [16]. In [17] the well-posed problems were analysed for the one-dimensional steady-state system of equations describing the classical electrode effect in the atmospheric surface layer; a complete classification of the solution types was obtained, their properties were investigated, and analytical expressions were derived for the dependence of the ion concentration on the electric field intensity. New classes of solutions to the system were found, characterized by the presence of layers with infinitely increasing conductivity and charge density.

2. The global electric circuit

The concept of the global electric circuit (GEC) is fundamentally important for the studies of atmospheric electricity, since it combines all electrical processes in the atmosphere into a single electric network. Over the last few years the interest in GEC has increased owing to the fact that its parameters can serve as indicators of the state of Earth’s climate system and Earth’s space environment.

Much attention has been given recently to modelling the GEC and its particular components, especially the most important part of the GEC composed of quasi-stationary distribution of the electric current, maintained by thunderstorm generators. In [18] steady-state and non-stationary GEC models were

constructed; in these models it is possible to uniquely determine the spatial distribution of the electric potential for arbitrary (known) distribution of conductivity in the atmosphere, once GEC generators are described in the form of a source current density distribution. An important distinctive feature of these models is the boundary value problem in which the ionospheric potential — one of the most important GEC parameters, defined as the potential difference between the Earth's surface and the ionosphere — is uniquely determined (as a constant or as a function of time) from the solution of equations for the potential and is not specified explicitly; furthermore, it was demonstrated that this boundary value problem is the only possible one, if the atmosphere has the geometry of a spherical layer. Besides the implementation of corresponding numerical models on the basis of the finite element method, it was shown that the ionospheric potential in many simple problems can be expressed analytically as a function of the problem parameters [18, 19]. A number of general questions concerning GEC modelling in both plane-parallel and spherical geometry were discussed in [20].

In [21] the impact of lightning discharges on the GEC was analysed and discussed. On the basis of a quasi-stationary GEC model it was shown that intracloud discharges and positive cloud-to-ground discharges result in a decrease in the ionospheric potential, whereas negative cloud-to-ground discharges result in its increase. Quantitative estimates demonstrated that the ionospheric potential variation due to negative cloud-to-ground discharges do not exceed 10% of its quasi-stationary value.

The interaction of the GEC with ionospheric and lithospheric processes is another important direction of research. In [22] an attempt was made to consider the influence of the ionospheric generator on the atmospheric electric field. The vertical profile of atmospheric conductivity was assumed to be piecewise-exponential, and at the upper boundary of the atmosphere a certain distribution of the potential was specified. Within the framework of the non-stationary problem the estimates were obtained for the stabilization time of the stationary electric field in the lower atmosphere when the ionospheric generator is turned on and for the dissipation time of the electric field in the absence of generators. In [23, 24] penetration of the electric field from the atmosphere near the Earth's surface to the ionosphere was modelled, which is important for the problem of ionosphere-lithosphere coupling. In such models the vertical component of the electric field at the Earth's surface is specified, and the equation for the potential, allowing for conductivity anisotropy, is solved. The authors calculated that the absolute value of the resulting electric field generated in the ionosphere by means of such mechanism is much less than it is usually supposed in connection with observations of the ionospheric precursors of earthquakes [24]. The coupling of lithospheric and ionospheric processes through the GEC was also discussed in [25]. In [26] hypothetical 'seismogenic currents' flowing between the tectonic

faults and the ionosphere were suggested as GEC generators in addition to thunderstorms in order to account for the observed variations of the ionospheric total electron content.

In [27] the relations were analysed between distributed GEC models and simplified equivalent-circuit models, where different parts of the atmosphere are replaced by equivalent resistors and capacitors; the limitations of such models were established. The influence of conductivity inhomogeneities on the ionospheric potential was also studied; it was shown that the account of conductivity reduction inside a thunderstorm generator may lead to substantial increase in its contribution to the GEC. The mechanisms whereby conductivity perturbations in the atmosphere have an impact on the ionospheric potential dynamics were also discussed in [25].

One of the main reasons for the increasing interest in the GEC during the last few years is the close connection between electrical processes in the atmosphere and the climate dynamics. In [28] the dynamics of the ionospheric potential on different time scales was studied using a general circulation model. A parameterization was suggested for the contribution to the ionospheric potential from convection regions, associated with electrified clouds, i.e. with GEC generators. The calculated diurnal and seasonal ionospheric potential variations turned out to agree with the experimental data; also, the decrease in the ionospheric potential by about 10% over the 21st century was predicted.

In [29] the principal criteria were formulated for the formation and maintenance of a GEC in the atmospheres of the Solar System planets. Having estimated the vertical conductivity profile in the atmosphere of Mars, the authors concluded that there is no stationary GEC on Mars, but the current still can flow in the circuit, if a high-power and extensive generator, presumably related to the electrification during the dust storms, is working.

3. Electrical processes in clouds and their simulation

The problem of generation and evolution of the intense convective systems is one of the most topical and complicated problems of the atmospheric physics. Investigation of electrical processes in convective systems is necessary for self-consistent analysis of the atmospheric dynamics and for increasing the precision of weather forecasts. During the period 2010–2015 in Russian Federation a number of attempts were made to include the main electrical processes in hydrodynamic numerical models of the atmosphere [30–33]. Numerical non-stationary three-dimensional model of a convective cloud with parameterized description of microphysical processes allowing for the electrification was developed by a scientific group from RosHydroMet Voeikov Main Geophysical Observatory. The spatio-temporal distribution of the main cloud characteristics,

including the volume charge density and the electric field, were estimated. The calculations showed that the electric structure of the cloud is different at various stages of its life, i. e., it varies from unipolar to dipolar and then to tripolar. These results are in a fair agreement with the field studies [30,31]. Numerical calculations of the convective cloud formation during unstable atmospheric stratification and in the presence of background wind were performed by means of the three-dimensional non-stationary model developed in RosHydroMet High Mountain Geophysical Institute with detailed description of hydrodynamic, thermodynamic, microphysical, and electric processes. The formation of the positive and negative volume electric charges was studied, and the electric field at various stages of cloud development was calculated with the help of this model. It was found that the precipitation particle growth time in an intense convective cloud decreases by 30% due to electric coagulation [32, 33]. A hazardous meteorological phenomenon, bora in Novorossiysk, was studied using the results of numerical modelling based on the WRF-ARW mesoscale atmospheric model, the SWAN model of wind waves and the observational data obtained during expeditions [34]. The WRF model proved to simulate bora qualitatively well; this fact shows that mesoscale atmospheric models could successfully reproduce such events.

Predicting lightning activity is important for different applications and fundamental research. Nowadays in most cases indirect nonelectrical indices are used for such forecasts. However, this method, which considers thermodynamic and microphysical features of the convective cloud evolution, but does not include non-local interaction of electrical charged particles, is not capable to predict lightning activity with high accuracy. Forecasts based on indirect indices depending on the parameterization of microphysical processes in the WRF model were studied in papers [35, 36]. A new algorithm of predicting lightning activity was proposed on the basis of direct calculation of the electric potential and the electric field in thunderclouds with the help of the WRF model data [35–38]. The results yielded by this model were shown to be in accordance with the experimental data concerning the electrical characteristics of thunderclouds. The simulation of real thunderstorms in Nizhny Novgorod region showed good correlation with the radar data.

Owing to an important role of lightning discharges in local and global electric phenomena in the Earth's atmosphere, simulation of the fields and currents during a lightning discharge is a topical problem, important for both direct and inverse electrodynamics problems. Researchers from the IAP RAS proposed a numerical model of large-scale electrodynamics of a lightning discharge based on the complete set of Maxwell's equations, which makes it possible to describe both the quasistatic and fast transient electric fields and currents in the atmosphere [39–41]. The proposed model of the electromagnetic response of the

atmosphere to a lightning discharge makes it possible to describe a number of parameters of different components of the discharge current by comparing the calculation results with the observational data on electromagnetic and quasistatic fields. Analysis of the form of quasistatic field pulse made it possible to estimate the distance to the discharge, the neutralized charge and the height of the discharge.

One of the most important and complicated problems of the cloud physics is the development of high-performance methods for the control of cloud-to-ground processes and precipitation growth processes by means of active influence. The development of scientifically grounded methods of active influence requires creation of a new class of the cloud microstructure control models. In such models the parameters of influence (the point of influence, the time of influence, the source power) should be determined as the solution of the optimal control problem for the set of equations describing transformation of spatial and temporal physical properties of the cloud. One of the directions of further development is improvement of the existing models of convective clouds for studying an artificial increase of precipitation, cloud atmosphere electrification and optimal control of the cloud microstructure.

Experiments on modelling upward and downward leaders during the evolution of a long spark and in an artificial electrified aerosol cloud were performed at High-Voltage Research Centre of the All-Russian Electrotechnical Institute [42–46]. As part of the experiments, the impact of upward and downward leaders on lightning strokes to ground and isolated objects was studied. It was found that in the case of the long spark, the upward negative leader is caused by a positive downward leader propagating from the high-voltage electrode of the Marx generator in the gap of length 9–12 m, and in the case of the electrified aerosol cloud, the upward positive leader is initialized by the electric field of the negatively charged cloud. All the phases typical for natural and trigger lightning were observed.

The system generating a unipolar electrified aerosol cloud and the registration system were developed and implemented. The electrical structure of a unipolar cloud was modelled numerically using the quasi-electrical approach. For the first time the infrared images were obtained for the discharges generated inside the artificial charged aerosol cloud.

Along with typical streamer and leader discharges, which are observed in laboratory experiments with long spark discharges, inside the charged cloud many non-conventional types of discharges were observed [45]. These discharges, named ‘stalks’, constitute a new class of discharge phenomena inside the electrified cloud medium. The variety of stalks was classified and analysed.

To understand the physics of lightning, the studies of the kinetics of the processes occurring in streamer and leader discharges in plasma are important. The

simulation of nitrogen molecules dissociation in a repetitively pulsed barrier discharge at atmospheric pressure was presented in [47]. It was shown that the quenching of basic predissociating conditions at this pressure is relatively low and the use of the cross-section of N_2 dissociation by electron impact makes it possible to adequately describe the recovery of the atoms in these experimental conditions at atmospheric pressure. The propagation of streamers along the gas jets for positive and negative polarity were simulated; the resulting patterns of the dynamics and structure of streamers in the two cases are similar to those observed in experiments with plasma jets [48].

The influence of ionic layer formed by corona discharge at ground level in the event of the attraction of lightning to tall objects was investigated. The properties of non-stationary corona supported by a multi-point ground system in the time-varying electric field of thunderstorms were studied numerically and analytically. The initialization of an upward leader from the ground-based system with natural conditions was modeled in [49].

Lightning protection remains one of the most important problems. Protection of industrial buildings from direct lightning strokes must be combined with the suppression of incomplete discharges from external buildings and even from lightning rods themselves [50].

Lightning flashes are one of the main sources of nitrogen oxides in the troposphere. The nitrogen oxides can make a significant contribution to the redistribution of radiation-active and chemically active gases, which affect the variation of the temperature fields, and thereby weather and climate change. In recent years a series of important studies was published on the feedbacks between thunderstorm activity, atmospheric composition and changes in weather and climate [51–53]. It was shown that, as the result of the variability of NO_x production by lightning and the subsequent variability of the concentrations of atmospheric gases, temperature varies most significantly in lower and middle stratosphere in tropical and polar regions [53].

4. Lightning location

Information being collected from a lightning location system (LLS) is applicable for solving different problems. Timely storm warning needs early thunderstorm detection and more precise storm cells positioning. Also, early thunderstorm detection may be useful for hydrological studies and the control of current stage and trend of cloud formation. Thunderstorms are often the precursors of other dangerous phenomena in the cloudy atmosphere; LLSs are useful for providing aviation safety. Regional thunderstorms climatology and typical lightning parameters, such as current magnitude and growth time, obtained by means of LLSs, play significant role for lightning protection purposes.

In recent years multi-point lightning location systems have been being actively developed in Russia [54–60]. A number of studies have been performed so as to investigate and improve the precision of LLSs [56,61], new systems and complexes have been created [54,55,57]. In other studies the LLS data have been used together with other sources of information about thunderstorm activity [62].

A multi-point LLS developed in the IAP RAS was put into operation in the Volga-Vyatka region. At the initial stage of development, this LLS covers Nizhny Novgorod region. During the period from 16 July 2014 until the end of the convective season the LLS registered about 160000 lightning discharges (including both cloud-to-ground and intracloud discharge types). The system is based on Boltek Stormtracker devices and special software developed in the IAR RAS. For validating the precision of the developed LLS, the data obtained from it were compared with the WWLLN data and the data from a Doppler weather radar; this validation showed good correlation. In the Nizhny Novgorod LLS a combined method of lightning detection is applied, including the time-of-arrival and direction finding methods [55, 63].

In the North Caucasus region the lightning detector LS8000, developed by Vaisala, was put into operation. LS8000 provides the coordinates, polarity, type (cloud-to-ground or intracloud) and other characteristics of lightning discharges. Combined cluster processing is planned of the LS8000 data and the map of the radio echo from clouds and precipitations, obtained from regional weather radars network in real time. Since 2008, during the period of LS8000 operation, the parameters of the currents for detected cloud-to-ground lightning discharges were studied [57].

During 2011, the Alves 9.07 LLS, developed jointly by Alves Ltd. and the department of atmospheric electricity of the Voeikov Main Geophysical Observatory, was modified. The Alves System is based on the time-of-arrival positioning method and covers the European part of Russia and the Urals. The new generation of lightning detectors was developed and put into operation. As of August 2014, the LLS consisted of 70 lightning detectors. During the convective seasons of 2013–2014 accuracy of the Alves was estimated using the data provided by the European LLS Blitzortung [58–60]. Also, the sources of inaccuracies caused by errors in the timing of atmospheric were investigated. Model and experimental estimates of these errors were made [56, 64]. Model estimates of the errors of lightning positioning algorithms were carried out for the case of a high-current lightning stroke represented by an arbitrarily oriented dipole under the influence of industrial noise [61].

In Eastern Siberia the features of the spatial distribution of positive lightning discharges detected by a one-point detector with the coverage radius of about 1200 km were studied for 2003–2007 seasons. The spatial distribution of positive lightning was found to be in general the same as the distribution of the total

lightning activity. Areas of thunderstorm activity, where the count of positive discharges is greater than the count of negative ones, were highlighted, and this fact was accounted for by geographical conditions, such as high altitude and the proximity of the Sea of Okhotsk; thus the influence of the relief on the inverted charge distribution inside the cloud was demonstrated [65].

Other lightning activity parameters were investigated in the region of Central Yakutia in 2009–2012. The percentage of cloud-to-ground discharges was found to be 40–60%, which agrees with the observations in Western Siberia (40–50%). Positive cloud-to-ground discharges count was 8–15%. Thunderstorm activity in Yakutsk was 3 times higher than that in the 400-km vicinity of Yakutsk [66].

An LLS based on three independent lightning detectors have been functioning in Yakutia for a long time; the detectors are located in Yakutsk, Neryungri, Mirnyi. It operates in the VLF range and has the positioning precision of a few kilometres. Using the LLS data helps to improve clustering algorithms. The results of data processing showed that mature thunderstorm cells are located at the cluster centre and dissipating cells are located at the downwind part of the cluster. The time of activity of a single cell is 20–30 minutes, whereas a multi-cell cluster can exist for several hours. Thunderstorms in a cluster are usually more intensive than those in isolated cells. According to the study of 227 thunderstorm cells, average cell area is 12 km², average cell lifetime is about 31 minute and average count of discharges in a cell is equal to 10. For the first time the data on thunderstorm climatology in the region are obtained [67].

5. High-altitude discharges and gamma flashes

In recent years high-altitude discharges in the atmosphere are given significant attention in the world. One of the main tools for the direct study of high-altitude discharges are satellite measurements. The main scientific objectives and engineering designs of the micro-satellite platform Chibis and the scientific equipment Thunderstorm, which are aimed at exploring new physical mechanisms of high-altitude electrical discharges in the atmosphere, are presented in [68]. In [69] the data are presented from a space experiment conducted at the satellite University-Tatiana, in which the UV radiation in the night-time atmosphere and fluxes of electrons with energies above 70 keV were measured simultaneously. Increases in the average intensity of the UV radiation are registered; presumably, they may be due to the acceleration of electrons in atmospheric electrical discharges, followed by the capture of electrons by the geomagnetic field and the electron precipitation at conjugate points of the geomagnetic field. The statistics of high altitude discharges detected by the university satellite Tatiana 2 was analyzed in [70]. High-altitude discharges occur most often in equatorial latitudes over land, and their duration is 1–128 ms. Sequences of

high-altitude discharges from 3 to 16 events were recorded, and single events occurred much less frequently than the series. Registration of flashes took place in the ultraviolet (240–400 nm) and red-infrared (610–800 nm) ranges of the night-time atmosphere emission spectrum [71].

A number of studies on modeling the electrical and chemical processes during fast discharge phenomena were carried out. Further development of the theory of discharge phenomena in the stratosphere and mesosphere (elves and sprites), which are initiated by tropospheric storm processes, was discussed in [72]. The redistribution of charges in the atmosphere was investigated quantitatively at the altitudes up to 150 km during the process of charging and discharging of a thundercloud. Long duration of high altitude discharges, which are developing in the residual polarization field, was explained by taking into account small electrical conductivity of the atmosphere.

The paper [73] was devoted to the study of the conditions for the initiation of two types of high-altitude discharges, sprites and halo. A quasi-electrostatic model was developed for generating the electric field in the middle atmosphere, which takes into account peculiarities of the charge distribution and its dynamics inside thundercloud, as well as the realistic atmospheric conductivity profile. Non-linear effects associated with the heating of electrons in the electric field were also considered. It was shown that the area where the electric field of the lightning flash exceeds the breakdown field, is centered around an altitude of about 75 km, which is consistent with the observations of sprites. It was found that the dynamics of the current and charge of the lightning flash plays an essential role in the initiation of high-altitude discharges in the atmosphere.

The influence of high-altitude discharges on the chemical composition of the mesosphere was investigated in [74,75] on the basis of a numerical model; a self-consistent plasma-chemical model was suggested for the diffusion region of a sprite in the altitude range 60–90 km. Perturbations were analyzed of the concentrations of ions, electrons and neutral components due to a sprite discharge and of the intensity of photon emission due to a sprite or a halo. Owing to the rapid displacement of the electric field at the top of the diffusion region of a sprite at the altitudes 78–81 km, the radiation at the discharge axis ceases earlier than in the outer region, i.e., toroidal structure of the electric field and sprite radiation is being formed. The electron density decreases during the development of a sprite discharge at the altitudes 83–87 km, which is the result of the increasing role of dissociative attachment to molecular oxygen, which significantly reduces the conductivity at these altitudes.

A number of studies were dedicated to the problem of initiation of lightning discharges and the runaway breakdown. The possibility of a self-discharge in a transverse field of a lightning leader in the regime of generating relativistic runaway electron avalanches was analyzed in [68]. A low threshold for feedback

was obtained for a leader of cylindrical geometry. It was shown that the discharge can be the source of the pulses of penetrating radiation observed to be correlated with thunderstorm activity; the characteristics of these pulses were reproduced in the model of a cylindrical leader.

The data obtained from the simultaneous recording of signals emitted during lightning discharges in the radio and gamma-ray ranges during the in situ observations in the Tien Shan were analyzed in [63, 76]. High correlation (0.9–0.95) between gamma waves and radio waves was shown. Measurements confirmed the theory of lightning initiation by relativistic runaway electron avalanches. It was demonstrated that the energy spectrum of gamma radiation corresponds to the characteristic spectrum of the runaway breakdown. In [76] detailed analysis was performed of the dynamics of electric pulses during the development of a lightning discharge, which indicated that the breakdown is determined by the runaway electrons. High magnitude of current pulses was explained by multiple micro-discharges on the hydrometeors, as a result of which, the vast region of ionic conductivity is formed in the cloud. It was shown that the charge transfer by ions plays a decisive part in the development of a lightning leader.

Conclusions

Over the last few years the studies of atmospheric electricity in Russian Federation have been actively being developed. A variety of experimental and theoretical studies of fair weather electricity, including the impact of atmospheric ions and aerosols, were performed. Experimental and theoretical research regarding the global electric circuit was carried out with the help of models of climate and chemistry. A numerical non-stationary three-dimensional model of a convective cloud allowing for the electrification was constructed, and a model of the cloud dynamics have been developed with a detailed description of microphysics. A number of experimental studies in the fields of lightning physics and lightning protection were performed, including experiments employing unique laboratory equipment and field experiments at the All-Russian Electrotechnical Institute facility in Istra. In many regions of Russia the climatology of the electrical processes in the atmosphere, regional meteorological peculiarities of thunderstorms and further development of methods for modelling and forecasting thunderstorm phenomena have been investigated. Several unique experimental studies of high-energy processes in the atmosphere correlated with lightning activity were performed. Discharges in the middle atmosphere were theoretically analysed, and new methods for their detection were developed. A number of studies were successfully performed at the Tatiana and Tatiana 2 micro-satellites; interesting results were obtained at Chibis satellite, which had been aimed at the study of high-energy phenomena in the atmosphere. RosHydroMet have been

developing a network of Doppler radars with cross-polarization capability (of which about 30 are already operating) and a lightning detection network. Another important achievement is the launch and successful operation of the LS800 lightning detection system in the Southern federal district and the Moscow region.

A number of factors conduced to the development of atmospheric electricity research in Russian Federation, including the improvement of technical equipment of the Federal Service for Hydrometeorology and Environmental Monitoring (RosHydroMet). For certain directions of research, the support from the Government of the Russian Federation (‘megagrants’) is an important factor; this support made it possible to involve world’s leading experts and to create new scientific laboratories, including the laboratory of lightning physics in the IAP RAS under the leadership of Prof. V.A. Rakov from the University of Florida.

Over the past four years several conferences dedicated to the problems of atmospheric electricity were organized in Russia. They include 7th All-Russian Conference on Atmospheric Electricity (St. Petersburg, 2012), 4th International Conference on Lightning Protection (St. Petersburg, 2014), 1st All-Russian Conference on the Global Electric Circuit (Borok, 2013). Russian researchers actively participated in 15th International Conference on Atmospheric Electricity (Oklahoma, USA, 2014), which is held every 4 years and is the world’s principal international forum for atmospheric electricity.

References

1. Anisimov S. V., Galichenko S. V., Shikhova N. M. Space charge and aeroelectric flows in the exchange layer: An experimental and numerical study // *Atmos. Res.* 2014. Vol. 135–136. P. 244–254.
2. Anisimov S. V. et al. Aeroelectric structures and turbulence in the atmospheric boundary layer // *Nonlinear Process. Geophys.* 2013. Vol. 20, № 5. P. 819–824.
3. Redin A. A., Kupovykh G. V., Boldyrev A. S. Electrodynamic Model of the Atmospheric Convective-Turbulent Surface Layer // *Radiophys. Quantum Electron.* 2014. Vol. 56, № 11–12. P. 739–746.
4. Anisimov S. V. et al. Electricity of the convective atmospheric boundary layer: Field observations and numerical simulation // *Izv. Atmos. Ocean. Phys.* 2014. Vol. 50, № 4. P. 390–398.
5. Anisimov S. V., Shikhova N. M. Intermittency of turbulent aeroelectric field // *Atmos. Res.* 2014. Vol. 135–136. P. 255–262.
6. Anisimov S. V., Afinogenov K. V., Shikhova N. M. Dynamics of Undisturbed Midlatitude Atmospheric Electricity: From Observations to Scaling // *Radiophys. Quantum Electron.* 2014. Vol. 56, № 11–12. P. 709–722.

7. Anisimov S. V., Shikhova N. M. Transport of electricity in atmospheric exchange layer // *Geophys. Res.* 2010. Vol. 11, № 1. P. 55–63.
8. Anisimov S. V., Galichenko S. V., Shikhova N. M. Formation of electrically active layers in the atmosphere with temperature inversion // *Izv. Atmos. Ocean. Phys.* 2012. Vol. 48, № 4. P. 391–400.
9. Petrov A. I. et al. Measuring complex for the study of atmospheric electricity boundary layer // *Izv. VUZov. Sev. Reg. Nat. Sci.* 2010. № 3. P. 47–52.
10. Redin A. A., Kupovykh G. V. On the global and local variations of the electric field near the Earth surface // *Izv. VUZov. Sev. Reg. Nat. Sci.* 2011. № 1. P. 87–90.
11. Kudrinskaya T. V. et al. The study of the atmospheric electric field at different levels near the ground // *Nauchnaya mysl' Kavk.* (in Russ.) 2012. № 4(72). P. 95–98.
12. Berezinskiy N. A. et al. Influence of earthquake preparation for radon concentration and electrical conductivity of surface atmosphere // *Geol. Geophys. South Russ.* (in Russ.) 2011. № 2. P. 14–22.
13. Kudrinskaya T. V., Kupovykh G. V., Redin A. A. Comparison of the mathematical modeling results of the electrode effect with the experimental data // *Izv. Yuzhnogo Fed. Univ. Tekhnicheskoye Nauk.* 2013. № 4(141). P. 72–80.
14. Boldyrev A. S. et al. On the atmosphere electric field monitoring using ground-based observations // *Mod. Probl. Sci. Educ.* 2013. № 6. P. 875.
15. Dmitriev E. M., Filippov V. A. The analytical solution of the surface atmosphere classical electrode effect problem // *Geophys. Res.* 2010. Vol. 11, № 4. P. 53–59.
16. Dmitriev E. M. An asymptotic solution of the surface atmosphere electrode effect problem under weak turbulent mixing // *Geophys. Res.* 2011. Vol. 12, № 4. P. 52–58.
17. Kalinin A. V. et al. Classification and Properties of Solutions for the System of Equations of Classical Electrode Effect Theory // *Radiophys. Quantum Electron.* 2014. Vol. 56, № 11–12. P. 747–768.
18. Kalinin A. V. et al. Stationary and nonstationary models of the global electric circuit: Well-posedness, analytical relations, and numerical implementation // *Izv. Atmos. Ocean. Phys.* 2014. Vol. 50, № 3. P. 314–322.
19. Mareeva O. V. et al. On the contribution of a convective generator into the global electric circuit // *Solnechno-zemnaya Fiz.* 2012. № 21(134). P. 115–118.
20. Slyunyaev N. N. et al. Calculation of the ionospheric potential in steady-state and non-steady-state models of the global electric circuit // *Int. Conf. Atmos. Electr. Norman, Oklahoma, USA, 2014.*
21. Morozov V. N. Influence of lightning discharges in thunderclouds on the global electric circuit // *Tr. GGO im. A. I. Voeikova.* 2013. № 569. P. 249–257.
22. Morozov V. N. Distribution of the electric field produced by the ionospheric generator in the lower layers of the atmosphere // *Tr. GGO im. A. I. Voeikova.* 2012. № 565. P. 205–215.
23. Denisenko V. V., Pomozov E. V. Penetration of electric field from the surface layer to the ionosphere // *Solnechno-zemnaya Fiz.* 2010. № 16. P. 70–75.
24. Denisenko V. V. et al. On electric field penetration from ground into the ionosphere // *J. Atmos. Solar-Terrestrial Phys.* 2013. Vol. 102. P. 341–353.

25. Pulinet S., Davidenko D. Ionospheric precursors of earthquakes and global electric circuit // *Adv. Sp. Res.* 2014. Vol. 53, № 5. P. 709–723.
26. Namgaladze A. A. Earthquakes and the global electric circuit // *Khimicheskaya Fiz.* 2013. Vol. 32, № 9. P. 9–13.
27. Slyunyaev N. N. et al. Influence of large-scale conductivity inhomogeneities in the atmosphere on the global electric circuit // *J. Atmos. Sci.* 2014. Vol. 71, № 11. P. 4382–4396.
28. Mareev E. A., Volodin E. M. Variation of the global electric circuit and ionospheric potential in a general circulation model // *Geophys. Res. Lett.* 2014. Vol. 41, № 24. P. 9009–9016.
29. Evtushenko A. A., Ilin N. V., Kuterin F. A. On the existence of a global electric circuit in the atmosphere of Mars // *Moscow Univ. Phys. Bull.* 2015. Vol. 70, № 1. P. 57–61.
30. Veremey N. E. et al. Study of the Evolution of the Electric Structure of a Convective Cloud Using the Data of a Numerical Nonstationary Three-Dimensional Model // *Radiophys. Quantum Electron.* 2014. Vol. 56, № 11–12. P. 801–810.
31. Veremey N. E. et al. Studies of the evolution of convective cloud electric structure with the use of numerical nonstationary three-dimensional model data // *VII All-Russian Conf. Atmos. Electr.* 2012. P. 47–48.
32. Ashabokov B. A. et al. Numerical Simulation of Thermodynamic, Microstructural, and Electric Characteristics of Convective Clouds at the Growth and Mature Stages // *Radiophys. Quantum Electron.* 2014. Vol. 56, № 11–12. P. 811–817.
33. Ashabokov B. A. et al. Some results of numerical studies in thermodynamic, microphysical and electric characteristics formation of convective clouds // *VII All-Russian Conf. Atmos. Electr.* 2012. P. 31–32.
34. Toropov P. A., Myslenkov S. A., Samsonov T. E. Numerical modeling of bora in Novorossiysk and associated wind waves // *Moscow Univ. Geogr. Bull.* 2013. № 2. P. 38–46.
35. Demytyeva S. O., Ilin N. V., Mareev E. A. Calculations of the Lightning Potential Index and Electric Field in Numerical Weather Prediction Models // *Izv. Atmos. Ocean. Phys.* 2015. Vol. 51, № 2. P. 186–192.
36. Demytyeva S. O., Ilin N. V. Calculation of Lightning Potential Index (LPI) for different microphysics parameterizations based on WRF model and its comparative analysis with electrical parameters // *15th Int. Conf. Atmos. Electr. (ICAE2014)*. 2014. P. P–04–05.
37. Demytyeva S. O., Ilin N. V., Mareev E. A. Calculations of thundercloud electric parameters in high-resolution numerical models // *XVIII All-Russian young Sci. Sch. “Atmospheric Compos. Atmos. Electr. Clim. Process.* 2014. P. 52–53.
38. Demytyeva S. O., Ilin N. V., Mareev E. A. Prediction of lightning activity based on direct electric field calculations // *Int. Symp. “Topical Probl. Nonlinear Wave Physics” (NWP 2014)*. 2014. P. 158–159.
39. Davydenko S. S., Mareev E. A., Sergeev A. S. Model of electromagnetic response of the atmosphere to the lightning discharge // *VII All-Russian Conf. Atmos. Electr.* 2012. P. 64–67.

40. Davydenko S.S. et al. Electromagnetic response of the inhomogeneous anisotropic atmosphere to a single lightning discharge // Int. Symp. "Topical Probl. Nonlinear Wave Physics" (NWP 2014). 2014. P. 149–150.

41. Davydenko S.S. et al. 3D modeling atmospheric electric and current caused by a lightning discharge // 15th Int. Conf. Atmos. Electr. (ICAE2014). 2014. P. P – 08–25.

42. Syssoev V.S. et al. A study of parameters of the counterpropagating leader and its influence on the lightning protection of objects using large-scale laboratory modeling // Radiophys. Quantum Electron. 2014. Vol. 56, № 11–12. P. 839–845.

43. Syssoev V.S. et al. Electrical structure of unipolar cloud // VII All-Russian Conf. Atmos. Electr. 2012. P. 238–240.

44. Bogatov N.A. et al. Microwave diagnostics for investigation of long spark and artificial charged aerosol cloud // 15th Int. Conf. Atmos. Electr. (ICAE2014). 2014. P. P – 03–09.

45. Andreev M.G. et al. First detailed observations of discharges within the artificial charged aerosol cloud // 15th Int. Conf. Atmos. Electr. (ICAE2014). 2014. P. O – 03–08.

46. Andreev M.G. et al. Return stroke initiated by the contact between a downward negative leader from the aerosol cloud and upward positive leader from the grounded plane // 15th Int. Conf. Atmos. Electr. (ICAE2014). 2014. P. P – 03–07.

47. Popov N.A. Dissociation of nitrogen in a pulse-periodic dielectric barrier discharge at atmospheric pressure // Plasma Phys. Reports. 2013. Vol. 39, № 5. P. 420–424.

48. Naidis G.V. Simulation of streamers propagating along helium jets in ambient air: Polarity-induced effects // Appl. Phys. Lett. 2011. Vol. 14. P. 141501.

49. Bazelyan E.M., Raizer Y.P., Aleksandrov N.L. The effect of corona space charge produced at ground level on lightning attachment to tall structures // 2012 31st Int. Conf. Light. Prot. ICLP 2012. 2012.

50. Bazelyan E.M. Lightning attacks the objects of oil and gas industry not only from the top // Territ. Neft. Russ. 2012. Vol. 9. P. 20–21.

51. Sukhodolov N.V., Smyshlyaev S.P., Mareev E.A. Modeling global aspects of lightning activity for investigation of feedbacks with climate change and atmosphere composition // VII All-Russian Conf. Atmos. Electr. 2012. P. 236–238.

52. Kolomeetz L.I., Smyshlyaev S.P. Modeling of feedbacks of lightning activity, atmosphere composition and climate change // XVIII All-Russian young Sci. Sch. Atmospheric Compos. Atmos. Electr. Clim. Process. 2014. P. 56–57.

53. Smyshlyaev S.P. et al. Simulating indirect effects that thunderstorm activity has on atmospheric temperature // Izvestiya, Atmos. Oceanic Phys., 2013. Vol. 49, № 5. P. 550–564.

54. Kuterin F.A., Shlyugaev Y.V., Bulatov A.A. Organization of database for multi-point lightning location system // IV Int. Conf. Light. Prot. 2014. P. 278–282.

55. Kuterin F.A., Bulatov A.A., Shlyugaev Y.V. The Development of the Lightning Detection Network based on Boltek StormTracker hardware // Int. Conf. Atmos. Electr. ICAE. Norman, OK, USA, 2014. P. P – 12–17.

56. Kononov I.I. et al. Accuracy characteristics of difference time of arrival system of lightning location // Proc. Voeikov A.I. Main Geophys. Obs. 2014. № 575. P. 131–141.

57. Adzhiev A.K., Stasenko V.N., Tapashkanov V.O. Lightning detection system in the North Caucasus // Russ. Meteorol. Hydrol. 2013. Vol. 38, № 1. P. 1–5.

58. <http://www.grozy.ru> [Electronic resource].
59. <http://www.lightnings.ru> [Electronic resource].
60. <http://alwes.ru> [Electronic resource].
61. Kononov I. I., Yusupov I. E., Kandaratskov N. V. Analysis of One-Point Methods for Lightning-Discharge Passive Location // Radiophys. Quantum Electron. 2014. Vol. 56, № 11–12. P. 788–800.
62. Bukharov M. V. Satellite diagnosis of thunderstorm probability // Russ. Meteorol. Hydrol. 2013. Vol. 38, № 8. P. 515–521.
63. Gurevich A. V. et al. Correlation of radio and gamma emissions in lightning initiation // Phys. Rev. Lett. 2013. Vol. 111, № 16.
64. Kononov I. I. et al. Systematic errors of thunderstorm cells positioning // XVII Int. Conf. “Radiolocation, Navig. Commun. Voronezh, 2011. P. 1990–2002.
65. Mullayarov V. A. et al. Patterns of spatial distribution of positive thunderstorm discharges in Eastern Siberia // Russ. Meteorol. Hydrol. 2009. Vol. 34, № 6. P. 364–370.
66. Kozlov V. I. et al. Parameters of thunderstorm activity and lightning discharges in Central Yakutia from 2009 to 2012 // Izv. Atmos. Ocean. Phys. 2014. Vol. 50, № 3. P. 323–329.
67. Shabaganova S. N. et al. Characteristics of storm cells from observations in Yakutia // Russ. Meteorol. Hydrol. 2013. Vol. 37, № 11–12. P. 746–751.
68. Kutsyk I. M., Babich L. P., Donskoi E. N. Self-sustained relativistic-runaway-electron avalanches in the transverse field of lightning leader as sources of terrestrial gamma-ray flashes // JETP Lett. 2011. Vol. 94, № 8. P. 606–609.
69. Veden'kin N. N. et al. Atmospheric ultraviolet light and comparison of its intensity with the variation of electron flux with energies higher than 70 keV in satellite orbit (according to Universitetskii-Tatiana satellite data) // Moscow Univ. Phys. Bull. 2009. Vol. 64, № 4. P. 450–454.
70. Garipov G. K. et al. Global transients in ultraviolet and red-infrared ranges from data of universitetsky-tatiana-2 satellite // J. Geophys. Res. Atmos. 2013. Vol. 118, № 2. P. 370–379.
71. Vedenkin N. N. et al. Atmospheric ultraviolet and red-infrared flashes from Universitetsky-Tatiana-2 satellite data // J. Exp. Theor. Phys. 2011. Vol. 113, № 5. P. 781–790.
72. Khodataev K. V. Discharge Processes in a Stratosphere and Mesosphere During a Thunderstorm (in Russian) // Eng. Phys. 2012. Vol. 2. P. 6–19.
73. Mareev E. A., Yashunin S. A. On conditions of initiation of electric discharges in the middle atmosphere // Izv. Atmos. Ocean. Phys. 2010. Vol. 46, № 1. P. 69–75.
74. Evtushenko A. A., Kuterin F. A. One-Dimensional Self-Consistent Model of the Sprite/Halo Influence on the Mesosphere Chemistry // Radiophys. Quantum Electron. 2014. Vol. 56, № 11–12. P. 853–871.
75. Evtushenko A. A., Kuterin F. A. Self-consistent model on night sprite (In printing) // Radiophys. Quantum Electron. 2015.
76. Gurevich A. V., Karashtin A. N. Runaway breakdown and hydrometeors in lightning initiation // Phys. Rev. Lett. 2013. Vol. 110, № 18.

Climate

I. I. Mokhov

A. M. Obukhov Institute of Atmospheric Physics RAS
mokhov@ifaran.ru

This review presents results of the Russian studies of climate and its changes (published in 2011–2014). Essential part of key results of climate change studies with analysis of impacts for Russia during last years is given in [1–233]. Previous similar review was published in [19, 23]. Information on climate studies in Russia is published regularly in the bulletin “Climate Change” (<http://meteorf.ru>). Various and detailed assessment of climate changes and their impacts in Russian regions was presented in [1].

Climate and its changes from observations, reanalyses and paleoreconstructions

Significant climate anomalies and changes have been noted during last time in various regions, including Russian regions [1–102]. In Russia, as a northern country, the warming is much faster than for the Earth as a whole. In recent decades, the rate of the surface warming in Russia in general was more than twice higher than the global one. In some regions it was more than 4 times larger. According to Roshydromet data (<http://www.meteorf.ru>) the trend of the annual-mean surface air temperature for Russia as a whole for the period 1976–2014 was equal to $0.42^{\circ}\text{C}/(10 \text{ years})$. Such a rapid warming in Russia is accompanied by considerable interannual variability. The obtained linear trend is associated with 40% of the variance of surface air temperature for Russia as a whole. The highest rate of the surface air warming in recent decades was observed in the Arctic regions up to $0.8^{\circ}\text{C}/(10 \text{ years})$ or more for annual means and up to $1^{\circ}\text{C}/(10 \text{ years})$ or more for the seasonal means.

The tendency of increase in the number and intensity of regional hydrometeorological anomalies under general climate warming is noted, for Russian regions, in particular (<http://www.meteorf.ru>). The number of hazardous hydrometeorological phenomena with significant economic and social damage was 2.4 times larger in Russia for the last five years (2010–2014) than for the last five years at the end of the 20th century (1996–2000). The largest number of such events was in 2012. Most often dangerous meteorological phenomena are observed in the summer months.

Particularly strong changes in climate have been noted in Arctic and subarctic latitudes, which are characterized by high variability and sensitivity to various

natural and anthropogenic forcings [1–44]. Regional increase in the surface temperature is accompanied by fast reduction of sea ice and significant change of snow cover. In the Arctic, changes in the carbon cycle, including the methane cycle, associated with climate changes, are of special importance [25–28]. The carbon dioxide exchange between the atmosphere and the ocean in the Arctic basin depends on the sea ice conditions [40]. New permafrost features (deep craters) have been noted as a response to local climate variations [34]. Such features can be new indicators of changes in the regional stability of contemporary permafrost [36, 37].

According to estimates [20] with the use of observation data from the mid-19th century the contribution of the CO₂ atmospheric content to the dispersion of global annual-mean surface air temperature is more than 3/4. For the Arctic, the contribution of CO₂ to long-term changes is estimated at slightly less than 1/2.

Recent global warming slowdown (hiatus) is discussed in [95].

Many studies are related with the analysis of regional climate extremes [45–56]. In particular, detailed and comprehensive analysis was done for the strongest heat wave in the European part of Russia in summer 2010 with a huge social, environmental and economic losses (e.g. [45–49]). In summer-fall 2013, a record flood occurred in the Amur River basin with severe consequences [16, 102,].

Different cyclic processes occurring in the climate system on different spatial and temporal scales significantly contribute to climate changes. Along with regular cycles a noticeable contribution is associated with different quasi-cyclic processes and phenomena such as the Quasi-Biennial Oscillation (QBO), the El Niño/Southern Oscillation (ENSO), the Atlantic Equatorial Mode (AEM), the North Atlantic Oscillation (NAO), the Arctic Oscillation (AO), the Atlantic Multidecadal Oscillation (AMO), the Pacific Decadal Oscillation (PDO) the cycles of solar activity, and others [1–3, 16, 88–94].

The results of an analysis of historical data and paleoreconstructions advance our understanding of the role of different climatic mechanisms [103–119]. In particular, analysis of the Antarctic snow pits and shallow cores shows multiple climate shifts during past three centuries [111]. Recent significant climatic shift was detected in the 1970s.

Climate theory and climate system modeling

Various aspects of the theory of climate and the modelling of the Earth's climate system are considered in [1–3, 120–160]. Models of different complexity (from conceptual models to the most detailed coupled models of general circulation, global and regional) are used to describe the global climate system (e.g. [120–128]).

Climate models development is related with the more detailed resolution with inclusion of additional effects and climate processes and also with the more

adequate simulation of interaction between different components of the climate system [128–136].

New estimates of climatic effects have been obtained with the use of new parameterizations and specially developed algorithms for description of comprehensive climate processes [127–136,182]. In particular, the ionospheric potential parameterization was used in the general circulation model of the atmosphere and ocean [182]. A coupled chemistry-climate model (including lower and middle atmosphere) was used to assess temperature variations in the atmosphere when its chemical composition is changed due to thunderstorm activity [199]. From ensemble of model simulations with the climate model of intermediate complexity with different scenarios a possibility of transient hysteresis is exhibited for the permafrost area in dependence on temperature [122]. The catastrophic flooding in the Amur River basin in the summer-fall of 2013 due to intense and prolonged rain was related to unique combination of different climatic processes and effects (including long atmospheric blocking anticyclone over the North Pacific during East Asian monsoon season) [16, 102, 198].

The mechanism of multidecadal climate variations in the Arctic and North Atlantic is analyzed in [159] on the basis of ensemble simulations with climate general circulation model. Arctic climate predictability is discussed. Significant topic is related with modeling of potential effects of methane hydrates associated with climate warming and permafrost degradation [133, 141, 142, 154, 164, 165, 169–171]. For long-term climate simulations and for adequate interpretation of paleoreconstructions it is necessary to develop corresponding ice sheet models [189–191].

Russian climate models are used in different international programs, initiatives and projects, including international comparisons of climate models and their blocks: CMIP5, EMICAR5, CORDEX, NEESPI, AOMIP, PMIP II, SnowMIP2, WETCHIMP, IMILAST and others.

Global and regional climate change simulations with assessment of natural and anthropogenic contribution

The estimates of climate changes, including model estimates of possible climate changes in Russian regions, are presented in [1–3, 161–210].

The rapid retreat and thinning of the Arctic sea ice extent is very clear manifestation of climate change and climate models project further general decrease of the Arctic sea ice extent in the 21st century [1–3,206]. According to model projections the navigation in the Arctic Ocean should be more accessible. At the same time, in connection to the changes in the sea ice extent in the Arctic, there should be expected corresponding changes in sea waves in the Arctic basin.

According to models simulations dangerous phenomena with strong winds and extreme sea waves in the Arctic Ocean (in particular along the Northern Sea Route) should be more frequent [175,176].

Characteristics of cyclones (frequency, intensity and size) and their changes in the Arctic in a warmer climate are analyzed in [162] with the use of regional climate model simulations with scenario of moderate anthropogenic forcings for the 21st century.

Possible changes in climate extremes in Russian regions in the 21st century are estimated in [202] from ensemble simulations with regional climate model. High resolution of the regional model enables to simulate the observed climate variations more realistically in comparison to the low-resolution models.

Model simulations show an overall increase in the risk (probability) of extreme precipitation runoff in the Amur River basin in the summer-fall monsoon seasons under scenarios of global warming in the 21st century [16, 198].

According to [184] model simulations show a general increase in the blocking frequency for the Euro-Atlantic region in winter, summer and for the entire year during the 21st century for analyzed RCP scenarios (RCP 2.6 and RCP 8.5), while changes of the opposite sign are characteristic for the Northern Hemisphere as a whole. It was also noted that there is a tendency for an increase in the blocking intensity in the Euro-Atlantic region during the winter from model simulations with both analyzed RCP scenarios for the 21st century. A significant increase is obtained in the Euro-Atlantic region for the likelihood of extreme winter with the total blocking duration longer than seven weeks. Also, a similar tendency is characteristic for the Euro-Atlantic region in summer.

Model estimates of possible permafrost degradation under global warming are presented in [1–3] (see also [164, 203]).

The chemistry-climate model SOCOL has been used in [209] to evaluate the contributions of key anthropogenic factors to the simulated changes of ozone and stratospheric dynamics in the 21st century.

Changes in the thunderstorm activity and lightning flash rate under global warming are assessed in [182] on the basis of simulations with a general circulation model of the atmosphere and ocean. According to obtained results the ionospheric potential is decreasing under global warming while the lightning flash rate is increasing.

Climate change impacts and problems of adaptation and mitigation

Various aspects of climate change impacts for Russian regions and problems of adaptation and possible mitigation are analyzed in [1–18, 211–233].

The problems of hydrometeorological safety in a changing climate with adaptation to climate changes were widely discussed at the Seveth All-Russian Meteorological Congress (<http://www.meteorf.ru/documents/21/8002/>) in 2014.

The effects of climate changes and the problems of adaptation to them and their possible mitigation are discussed and analyzed in [1, 8, 10–12, 14, 17, 18, 217–222] taking into account tendencies in the world economy, power engineering, and the corresponding strategy in Russia. Problems associated with climate changes in northern Eurasia and their different impacts are noted in [13]. Problems related to the optimal adaptation, specifically of the Russian economy, to the hazardous effects of climate changes and the questions related to hydrometeorological security are analyzed in [1]. Changes in the health of Russia's population under the conditions of a varying climate are considered in [17].

The key point of the widely debated problem of global warming is the question of maximum permissible changes. It is necessary to develop objective criteria for estimating both global and regional climate changes and permissible risks [23, 211, 212].

Problem of the climate change mitigation is discussed in [225–230]. In particular, model simulations with aerosol injections in the stratosphere (geoengineering) are analyzed [226–229]. Reduction of short-lived atmospheric pollutant emissions are considered in [230] as an alternative strategy for climate moderation.

An adequate consideration for the carbon balance of Russian boreal forests, wetlands and other terrestrial ecosystems is necessary for a more detailed and comprehensive analysis of the carbon cycle influence in the Earth's climate system [23]. In particular, according to [223] the carbon sink to Russian forests have increased three times from the end of 1980s to the end of 2000s. Such quantitative estimates are necessary for consideration of post-Kyoto agreements [23].

References

1. Second Assessment Report of Roshydromet on climate changes and their impact on the territory of the Russian Federation, 2014: Roshydromet, Moscow, 1535 p. (in Russian)
2. IPCC, 2013: Climate Change 2013: The Physical Science Basis. Contribution of Working Group I to the Fifth Assessment Report of the Intergovernmental Panel on Climate Change. [T.F. Stocker, D. Qin, G.-K. Plattner et al. (eds.)] Cambridge Univ. Press, Cambridge/New York, 1535 p.
3. IPCC, 2014: Climate Change 2014: Impacts, Adaptation, and Vulnerability. Part B: Regional Aspects. Contribution of Working Group II to the Fifth Assessment Report of the Intergovernmental Panel on Climate Change [V.R. Barros, C. B. Field, D.J. Dokken et al. (eds.)]. Cambridge Univ. Press, Cambridge/New York, 688 p.

4. Extremal Natural Phenomena and Catastrophes (vol. II) 2011: IPE RAS, Moscow, 344 p. (in Russian)
5. Meteorological and Geophysical Researches. Moscow, Paulsen, 2011, 349 p. (in Russian)
6. Oceanography and Sea Ice, 2011: Paulsen, Moscow, 432 p. (in Russian)
7. Polar Cryosphere and Continental Waters, 2011: Paulsen, Moscow, 320 p. (in Russian)
8. Assessment of Macroeconomic Impacts of Climate Change over the Territory of Russian Federation till 2030 and beyond, 2011: Roshydromet, 252 p. (in Russian)
9. Snow, Water, Ice and Permafrost in the Arctic (SWIPA): Climate Change and the Cryosphere, 2011: AMAP, Oslo, 538 p.
10. Methods of Assessment of Climate Change Consequences for Physical and Biological Systems, 2012: Planeta, Moscow, 512 p. (in Russian)
11. Investigation of Possibilities of Climate Stabilization Using New Technologies, 2012: Moscow, Roshydromet, 178 p.
12. Fundamental Problems of Spatial Development of the Russian Federation: Interdisciplinary Synthesis. Moscow, Media-Press, 2013, 664 p. (in Russian)
13. Regional Environmental Changes in Siberia and Their Global Consequences, 2013: Dordrecht: Springer. 354 p.
14. Natural Environment of Russia: Adaptation Processes in Conditions of Changing Climate and Development of Nuclear Energy, 2014: IPE RAS, Moscow, 344 p. (in Russian)
15. Turbulence, Atmosphere and Climate Dynamics, 2014: GEOS, Moscow, 696 p. (in Russian)
16. Extreme Floods in the Amur River Basin: Causes, Forecasts, and Recommendations, 2014: Roshydromet, Moscow, 207 p. (in Russian)
17. Health of the Russian Population: Influence of the Environment in a Changing Climate. Moscow, Nauka, 2014, 428 p. (in Russian)
18. Strategic Resources and Conditions for Sustainable Development of the Russian Federation and its Regions, 2014: IG RAS, Moscow, 166 p. (in Russian)
19. Russian National Report. Meteorology and Atmospheric Sciences. 2007–2010. Ed. by I. I. Mokhov and A. A. Krivolutsky, 2011: MAKS Press, Moscow, 213 p.
20. Gruza G. V., Rankova E. Ya., 2012: Observed and Expected Climate Changes over Russia: Surface Air Temperature. ARIHMI-WDC, Obninsk, 194 p. (in Russian)
21. Perevedentsev Yu. P., Mokhov I. I., Eliseev A. V. et al., 2013: Theory of Atmospheric General Circulation. Kazan', Kazan State Univ., 224 p. (in Russian)
22. Diansky N. A., 2013: Modelling of the circulation of the ocean and study of its response to short-term and long-term atmospheric forcings. Fizmatlit, Moscow, 272 p. (in Russian)
23. Mokhov I. I., 2013: Results of Russian climate studies in 2007–2010. Izvestiya, Atmos. Oceanic Phys., 49(1), 1–15.
24. Alekseev G. V., 2014: Arctic dimension of global warming. Ice and snow, 2(126), 53–68 (in Russian)

25. Sergienko V.I., Lobkovsky L.I., Semiletov I.P. et al., 2012: The degradation of submarine permafrost and the destruction of hydrates on the shelf of east arctic seas as a potential cause of the “Methane Catastrophe”. *Doklady Earth Sci.*, 446(1), 1132–1137.
26. Lobkovsky L.I., Nikiforov S.L., Shakhova N.E. et al., 2013: Mechanisms responsible for degradation of submarine permafrost on the eastern arctic shelf of Russia. *Doklady Earth Sci.*, 449(1), 280–283.
27. Shakhova N., Semiletov I., Leifer I. et al., 2014: Ebullition and storm-induced methane release from the East Siberian Arctic shelf. *Nature Geosci.*, 7(1), 64–70.
28. Anisimov O.A., Zaboikina Yu.G., Kokorev V.A., Yurganov L.N., 2014: Possible causes of methane release from the East Arctic seas shelf. *Ice and Snow*, 2(126), 69–81. (in Russian)
29. Anderson L.G., Bjork G., Jutterstrom S. et al., 2011: East Siberian Sea, an Arctic region of very high biogeochemical activity. *Biogeosci.*, 8(6), 1745–1754.
30. Anisimov O.A., Zhiltsova E.L., 2012: Climate change estimates for the regions of Russia in the 20th century and in the beginning of the 21st century based on the observational data. *Russ. Meteorol. Hydrol.*, 37(6), 421–429.
31. Bulygina O.N., Groisman P.Ya., Razuvaev V.N., Korshunova N.N., 2011: Changes in snow cover characteristics over Northern Eurasia since 1966. *Environ. Res. Lett.*, 6, 045204 doi:10.1088/1748-9326/6/4/045204.
32. Callaghan T.V., Johansson M., Brown R.D. et al., 2011: The changing face of Arctic snow cover: A synthesis of observed and projected changes. *Ambio*, 40, Suppl. 1, 17–31.
33. Callaghan T.V., Johansson M., Brown R.D. et al., 2011: Multiple effects of changes in Arctic snow cover. *Ambio*, 40, Suppl. 1, 32–45.
34. Frolov I.E., Gudkovich Z.M., Karklin V.P., Smolyanitsky V.M., 2011: Regional features of climatic changes of sea ice cover in the XX – beginning of XXI century and their causes. *Ice and snow*, 3(115), 91–104. (in Russian)
35. Golubyatnikov L.L., Kazantsev V.S., 2013: Contribution of tundra lakes in western Siberia to the atmospheric methane budget. *Izvestiya, Atmos. Oceanic Phys.*, 49(4), 395–403.
36. Malkova G.V., Pavlov A.V., Skachkov Yu.B., 2011: Evaluation of stability of frozen strata in contemporary climate change. *Earth’s Cryosphere*, XV(4), 33–36. (in Russian)
37. Konishchev V.N., 2011: Permafrost response on climate warming. *Earth’s Cryosphere*, XV(4), 15–18.
38. Leibman M.O., Kizyakov A.I., Plekhanov A.V., Streletskaia I.D., New permafrost feature-deep crater in Central Yamal (West Siberia, Russia) as a response to local climate fluctuations. *Geography. Environment. Sustainability*, 7(4), 68–80.
39. Meier W.N., Hovelsrud G.K., van Oort B.E.H. et al., 2014: Arctic sea ice in transformation: A review of recent observed changes and impacts on biology and human activity. *Rev. Geophys.*, 51, doi: 10.1002/2013RG000431.
40. Nedashkovsky A.P., 2012: Emission and absorption of CO₂ during the sea ice formation and melting in the high Arctic. *Ice and snow*, 1(117), 75–84. (in Russian)

41. Radionov V.F., Aleksandrov E.I., Bryazgin N.N., Dementiev A.A., 2013: Changes in temperature, precipitation and snow cover in the Arctic Seas region, 1981–2010. *Ice and Snow*, 1(121), 61–68. (in Russian)
42. Semenov E.K., Sokolikchina N.N., Tudrii K. O., 2013: The warm winter in the Russian Arctic and anomalous cold in Europe. *Russ. Meteorol. Hydrol.*, 38(9), 614–621.
43. Smedsrud L.-H., Esau I., Ingvaldsen R.B. et al., 2014: The role of the Barents Sea in the Arctic climate system. *Rev. Geophys.*, 51(3), 415–449.
44. Tilinina N., Gulev S.K., Bromwich D.H., 2014: New view of Arctic cyclone activity from the Arctic system reanalysis. *Geophys. Res. Lett.*, 41(5), 1766–1772.
45. Gruza G.V., Rankova E. Ya., 2011: Estimation of probable contribution of global warming to the genesis of abnormally hot summers in the European part of Russia. *Izvestiya, Atmos. Oceanic Phys.*, 47(6), 661–664.
46. Mokhov I.I., 2011: Specific features of the 2010 summer heat formation in the European territory of Russia in the context of general climate changes and climate anomalies. *Izvestiya, Atmos. Oceanic Phys.*, 47(6), 709–716.
47. Popova V.V., 2014: Summertime warming in the European part of Russia and extreme heat in 2010 as manifestation of large-scale atmospheric circulation trends in the late 20th-early 21st centuries. *Russ. Meteorol. Hydrol.*, 39(3), 159–167.
48. Shmakin A.B., Chernavskaya M.M., Popova V.V., 2013: 2010 great drought at the East European plain: Historical analogies and circulation mechanisms. *Izvestiya, Geogr.*, 6, 59–75. (in Russian)
49. Shukurov K.A., Mokhov I.I., Shukurova L.M., 2014: Estimate for radiative forcing of smoke aerosol from 2010 summer fires based on measurements in the Moscow region. *Izvestiya, Atmos. Oceanic Phys.*, 50(3), 256–265.
50. Tishchenko V.A., Khan V.M., Vil'fand R.M., et al, 2013: Studying the development of atmospheric processes associated with blocking and quasistationary anticyclones in the Atlantic European sector. *Russ. Meteorol. Hydrol.*, 38(7), 444–455.
51. Vinogradova V.V., 2014: Heat waves in the European Russia at the beginning of the 21st century. *Izvestiya, Geogr.*, 1, 47–55. (in Russian)
52. Cherenkova E.A., 2013: Quantitative evaluation of atmospheric drought in federal districts of the European Russia. *Izvestiya, Geogr.*, 38(6), 76–85. (in Russian)
53. Vyazilova N.A., Vyazilova A.E., 2012: On the North Atlantic extreme cyclone activity. *Russ. Meteorol. Hydrol.*, 37 (11–12), 689–695.
54. Zolina O., Simmer C., Belyaev K. et al., 2013: Changes in the duration of European wet and dry spells during the last 60 years. *J. Clim.*, 26(6), 2022–2047.
55. Kurgansky M.V., Chernokulsky A.V., Mokhov I.I., 2013: The tornado over Khanty-Mansiysk: An exception or a symptom? *Russ. Meteorol. Hydrol.*, 38(8), 539–546.
56. Mokhov I.I., Dobryshman E.M., Makarova M.E., 2014: Transformation of tropical cyclones into extratropical: The tendencies of 1970–2012. *Doklady Earth Sci.*, 454(1), 59–63.
57. Anisimov O., Kokorev V., Zhiltsova Y., 2013: Temporal and spatial patterns of modern climatic warming: case study of Northern Eurasia. *Clim. Change*, 118(3–4), 871–883.

-
58. Chernokulsky A. V., Bulygina O. N., Mokhov I. I., 2011: Recent variations of cloudiness over Russia from surface daytime observations. *Environ. Res. Lett.*, 6, 035202.
59. Samukova E. A., Gorbarenko E. V., Erokhina A. E., 2014: Long-term variations of solar radiation in Europe. *Russ. Meteorol. Hydrol.*, 39(8), 514–520.
60. Sarafanov A. A., Falina A. S., Sokov A. V., 2013: Long-term changes in the characteristics and circulation of deep waters in the northern North Atlantic: The role of regional and external factors. *Doklady Earth Sci.*, 450(2), 643–646.
61. Semenov E. K., Platonov V. S., Sokolikhina E. V., 2012: Synoptic aspects of the catastrophic flood formation in the northeast of Australia during extreme La Nina 2010–2011. *Russ. Meteorol. Hydrol.*, 37(2), 90–97.
62. Groisman P. Ya., Bogdanova E. G., Alexeev V. A., Cherry J. E., Bulygina O. N., 2014: Impact of snowfall measurement deficiencies on quantification of precipitation and its trends over Northern Eurasia. *Ice and snow*, 2(126), 29–43. (in Russian)
63. Popova V. V., 2011: The snow storage contribution in major changes of river runoff in the Arctic Ocean drainage basin during the current warming period. *Ice and snow*, 3(115), 69–78. (in Russian)
64. Popova V. V., Polyakova I. A., 2013: Change of stable snow cover destruction dates in northern Eurasia, 1936–2008: impact of global warming and the role of large-scale atmospheric circulation. *Ice and snow*, 2(122), 29–39. (in Russian)
65. Gruza G. V., Rankova E. Ya., 2012: Dynamic normals of surface air temperature. *Russ. Meteorol. Hydrol.*, 37(11–12), 717–727.
66. Akperov M. G., Mokhov I. I., 2013: Estimates of the sensitivity of cyclonic activity in the troposphere of extratropical latitudes to changes in the temperature regime. *Izvestiya, Atmos. Oceanic Phys.*, 49(2), 113–120.
67. Borzenkova A. V., Shmakin A. B., 2013: Modern climate change of heating period in Russia and its relation to atmospheric circulation. *Izvestiya, Geogr.*, 4, 59–69. (in Russian)
68. Bekoryukov V. I., Glazkov V. N., Fedorov V. V., 2011: Analysis of time series of global mean values of thermodynamic and circulation parameters of the atmosphere and concentrations of ozone and water vapor. *Izvestiya, Atmos. Oceanic Phys.*, 47(1), 67–76.
69. Gulev S. K., Latif M., Keenlyside N. et al., 2013: North Atlantic Ocean control on surface heat flux on multidecadal timescales. *Nature*, 499(7459), 464, DOI: 10.1038/nature12268.
70. Panin G. N., Diansky N. A., 2014: On the correlation between oscillations of the Caspian Sea level and the North Atlantic climate. *Izvestiya, Atmos. Oceanic Phys.*, 50(3), 266–277.
71. Perevedentsev Yu. P., Shantalinsky K. M., 2014: Estimation of contemporary observed variations of air temperature and wind speed in the troposphere of the Northern Hemisphere. *Russ. Meteorol. Hydrol.*, 39(10), 650–659.
72. Chernokulsky A. V., Mokhov I. I., 2012: Climatology of total cloudiness in the Arctic: An intercomparison of observations and reanalyses. *Adv. Meteorol.*, 2012, Art. ID542093, doi:10.1155/2012/542093.

73. Chubarova N.E., Nezval E.I., Belikov I.B. et al., 2014: Climatic and environmental characteristics of Moscow megalopolis according to the data of the Moscow State University Meteorological Observatory over 60 years. *Russ. Meteorol. Hydrol.*, 9, 602–613.
74. Khokhlova A.V., Timofeev A.A., 2011: Long-term variations of wind regime in the free atmosphere over the European territory of Russia. *Russ. Meteorol. Hydrol.*, 36(4), 229–238.
75. Romankevich E.A., Vetrov A.A., 2013: Masses of carbon in the Earth's hydrosphere. *Geochem. Intern.*, 51(6), 431–455.
76. Adushkin V.V., Kudryavtsev V.P., 2013: Estimating the global flux of methane into the atmosphere and its seasonal variations. *Izvestiya, Atmos. Oceanic Phys.*, 49(2), 128–136.
77. Ginzburg A.S., Vinogradova A.A., Fedorova E.I., 2011: Some features of seasonal variations in the methane content in the atmosphere over northern Eurasia. *Izvestiya, Atmos. Oceanic Phys.*, 47(1), 45–58.
78. Kononova N.K., Khmelevskaya L.V., 2011: Long-term fluctuations of beginning dates and duration of circulation seasons of extra-tropical latitudes of Northern Hemisphere. *Izvestiya, Geogr.*, 3, 43–62. (in Russian)
79. Kotlyakov V.M., Moskalevskiy M.Y., Vasil'ev L.N., 2011: Changes in the mass balance of the Antarctic ice sheet over 50 years. *Doklady Earth Sci.*, 438(1), 686–689.
80. Krenke A.N., Cherenkova E.A., Chernavskaya M.M., 2012: Stability of snow cover on the territory of Russia in relation to climate change. *Ice and Snow*, 1(117), 29–37.
81. Nigmatulin R.I., 2012: Notes on global climate and ocean currents. *Izvestiya, Atmos. Oceanic Phys.*, 48(1), 30–36.
82. Vyazilova N.A., 2012: Cyclone activity and circulation oscillations in the North Atlantic. *Russ. Meteorol. Hydrol.*, 37(7), 431–437.
83. Vyazilova N.A., Vyazilova A.E., 2014: Storm cyclones in the North Atlantic. *Russ. Meteorol. Hydrol.*, 39(6), 371–377.
84. Sidorenkov N.S., Sumerova K.A., 2012: Temperature fluctuation beats as a reason for the anomalously hot summer of 2010 in the European part of Russia. *Russ. Meteorol. Hydrol.*, 37(6), 411–420.
85. Vetrov A.A., Romankevich E.A., 2011: Primary production and fluxes of organic carbon to the seabed in the Russian Arctic Seas as a response to the recent warming. *Oceanology*, 51(2), 255–266.
86. Vinogradova G.M., Zavalishin N.N., 2011: Anticyclonogenesis of surface pressure field in winter season, blocking, and variability of the Earth angular velocity. *Russ. Meteorol. Hydrol.*, 36(11), 731–736.
87. Zhrebtsov G.A., Kovalenko V.A., 2012: Solar activity effect on weather-climatic characteristics of the troposphere. *Solar-Terrest. Phys.*, 21, 98–106. (in Russian)
88. Byshev V.I., Neiman V.G., Romanov Yu.A., Serykh I.V., 2012: El Nino as a consequence of the global oscillation in the dynamics of the Earth's climatic system. *Doklady Earth Sci.*, 446(1), 1089–1094.

89. Byshev V.I., Neiman V.G., Ponomarev V.I. et al., 2014: The influence of global atmospheric oscillation on formation of climate anomalies in the Russian Far East. *Doklady Earth Sci.*, 458(1), 1116–1120.
90. Privalsky V., Muzylev S., 2013: An experimental stochastic model of the El Niño — Southern Oscillation system at climatic time scales. *Univers. J. Geosci.*, 1(1), 28–36.
91. Mokhov I.I.; Timazhev A. V., 2013: Climatic anomalies in Eurasia from El Niño/La Niña effects. *Doklady Earth Sci.*, 453(1), 1141–1144.
92. Mokhov I. I., Smirnov D. A., Nakonechny P. I. et al., 2012: Relationship between El-Niño/Southern Oscillation and the Indian monsoon. *Izvestiya, Atmos. Oceanic Phys.*, 48(1), 47–56.
93. Smirnov D.A., Mokhov I.I., 2013: Estimation of interaction between climatic processes: Effect of sparse sample of analyzed data series. *Izvestiya, Atmos. Oceanic Phys.*, 49(5), 485–493.
94. Mokhov I. I., Smirnov D. A., Nakonechny P. V., Kozlenko S. S., Seleznev E. P., Kurths J., 2011: Alternating mutual influence of El-Niño/Southern Oscillation and Indian monsoon. *Geophys. Res. Lett.*, doi: 10.1029/2010 GL 045932.
95. Klimenko V. V., 2011: Why is global warming slowing down? *Doklady Earth Sci.*, 440(2), 1419–1422.
96. Mokhov I. I., Smirnov D. A., Karpenko A. A., 2012: Assessments of the relationship of changes of the global surface air temperature with different natural and anthropogenic factors based on observations. *Doklady Earth Sci.*, 443(1), 381–387.
97. Elansky N. F., Lavrova O. V., Mokhov I. I., et al., 2012: Heat island structure over Russian towns based on mobile laboratory observations. *Doklady Earth Sci.*, 443(1), 420–425.
98. Aleksandrov G. G., Belova I. N., Ginzburg A. S., 2014: Anthropogenic heat flows in the capital agglomerations of Russia and China. *Doklady Earth Sci.*, 457(1), 850–854.
99. Ginzburg A. S., Belova I. N., Raspletina N. V., 2011: Anthropogenic heat fluxes in urban agglomerations. *Doklady Earth Sci.*, 439(1), 1006–1009.
100. Mokhov I. I., Semenov A. I., 2014: Nonlinear temperature changes in the atmospheric mesopause region of the atmosphere against the background of global climate changes, 1960–2012. *Doklady Earth Sci.*, 456(2), 741–744.
101. Manney G. L., Santee M. L., Rex M. et al., 2011: Unprecedented Arctic ozone loss in 2011. *Nature*, 478, 469–475.
102. Danilov-Danil'yan V. I., Gel'fan A. N., 2014: The extraordinary flood in the Amur River basin. *Herald of the RAS*, 84(5), 335–343.
103. Vakulenko N. V., Kotlyakov V. M., Sonechkin D. M., 2014: Increase in the global climate variability from about 400 ka BP until present. *Doklady Earth Sci.*, 456(2), 745–748.
104. Osipov E. Y., Khodzher T. V., Golobokova L. P. et al., 2014: High-resolution 900 year volcanic and climatic record from the Vostok area, East Antarctica. *Cryosphere*, 8(3), 843–851.
105. Bazin L., Landais A., Lemieux-Dudon B. et al., 2013: An optimized multi-proxy, multi-site Antarctic ice and gas orbital chronology (AICC2012): 120–800 ka. *Clim. Past*, 9(4), 1715–1731.

106. Bazin L., Landais A., Lemieux-Dudon B. et al., 2013: An optimized multi-proxy, multi-site Antarctic ice and gas orbital chronology (AICC2012): 120–800 ka. *Clim. Past.*, 9(4), 1715–1731.
107. Bezverkhny V.A., 2014: Correlation between 41000-year rhythms in variations in the inclination of earth, violent volcanic eruptions, and temperature of deep ocean waters. *Izvestiya, Atmos. Oceanic Phys.*, 50(6), 657–659.
108. Bezverkhny V.A., 2013: Manifestation of characteristic periods of oscillations of the Earth's orbital parameters in the paleoclimatic data. *Doklady Earth Sci.*, 451(1), 779–783.
109. Solomina O.N., 2014: Holocene glacier variations and their potential orbital, solar, volcanic and anthropogenic forcings. *Ice and snow*, 3(127), 81–90. (in Russian)
110. Dahl-Jensen D., Albert M.R., Aldahan A. et al., 2013: Eemian interglacial reconstructed from a Greenland folded ice core. *Nature*, 493(7433), 489–494.
111. Ekaykin A.A., Kozachek A.V., Lipenkov V. Ya. et al., 2014: Multiple climate shifts in the Southern Hemisphere over the past three centuries based on central Antarctic snow pits and core studies. *Annals of Glaciology*, 55(66), 259–266.
112. Leichenkov G.L., 2014: Environmental and climate changes in Antarctica in the geological past. *Ice and Snow*, 4(128), 107–116. (in Russian)
113. Levitan M.A., Leichenkov G.L., 2014: Genozoic glaciation of Antarctica and sedimentation in the Southern Ocean. *Lithology and Mineral Resources*, 49(2), 117–137.
114. Lipenkov V.Y., Raynaud D., Loutre M.F., Duval P., 2011: On the potential of coupling air content and O-2/N-2 from trapped air for establishing an ice core chronology tuned on local insolation. *Quatern. Sci. Rev.*, 30(23–24), 3280–3289.
115. Parrenin F., Petit J.-R., Masson-Delmotte V. et al., 2012: Volcanic synchronisation between the EPICA Dome C and Vostok ice cores (Antarctica) 0–145 kyr BP. *Clim. Past*, 8(3), 1031–1045.
116. Vandenberghe J., Renssen H., Roche D.M. et al., 2012: Eurasian permafrost instability constrained by reduced sea-ice cover. *Quatern. Sci. Rev.*, 34, 16–23.
117. Vandenberghe J., French H.M., Gorbunov A. et al., 2014: The Last Permafrost Maximum (LPM) map of the Northern Hemisphere: permafrost extent and mean annual air temperatures, 25–17ka BP. *BOREAS*, 43(3), 652–666.
118. Velichko A.A., Borisova O.K., 2011: Paleoanalogues of global warming in the 21st century. *Doklady Earth Sci.*, 438(1), 681–685.
119. Fischer H., Severinghaus J., Brook E. et al., 2013: Where to find 1.5 million yr old ice for the IPICS “Oldest-Ice” ice core. *Clim. Past*, 9(6), 2489–2505.
120. Eby M., Weaver A.J., Alexander K. et al., 2013: Historical and idealized climate model experiments: an EMIC intercomparison. *Clim. Past*, 9(3), 1111–1140.
121. Alexandrov G.A., 2014: Explaining the seasonal cycle of the globally averaged CO₂ with a carbon-cycle model. *Earth System Dyn.*, 5(2), 345–354.
122. Eliseev A.V., Demchenko P.F., Arzhanov M.M., Mokhov I.I., 2014: Transient hysteresis of near-surface permafrost response to external forcing. *Clim. Dyn.*, 42(5–6), 1203–1215.

-
123. Ghil M., Yiou P., Hallegatte S. et al., 2011: Extreme events: dynamics, statistics and prediction. *Nonlin. Processes Geophys.*, 18, 295–350.
124. Ginzburg A. S., 2011: Regional air temperature maxima and the possibility of their simple energy-balance estimates. *Izvestiya, Atmos. Oceanic Phys.*, 47(6), 665–671.
125. Golitsyn G. S., 2012: Statistics and Dynamics of Natural Processes and Phenomena: Methods, Tools and Results. KRASAND, Moscow, 400 p. (in Russian)
126. Kislov A. V., Konstantinov P. I., 2011: Detailed spatial modeling of temperature in Moscow. *Russ. Meteorol. Hydrol.*, 36(5), 300–306.
127. Shkolnik I. M., Efimov S. V., 2013: Cyclonic activity in high latitudes as simulated by a regional atmospheric climate model: added value and uncertainties. *Environ. Res. Lett.*, 8(4), AN045007, DOI: 10.1088/1748–9326/8/4/045007.
128. Volodin E. M., 2013: The mechanism of multidecadal variability in the Arctic and North Atlantic in climate model INMCM4. *Environ. Res. Lett.*, 8(3), A.N. 035038, DOI: 10.1088/1748–9326/8/3/035038.
129. Ibraev R. A., Khabeev R. N., Ushakov K. V., 2012: Eddy-resolving 1/10o model of the World Ocean. *Izvestiya, Atmos. Oceanic Phys.*, 48(1), 37–46.
130. Melton J. R., Wania R., Hodson E. L. et al., 2013: Present state of global wetland extent and wetland methane modelling: conclusions from a model intercomparison project (WETCHIMP). *Biogeosci.*, 10(2), 753–788.
131. Wania R., Melton J. R., Hodson E. L. et al., 2013: Present state of global wetland extent and wetland methane modelling: Methodology of a model intercomparison project (WETCHIMP). *Geosci. Model Devel.*, 6(3), 617–641.
132. Golubyatnikov L. L., Mokhov I. I., Eliseev A. V., 2013: Nitrogen cycle in the Earth climatic system and its modeling. *Izvestiya, Atmos. Oceanic Phys.*, 49(3), 229–243.
133. Nicolsky D. J., Romanovsky V. E., Romanovskii N. N. et al., 2012: Modeling sub-sea permafrost in the East Siberian Arctic shelf: The Laptev Sea region. *J. Geophys. Res.*, 117, 429–436.
134. Stepanenko V. M., Machul'skaya E. E., Glagolev M. V. et al, 2011: Numerical modeling of methane emissions from lakes in the permafrost zone. *Izvestiya, Atmos. Oceanic Phys.*, 47(2), 252–264.
135. Eliseev A. V., Mokhov I. I., Chernokulsky A. V., 2014: Influence of ground and peat fires on CO₂ emissions into the atmosphere. *Doklady Earth Sci.*, 459(2), 1565–1569.
136. Yurova A. Yu., Volodin E. M., 2011: Coupled simulation of climate and vegetation dynamics. *Izvestiya, Atmos. Oceanic Phys.*, 47(5), 531–539.
137. Ananicheva M. D., Krenke A. N., Semenov A. E., Turkov D. V., 2011: Dependence of snow accumulation in Antarctica on the sea ice area. *Ice and Snow*, 4(116), 47–56. (in Russian)
138. Baidin A. V., Meleshko V. P., 2014: Response of the atmosphere at high and middle latitudes to the reduction of sea ice area and the rise of sea surface temperature. *Russ. Meteorol. Hydrol.*, 6, 361–370.
139. Dzyuba A. V., Eliseev A. V., Mokhov I. I., 2012: Estimates of changes in the rate of methane sink from the atmosphere under climate warming. *Izvestiya, Atmos. Oceanic Phys.*, 48(3), 332–342.

140. Ba J., Keenlyside N. S., Latif M. et al., 2014: A multi-model comparison of Atlantic multidecadal variability. *Cli. Dyn.*, 43(9–10), 2333–2348.
141. Arzhanov M. M., Mokhov I. I., 2014: Model assessments of organic carbon amounts released from long-term permafrost under scenarios of global warming in the 21st century. *Doklady Earth Sci.*, 455(1), 346–349.
142. Arzhanov M. M., Mokhov I. I., 2013: Temperature trends in the permafrost of the Northern Hemisphere: Comparison of model simulations with observations. *Doklady Earth Sci.*, 449(1), 319–323.
143. Denisov S. N., Arzhanov M. M., Eliseev A. V. et al., 2011: Sensitivity of methane emissions from West Siberian wetlands to climate changes: Multimodel estimates. *Atmos. Oceanic Optics*, 24(4), 319–322.
144. Eliseev A. V., Mokhov I. I., Chernokulsky A. V., 2014: An ensemble approach to simulate CO₂ emissions from natural fires. *Biogeosciences*, 11(12), 3205–3223.
145. Eliseev A. V., Demchenko P. F., Arzhanov M. M. et al., 2012: Hysteresis of the surface permafrost area dependence on the global temperature. *Doklady Earth Sci.*, 444(2), 725–728.
146. Hoffman F. M., Randerson J. T., Arora V. K. et al., 2014: Causes and implications of persistent atmospheric carbon dioxide biases in Earth System Models. *J. Geophys. Res.* — *Biogeosci.*, 119(2), 141–162.
147. Gorchakova I. A., Mokhov I. I., 2012: The radiative and thermal effects of smoke aerosol over the region of Moscow during the summer fires of 2010. *Izvestiya, Atmos. Oceanic Phys.*, 48(5), 496–503.
148. Gusev A. V., Diansky N. A., 2014: Numerical simulation of the world ocean circulation and its climatic variability for 1948–2007 using the INMOM. *Izvestiya, Atmos. Oceanic Phys.*, 50(1), 1–12.
149. Iakovlev N. G., 2012: On the simulation of temperature and salinity fields in the Arctic Ocean. *Izvestiya, Atmos. Oceanic Phys.*, 48(3), 86–101.
150. Jin L., Schneider B., Park W. et al., 2014: The spatial-temporal patterns of Asian summer monsoon precipitation in response to Holocene insolation change: a model-data synthesis. *Quatern. Sci. Rev.*, 85, 47–62.
151. Johnson M., Proshutinsky A., Aksenov Y. et al., 2012: Evaluation of Arctic sea ice thickness simulated by Arctic Ocean Model Intercomparison Project models. *J. Geophys. Res.* — *Oceans*, 117, AN C00D13, DOI: 10.1029/2011JC007257.
152. Karol I. L., Kiselev A. A., Frol'kis V. A., 2011: Indices of the factors that form climate changes of different scales. *Izvestiya, Atmos. Oceanic Phys.*, 47(4), 415–429.
153. Karol I. L., Kiselev A. A., Frol'kis V. A., 2012: Radiation indices of climate-forming factors and their estimates under anthropogenic climate changes. *Russ. Meteorol. Hydrol.*, 5, 298–306.
154. Malakhova V. V., Golubeva E. N., 2014: Modeling of the dynamics subsea permafrost in the East Siberian Arctic shelf under the past and the future climate changes. *Proc. SPIE*, 9292, A.N. 9292D, doi:10.1117/12.2075137.
155. Neu U., Akperov M. G., Benestad R. et al., 2013: IMILAST — a community effort to intercompare cyclone detection and tracking algorithms: quantifying method-related uncertainties. *Bull. Amer. Meteorol. Soc.*, 94(4), 529–547.

156. Semenov S.M., Popov I.O., 2011: Comparative estimates of influence of changes in carbon dioxide, methane, nitrous oxide, and water vapor concentrations on radiation-equilibrium temperature of Earth's surface. *Russ. Meteorol. Hydrol.*, 36(2), 124–129.
157. Tarko A.M., Usatyuk V.V., 2013: Simulation of the global biogeochemical carbon cycle with account for its seasonal dynamics and analysis of variations in atmospheric CO₂ concentrations. *Doklady Earth Sci.*, 448(2), 258–261.
158. Tolstykh M.A., Diansky N.A., Gusev A.V. et al., 2014: Simulation of seasonal anomalies of atmospheric circulation using coupled atmosphere-ocean model. *Izvestiya, Atmos. Oceanic Phys.*, 50(2), 111–121.
159. Volodin E.M., 2013: The mechanism of multidecadal variability in the Arctic and North Atlantic in climate model INMCM4. *Environ. Res. Lett.*, 8(3), A.N. 035038, doi:10.1088/1748–9326/8/3/035038.
160. Volodin E.M., 2014: Possible reasons for low climate-model sensitivity to increased carbon dioxide concentrations. *Izvestiya, Atmos. Oceanic Phys.*, 50(4), 350–355.
161. Dymnikov V.P., Lykosov V.N., Volodin E.M., 2012: Modeling climate and its changes: Current problems. *Herald of the RAS*, 82(2), 111–119.
162. Akperov M., Mokhov I.I., Rinke A., Dethloff K., Matthes H., 2014: Cyclones and their possible changes in the Arctic by the end of the twenty first century from regional climate model simulations. *Theor. Appl. Climatol.*, doi: 10.1007/s00704–014–1272–2.
163. Arpe K., Leroy S.A.G., Wetterhall F. et al., 2014: Prediction of the Caspian Sea level using ECMWF seasonal forecasts and reanalysis. *Theor. Appl. Climatol.*, 117, 41–60.
164. Arzhanov M.M., Eliseev A.V., Mokhov I.I., 2013: Impact of climate changes over the extratropical land on permafrost dynamics under RCP scenarios in the 21st century as simulated by the IAP RAS climate model. *Russ. Meteorol. Hydrol.*, 38(7), 456–464.
165. Arzhanov M.M., Eliseev A.V., Mokhov I.I., 2012: A global climate model based, Bayesian climate projection for northern extra-tropical land areas. *Glob. Planet. Change*, 86–87, 57–65.
166. Bardin M. Yu., 2011: Scenario forecasts of air temperature variations for the regions of the Russian Federation up to 2030 using the empirical stochastic climate models. *Russ. Meteorol. Hydrol.*, 36(4), 217–228.
167. Eliseev A.V., Mokhov I.I., 2011: Uncertainty of climate response to natural and anthropogenic forcings due to different land use scenarios. *Adv. Atmos. Sci.*, 28(5), 1215–1232.
168. Cherenkova E.A., Zolotokrylin A.N., 2012: Model estimates of moistening conditions on the Russian plains by the middle of the 21st century. *Russ. Meteorol. Hydrol.*, 37, 704–710.
169. Denisov S.N., Arzhanov M.M., Eliseev A.V. et al., 2011: Assessment of the response of subaqueous methane hydrate deposits to possible climate change in the twenty-first century. *Doklady Earth Sci.*, 441(2), 1706–1709.

170. Denisov S.N., Arzhanov M.V., Eliseev A.V., et al, 2013: Assessments of stability of methane hydrates in the Lake Baikal system. *Doklady Earth Sci.*, 449(1), 346–348.
171. Denisov S.N., Eliseev A.V., Mokhov I.I., 2013: Climate change in IAP RAS global model taking account of interaction with methane cycle under anthropogenic scenarios of RCP family. *Russ. Meteorol. Hydrol.*, 11, 741–749.
172. Eliseev A.V., 2011: Estimation of changes in characteristics of the climate and carbon cycle in the 21st century accounting for the uncertainty of terrestrial biota parameter values. *Izvestiya, Atmos. Oceanic Phys.*, 47(2), 131–153.
173. Eliseev A.V., Mokhov I.I., 2011: Effect of including land-use driven radiative forcing of the surface albedo of land on climate response in the 16th-21st centuries. *Izvestiya, Atmos. Oceanic Phys.*, 47(1), 15–30.
174. Eliseev A.V., Mokhov I.I., Muryshev K.E., 2011: Estimates of climate changes in the 20th-21st centuries based on the version of the IAP RAS climate model including the model of general ocean circulation. *Russ. Meteorol. Hydrol.*, 36(2), 73–81.
175. Khon V.C., Mokhov I.I., Pogarsky F.A., 2013: Estimating changes of wind-wave activity in the Arctic Ocean in the 21st century using the regional climate model. *Doklady Earth Sci.*, 452(2), 1027–1029.
176. Khon V.C., Mokhov I.I., Pogarsky F.A., Babanin A., Dethloff K., Rinke A., Matthes H., 2014: Wave heights in the 21st century Arctic Ocean simulated with a regional climate model. *Geophys. Res. Lett.*, 41(8), 2956–2961.
177. Khon V.C., Park W., Latif M., Mokhov I.I., Schneider B., 2012: Tropical circulation and hydrological cycle response to orbital forcing. *Geophys. Res. Lett.*, 39(15), L15708.
178. Kislov A.V., Panin A.V., Toropov P.A., 2014: Present-day variations and paleodynamics of the Caspian Sea level as a standard for climate modeling data verification. *Russ. Meteorol. Hydrol.*, 39(5), 328–334.
179. Khon V.C., Mokhov I.I., 2012: The hydrological regime of large river basins in Northern Eurasia in the XX–XXI centuries. *Water Resources*, 39(1), 1–10.
180. Kuzin V.I., Platov G.A., Golubeva E.N., et al, 2012: Certain results of numerical simulation of processes in the Arctic Ocean. *Izvestiya, Atmos. Oceanic Phys.*, 48(1), 102–119.
181. Lehmann J., Coumou D., Frieler K., Eliseev A.V., Levermann A., 2014: Future changes in extratropical storm tracks and baroclinicity under climate change. *Environ. Res. Lett.*, 9(8), 084002.
182. Mareev E.A., Volodin E.M., 2014: Variation of the global electric circuit and ionospheric potential in a general circulation model. *Geophys. Res. Lett.*, 41(24), 9009–9016.
183. Mokhov I.I., Semenov V.A., Khon V.C., Pogarsky F.A., 2013: Change of sea ice extent in the Arctic and the associated climatic effects: detection and simulation. *Ice and Snow*, 2(122), 53–62. (in Russian)
184. Mokhov I.I., Timazhev A.V., Lupo A.R., 2014: Changes in atmospheric blocking characteristics within Euro-Atlantic region and Northern Hemisphere as a whole in

the 21st century from model simulations using RCP anthropogenic scenarios. *Glob. Planet. Change*, 122, 265–270.

185. Morozova P.A., 2014: Influence of the Scandinavian ice sheet on the climatic conditions of the East European Plain evidenced from the numerical simulation project PMIP II. *Ice and Snow*, 1(125), 113–124. (in Russian)

186. Zickfeld K., Eby M., Weaver A.J. et al., 2013: Long-term climate change commitment and reversibility: An EMIC intercomparison. *J. Clim.*, 26(16), 5782–5809.

187. Moshonkin S.N., Alekseev G.V., Diansky N.A., et al, 2011: Reproduction of the large-scale state of water and sea ice in the arctic ocean in 1948–2002: Part I. Numerical model. *Izvestiya, Atmos. Oceanic Phys.*, 47(5), 628–641.

188. Nadezhina E.D., Mol'kentin E. K., Kiselev A.A., et al, 2011: Investigation of parameterization effect on the methane flux estimation from the regional climate model of the main geophysical observatory for the territory of Russia. *Russ. Meteorol. Hydrol.*, 6, 371–382.

189. Rybak O.O., Fürst J.J., Huybrechts P., 2013: Mathematical modeling of ice flow in the north-western Greenland and interpretation of deep drilling data at the NEEM camp. *Ice and Snow*, 1(121), 16–15. (in Russian)

190. Rybak O.O., Huybrechts P., 2012: Mathematical modeling of ice flow in Queen Maud Land, Antarctica, and its application to the Late Quaternary climate paleoreconstructions. *Ice and Snow*, 3(119), 5–16. (in Russian)

191. Rybak O.O., Huybrechts P., 2014: The Greenland ice sheet at the peak of warming during the previous Interglacial. *Ice and Snow*, 2(126), 91–101. (in Russian)

192. Semenov V.A., 2011: Climate-related changes in hazardous and adverse hydrological events in the Russian rivers. *Russ. Meteorol. Hydrol.*, 36(2), 124–129.

193. Semenov V.A., 2014: Role of sea ice in wintertime Arctic temperature anomalies. *Izvestiya, Atmos. Oceanic Phys.*, 50(4), 343–349.

194. Semenov V.A., Mokhov I.I., Latif M., 2012: Influence of the ocean surface temperature and sea ice concentration on regional climate changes in Eurasia in recent decades. *Izvestiya, Atmos. Oceanic Phys.*, 48(4), 355–372.

195. Semenov V.A., Shelekhova E.A., Mokhov I.I. et al. Influence of the Atlantic Multidecadal Oscillation on settling anomalous climate regimes in Northern Eurasia based on model simulation. *Doklady Earth Sci.*, 459(2), 1619–1622.

196. Overland J.E., Wang M.Y., Bond N.A. et al., 2011: Considerations in the selection of global climate models for regional climate projections: The Arctic as a case study. *J. Clim.*, 24(6), 1583–1597.

197. Semenov V.A., Mokhov I.I., Polonsky A.B. Modeling of impact of natural long-period variability in the North Atlantic upon formation of climate anomalies. *Marine Hydrophysical J.*, 4, 14–27. (in Russian)

198. Mokhov I.I., 2014: Hydrological anomalies and tendencies of change in the basin of the Amur River under global warming. *Doklady Earth Sci.*, 455(2), 459–462.

199. Mokhov I.I., Akperov M.G., Prokofyeva M.A. et al., 2013: Blockings in the Northern hemisphere and Euro-Atlantic region: Estimates of changes from reanalysis data and model simulations. *Doklady Earth Sci.*, 449(2), 430–433.

200. Mokhov I. I.; Eliseev A. V., 2012: Modeling of global climate variations in the 20th-23rd centuries with new RCP scenarios of anthropogenic forcing. *Doklady Earth Sci.*, 443(2), 532–536.
201. Sherstyukov B. G., Sherstyukov A. B., 2014: Assessment of increase in forest fire risk in Russia till the late 21st century based on scenario experiments with fifth-generation climate models. *Russ. Meteorol. Hydrol.*, 39(5), 292–301.
202. Shkolnik I. M., Meleshko V. P., Efimov S. V., Stafeeva E. N., 2012: Changes in climate extremes on the territory of Siberia by the middle of the 21st century: An ensemble forecast based on the MGO regional climate model. *Russ. Meteorol. Hydrol.*, 2, 71–84.
203. Shkolnik I. M., Nadyozhina E. D., Pavlova T. V. et al., 2012: Simulation of the regional features of the seasonal thawing layer in the Siberian permafrost zone. *Earth's Cryosphere*, *Russ. Meteorol. Hydrol.*, XVI(2), 52–59. (in Russian)
204. Smyshlyayev S. P., Mareev E. A., Galin V. Y., Blakitnaya P. A., 2013: Simulating indirect effects that thunderstorm activity has on atmospheric temperature. *Izvestiya, Atmos. Oceanic Phys.*, 49(5), 504–518.
205. Sporyshev P. V., Kattsov V. M., Matyugin V. A., 2012: A correspondence between the model ensemble simulations and observations of temperature changes on the territory of Russia. *Russ. Meteorol. Hydrol.*, 37(1), 1–11.
206. Stroeve J. C., Kattsov V., Barrett A. et al., 2012: Trends in Arctic sea ice extent from CMIP5, CMIP3 and observations. *Geophys. Res. Lett.*, 39, L16502, doi:10.1029/2012GL052676.
207. Ulbrich U., Leckebusch G. C., Grieger J. et al., 2013: Are greenhouse gas signals of Northern Hemisphere winter extra-tropical cyclone activity dependent on the identification and tracking algorithm? *Meteorol. Z.*, 22(1), 61–68.
208. Volodin E. M., Diansky N. A., Gusev A. V., 2013: Simulation and prediction of climate changes in the 19th to 21st centuries with the Earth's climate system model IN-MCM4. *Izvestiya, Atmos. Oceanic Phys.*, 49(4), 347–366.
209. Zubov V., Rozanov E.; Egorova T. et al., 2013: Role of external factors in the evolution of the ozone layer and stratospheric circulation in 21st century. *Atmos. Chem. Phys.*, 13(9), 4697–4706.
210. Zubov V. A., Rozanov E. V., Rozanova I. V., et al, 2011: Simulation of changes in global ozone and atmospheric dynamics in the 21st century with the chemistry-climate model SOCOL. *Izvestiya, Atmos. Oceanic Phys.*, 47(3), 301–312.
211. Anisimov O. A., Zhiltsova E. L., Reneva S. A., 2011: Estimation of critical levels of climate change influence on the natural terrestrial ecosystems on the territory of Russia. *Russ. Meteorol. Hydrol.*, 36(11), 723–730.
212. Mokhov I. I., Malyshkin A. V., 2011: Analytical estimate of the critical global-warming level for the Antarctic ice sheet mass gain-to-loss transition. *Doklady Earth Sci.*, 436(1), 155–158.
213. Vonk J. E. Sanchez-Garcia L., van Dongen B. E. et al., 2012: Activation of old carbon by erosion of coastal and subsea permafrost in Arctic Siberia. *Nature*, 489(7414), 137–140.

214. Grabar V.A., Gityarsky M.L., Dmitrieva T.M. et al., 2011: Assessment of greenhouse gases emissions from civil aviation in Russia. *Russ. Meteorol. Hydrol.*, 36(1), 18–24.
215. Arzhanov M.M., Eliseev A.V., Klimenko V.V., Mokhov I.I., Tereshin A.G., 2012: Estimating climate changes in the northern hemisphere in the 21st century under alternative scenarios of anthropogenic forcing. *Izvestiya, Atmos. Oceanic Phys.*, 48(6), 573–584.
216. Danilov A.I., Alekseev G.V., Klepikov A.V., 2014: The consequences of climate change for maritime activity in the Arctic. *Ice and snow*, 3(127), 91–99. (in Russian)
217. Kattsov V.M., Porfiriyev B.N., 2011: Assessment of Macroeconomic Consequences of Climate Change. *Roshydromet, Moscow*, 251 p. (in Russian)
218. Kattsov V.M., Porfiriyev B.N., 2012: Climate change in the Arctic: Consequences for the environment and economy. *Arctic: Ecology and Economy*, 2(6), 66–79. (in Russian)
219. Costs and Benefits of Low-Carbon Economy and Transformation of Society in Russia. Perspectives Before and After 2050, 2014: Moscow. CENEF. 208 pp.
220. Klimenko V.V., 2012: Influence of climatic and geographical conditions on the level of energy consumption. *Doklady Earth Sci.*, 443(1), 392–395.
221. Klimenko V.V., Tereshin A.G., 2013: Unconventional gas and transformation of the global carbon balance. *Doklady Earth Sci.*, 453(1), 1113–1116.
222. Khlebnikova E.I., Sall' I.A., Shkol'nik I.M., 2012: Regional climate changes as the factors of impact on the objects of construction and infrastructure. *Russ. Meteorol. Hydrol.*, 37(11–12), 735–745.
223. Zamolodchikov D.G., Grabovsky V.I., Kraev G.N., 2011: A twenty year retrospective on the forest carbon dynamics in Russia. *Contemp. Probl. Ecol.*, 4(7), 706–715.
224. Zamolodchikov D.G., Grabovsky V.I., Korovin G.N. et al., 2013: Carbon budget of managed forests in the Russian Federation in 1990–2050: Post-evaluation and forecasting. *Russ. Meteorol. Hydrol.*, 10, 701–714.
225. Uvarova N.E., Kuzovkin V.V., Paramonov S.G., Gityarsky M.L., 2014: The improvement of greenhouse gas inventory as a tool for reduction emission uncertainties for operations with oil in the Russian Federation. *Clim. Change*, 124, 535–544.
226. Izrael Yu.A., Volodin E.M., Kostrykin S.V. et al., 2014: The ability of stratospheric climate engineering in stabilizing global mean temperatures and an assessment of possible side effects. *Atmos. Sci. Lett.*, 15(2), 140–148.
227. Volodin E.M., Kostrykin S.V., Ryaboshapko A.G., 2011: Simulation of climate change induced by injection of sulfur compounds into the stratosphere. *Izvestiya, Atmos. Oceanic Phys.*, 47(4), 430–438.
228. Izrael Yu.A., Volodin E.M., Kostrykin S.V. et al., 2013: Possibility of geoengineering stabilization of global temperature in the 21st century using the stratospheric aerosol and estimation of potential negative effects. *Russ. Meteorol. Hydrol.*, 38(6), 371–381.
229. Meleshko V.P., Kattsov V.M., Karol I.L., 2011: An answer to the paper of A.G. Ryaboshapko “On the taboo on researching in the field of global climate geoengineering”. *Russ. Meteorol. Hydrol.*, 8, 566–568.

230. Karol' I. L., Kiselev A. A., Genikhovich E. L. et al., 2013: Reduction of short-lived atmospheric pollutant emissions as an alternative strategy for climate-change moderation. *Izvestiya, Atmos. Oceanic Phys.*, 49(5), 461–478.

231. Romanovskaya A. A., Korotkov V. N., Smirnov N. S. et al., 2014: Land use contribution to the anthropogenic emission of greenhouse gases in Russia in 2000–2011. *Russ. Meteorol. Hydrol.*, 39(3), 137–145.

232. Shvidenko A., Schepaschenko D., Vaganov E. A. et al., 2011: Impacts of wildfire in Russia between 1998–2010 on ecosystems and the global carbon budget. *Doklady Earth Sci.*, 441(2), 1678–1682.

233. Zamolodchikov D. G., Grabovsky V. I., Shulyak P. P., Chestnykh O. V., 2013: The impacts of fires and clear-cuts on the carbon balance of Russian forests. *Contemp. Probl. Ecol.*, 6(7), 714–726.

Clouds and Precipitation

*N. A. Bezrukova*¹, *A. V. Chernokulsky*²

¹ Central Aerological Observatory

bezrukova@cao-rhms.ru

² A. M. Obukhov Institute of Atmospheric Physics RAS

a.chernokulsky@ifaran.ru

1. Cloud physics

1.1. Observations and investigation of different cloud types and precipitation characteristics

Clouds are an important element of the Earth's climate system; they take part in the hydrological cycle of the planet and influence its radiation balance. However, the description of cloud processes in up-to-date weather and climate models is still no well-developed. The response of cloud characteristics to changes in the characteristics of atmospheric dynamics and thermodynamics varies among different models. Therefore, clouds are a source of the greatest climate models' uncertainty in estimating the response to external forcing. Moreover, observational data on macro- and microscale cloud characteristics varies considerably. In this connection, solving the general problems of cloud and precipitation physics and analyzing the generalized results of cloud and precipitation observations is still given much attention.

Considerable work to evaluate all known systematic bias in precipitation measurements throughout Russia has been done, and a new, corrected, quasi-uniform precipitation time series for several hundred Russian weather stations is presented in [1]. The measured and corrected mean annual precipitation values, on average, differ by 15–20%, with the largest differences (of up to 100% at windy sites) observed in winter. It is shown that measured mean annual precipitation corrections for practically the whole of Russia are gradually decreasing due to such factors as climate warming during transitional seasons, slower winter wind speeds a decrease of winter wind speeds in the Arctic, and the 1966 jump in observed precipitation values caused by introducing corrections for moisturizing. Time non-uniformity of corrections mainly affects the evaluation of winter precipitation trends. In particular, the precipitation enhancement trend throughout most of Russia (based on the initial data) is absent from the corrected data; moreover, in the arctic regions of Asia, a statistically significant precipitation decrease is observed. The influence of wind on the amount of precipitation measured with standard rain gages is also analyzed in [2].

Papers [3, 4] analyze cloud changes (cloud amount and type) for Russia using ground-based observations, with special emphasis on the last decades. The total cloud amount, especially during transitional seasons, and the frequency of high-level and vertically developed clouds were found to increase. The patterns of the total cloud cover and low-level clouds in different regions of Russia, as well as their changes are discussed in [5–11]. Based on the analysis of these cloud features, an applied climatic zoning of Siberia is fulfilled in [12, 13], with uniform cloud regions distinguished and local cloud models of the atmosphere developed.

Papers [14, 15] includes a detailed comparative analysis of the current databases on clouds: satellite- and ground-based observations and re-analysis data (on the whole, 16 databases are used) for the polar regions of the Northern Hemisphere (north of 60°N). It is shown that cloud observations agree better in summer, and over the ocean, than in winter, and over land. This is basically due to differences in cloud detection algorithms, which are more prominent above snow and ice surfaces (throughout the year) and over regions with strong surface temperature inversions (in winter). On average, based on observations, total cloud fraction over the whole Arctic is 0.70 ± 0.03 ; it is larger (0.74 ± 0.04) over the ocean and less (0.67 ± 0.03) over land. The annual variation is marked by maximal cloud fraction in the fall and minimal in spring. It is pointed out that generally up-to-date reanalyses fail to adequately reproduce the Arctic total cloud cover, either its spatial distribution or within-year dynamics.

The global climatology of a cloud overlap parameter, based on satellite data, is assessed in [16]. It is shown that the global cloud cover tends to overlap randomly. Maximum cloud overlap is associated with small values of cloud fraction, and occurs in subtropical highs over the ocean and in subtropical and polar deserts over land, while random cloud overlap occurs in regions with large values of cloud fraction (e.g. ITCZ and mid-latitude storm tracks). It is speculated that over the vast regions of the Southern Ocean (around 60S) an assumption of minimum overlap of cloud layers should be used due to the strong baroclinic instability and high values of wind shear.

The influence of various factors — local (terrain and underlying surface properties), large-scale (variability of the centers of action of the atmosphere and quasi-periodic atmospheric processes), and external, relative to the climate system (solar and geomagnetic activity) — on the characteristics of clouds and precipitation is analyzed and discussed in [17–25].

A possible mechanism of the influence of cosmic rays on the formation of neutral water drops and ice crystals in the Earth's atmosphere is suggested in paper [19]. This mechanism is based on a small-percentage change in atmospheric transparency that can be due to cosmic rays penetrating to the atmosphere, which causes the vertical temperature distribution to change and influences water drop and active condensation nuclei accretion, and ice crystal formation.

A 2–3-fold increase of the probability of anomalously intense winter and summer precipitation in Western Siberia conditioned by anomalous thermal currents in the Arctic and Atlantic (i. e., in a positive phase of the Atlantic multi-decadal oscillation) has been revealed based on numerical experiments in [25].

The influence of the Siberian High on the characteristics of winter cloud cover (cloud fraction and type) has been evaluated based on ground-based observations on the Russian territory [17]. A long-term relation between cloud cover and the Siberian High has been established. It is shown that a 1 hPa enhancement of the Siberian High leads, on average, to one additional cloudless day in the south of Siberia, which is primarily related with a decrease of stratiform clouds and rainclouds. A decrease in winter Siberian cloud cover during the last years, which has also been noted in [7, 8], can be explained by the observed enhancement of the Siberian High.

Based on a 25-year series of observations in different parts of Nizhniy Novgorod and Kirov Regions, cases of freezing precipitation and various glaze-and-rime phenomena hazardous to communication lines and transportation have been investigated, as described in [26]. Based on the obtained data, some physical-statistical traffic-climate models are proposed. These models are employed by meteorologists for the needs of road maintenance services.

As a result of complex data analysis, a permanent presence of amorphous-phase liquid water (referred to as ‘A-water’) in definitely ice-containing clouds has been suggested in [27]. The author describes this water phase as possessing physical properties largely different from those of common supercooled water. Additionally, it was concluded that in cold clouds, which are generally thought of as purely liquid-water ones, a fine, and thus previously undetected ice fraction coexists with common supercooled water. The author believes the new results and conclusions can radically change the conventional notion of the optical, radiation, and other properties of ice-containing clouds as a physical disperse medium. As a consequence, conventional knowledge of liquid polymorphous water should broaden, thus serving the needs of both cold cloud physics and water physical chemistry.

1.2. Convection, convective cloud characteristics and cloud water content

Atmospheric convection and convective fluxes resulting from ordered vertical air movement are processes associated with the whole class of hazardous weather phenomena. Therefore, investigation of convective clouds as the main visual indicator of convection is conventionally given much attention. Considering the vastness of the Russian territory, which explains the local peculiarities

of convection processes, convection as a mesoscale phenomenon is usually studied on a regional scale. The results obtained, which are reflective of the local features of convection, are further used in modeling and predicting regional-scale hazardous phenomena. They serve to develop special forecasts for all branches of economy, but basically for aviation and transport in general, as well as for the needs of an energy sector.

Regional studies of convection. Daily data on the formation of convective clouds and phenomena of convective nature during the warm season of 2008 have been analyzed for the Far-East area. The relevant statistics is presented and comparison with the climatic data performed. Typical synoptic situations accompanied by hazardous convective weather phenomena are described [28]. Based on radar data, over two hundred summer mesoscale convective systems (MCS) have been investigated in central Russia, over an area with a 200-km radius around Moscow, which have been classified by their morphology. The morphology of such systems is the basis for predicting weather hazards including lines with heavy showers and squalls [29]. Three types of lines are distinguished: lines with 100-km monolithic segments of over a 40 dBZ reflectivity; lines of intermittent convection — combinations of linear and node-like amorphous storms, as well as convex and concave arched systems frequently forming families of occlusion spirals. Nonlinear MCSs include circular radio echo structures similar to open mesoscale cells, or small 30-km arcs. However, the most severe storms occur along extended MCS development axes [29].

Climatic descriptions of Western Siberia convective resources are presented [30]; the influence of local physiographic features on the convective potential of the atmosphere of Western Siberia has been studied [31]. Convection characteristics on stormy days have been studied in Gorny Altai [32].

The characteristics of thunderstorm cells have been investigated based on observations in Yakutia [33]. Using thunderstorm location network data, it has been established that increasing thunderstorm activity (lightning density in the region) results in a larger number of thunderstorm centers and thunderstorm cells. It was concluded that the size and lifetime of thunderstorm cells in Yakutia correspond to the data for North America and the European part of Russia. It was shown that the larger the extension of thunderstorm cells, the higher is the lightning intensity in the cells.

Statistical analysis based on hail hazard radar data, using automated identification of convective cells and estimation of their parameters, has been fulfilled for Stavropol Territory and the Crimea [34]. Automatic data processing has shown that >56% and 49% of hail convective cells in Stavropol area and the Crimea, respectively, are soft-shower and small-hail ones causing no damage, and 30% of convective cell reach mean intensity in both regions, with only 8% in Stavropol area and 17% in the Crimea developing to cause severe hail damage.

This analysis of hailstorm activity builds on several years of radar observations. Monthly statistics has been obtained, which is of practical importance.

Intense convection on the Perm Territory was studied using the WRF-ARW model. The development of a short-lived convective system accompanied by severe storms, shower rains, squalls with wind speed up to 22 m/s and hail with hailstone diameter reaching 200 mm or more on 9 June 2012 was analyzed. The model estimation of convection development shows that the WRF-ARW model, though adequately reproducing convective system origination, does not always correctly indicate the areas of intense precipitation, and more over, fails to reproduce hail formation [35]. In [36] a possibility to apply the WRF model for thunderstorm forecast, using different indices of convective instability, is discussed. Ten different indices and several methods to assess the forecast skill score are considered. The value of the energy of convective inhibition, CIN, was found to be the most successful thunderstorm forecast index (for several cases considered).

It is worth noting that under the conditions of the global climate change, the statistical characteristics of convective clouds and precipitation are observed to have changed, too. In particular, in the second half of the XX century, in Siberia, the number of events with extremely intensive precipitation (mainly caused by thermal and dynamic convection) increased, with a positive trend of 2.2%/decade for the 95th percentile of the diurnal precipitation and 3.5%/decade for the 99th percentile [37]. According to observations, the function of distribution for precipitation in the European part of Russia and in Western Europe has changed [38–43]. Thus in Germany, the duration of extremely long rainy periods has grown by 2–3%, with precipitation intensity increasing by up to 10% for rainy periods lasting over 5 days [41].

Over the larger part of Russia, along with precipitation change, a statistically significant increase of the occurrence of cumulonimbus clouds and decrease of the occurrence of nimbostratus clouds are observed [3]. In particular, in Western Siberia, the number of days with cumulonimbus clouds during the warm seasons from April to October increased by 10–15% over the first decade of the XXI century, compared with the last decade of the XX century, while the number of days with nimbostratus clouds during the same periods decreased by 5–10% [3]. During the 1965–2010, in Khanty-Mansiysk area, the linear trend of the occurrence (number of days) of cumulonimbus clouds in summer was 3.0% over a decade; in 2012, a tornado was observed there, which is an extremely rare phenomenon for such a high latitude (61° N) [44].

Convection studies using simulation techniques. At Stavropol State University, 2D simulation of the formation of moist air convection in the surface atmospheric layer has been carried out [45]; a 2D convection model provided analytical solutions of thermal convection equations and described conditions for the formation of moist air convection, which determine the influence of surface

layer parameters on convection. Irkutsk State University has carried out a study of convection, using Kain-Fritsch numerical model [46].

Numerical experiments are being carried out to study the formation of microstructure characteristics of hailstorm clouds, using a 3D non-stationary convective cloud model developed at the High-Mountain Geophysical Institute [47–50], with detailed description of hydrothermodynamic, microphysical, and electric processes; numerical experiments have been fulfilled to study microstructure and thermodynamic parameters of convective clouds under conditions of unstable atmospheric stratification. Thermodynamic and microstructure parameters in the zone of convective clouds and at different times have been determined and air circulation character investigated. Electric field characteristics at different stages of development have been calculated with electric coagulation processes taken into account. The numerical experiments have confirmed that dynamic processes considerably influence the formation of thermodynamic cloud characteristics, the latter also affecting microphysical processes and precipitation particle growth. The formation peculiarities of thermal atmospheric convection in the presence of a horizontal temperature gradient have been investigated. [51].

Investigation of the microphysical characteristics of cumulonimbus clouds was also presented in [52–57].

In [52, 53], based on the measurements carried out aboard the Russian aircraft laboratory “Geophysika”, significant differences were revealed in the microphysical properties of the anvils of tropical clouds with deep convection, depending on the phase of their development. In the onset phase, clouds include small ice crystals (10–100 μm) with homogeneous morphology. During the phase of maximal cloud development, ice crystals have a non-uniform composition, irregular shape and large size (1 mm or more); the values of ice crystal concentration, moisture content and effective radius are the largest in contrast to the smallest values of these parameters during cloud onset. During cloud dissipation phase, ice crystal sizes do not exceed 200–300 μm .

Paper [54] is devoted to the evaluation of water content and water reserve of 142 Cb centers with shower rains and hail. The values of these parameters are calculated based on radar characteristics and using empirical relationships.

Paper [55] analyzed the evolution of a long-lived cumulonimbus cloud in Saudi Arabia desert area on 10 April 2008, based on continuous satellite-borne and radar observations and numerical simulation using a non-stationary 1.5-dimensional model. Precipitation intensity in the cloud was estimated to be about 100 mm/hr. The anvil characteristics in the zone its formation just above the cloud differed considerably from those observed in the anvil moving away from the formation zone. In particular, the temperature in the anvil formation zone reached $-50\text{ }^{\circ}\text{C}$ with 92% albedo, and increased to $-30\text{ }^{\circ}\text{C}$ with the albedo falling to 68%. According to the authors’ estimates, during the period of the anvil’s

active formation (about 100 minutes), as a result of the vertical transport, up to $1,8 \times 10^9$ kg of ice crystals could have moved to the upper tropospheric layers. It was established that radar underestimated the horizontal dimensions of the anvil and, due to the presence of large hail particles, overestimated precipitation intensity. Paper [56], discusses a case of the development of a cumulonimbus cloud with highly intensive precipitation in the southwestern part of Saudi Arabia; the cloud height being 14 km, the radar reflectivity was 60 dBZ. The data of the remote measurements of precipitation intensity obtained by radar (based on the reflectivity to precipitation intensity ratio) and satellite-borne IR-radiometer SEVIRI on Meteosat-8 are compared. The Z-R ratios for radar precipitation intensity estimates are analyzed. The best ratios are chosen for the evaluation of precipitation intensity based on radar and satellite-borne measurement data that agree with ground-based raingauge measurements the best.

The optical parameters of a developing convective cloud are estimated in [57]. An inverse relationship has been revealed between the values of the scattering indicatrix and polarization (depolarization) at scattering angles for which the scattering indicatrix is maximal, while polarization and depolarization are minimal.

The relationship of precipitation intensity and atmospheric convective instability is assessed in [58]. It is found that convective instability in the deep layers (of large vertical thickness) mostly results in heavy precipitation, while shallow instability (of small vertical thickness) mostly in light precipitation. It is expressed in monotonous growth of the frequency of moderate, heavy, and very heavy precipitation with the growing of neutral buoyancy level and frontal parameter that characterize baroclinic instability; on the contrary, light precipitation frequency is maximum at the level of neutral buoyancy around 2–3 km.

Paper [59] uses the authors' local model of a convective cloud. The model uses grid data of ERA-40 reanalysis as initial ones. It is shown that the acquired distribution of the number of days with thunderstorms and days with convective precipitation over the territory of Russia, as well as their meaningful time correlation, on the whole, agree with the data obtained by weather observational stations. In most regions of Russia, July is the period with a maximal thunderstorm frequency (up to 8 days per month in separate regions).

During the reference period, basic cumulus cloud characteristics, such as temperature fields, were studied. A method is proposed to determine the heights of isotherm surfaces in convective clouds based on the classical model of cloud development used in atmospheric physics [60]. The method proposed can be realized using data from standard surface-layer weather observations.

At the Main Geophysical Observatory, the peculiarities of water content statistics for cloud fields with superficial convection have been investigated [61] based on LES modeling. The function of water content distribution is shown to decrease exponentially. It has been found that in practically all cases there exists

a point on the water content axis at which the rate of exponential decrease changes abruptly. The corresponding value can be taken as a certain characteristic scale of water content. A similar feature can also be found in experimental data.

Microphysics issues have been investigated: e.g. the role of an ice phase in the formation of convection has been analyzed [62]; also considered were some theoretical problems, such as Rayleigh convective instability under phase transition conditions [63], and experimental studies of spectral characteristics of turbulence and turbulent fluxes in convective clouds at middle latitudes and in the tropical zone (Cuba) have been fulfilled [64] (see also section Turbulence).

In connection with the beginning deployment of a new weather radar network DMRL–C (with 22 observation stations already operating), operating instructions on the use of new Doppler radar for the needs of weather forecast services and aviation are being developed [65].

1.3. Experimental studies, measurement instruments and procedures, data processing techniques, field observational data on clouds and precipitation, and instruments for cloud observations. Modeling of cloud and microphysical processes

An important aspect of studying cloud processes is the accuracy of observations and their feasibility at different space and time scales. Due to the intrinsic limitations of conventional meteorological observations, remote hydrometeor sounding techniques, both passive and active, have developed significantly. A number of problems connected, e.g., with the response of cloud and precipitation characteristics to dynamic and thermodynamic atmospheric processes, composition of cloud elements (the number and properties of condensation nuclei) can be partly solved by numerical modeling. However, for more detailed investigation into the fine cloud structure and validation of remote techniques and numerical simulation results, in situ observations inside cloud layers are required. Such observations can be carried out aboard aircraft equipped with measurement systems. In 2014, a new-generation aircraft laboratory aboard a production YAK-42D airplane became operational. The laboratory is equipped with modern instruments to measure air temperature, pressure, density, and humidity, wind and turbulence, to study the microphysical structure of clouds and precipitation, gas and aerosol atmospheric composition, atmospheric radiation, atmospheric electricity, radar characteristics of clouds and local relief, radiation and thermal physical characteristics of the underlying surface, as well as radioactive pollution of the atmosphere and underlying surface. The studies fulfilled and technical procedures are discussed in [66–68].

A new-generation DMRL–C radar network is being developed in Russia to carry out observations of clouds, precipitation, and hazardous weather

phenomena. At present, about twenty DMRL–C radar stations are in operation. Workstations to display radar weather data have been organized at Roshydromet Situational Center and the Hydrometcenter of Russia; every 10 minutes they receive information about the height of an upper cloud boundary, precipitation intensity, observed weather phenomena, etc. (<http://meteorad.ru>). Twelve DMRL–C stations have already been adapted to meteorological use. Twenty four sites have been chosen to install DMRL–C stations in 2015. A document entitled “User’s Guide on the Application of Doppler DMRL–C Weather Radar Data in Synoptic Practice” has been developed and introduced.

Cloud and precipitation detection algorithms and peculiarities of determining basic cloud characteristics based on observations from space-borne platforms are analyzed and discussed in [69–80]. Papers [81, 82] compare space-borne and ground-based radar measurements of cloud and precipitation parameters. Using ground-based radar in detecting cloud and precipitation characteristics is also discussed in [83–85].

A complex threshold technique of automatic pixel-by-pixel classification of SEVIRI radiometer measurement data from a geostationary Meteosat satellite and AVHRR radiometer data from a polar-orbiting NOAA satellite is presented in papers [78–80]. The technique is intended for 24-hr retrieving of the parameters of cloud cover, precipitation and hazardous weather phenomena over the European part of Russia (ER), independent of the type of underlying surface. It is shown that the estimates of diurnal, monthly and annual precipitation totals obtained by this technique agree well with the ground-based observations, and are available for visual monitoring of moistening in the ER. The high accuracy of the estimates achieved is due to the use of combined AVHRR and SEVIRI space images, which allows avoiding the drawbacks inherent in any type of initial information. The technique is expected to be used in processing data from MSU-MP instrument (a multi-zonal low-resolution scanning unit) mounted on the Russian satellite Meteor-M2 (launched 8 July 2014) and, later, in processing data from the satellite Electro-2.

A reliable and fast algorithm of automatic cloud object segmentation on spectral zonal images of the earth surface is presented in [77]. It is based on taking into account a stereo effect exhibited in a mutual shift of upper-level objects. The algorithm is accelerated by applying this effect to cloud object “candidates” distinguished by using a colorimetry algorithm and Bayes classifier. At present, this algorithm is being implemented in the system of processing data from the Russian Canopus-B satellite (launched 22 July 2012), and is to be further used in the data processing system for Resurs-P satellite.

In papers [70–72] is developed an algorithm of cloud field segmentation on space images and cloud type classification based on neural networks and information about the characteristic texture of images of different cloud types.

Various aspects of lidar observations of clouds and precipitation are discussed in papers [86–98].

A numerical solution of the problem of light scattering on chaotically oriented hexagonal ice crystals in cirrus clouds first obtained in a physical optics approximation is given in [93]. It is shown that the size and form of such ice crystals can be determined from lidar signal depolarization ratio.

A new two-channel rain gage using an up-to-date optoelectronic circuitry is presented in [86, 87, 90, 91]. The uncertainty of measuring particle size and rate as well as precipitation amount is shown to be no more than 5%. Preliminary field measurement data on precipitation parameters has been obtained.

Some aspects of the propagation of sonic and infrasonic waves in a cloud medium are examined in [99, 100]. For typical values of cloud parameters, the coefficient of infrasonic absorption is estimated in [100] to be about 0.1 km⁻¹, the basic absorption mechanism, in this case, being the relaxation processes related with the phase transition 'vapor — water drop' caused by an infrasonic wave. Acoustic waves in a cloud medium are shown to be subject to notable dispersion at frequencies comparable with the inverse relaxation time.

In paper [99] is examined the dependence of the refraction angle on the frequency and angle of acoustic wave incidence upon an 'air-fog' interface. Based on the analytic expressions obtained and analysis of numerical calculations, it is established that in the case when the wave is incident from the fog onto the interface, exceeding a certain critical angle results in complete internal reflection.

Apart from remote techniques, sky status exploring techniques based on special processing of images from the so-called 'all-sky' cameras, or cloud cameras (superwide-angle lens cameras) used to evaluate cloud amount, as well as cloud height and speed, have dynamically developed, as is discussed in [101–104] and [105], respectively.

An automatic technique to determine cloud amount from images obtained in a visible range, using SBIG AllSky-340B all-sky camera installed at Sayany Observatory, has been developed and described in [102]. An empirical formula to calculate cloud amount on an 8-number scale is presented; the formula represents a function of the parameters of a sky brightness histogram profile. The difference between cloud amounts obtained using automatic and visual techniques was not more than 2.

Paper [101] is devoted to the development of a cloud observation system designed for automatic cloud cover evaluation under marine observational conditions. Apart from the cloud camera, this system includes a gyroscope, an accelerometer, and a global positioning sensor. The latter permits the position of the sun to be accurately determined during sky scanning, and a solar illumination effect to be taken into account.

A method to determine total cloud amount from color panoramic all-sky images by analyzing color components of each image point, using RGB-model

color synthesis (a method of evaluating the so-called ‘blue of the sky’) is proposed in [103, 104]. Comparisons between visual measurements and automatic cloud amount determination have revealed considerable disagreement in the presence of cirrus clouds.

Paper [106] proposes a way to determine the parameters of every single raindrop (frequency and mode of oscillation, size, and shape) by taking pictures of the color tracks of raindrops illuminated with white light from below and at scattering angles near the rainbow of the first order. Color tracks of abnormally high modulation of light scattered by oscillating raindrops are recorded. Also recorded and described are different types of double and triple tracks (multitracks) whose form and color depend on the mode composition of raindrop oscillation. Decoding the form of the multitracks seems to permit the acquisition of valuable data on such a complex and poorly explored process as raindrop deformation and oscillation.

Papers [107–115] are devoted to modeling clouds and cloud processes. Local models of clouds and precipitation (one- and three-dimensional) [107–109, 115], as well as the scheme of calculating cloud and precipitation characteristics in global climate models [110, 111, 114], including climate models of intermediate complexity [110], have been developed and analyzed.

1.4. Tropospheric aerosol, cloud condensation nuclei, ice nuclei

Tropospheric aerosol particles which act as condensation nuclei play an important role in the formation of clouds and precipitation. Papers [116–121] are devoted to the discussion of various aspects of aerosol interaction with cloud medium, while papers [122–126] analyze aerosol condensation activity and its relation with chemical aerosol components and air humidity.

It is shown in [118, 120] that aerosol-induced ice nucleation increase significantly influences the evolution of a cumulonimbus cloud of large vertical extension by changing precipitation intensity time distribution and precipitation rate. Papers [116, 117] further develop an analytical scheme for the parameterization of homogeneous and heterogeneous nucleation as well as for the calculation of ice nuclei concentration in cloud medium. This scheme builds upon the nucleation dependence on both temperature and saturation level, and is intended for the numerical simulation of weather and climate. In [127], the author distinguishes four basic groups of ice nuclei shapes in the atmosphere based on their height to cross-section ratios. In [122], the condensation activity of surface aerosol including nitrates has been found to diminish with increasing relative air humidity.

Spatiotemporal aerosol characteristics (aerosol optical thickness, AOT; microphysical properties) have been investigated for different regions of Russia and

other countries [128–145], including polar regions [146–155], and sea regions [156–160]. In papers [161–165], chemical aerosol properties, including ion composition, have been studied.

A number of aerosol characteristics for the Siberian region have been obtained based on 302-m weather tower measurements. The tower ZOTTO had been built by Russian specialists with the financial support of the German party to provide measurements of atmospheric composition in the boundary layer over the northern Eurasian region far from anthropogenic aerosol sources. In [129, 132, 133] using ZOTTO measurements, the basic aerosol sources have been revealed, and the annual aerosol variation, with a maximum in December and minimum in June, obtained based on solving an inverse trajectory problem. The June minimum in the annual variation of aerosol concentration (for 0.02–1 μm size spectrum) is also observed in Moscow area [20], and the December maximum (along with two secondary ones in spring and late summer) in Tomsk area [128]. Apart from the annual cycle, a diurnal one for aerosol characteristics has been distinguished for Siberian cities [134] and Moscow area [135] based on observations. According to [145], not only a diurnal cycle, but also the so-called ‘weekend effect’ is observed over such a megacity as London. In Moscow region, the weekly cycle based on ground-based data is not pronounced [131]; however, it is notable for meteorological variables in the free troposphere [166, 167]. Based on satellite data, the weekly AOT cycle over Moscow region, which in turn can modulate the weekly cycle for precipitation, is pointed out in [168]. It is also noted that an enhanced and reduced amount of intense precipitation (more than 5 mm) is observed in Moscow on Tuesday-Wednesday and Sunday-Monday, respectively.

The influence of various factors on the amount and characteristics of tropospheric aerosol has been analyzed in [159–162]. Paper [162] based on observational data estimates the influence of precipitation on aerosol concentration in the surface atmospheric layer as limited: a washing-out effect is only observed for particles within the size range of 0,03–0,1 μm in winter, not exceeding 30%, and 0,03–1,0 μm in summer, not exceeding 10–20% and being very short-term. Based on experimental studies, it is shown in [161] that the generation of a coronal discharge under conditions without fog is accompanied by aerosol size spectrum shifting toward larger mean particle size, while in the presence of fog, aerosol concentration was observed to decrease, which could result in complete disappearance of all aerosols, including those of a nanometer size.

Variations of the characteristics of atmospheric aerosol due to forest fires have been investigated and discussed in [163–180]. In the central regions of Yakutia, during the peak phase of fire activity, the AOT values were measured to have increased manifold compared with the peak background values, and burning products were found at a distance of up to 3 thousand kilometers from the

fire source, according to [64, 65]. Based on the data of field observations, during the 2012 summer period of severe smoke in Siberia, an effective aerosol particle radius was 220 nm, the mean single scattering albedo at a 525 nm wavelength was about 0.91, and aerosol acidity was increased [173, 176, 177].

A comprehensive study of aerosol characteristics during the 2010 severe smoke blanketing in the European part of Russia has been carried out based on the data of ground-based monitoring [181–185], satellite-borne sounding [186, 187], and numerical simulation [188].

In Moscow region, maximum permissible mass aerosol concentrations PM10 were found to have increased 5-fold (up to 1.7 mg/m³) [182]. The characteristic particle size was 0.1–3 μm, while particles over 5 μm in size were not practically observed [189]. On 7 August, according to ground-based observations, the AOT value at a 500 nm wavelength was as high as 6.4 in Moscow and 5.9 in Moscow environs [190]; according to satellite-borne observations, AOT (at a 500 nm wavelength) reached a maximum of 4.86 [191]. The characteristic features of AOT distribution and atmospheric turbidity factor, depending on weather parameters, have been revealed [191, 192], and weekly synchronization of AOT and meteorological parameters has been pointed out [193].

It is shown in [181] that solar radiation attenuation in 2010 was greater than during the 1972 and 2002 periods of fire. The maximal values of shortwave aerosol radiation forcing on the earth surface were up to 360 W/m² [184], and from 150 W/m² [184] to 167 W/m² [190] at the top of atmosphere. At the same time, with extreme AOT values, the downward long-wave radiation increase was estimated to be from 20 to 50 W/m², according to different estimates [181, 194]. The thermal aerosol effect (surface air temperature decrease) was estimated to be 4–6 degrees [184, 194]. The chemical composition of aerosol is thoroughly analyzed in [185]; an abnormally intensive condensation activity (Henel parameter) of the 2010 smoke (0.2–0.4) is pointed out, which proved to be significantly higher than that for the 2002 smoke (0.1–0.15) [195]. During the smoke period, almost a 20-fold increase of the amount of active condensation nuclei was revealed, which produced conditions for aerosol particle moisturizing and acid smog formation [189].

Paper [174] compares the periods of severe forest fire smoke on the European territory of Russia (5–9 August 2010) and in Western Siberia (27–31 July 2012), using ground-based and satellite-borne observations. With close mean regional AOT values, the local AOT was larger in Western Siberia; a greater (by module) radiation aerosol forcing was observed in Siberia. Apart from the characteristics of aerosols in forest fire burning products, the characteristics of tropospheric aerosols of a different origin were estimated, including a pollen aerosol component [196–198], saltating sand particles in arid regions [199–201], dust aerosol [202], and anthropogenic aerosol [203, 204].

In [205], a model of the vertical transport of dust in a convectively unstable atmospheric boundary layer is proposed. A numerical model is constructed in [199, 200] describing the movement of a saltating sand particles in the surface atmospheric layer; an average sand-grain charge-to-mass ratio in the lower flipping layer is $33 \mu\text{A}\cdot\text{s}/\text{kg}$, while a restored charge-to-mass ratio of positively charged sand-grains is $44 \mu\text{A}\cdot\text{s}/\text{kg}$, on average [201]. In [203], the influence of a large urban area, such as Moscow, on AOT values is evaluated: under urban conditions, AOT values are by 0,02 higher compared with the background conditions (a winter increase of up to 26% is maximal); the differences in the radiation forcing at the upper atmospheric boundary are of the order of $-0.9 \text{ W}/\text{m}^2$.

Much attention is given to measurement methods [206–227], modeling [116, 117, 228, 229], and methods of tropospheric aerosol prediction [230–232].

In paper [210, 211], an algorithm is proposed and tested which combines iteration retrieval of the optical characteristics of single scattering directly from photometry measurement data with the inverse problem solution, thus permitting the retrieval of the microstructure of homogeneous aerosol particles and a complex refraction index of aerosol matter.

In [218], a new differential analyzer to study hygroscopic aerosol properties is proposed and tested; it uses the technique of studying the hygroscopic properties of aerosol particles deposited on a filter, based on a thermal conductivity measurement of the amount of water vapor absorbed by an aerosol sample. This technique has a number of advantages, including higher sensitivity permitting measurements with not more than 0.1 mg of deposited particle mass, a wider range of relative humidity change (up to 99% with a 0.06% accuracy at the upper limit of the range), the absence of intermediate measurement phases necessitating taking into account water adsorption on the measurement system units, and the absence of particle size and shape restrictions.

A generalized empirical model of the optical characteristics of aerosol in the lower 5-km atmospheric layer of Western Siberia has been created based on long-term aircraft measurements of the vertical profiles of small-angle scattering coefficients, dispersion composition of atmospheric aerosol and the amount of absorbing particles [231]. The model permits the retrieval of aerosol optical characteristics in the optical and near IR spectrum ranges (a complex refraction index, scattering and absorption coefficients, and optical thickness).

In [217], a unique instrumentation system for simultaneous observations of a great number of optical, microphysical, and radiation parameters of the atmosphere and atmospheric aerosol is described. The system is intended for ground-based observations at several specialized stations, aircraft observations, as well as observations using sodar, lidar, solar photometers, Fourier spectrometers, and other instruments. The system operability has been validated by comparison with satellite-borne observations exemplified by the 22 May 2012 measurements.

1.5. Cloud microphysics

During the last years, considerable progress has been made in describing microphysical and thermodynamic cloud process using numerical models of weather and climate. The so-called ‘cloud resolving’ models have been dynamically developed. Understanding the microphysical properties of clouds and precipitation is critical for solving the problems of intended weather modification.

Most of the current notions of cloud thermodynamics, kinetics, and microphysics are summarized in the monograph [233]. The monograph incorporates the theoretical foundations of the processes of cloud formation (the emergence of cloud droplets and crystals), cloud evolution, and precipitation formation. Here are presented some up-to-date patterns of the parameterization of basic microphysical cloud processes, which can be used in numerical models of clouds as well as in models of weather and climate.

Various aspects of cloud microphysics and optics are also discussed in [234–244].

Based on laboratory experiments, the signs of the spatial ordering of fog have been revealed in [242, 243]. It is shown that the carriers of the fog structure are droplet chains including 2 to 10 droplets separated by a fixed space. The influence of droplet ordering on the surface tension and shear viscosity of clouds and fogs is evaluated.

In paper [234], based on experimental studies, droplet movements and deformations in a swirling flow of viscose fluid at small Reynolds numbers are evaluated. It is first demonstrated that, at small Reynolds number, a droplet is deformed when the Bond number reaches a certain critical value. The relationship between this value and a droplet movement pattern within the range of Reynolds numbers ($Re = 0,03–0,84$) is obtained experimentally.

The process of the cooling of falling drops is numerically simulated and their temperature calculated in [240]. Large drops do not have enough time to become overcooled and thus have a positive temperature when reaching the ground, while smaller ones are cooled to below 0°C . The evaluation of the process of falling drop transformation into ice during overcooled water crystallization has shown that the portion of an ice cover on the drop surface at phase transition is never more than 3% even under the most favorable cooling conditions.

1.6. Turbulence and air fluxes in clouds

Turbulence is an important factor of energy and water vapor exchange between the earth surface (land or water) and the atmosphere, and thus one of the basic sources of cloud development. Therefore, certain investigations of the boundary layer can also be referred to those of cloud turbulence.

Mathematical methods. Based on processing experimental data, three basic types of structural functions have been distinguished, and models of their parameterization within the range of shears referring to the inertial turbulence interval have been suggested. The frequency of occurrence of the distinguished structural functions during different seasons at an observation station in an urban area has been estimated [245, 246].

Using numerical and mathematical simulation, stably stratified turbulent fluxes over the surface in urban areas have been investigated. Calculations of stably stratified turbulent fluxes over surfaces with explicitly specified roughness elements have been fulfilled using a LES model. The calculation results for different height distributions of external dynamic forcing are discussed and compared. The results of analyzing the structural functions of surface layer air temperature over an inhomogeneous underlying surface are presented [247, 248].

Experimental methods. Experimental studies of the nature and conditions of breeze circulation dependent on the diurnal variation have been carried out based on measurements on the sea shore in Bulgaria (Akhtopol). The front of the sea-land breeze circulation has been effectively discovered by measuring wind speed and direction as well as the surface air temperature. A measurement series using a three -component acoustic thermometer, sodar and synoptic charts can also characterize breeze circulation and turbulence structure in the surface layer [249]. The same authors studied the vertical variability of turbulence characteristics using a weather tower (Obninsk) [250].

Aircraft weather laboratory equipped with different measurement systems have proved effective in studying turbulence. The characteristics of turbulent fluxes in clouds have been investigated; statistical and spectral characteristics of turbulence in a cloudy atmosphere at middle latitudes (Russia) and tropical latitudes (Cuba) are presented based on the results of aircraft measurements. The influence of cloud water content on calculations of the spectral characteristics of temperature fields and turbulent heat fluxes in cumulus clouds have been estimated [251]. An empirical model of turbulence in a cloudy atmosphere, based on aircraft observations, is proposed [64, 252, 253].

2. Weather modification. Seeding agents and technical aids

2.1. Weathering

Intended weather modification aims at preventing or diminishing the effects of hazardous weather phenomena related with the formation of clouds and precipitation on the economic and other aspects of human activity. This refers to intended modification of stratiform clouds and fogs leading to their dispersal, modification of rain clouds resulting in precipitation redistribution, preventive

modification of fast growing cumulus clouds aimed at their dispersal on special occasions, prevention of hail damage, and mitigation of draughts.

The work devoted to intended modification of clouds proceeds in several directions. First, the object proper is investigated: clouds of various forms and geneses, their characteristics, including the characteristics and properties of cloud elements and precipitating hydrometeors. Another aspect directly related with the first one is the development of new techniques and means of weather modification: development of seeding agents, testing their effectiveness, etc. Concurrently with the above activities, methodological work consisting in drawing up reference documents, instructions, user's guides and optimizing the developed techniques is being carried out. One more important direction deals with the assessment of cloud seeding effects and development of methods to assess the practicability of intended cloud modification.

Methods and technical means. Investigation of clouds and cloud processes aimed at their intended modification is carried out using various methods and technical aids. Theoretical studies, laboratory experiments, laboratory simulation, field observations aboard aircraft labs, as well as experimental operations using all available remote techniques serve to this end. Radio sounding, satellite-borne and, particularly, weather radar observations traditionally play an important role in this field. Radar systems are used to study clouds and convective processes related with weather hazards (shower rains, hail damage, tornados, squalls, etc.) in different parts of Russia and CIS countries; they help to study the development of hail formation processes in southern regions such as Stavropol Territory, North Caucasus, and Moldova, where hail causes great damage. Radar is indispensable in complex studies of precipitation production convective air-mass and cloud frontal processes accompanied by hazardous weather phenomena in middle latitudes, aimed at the development of intended weather modification techniques.

Investigation of hail processes. The best progress in this direction has been made in the southern, North Caucasus region of Russia. A fundamental review prepared at the High-Mountain Geophysical Institute (HGI) [254] discusses the state-of-the-art in studying the physics of hail clouds and their intended modification. It is noted that this research field is on the way to a new phase in studying hail processes taking into account their system properties. Some difficulties in solving this problem are outlined. Investigation based on the regression analysis of atmospheric parameters that condition the formation of hail embryos of different types has been fulfilled at the HGI [255]. The results of the multiple regression analysis of thermodynamic and microphysical atmospheric parameters leading to hail embryo formation have been presented.

Microphysical aspects of hail processes due to hail cloud seeding are discussed in [256] (Nomangan State University). To date, submicron AgI particles

are used in seeding hail clouds to create embryos competing with natural ones for supercooled liquid water, or accelerate precipitation formation. However, the investigations fulfilled confirm the leading role of gigantic and super-gigantic particles that also occur at high levels (5 km or more) in the formation of convective precipitation embryos. As cloud and precipitation particle accretion is mainly due to coagulation, cloud seeding by submicron AgI particles is not likely to be highly effective in hail mitigation. The fact that the seeded agent is found in hail layers rather than in hail embryos indicates that the agent is mainly spent on intensifying (or accelerating) the coagulation accretion of much more natural cloud and precipitation particles rather than on creating additional precipitation embryos. It is pointed out that this can be one of the main cloud modification mechanisms.

Radar observations aimed at predicting convective storm evolution are summarized in [257] (Special Weather Modification Service of Moldova)

The results of studying the evolution of convective storms and analysis of their radio echo and wind hodograph in the troposphere have been summed up. The peculiarities of the formation and evolution of cumulonimbus clouds have been established based on their radio echoes in the Lagrange (moving) reference frame. The peculiarities of the evolution of thick Cb with significant wind shear have been revealed. Based on the troposphere wind hodograph constructed in a moving reference frame, the direction and peculiarities of Cb evolution can be predicted. The results of the studies are used by the Special Weather Modification Service of Moldova in hail mitigation operations, in predicting the location of new convective cell formation, and in optimizing the size of the sites for seeding crystallizing agents.

The efficiency of precipitation redistribution operations. The efficiency of cloud seeding to redistribute precipitation in the middle latitudes remains to be topical. This problem is regularly on the agenda of conferences devoted to this research direction. In particular, recommendations for the application of methods and technical aids to modify convective clouds have been elaborated [258]. Studies of the practicability and effectiveness of seeding operations in redistributing both summer and winter precipitation are under way [259].

Draught mitigation. For areas suffering from water deficit, in steppe areas where vegetation period partly coincides with the period of precipitation deficiency, the development of a new experimental direction devoted to precipitation enhancement during periods most important for vegetation is of primary importance. During the last years, research in this direction has been given a new impulse due to increasingly frequent summer draughts not only in southern regions, but also in the central part of Russia, which occur against the background of the global warming. Sound preparatory work has been done, and the basic principles of organizing and operating the system of draught mitigation in the Russian Federation through intended precipitation enhancement have been grounded [260].

Cloud and fog modification. A large weather modification work series is devoted to intended cloud and fog dissipation. A monograph entitled "Methods and means of modifying clouds, precipitation and fogs" was published [261].

Numerical simulation methods in intended weather modification. The results of modifying low stratified clouds and fogs with large artificial water drops aimed at their dissipation have been analyzed using numerical simulation [262, 263]. The amount of water required for fog dissipation over a runway has been estimated, and calculations to allow for wind fulfilled. Practicability of the results obtained in producing or enhancing precipitation from stratified clouds and inhibiting convective clouds has been established.

Recommendations for the application of methods and means of modifying warm airmass stratiform clouds and fogs have been worked out by A. F. Mozhaisky Space Academy jointly with the Kabardino-Balkaria Research Center of the Russian Academy of Sciences (RAS) [264]. The recommendation will not only help optimize the procedures of using these methods and improve the effectiveness of cloud and fog dispersal operations, but also solve a wide range of applied problems.

Many of the earlier methods continue to be successfully used for various applied purposes. For example, field experiments to clear warm stratiform clouds in a foothill area were fulfilled in Kabardino-Balkaria. The experiments aimed at widening the prospects of optical observations of the atmosphere and cosmic space from the Earth, and vice versa, in the presence of stratiform clouds. Clearances were produced in stratiform clouds, using weather modification methods and technical aids described in [265]. Such clouds cover considerable areas and can persist over a single region for a long time.

Experimental work. Experimental weather modification operations are rather complicated and costly, while it is difficult to assess their effectiveness without making numerous experiments in order to collect significant statistics. As it is impossible to repeat numerous series of experiments, new ways of assessing the efficiency of weather modification techniques have to be found. The paper [266] analyzes a change in the characteristics of a cumulonimbus cloud, Cb, caused by its merging with feeder clouds having large water content. Seeding agent was introduced to feeder clouds in the immediate vicinity of the main Cb from board an aircraft, which usually crossed the clouds during seeding. The seeding procedure resulted in the crystallization heat emission, which stimulated vertical feeder cloud development and thus its merging with the Cb cloud, while the presence of artificially produced ice nuclei lead to the formation of additional precipitation. Cb dynamics changed, too: falling out precipitation gradually washed out the rear side of the Cb cloud, the updraft shifted into the zone of development of the feeder clouds, thus conditioning their vertical growth and merging with the Cb cloud. The analysis was made based on continuous 6-hr. radar and

satellite-borne observations of the development of a long-lived Cb cloud in Saudi Arabia on 4 July 2008. Also fulfilled was the numerical simulation of Cb development, using a non-stationary 1.5-dimensional model. It was established that processes of Cb merging with feeder clouds developing in the vicinity of Cb lead to longer lifetime and higher level of Cb upper boundary, higher radar reflectivity, higher intensity and longer duration of precipitation. Intended modification of feeder clouds can accelerate their development and further considerably influence a Cb cloud.

The same research team [267] presented the results of radar studies of cloud merging both during their natural development cycle and when seeded in the southwest of Saudi Arabia in 2008. It was established that cloud merging processes proceeded in a highly unstable atmosphere with instability energy reserve exceeding 3000 J/kg. Cloud merging considerably influences their development. Cloud mass and precipitation flow were observed to change the most, increasing 2–3-fold due to this process. The influence of cloud merging on cloud characteristic was found to exceed considerably the effect of seeding feeder clouds. Paper [268] analyzes the development of three closely spaced Cb clouds in Saudi Arabia after crystallizing agent seeding. Continuous satellite-borne and radar observations were being carried out during 5 hours. The authors assessed the seeding effect based on a thorough analysis of changes in cloud characteristics due to seeding and their comparison with the ones expected in accordance with the physical seeding concept. Data on the development dynamics of Cb clouds and their anvils were obtained. Upon seeding, Cb clouds were observed to develop vertically, while radar reflectivity and precipitation amount increased. In all three cases, precipitation enhancement was quite considerable (up to 200%). The data obtained agree with the theoretical notions of the effect of intended modification on the dynamic cloud properties and precipitation characteristics. The data indicate that intended modification of clouds is highly promising for Cb precipitation enhancement.

New cloud modification techniques. Some new alternative cloud modification techniques are proposed to change electric cloud structure, induce precipitation with negative ion fluxes and microwave radiation. Paper [269] describes an installation producing fluxes of negative ions to influence atmospheric processes in order to clear fogs, induce precipitation, etc. The authors present the results of balloon measurements of a flux of charged particles produced by a coronal discharge in the atmosphere. The graphs of the concentration of negative ions versus height above the Earth surface, based on model calculations, are also presented

Paper [270] discusses a radio optical mechanism of both natural and intended modification of weather and climate characteristics. The author proposes a method of intended modification of the atmosphere based on using a microwave radiation source at altitudes of 2–4 km.

To change the electric structure of clouds, experiments in accelerating the formation of and separating volume electric charges in stratified clouds were carried out [271]. Experimental results of stratified cloud modification with ultra-long conductive filaments to change electric characteristics of clouds, produce volume electric charges in them and induce lightnings are presented.

Cloud seeding efficiency. Paper [272] considers the efficiency of seeding convective clouds with crystallizing agents to enhance precipitation. In [273], based on numerical simulation, a comparative evaluation of the efficiency of hygroscopic agents in modifying convective clouds to enhance precipitation is fulfilled. It is shown that polydisperse salt powders are considerably more efficient than the other hygroscopic agents presently available. Salt powders are effective at one order lower mass concentrations of hygroscopic particles compared with pyrotechnical flares. They can even induce precipitation from warm convective clouds, without 'overseeding' effect observed, while this effect can occur when seeding hygroscopic agents with narrow particle size spectra.

The effectiveness of cloud seeding operations to improve weather conditions in big cities (preventing precipitation during mass festivities) has been estimated [274]. Operations aimed at cloud dissipation and precipitation control employed up to 12 airplanes equipped with all necessary measuring instruments, technical aids, and means of radio data exchange. Liquefied nitrogen, carbon dioxide, silver iodide, or coarsely dispersed powders were used as seeding agents. Ground-based automated weather radar systems controlled aircraft operations and cloud seeding effect. The positive results of over 40 large-scale weather modification aircraft operations fulfilled to redistribute atmospheric precipitation in different regions of Russia and abroad since 1995 testify to the practicability of cloud seeding techniques and technical aids developed at Roshydromet. A study fulfilled at the High-Mountain Geophysical Institute and discussed in [275] is devoted to the methods and results of investigating the physical and economic efficiency of intended weather modification aimed at hail damage mitigation.

Constructing a 3-D model of Cb cloud and simulating intended weather modification. Work series [276, 277] is devoted to the development of a 3D model of a thunderstorm Cb cloud to calculate the parameters of liquid and solid precipitation under conditions of both natural and artificially modified Cb development. A series of numerical experiments with the 3D model for the conditions of weather modification by hygroscopic, ice-forming, and combined methods have provided quantity estimates indicating that maximal precipitation enhancement by the combined method can be up to 20%. An experience of using base blocks developed at the Main Geophysical Observatory for numerical simulation of thunderstorm Cb cloud seeding with ice-forming substances is described. In developing the 3D Cb model, numerical simulation of thunderstorm Cb modification using hygroscopic species has been fulfilled.

2.2. Seeding agents and technical aids

The High-Mountain Geophysical Institute jointly with Kabardino-Balkaria University [278–280] investigated condensation processes in a cloud of explosive gas including crystallizing agent vapor. It was demonstrated that critical viable condensation nuclei mainly form at an instant of the transition of the detonation products of explosives to an ideal gas. The rate of the origination of agent embryos capable of further growth has been calculated. The kinetics of condensation processes in disperse systems formed due to crystallizing agent dispersal by using an artillery technique has been developed. The number and mean radii of crystals produced per 1 g of crystallizing agent have been calculated. For AgI, these values are of an order of 10^{12} and $10\text{--}7$ m, respectively. The kinetics of Brownian coagulation in disperse systems formed due to crystallizing agent dispersal by explosion has been analyzed. It is shown that crystals formed upon the termination of exploding gas cloud expansion processes acquire charges whose magnitude is, on average, of an order of one thousand elementary charges. The characteristic origination rate of viable condensation nuclei for most frequently used explosives is of an order of $10^{28} \text{ m}^{-3} \cdot \text{s}^{-1}$.

The estimates of the transport of ice-forming particles from ground-based dispensers have been obtained [281]. The effect of acting upon clouds with salt powders has been studied experimentally [282]. Laboratory studies of the mechanisms of the action of powder agents promising for cloud and fog dissipation have been carried out [283]. The influence of water phase transitions on the parameters of clouds and cloud systems developing both naturally and when acted upon by particles of ice-forming agents has been analyzed [284].

References

1. Groisman, P. Y., Bogdanova E. G., Alexeev V.A. et al. Impact of snowfall measurement deficiencies on quantification of precipitation and its trends over Northern Eurasia. *Ice and Snow*. 2014. No. 2, p. 29–43.
2. Yang D., Simonenko A. Comparison of Winter Precipitation Measurements by Six Tretyakov Gauges at the Valdai Experimental Site. *Atmosphere–Ocean*. 2014. Vol. 52. No. 1, p. 39–53.
3. Chernokulsky, A.V., Bulygina O.N., Mokhov I.I. Recent variations of cloudiness over Russia from surface daytime observations. *Environmental Research Letters*. 2011. Vol. 6. No. 3, p. 035202.
4. Khlebnikova, E.I., Makhotkina E.L., Sall I.A. Cloud cover and solar radiation regime over Russia: observed climatic changes. *The Transactions of the Main Geophysical Observatory*. 2014. No. 573, p. 65–91 (in Russian).

5. Chubarova, N.E., Nezval' E.I., Belikov I.B. et al. Climatic and environmental characteristics of Moscow megalopolis according to the data of the Moscow State University Meteorological Observatory over 60 years. *Russian Meteorology and Hydrology*. 2014, Vol. 39. No. 9, p. 602–613.
6. Komarov, V.S., Il'in S.N., Lavrinenko A. V. et al. Climate conditions of low clouds over the territory of Siberia and its modern change. Part 1. Features of low clouds conditions. *Atmospheric and Oceanic Optics*. 2013. Vol. 26. No. 7, p. 579–583 (in Russian).
7. Komarov, V.S., Il'in S.N., Lavrinenko A. V. et al. Climate conditions of low clouds over the territory of Siberia and its modern change. Part 2. Changes of low clouds conditions. *Atmospheric and Oceanic Optics*. 2013. Vol. 26. No. 7, p. 584–589 (in Russian).
8. Komarov, V.S., Matvienko G. G., Il'in S.N., Lomakina N. Ya. Regional features of long-term changes of cloud cover in the Siberian sector of the Northern hemisphere during the last 45 years (from 1969 to 2013). *Atmospheric and Oceanic Optics*. 2014. Vol. 27. No. 12, p. 1079–1084 (in Russian).
9. Shakina, N.P., Skriptunova E. N., Vetrova E. I. et al. The occurrence of low cloudiness over the European part of the former USSR from airport observations. *Transactions of Russian Hydrometeorcenter*. 2012. No. 348, p. 99–129 (in Russian).
10. Troshkin D. N., Kabanov M. V., Pavlov V. E. et al. Repetition of cloudiness situations and cloud optical thickness over the West-Siberian plain on the basis of ENVISAT data. *Atmospheric and Oceanic Optics*. 2012. Vol. 25. No. 9, p. 784–787 (in Russian).
11. Vetrova, E.I., Skriptunova E. N., Shakina N. P. Low clouds and their forecast at the airports of the European part of the former USSR. *Russian Meteorology and Hydrology*. 2013. Vol. 38. No. 1, p. 6–19.
12. Komarov, V.S., Nakhtigalova D. P., Il'in S.N. et al. Climatic zoning of the Siberia territory according to the total and lower cloudiness conditions as a basis for construction of local cloud atmosphere models. Part 1. Methodical bases. *Atmospheric and Oceanic Optics*. 2014. Vol. 27. No. 10, p. 895–898 (in Russian).
13. Komarov, V.S., Nakhtigalova D. P., Il'in S.N. et al. Climatic zoning of the Siberia territory according to the total and lower cloudiness conditions as a basis for construction of local cloud atmosphere models. Part 2. The results of climatic zoning. *Atmospheric and Oceanic Optics*. 2014. Vol. 27. No. 10, p. 899–905 (in Russian).
14. Chernokulsky, A. V. Cloudiness climatology in the arctic and subarctic regions from satellite and surface observations and reanalysis data. *Solar-Terrestrial Physics*, 2012. No. 21, p. 73–78 (in Russian).
15. Chernokulsky, A.V., Mokhov I.I. Climatology of total cloudiness in the Arctic: An intercomparison of observations and reanalyses. *Advances in Meteorology*. 2012. Vol. 2012, Article ID542093, 15 pages. DOI: 10.1155/2012/542093.
16. Chernokulsky, A.V., Eliseev A. V. Climatology of satellite-derived cloud overlap parameter. *Research Activities in Atmospheric and Oceanic Modelling*. A. Zadra (ed.), 2013. Rep. 43, p.02.03–02.05
17. Chernokulsky, A.V., Mokhov I.I., Nikitina N.G. Winter cloudiness variability over Northern Eurasia related to the Siberian High during 1966–2010. *Environmental Research Letters*, 2013. Vol. 8. No. 4, p. 045012.

18. Erlykin, A.D., Wolfendale A. W. Cosmic ray effects on cloud cover and their relevance to climate change. *Journal of Atmospheric and Solar-Terrestrial Physics*. 2011. Vol. 73. No. 13, p.1681–1686.
19. Kudryavtsev, I.V., Jungner H. Variations in atmospheric transparency under the action of galactic cosmic rays as a possible cause of their effect on the formation of cloudiness. *Geomagnetism and Aeronomy*. 2011. Vol. 51. No. 5, p. 656–663.
20. Makarieva, A.M., Gorshkov V.G., Sheil D. et al. Why Does Air Passage over Forest Yield More Rain? Examining the Coupling between Rainfall, Pressure, and Atmospheric Moisture Content. *J. Hydrometeor.* 2014. Vol. 15, p. 411–426.
21. Murav'ev, A.V., Kulikova I.A. Interrelation of total precipitation over Eurasia with atmospheric centers of action of the northern hemisphere and with major modes of the North Atlantic surface temperature variability. *Russian Meteorology and Hydrology*. 2011. Vol. 36. No. 5, p. 285–293.
22. Murav'ev, A.V., Resnyanskii Y.D. Interrelation of the intraseasonal precipitation variability over Eurasia to the Eliassen-Palm flux characteristics over the Northern Hemisphere. *Russian Meteorology and Hydrology*. 2011. Vol. 36. No. 11, p. 712–722.
23. Onuchin, A.A., Danilova I. V. Orographic effects of precipitation distribution in the near-Enisey Siberian regions. *Geography and Natural Resources*. 2012. No. 3, p. 85–92 (in Russian).
24. Rubtsova, O.A., Kovalenko V.A., Molodykh S.I. Peculiarities of changing the atmospheric precipitation and their correlation with geomagnetic activity. *Solar-Terrestrial Physics*. 2012. N. 21, p. 107–109 (in Russian).
25. Semenov, V.A., Shelekhova E.A., Mokhov I.I. et al. Influence of the Atlantic Multidecadal Oscillation on settling anomalous climate regimes in Northern Eurasia based on model simulation. *Doklady Earth Sciences*. 2014, Vol. 459, No. 2, p. 1619–1622.
26. Bezrukova, N., Stulov E., Sokolov V. et al. Cold season precipitation on the territory of Verhniaya Volga during the last 25 years. *Proceedings of the 16th International Conference on Clouds and Precipitation*. Leipzig, Germany. 30–03 August 2012. Abstract No. 174.
27. Nevzorov, A. *Microphysics of cold clouds: liquid phase phenomenon*. Lambert Academic Publishing, 2014, 70 p.
28. Bobrikova, I.V., Ignatenko L.A. Synoptic conditions for the occurrence of hazardous convective phenomena in the Far-East region. *Collection of papers. Far-East Region Research Institute. Vladivostok: Dalnauka*, 2010, p. 243–259 (in Russian).
29. Abdullaev, S.M., Lenskaya O. Y., Zhelnin A.A. The structure of mesoscale convective systems in central Russia. *Russian Meteorology and Hydrology*. 2012. Vol. 37. No. 1, p.12–20.
30. Zolotukhina, O.I., Konstantinova D.A. Parameters of Western Siberia convection on days with hazardous phenomena. *Geosystems: development factors, rational nature management, management methods. Collection of papers. 2nd International Theoretical and Practical Conference, Tuapse, 4–8 October 2011. Krasnodar 2011*, p. 155–157 (in Russian).

31. Tunaev, E.L., Konstantinova D.A. The influence of local physiographic peculiarities on the atmospheric convective potential of Western Siberia. Geosystems: development factors, rational nature management, management methods. Collection of papers. 2nd International Theoretical and Practical Conference, Tuapse, 4–8 October 2011. Krasnodar 2011, p. 209–211 (in Russian).
32. Gorbatenko, V.P., Konstantinova D.A. Characteristics of convection over Gorny Altai on days with thunderstorms. Climatology and Glaciology of Siberia: International Theoretical and Practical Conference, Tomsk, 16–20 October, 2012. Proceedings. Tomsk, 2012, p. 94–95 (in Russian).
33. Shabaganova, S.N., Karimov R.R., Kozlov V.I., Mullayarov V.A. Characteristics of storms cells from observations in Yakutia. Russian Meteorology and Hydrology. 2012. Vol. 37. No. 11–12, p. 746–751.
34. Zharashuev V.P. Statistical analysis of hailstorm activity on Stavropol krai and Crimea. Russian Meteorology and Hydrology. 2012. Vol. 37. No. 7, p. 37–43.
35. Kalinin, N.A., Vetrov A.L., Sviyazov E.M., Popova E.V. Studying intensive convection in Perm krai using the WRF model. Russian Meteorology and Hydrology. 2013. Vol. 38. No. 9, p. 598–604.
36. Gubenko, I.M., Rubinshtein K.G. An example of the comparison of middle troposphere instability indices in the prognostic model with the thunderstorm activity data. Russian Meteorology and Hydrology. 2014. Vol. 39, No. 5, p. 308–318.
37. Groisman, P. Ya., Blyakharchuk T.A., Chernokulsky A.V. et al. Climate Changes in Siberia. In: Regional Environmental Changes in Siberia and Their Global Consequences (P. Ya. Groisman and G. Gutman eds.). Dordrecht: Springer. 2012, p. 57–109.
38. Lockhoff, M., Zolina O., Simmer C., Schulz J. Evaluation of satellite-retrieved extreme precipitation over Europe using gauge observations. J. Climate. 2014. Vol. 27, p. 607–623.
39. Zolina, O. Changes in the duration of synoptic rainy periods in Europe from 1950 to 2008 and their relation to extreme precipitation. Doklady Earth Sci., 2011, Vol. 436. No. 2, p. 279–283.
40. Zolina, O. Changes in Intense Precipitation in Europe. In: “Changes in Flood Risk in Europe”, CRC Press, edited by Zbigniew W. Kundzewicz, 2012, p. 97–119.
41. Zolina, O. Multidecadal trends in the duration of wet spells and associated intensity of precipitation as revealed by a very dense observational German network. Environmental Research Letters. 2014. Vol.9. No.2. p. 025003.
42. Zolina, O., Simmer C., Belyaev K.P. et al. Changes in European wet and dry spells over the last decades. J. Climate. 2013. Vol. 26, p. 2022–2047.
43. Zolina, O., Simmer C., Kapala A. et al. New view on precipitation variability and extremes in Central Europe from a German high resolution daily precipitation dataset: Results from the STAMMEX project. Bull. Amer. Meteor. Soc. 2014. Vol. 95, p. 995–1002.
44. Kurgansky, M.V., Chernokulsky A.V., Mokhov I.I. The tornado over Khanty-Mansiysk: An exception or a symptom? Russian Meteorology and Hydrology. 2013. Vol. 38. No. 8, p. 539–546.

45. Simakhina, M.A., Larchenko I.N., Krupkin A.A. Origination of moist air convection in the atmospheric surface layer in a two-dimensional model. The Herald of Stavropol State University, 2011, No. 75, p. 63–68 (in Russian).
46. Zhambazhamts, Lkhazhavyn, Tsool Manalzhavyn, Arguchintsev V.K. Studying convection using Kain-Fritsch numerical model. Bulletin of Irkutsk State University. Series “Earth Sciences”, 2012, No.1, p. 186–194 (in Russian).
47. Ashabokov, B.A., Shapovalov A. V., Kuliev D. D. et al. Numerical simulation of thermodynamic, microstructural, and electric characteristics of convective clouds at the growth and maximum-development stages. Bulletin of Universities. Radiophysics. 2013. Vol. 56. No. 11–12, p. 900–907 (in Russian).
48. Ashabokov, B.A., Shapovalov V.A., Ezaova A.G., Shapovalov M.A. Investigation of nucleation in the thunderstorm clouds based on three-dimensional numerical model. Natural and Technical Sciences. 2014. No. 5 (73), p. 78–83. (in Russian).
49. Shapovalov, A.V., Shapovalov V.A., Ezaova A.G., Prodan K.A. Modeling of spectra of particles in convective clouds with mixed phase structure and their radiating properties. Bulletin of Kabardino-Balkaria scientific center of RAS. 2013. No. 5(55), p. 63–72 (in Russian).
50. Ashabokov, B.A., Fedchenko L.M., Shapovalov A. V., Ezaova A. G. Numerical experiments to study microstructure characteristics of thunderstorm clouds. Bulletin of Universities. Northern Caucasian region. Natural sciences. 2014, No. 3, p. 40–44 (in Russian).
51. Sukhov, S.A. Peculiarities of the formation of thermal convection in the atmosphere in the presence of a horizontal temperature gradient. Author’s abstract. High-Mountain Geophysical Institute, Nalchik. 2013. 19 p. (in Russian).
52. Frey, W., Borrmann S., Fierli F. et al. Tropical deep convective life cycle: Cb-anvil cloud microphysics from high-altitude aircraft observations. Atmos. Chem. Phys. 2014. Vol. 14, p. 13223–13240.
53. Frey, W., Borrmann S., Kunkel D., et al. In situ measurements of tropical cloud properties in the West African Monsoon: upper tropospheric ice clouds, Mesoscale Convective System outflow, and subvisual cirrus. Atmos. Chem. Phys., 2011. Vol. 11, p. 5569–5590.
54. Kalinin, N.A., Smirnova A.A. Determination of liquid water content and reserve of cumulonimbus cloudiness from meteorological radar information. Russian Meteorology and Hydrology. 2011. Vol. 36. No. 2, p. 91–101.
55. Krauss, T.W., Sin’kevich A.A., Veremei N.E. et al. Complex study of characteristics of a Cb cloud developing over the Arabian Peninsula under high dew point deficit in the atmosphere. Part 1. Field observations and numerical modeling. Russian Meteorology and Hydrology. 2011a. Vol. 36. No. 2, p.102–111.
56. Krauss, T.W., Sin’kevich A.A., Veremei N.E. et al. Complex study of characteristics of a Cb cloud developing over the Arabian Peninsula under conditions of high dew point deficit in the atmosphere. Part 2. Analysis of the Meteosat data. Russian Meteorology and Hydrology. 2011b. Vol. 36. No. 3, p. 167–174.
57. Zhekamukhov, Kh.M. Numerical simulation of the scattering indicatrix, linear polarization rate, and depolarization factor in the developing convective cloud for

millimeter and centimeter wavelengths. *Russian Meteorology and Hydrology*. 2014, Vol. 39. No. 10, p. 670–676.

58. Shakina, N.P., Skriptunova E.N. Diagnosis and forecasting of the probability spectra of precipitation rate ranges / *Russian Meteorology and Hydrology*. 2011. Vol. 36. No. 8, p. 499–510.

59. Veremei, N.E., Dovgalyuk Yu.A., Efimov S.V. et al. Studying the showers and thunderstorms on the territory of Russia using the numerical model of convective cloud and the reanalysis data. *Russian Meteorology and Hydrology*. 2013. Vol. 38. No. 1, p. 20–27.

60. Neizhmak, A.N., Zhalnin M. V. A method of estimating the height of an isotherm position in convective clouds. Safeguarding in emergency situations: Proceedings, 7th International Theoretical and Practical Conference, Voronezh, 21 December 2011. Part 1. Voronezh, 2011, p. 111–116 (in Russian).

61. Dovgaliuk, Yu.A., Ignatiev A. A. Some statistics peculiarities of the water content of clouds with superfluous convection. *Transactions of the Main Geophysical Observatory*, 2012, No. 566, p. 128–138 (in Russian).

62. Tabalchuk, T.G., Borodko S. K. The role of an ice phase in forming convective cells. Atmospheric composition. Atmospheric electricity. Climatic effects: Proceedings 12 International conference of young specialists. Zvenigorod, 28 May – 1 June 2012. Moscow 2012, p. 193–196 (in Russian).

63. Shmerlin, B. Ya., Kalashnik M. V. Rayleigh convective instability in the presence of phase transitions of water vapor. The formation of large-scale eddies and cloud structures. *Physics-Uspokhi*. 2013. Vol. 56. No. 5, p. 473.

64. Strunin, A.M., Strunin M. A. Spectral characteristics of turbulence and turbulent fluxes in convective clouds over Cuba based on aircraft observations. Reports. All-Russia open conference on cloud physics and intended modification of hydrometeorological processes, Nalchik, 7–9 October 2014, High-Mountain Geophysical Institute, p. 234–243.

65. User's Guide. Roshydromet document № 52 of 14.02.2014.

66. Borisov, Y., Petrov V., Strunin M. et al. New Russian aircraft-laboratory Yak-42D «Atmosphere» for environmental research and cloud modification. 16th International Conference on Clouds and Precipitation. July 30 – August 03, 2012. Leipzig, Germany. Abstract No 184.

67. Strunin, A.M., Zhivoglotov D.N. A method to determine true air temperature fluctuations in clouds with liquid water fraction and estimate water droplet effect on the calculations of the spectral structure of turbulent heat fluxes in cumulus clouds based on aircraft data. *Atmospheric Research*. 2014. Vol. 138. p. 98–111.

68. Zhivoglotov, D.N. Estimation of liquid water content effects on the air temperature measurements in the clouds based on the wind tunnel experiments. *Russian Meteorology and Hydrology*. 2013. Vol. 38. No. 8, p. 531–538.

69. Afonin, S. V. On the relation between radiation temperature of clouds in MODIS IR channels and cloud characteristics. *Atmospheric and Oceanic Optics*. 2012. Vol. 25. No. 2, p. 154–156.

70. Astafurov, V.G., Evsyutkin T. V., Kuryanovich K. V., Skorokhodov A. V. Statistical model of the texture of images of various cloudiness types from MODIS data. The

contemporary problems of the Earth remote sensing. 2013. Vol. 10. No. 47, p. 188–197 (in Russian).

71. Astafurov, V.G. and Skorokhodov A. V. Segmentation of Satellite Images by Textural Parameters Based on Neural Network Technologies. *Earth Research from Space*. 2011. No. 6, p. 10–20 (in Russian).

72. Astafurov, V.G. and Skorokhodov A. V. Classification of clouds in satellite images based on the technology of neural networks. The contemporary problems of the Earth remote sensing. 2011. Vol. 8. No. 1, p. 65–72 (in Russian).

73. Fomin, B.A., Falaleeva V.A. The vertical structure of aerosols and clouds derived from satellites equipped with high-resolution polarization sensors. *International Journal of Remote Sensing*. 2014. Vol. 35, No. 15, p. 5800–5811.

74. Nerushev, A.F., Chechin D. E. Determination of Atmospheric Precipitation Characteristics Based on Optical Satellite Measurements. *Earth Research from Space*. 2014. No. 5, p. 29–38 (in Russian).

75. Solomatov, D.V., Afonin S. V., Belov V. V. Construction of cloud mask and removal of semitransparent clouds on ETM+/Landsat-7 satellite images. *Atmospheric and Oceanic Optics*. 2013. Vol. 26. No. 9, p. 798–803 (in Russian).

76. Sukhonin, E. V. On the issue of combined active-passive radio sounding of precipitation on radio-occultation paths. *Journal of Communications Technology and Electronics*. 2013, Vol. 58. No. 2, p. 124–127.

77. Vetrov, A.A., Kuznetsov A. E. Automatic Clouds Segmentation on High Resolution Earth's Imagery. *Earth Research from Space*. 2014. No. 2, p. 27–34 (in Russian).

78. Volkova, E. V. Utilization of a complex threshold method's estimation of cloud cover parameters obtained by SEVIRI/METEOSAT-9 for climatic observations. The contemporary problems of the Earth remote sensing. 2012. Vol. 9. No. 2, p. 200–206 (in Russian).

79. Volkova, E. V. Automatic estimation of cloud cover and precipitation parameters obtained by AVHRR NOAA for day and night conditions. The contemporary problems of the Earth remote sensing. 2013. Vol. 10. No. 3, p. 66–74 (in Russian).

80. Volkova, E. V. Estimation of precipitation amount using SEVIRI/Meteosat-9 and AVHRR/NOAA data for the European territory of Russia. The contemporary problems of the Earth remote sensing. 2014. Vol. 11. No. 4, p. 163–177 (in Russian).

81. Krauss, T.W., Sin'kevich A.A., Ghulam A. S. High-intensity precipitation measurement using remote methods. *Russian Meteorology and Hydrology*. 2012. Vol. 37. No. 7, p. 438–447.

82. Tolmacheva, N.I., Ermakova L. N. Research of parameters of overcast and the phenomena according to satellite and radar-tracking sounding. *The Geographical Herald*. 2011. No. 3, p. 59–68 (in Russian).

83. Dorofeev, E.V., Lvova M. V., Popov I. B., Tarabukin I. A. Applying of thunderclouds discrimination criteria in algorithms of new type weather radar data processing. *The transactions of the Main Geophysical Observatory*. 2014. No. 572, p.140–152 (in Russian).

84. Kadygrov, E.N., Gorelik A.G., Tochilkina T.A. Study of liquid water in clouds with the “Microradkom” radiometric system. *Atmospheric and Oceanic Optics*. 2014. Vol. 27. No. 6, p. 596–604.
85. Pomortseva, A.A. Space structure of radar reflectivity of convective cloud cover in the Ural. *The Geographical Herald*. 2012. No. 4, p. 41–45 (in Russian).
86. Azbukin, A.A., Kalchikhin V.V., Kobzev A.A. et al. Optoelectronic precipitation parameters gage. *Instruments and Experimental Techniques*. 2013. No. 4, p. 140–141 (in Russian).
87. Azbukin, A.A., Kalchikhin V.V., Kobzev A.A. et al. Determination of calibration parameters of an optoelectronic precipitation gage. *Atmospheric and Oceanic Optics*. 2014, Vol. 275, No. 5, p. 432–437.
88. Burnashov, A.V., Konoshonkin A.V. Scattering of the light on bullet and droxtal ice crystals of cirrus clouds preferably oriented in a horizontal plane with zenith flutter. *Atmospheric and Oceanic Optics*. 2014. Vol. 27, No. 9, p. 807–811 (in Russian).
89. Kabkukova, E.G., Kargin B.A., Lisenko A.A. et al. Numerical statistical simulation of terahertz radiation propagation in cloudiness. *Atmospheric and Oceanic Optics*. 2014, Vol. 27, No. 11, p. 939–948.
90. Kalchikhin, V.V., Kobzev A.A., Korolkov V.A., Tikhomirov A.A. On the choice of the measuring area for dual-channel optical rain gauge. *Atmospheric and Oceanic Optics*. 2011. Vol. 24. No. 11, p. 990–996 (in Russian).
91. Kalchikhin, V.V., Kobzev A.A., Korolkov V.A., Tikhomirov A.A. Optoelectronic dual-channel precipitation gauge. *Atmospheric and Oceanic Optics*. 2013, Vol. 26. No. 2, p. 155–159 (in Russian).
92. Konoshonkin, A.V., Borovoi A.G. Specular scattering of light on cloud ice crystals and wavy water surface. *Atmospheric and Oceanic Optics*. 2013, Vol. 26. No. 5, p. 438–443.
93. Konoshonkin, A.V., Kustova N.V., Borovoi A.G. Peculiarities of the depolarization ratio in lidar signals for randomly oriented ice crystals of cirrus clouds. *Atmospheric and Oceanic Optics*. 2013. Vol. 26. No. 5, p. 385–387 (in Russian).
94. Konoshonkin, A.V., Kustova N.V., Borovoi A.G. Limits to applicability of geometrical optics approximation to light backscattering by quasihorizontally oriented hexagonal ice plates. *Atmospheric and Oceanic Optics*. 2015. Vol. 28. No. 1, p. 74–81.
95. Kryuchkov, A.V., Grishin A.I. Instrument for measuring cloud base height. *Instruments and Experimental Techniques*. 2011. No. 6, p. 143–144 (in Russian).
96. Kryuchkov, A.V., Grishin A.I. Eye-safe lidar for measuring cloud base height. *Instruments and Experimental Techniques*. 2013. No. 4, p. 142–143 (in Russian).
97. Sakai, T., Whiteman D.N., Russo F. et al. Liquid Water Cloud Measurements Using the Raman Lidar Technique: Current Understanding and Future Research Needs. *J. Atmos. Oceanic Technol.* 2013. Vol. 30, p. 1337–1353.
98. Vostretsov, N.A., Zhukov A.F. Distribution probability of fluctuation intensity of divergent laser beam in the ground atmosphere at snowfalls (0.63 μm). *Atmospheric and Oceanic Optics*. 2011. Vol. 24. No. 8, p. 706–710 (in Russian).

99. Shagapov, V. Sh., Sarapulova V.V. Features of sound refraction in the atmosphere in fog. *Izvestiya, Atmospheric and Oceanic Physics*. 2014, Vol. 50. No. 6, p. 602–609.
100. Svirkunov, P.N., Kozlov S. V. Absorption of infrasonic waves in a cloudy medium. *Izvestiya. Atmospheric and Oceanic Physics*. 2012. Vol. 48. No. 6, p. 625–630.
101. Krinitskiy, M., Sinitsyn A., Gulev S. New optical package and algorithms for accurate estimation and interactive recording of the cloud cover information over land and sea. *Geophysical Research Abstracts*. 2014. Vol. 16. Abstract No. EGU2014–2566.
102. Zagainova, Yu.S., Karavayev Yu.S. Estimation of cloudiness conditions on eight-point scale using the histogram technique applied to optical range images from all-sky camera. *Solar-Terrestrial Physics*, 2013. No. 23, p. 120–128 (in Russian).
103. Zuev, S.V., Gochakov A. V., Krasnenko N.P., Kolker A. B. Application of RGB and wavelet methods for instrumental determination of total cloudiness. *Atmospheric and Oceanic Optics*. 2014, Vol. 27. No. 9, p. 846–848 (in Russian).
104. Zuev, S.V., Levikin V.A. Definition of total cloudiness using the intensity blue in the sky image. *Atmospheric and Oceanic Optics*. 2013. Vol. 26. No. 6, p. 510–512 (in Russian).
105. Galileyskii, V.P., Grishin A. I., Morozov A. M. The passive monostatic method of estimation of the height and speed of the clouds movement. *Atmospheric and Oceanic Optics*. 2013. Vol. 26, No. 3, p. 253–257 (in Russian).
106. Sterlyadkin, V.V., Guseinov T. N., Kulikovskiy K. V. Recording of photo tracks of anomalously high light modulation in rains. *Atmospheric and Oceanic Optics*. 2012. Vol. 25, No. 8, p. 708–713 (in Russian).
107. Ashabokov, B.A., Fedchenko L. M., Kupovykh G. V. et al. Convective Cloud Model with the Influence of Physical Processes on Its Characteristics. *Bulletin of Universities. Northern Caucasian region. Natural sciences*. 2012. No. 6 (172), p. 58–62 (in Russian).
108. Ashabokov, B.A., Fedchenko L. M., Shapovalov A. V., Shapovalov V. A. Three-dimensional numerical model of the convective cloud with correlation to electric processes: some results of calculations of the hail storm clouds' parameters. *Bulletin of Kabardino-Balkaria scientific center of RAS*. 2014. No. 6 (62), p. 9–15.
109. Ashabokov, B.A., Fedchenko L. M., Shapovalov A. V. et al. Numerical Experiments on Research of Formation of Microstructural Characteristics of Thunderstorm Clouds. *Bulletin of Universities. Northern Caucasian region. Natural sciences*. 2014. No. 3. p. 40–44 (in Russian).
110. Eliseev, A.V., Coumou D., Chernokulsky A. V. et al. Scheme for calculation of multi-layer cloudiness and precipitation for climate models of intermediate complexity. *Geosci. Model Dev*. 2013. Vol. 6. p. 1745–1765.
111. Jiang, J.H., Su H., Zhai C. et al Evaluation of cloud and water vapor simulations in CMIP5 climate models using NASA “A-Train” satellite observations. *Journal of Geophysical Research: Atmospheres*. 2012. Vol. 117, No. D14, p. D14105. doi:10.1029/2011JD017237.
112. Ogorodnikov, V.A., Sereseva O. V. Approximate numerical modelling of inhomogeneous stochastic fields of daily sums of liquid precipitation. *Russian Journal of Numerical Analysis and Mathematical Modelling*. 2014. Vol. 29. No. 6, p. 375–382.

113. Smorodin, B.L., Kalinin N.A., Davydov D.V. Simulation of the variations of the temperature of droplets in freezing precipitation. *Russian Meteorology and Hydrology*. 2014. Vol. 39. No. 9, p. 590–595.
114. Su, H., Jiang J.H., Zhai C. et al. Diagnosis of regime-dependent cloud simulation errors in CMIP5 models using “A-Train” satellite observations and reanalysis data. *Journal of Geophysical Research: Atmospheres*. 2013. Vol. 118. No. 7, p. 2762–2780.
115. Vasilevsky, K.D., Sadokov V.P. One-dimensional model of convective precipitation. *Transactions of Russian Hydrometcenter*. 2012. No. 348, p. 173–183 (in Russian).
116. Curry, J.A., Khvorostyanov V.I. Assessment of some parameterizations of heterogeneous ice nucleation in cloud and climate models. *Atmos. Chem. Phys.* 2012. Vol. 12, p. 1151–1172.
117. Khvorostyanov, V.I., Curry J.A. Parameterization of homogeneous ice nucleation for cloud and climate models based on classical nucleation theory. *Atmos. Chem. Phys.* 2012. Vol. 12. p. 9275–9302.
118. Sinkevich, A.A., Krauss T.W., Pavar S.D. et al. Investigation of the effects of high atmospheric aerosol pollution on the development of the high-depth cumulonimbus cloud. *Russian Meteorology and Hydrology*, 2014, Vol. 39, No.9, p. 577–589.
119. Smirnov, V.V. Interrelation between variations of condensation nuclei concentration and cloud spectrum. *Russian Meteorology and Hydrology*. 2011. Vol. 36. No. 3, p. 155–166.
120. Veremey, N.E., Dovgaluk Yu.A., Dorofeev E.V. et al. Numerical simulation of the impact of soot aerosol particles on Cu development at the conditions of high atmospheric pollution. *Transactions of the Main Geophysical Observatory*. 2014. No. 572, p. 30–43 (in Russian).
121. Weigel, R., Borrmann S., Kazil J. et al. In situ observations of new particle formation in the tropical upper troposphere: the role of clouds and the nucleation mechanism. *Atmos. Chem. Phys.* 2011. Vol. 11, p. 9983–10010.
122. Gruzdev, A.N., Isakov A.A., Shukurova L.M. Analysis of relationship between condensation activity of surface aerosol and its chemical composition and relative air humidity according to measurements at the Zvenigorod Scientific Station. *Atmospheric and Oceanic Optics*. 2014, Vol. 27. No. 2, p. 169–175.
123. Isakov, A.A., Tikhonov A.V., Romashova E.V. Statistical characteristics of spectral dependencies of parameter of condensate activity of near-land aerosol. *The Herald of Tambov University*. 2013. Vol. 18. No. 4–1, p. 1383–1385 (in Russian).
124. Keskinen, H., Virtanen A., Joutsensaari J. et al. Evolution of particle composition in CLOUD nucleation experiments. *Atmos. Chem. Phys.*, 2013, Vol.13, p. 5587–5600.
125. Mikhailov, E.F., Vlasenko S.S., Rose D., Pöschl U. Mass-based hygroscopicity parameter interaction model and measurement of atmospheric aerosol water uptake. *Atmos. Chem. Phys.*, 2013. Vol. 13, p. 717–740.
126. Sinkevich, A.A., Pawar S.D., Kurov A.B. et al. Laboratory investigations of the impact of sand and clay particles on water drop crystallization processes. *The transactions of the Main Geophysical Observatory*. 2014. No. 570, p. 197–210 (in Russian).

127. Golubev V.N. Nucleation and growth of ice crystals in the atmosphere. *Ice and Snow*. 2013. No. 1(121), p. 53–60.
128. Arshinov, M. Yu., Belan B. D. Study of the aerosol size distribution during spring haze and biomass burning events. *Atmospheric and Oceanic Optics*. 2011. Vol. 24. No. 6, p. 468–477 (in Russian).
129. Chi, X., Winderlich J., Mayer J.-C. et al. Long-term measurements of aerosol and carbon monoxide at the ZOTTO tall tower to characterize polluted and pristine air in the Siberian taiga. *Atmos. Chem. Phys.*, 2013, Vol. 13, p. 12271–12298.
130. Glazkova, A.A., Kuznetsova I.N., Shalygina I. Yu., Semutnikova E. G. The diurnal variation of aerosol concentration (PM10) in summer in the Moscow region. *Atmospheric and Oceanic Optics*. 2012. V.25. No. 6, p. 495–500 (in Russian).
131. Gruzdev, A.N., Isakov A.A., Elokhov A. S. Analysis of weekly cycles in surface aerosol and NO₂ at Zvenigorod Scientific Station, IAP RAS. *Atmospheric and Oceanic Optics*. 2012. Vol. 25. No. 10, p. 884–889 (in Russian).
132. Heintzenberg, J., Birmili W., Otto R. et al. Aerosol particle number size distributions and particulate light absorption at the ZOTTO tall tower (Siberia), 2006–2009. *Atmos. Chem. And Phys.* 2011. Vol. 11, p. 8703–8719.
133. Heintzenberg, J., Wolfram B., Seifert P. et al. Mapping the aerosol over Eurasia from the Zotino Tall Tower. *Tellus B*. 2013, Vol. 65, p. 20062.
134. Kabanov, D.M., Beresnev S.A., Gorda S. Yu. et al. Diurnal behavior of the aerosol optical depth of the atmosphere in some regions of Asian part of Russia. *Atmospheric and Oceanic Optics*. 2013, Vol. 26, N6, p. 466–472.
135. Plaude, N.O., Stulov E.A., Parshutkina I.P. et al. Peculiarities of seasonal variations of atmospheric aerosol concentration in the surface air of Moscow environs. *Russian Meteorology and Hydrology*. 2012. Vol. 37. No. 1, p. 21–27.
136. Poddubny, V.A., Luzhetskaya A.P., Markelov Y.I. et al. Features of optical characteristics of atmospheric aerosol in the Middle Urals. *Izvestiya. Atmospheric and Oceanic Physics*. 2013. Vol. 49. No. 3, p. 285–293.
137. Pol'kin, V.V., Panchenko M. V., Uzhegov V.N. et al. On medium-sized particles in the ground aerosol during the winter-spring change. *Atmospheric and Oceanic Optics*. 2014. Vol. 27. No.9, p. 775–781 (in Russian).
138. Sakerin, S.M., Andreev S. Yu., Bedareva T.V., Kabanov D.M. Specific features of the spatial distribution of the atmospheric aerosol optical depth in the Asian part of Russia. *Atmospheric and Oceanic Optics*. 2012. Vol. 25. No. 6, p. 484–490 (in Russian).
139. Sakerin, S.M., Andreev S. Yu., Bedareva T.V. et al. Spatiotemporal variations in the atmospheric aerosol optical depth on the territory of Povolzhye, Urals, and Western Siberia. *Atmospheric and Oceanic Optics*. 2012. Vol. 25. No. 11, p. 958–962 (in Russian).
140. Samoilova, S.V., Balin Yu.S., Kokhanenko G.P., Penner I.E. Investigation of the vertical distribution of tropospheric aerosol layers using the data of multiwavelength lidar sensing. Part 3. Spectral peculiarities of the vertical distribution of the aerosol optical characteristics. *Atmospheric and Oceanic Optics*. 2012, Vol. 25. No. 3, p. 208–215.

141. Sitnov, S.A. Spatial-temporal variability of the aerosol optical thickness over the central part of European Russia from MODIS data. *Izvestiya. Atmospheric and Oceanic Physics*. 2011. Vol. 47. No. 5, p. 584–602.
142. Sukovatov, K. Yu., Bezuglova N. N., Shutova K. O. Functions of aerosol probability density and concentration in air of an industrial city (Barnaul city, as an example). *Atmospheric and Oceanic Optics*. 2013. Vol. 26. No.3, p. 194–195 (in Russian).
143. Talovskaya, A.V., Simonenkov D.V., Filimonenko E.A. et al. Study of aerosol composition in Tomsk region background and urban stations (the winter period 2012/13). *Atmospheric and Oceanic Optics*. 2014. Vol. 27. No.11, p. 999–1005 (in Russian).
144. Uzhegov, V.N., Pkhalagov Yu.A., Kabanov D.M., Sakerin S.M.. Coarse aerosol and its role in shaping the height of the homogeneous aerosol atmosphere. *Atmospheric and Oceanic Optics*. 2012. Vol. 25. No. 12, p. 1023–1027 (in Russian).
145. Zvyagintsev, A.M., Kuznetsova I. N., Tarasova O.A., Shalygina I. Yu. Variations in the concentrations of main air pollutants in London. *Atmospheric and Oceanic Optics*. 2014. Vol. 27. No. 5, p. 417–427.
146. Golobokova, L.P., Pol'kin V.V., Kabanov D.M. et al. Studies of atmospheric aerosols in the Russia Arctic regions. *Ice and Snow*. 2013. No. 2 (122), p. 129–136 (in Russian).
147. Pol'kin, V.V., Pol'kin V.V., Panchenko M. V. Annual variations of microphysical properties of aerosol at the station “Vostok” in 2009 and 2011. *Atmospheric and Oceanic Optics*. 2012. Vol. 25. No.11, p. 963–967 (in Russian).
148. Sakerin, S.M., Chernov D.G., Kabanov D.M. et al. Preliminary results of aerosol characteristics investigation in the atmosphere in Barentsburg region (Svalbard). *Problems of Arctic and Antarctic*. 2012. No.1 (91), p. 20–31 (in Russian).
149. Sakerin, S.M., Andreev S. Yu., Kabanov D.M. et al. On results of studies of atmospheric aerosol optical depth in Arctic regions. *Atmospheric and Oceanic Optics*. 2014. Vol. 27. No. 6, p. 517–528.
150. Stock, M., Ritter C., Herber A. et al. Springtime Arctic aerosol: Smoke versus haze, a case study for March 2008. *Atmospheric Environment*. 2012. Vol. 52, p. 48–55.
151. Vinogradova, A.A., Ivanova Yu.A. Pollution of central Karelia environment under long-range atmospheric transport of anthropogenic pollutants. *Izvestiya RAS, Geography*. 2013. No. 5, p. 98–108 (in Russian).
152. Vinogradova, A.A., Ivanova Yu.A. Anthropogenic pollution of Kostomuksha reserve (Karelia) environment under long-range atmospheric transport of aerosols. *Atmospheric and Oceanic Optics*. 2011, Vol. 24, No. 6, p. 493–501 (in Russian).
153. Vinogradova, A.A., Ponomareva T. Ya. Atmospheric transport of anthropogenic impurities to the Russian Arctic (1986–2010). *Atmospheric and Oceanic Optics*. 2012. Vol. 25. No. 6, p. 414–422.
154. Vinogradova, A.A., Veremeichik A.O. Potential sources of aerosol pollution of the atmosphere near the Nenetsky Nature Reserve. *Atmospheric and Oceanic Optics*. 2013a. Vol. 26, No. 2, p.118–125.
155. Vinogradova, A.A., Veremeichik A.O. Model estimates of anthropogenic black carbon concentration in the Russian Arctic atmosphere. *Atmospheric and Oceanic Optics*. 2013b, Vol. 26. No. 6, p. 443–451 (in Russian).

156. Nasrtdinov, I.M., Zhuravleva T. B., Sakerin S. M. Estimates of the aerosol radiative forcing for three regions of World Ocean. *Atmospheric and Oceanic Optics*. 2013, Vol. 26. No. 6, p. 517–523.
157. Pol'kin, V.V., Pol'kin V.V., Panchenko M. V., Golobokova L. P. Comparative studies of optical and microphysical characteristics and chemical composition of aerosol over water basin of Caspian Sea in the 29th and 41st cruises of RV Rift. *Atmospheric and Oceanic Optics*. 2014, Vol. 27. No. 1, p. 16–23.
158. Pol'kin, V.V., Pol'kin V.V., Golobokova L. P. et al. On the interannual variability of the latitudinal distribution of microphysical and chemical parameters of near-water aerosol of Eastern Atlantic in 2006–2010. *Atmospheric and Oceanic Optics*. 2013. Vol. 26. No.6, p. 519–524 (in Russian).
159. Sakerin, S.M., Vlasov N.I., Kabanov D.M. et al. Results of spectral measurements of aerosol optical depth of the atmosphere with solar photometers during the 58th Russian Antarctic expedition. *Atmospheric and Oceanic Optics*. 2013. Vol. 26. No. 12, p. 1059–1067 (in Russian).
160. Shmirko, K.A., Pavlov A. N., Stolyarchuk S. Yu. et al. Variations of aerosol microphysical parameters in the ground atmospheric layer of the transitional zone “land–ocean”. *Atmospheric and Oceanic Optics*. 2013. Vol. 26. No. 8, p. 619–627 (in Russian).
161. Golobokova, L.P., Filippova U. G., Marinaite I. I. et al. Chemical composition of atmospheric aerosol above the Lake Baikal area. *Atmospheric and Oceanic Optics*. 2011. Vol. 24. No. 3, p. 236–241 (in Russian).
162. Pavlov, V.E., Golobokova L. P., Zhamsueva G. S. et al. Correlation ratios between concentrations of ions in dissolved fractions of aerosols at the Asian continent. *Atmospheric and Oceanic Optics*. 2011. Vol. 24. No. 6, p. 483–487 (in Russian).
163. Pol'kin, V.V., Golobokova L. P. Comparative analysis of aerosol chemical compositions in complex experiments in Primorje. *Atmospheric and Oceanic Optics*. 2011. Vol. 24. No. 8, p. 675–683 (in Russian).
164. Zhamsueva, G.S., Zayakhanov A. S., Starikov A. V. et al. Results of studies of the ionic composition of aerosols in Mongolia. *Atmospheric and Oceanic Optics*. 2013. Vol.26. No. 6, p. 472–477 (in Russian).
165. Zhamsueva, G.S., Zayakhanov A. S., Starikov A. V. et al. Chemical composition of aerosols in the atmosphere of Mongolia. *Russian Meteorology and Hydrology*. 2012. Vol. 37. No. 8, p. 546–552.
166. Gruzdev A. N. Weekly Cycle in the Atmosphere. *Doklady Earth Sciences*. 2011. Vol. 439. No. 1, p. 1034–1038
167. Gruzdev A. N. Analysis of the Weekly Cycle in the Atmosphere near Moscow. *Izvestiya, Atmospheric and Oceanic Physics*. 2013. Vol. 49, No. 2, p. 137–147.
168. Sitnov S. A. Weekly variations in temperature and precipitation in Moscow: Relation with weekly cycles of air pollutants and synoptic variability. *Izvestiya, Atmospheric and Oceanic Physics*. 2011. Vol. 47. No. 4, p. 445–456.
169. Gryazin, V.I., Beresnev S. A. About vertical motion of fractal-like particles in the atmosphere. *Atmospheric and Oceanic Optics*. 2011. Vol. 24. No. 6, p. 506–509 (in Russian).

170. Isakov A.A., A.V. Tikhonov. Relationship between aerosol parameters and air masses in central Russia. *Atmospheric and Oceanic Optics*. 2014. Vol. 27. No. 6, p. 475–478.
171. Lapshin V.B., Paley A.A., Balyshv A. V. et al. Evolution of nanometer-size aerosol in dry and humid environment under the influence of corona discharge. *Atmospheric and Oceanic Optics*. 2012. Vol. 25. No. 2, p. 171–175.
172. Plaude N.O., Stulov E.A., Parshutkina I. P. et al. Precipitation effects on aerosol concentration in the atmospheric surface layer. *Russian Meteorology and Hydrology*. 2012. Vol. 37. No. 5, p. 324–331.
173. Bizin S.A., Popova M.A., Chankina O.V. et al. The effect of forest fires on mass concentration, disperse and chemical composition of atmospheric aerosols on a regional scale. *Atmospheric and Oceanic Optics*. 2013. Vol. 26. No. 6, p. 484–489 (in Russian).
174. Gorchakov G.I., Sitnov S.A., Sviridenkov M.A. et al. Satellite and ground-based monitoring of smoke in the atmosphere during the summer wildfires in European Russia in 2010 and Siberia in 2012. *International Journal of Remote Sensing*. 2014. Vol. 35. No. 15, p. 5698–5721.
175. Kozlov V.S., Yausheva E. P., Terpugova S.A. Optical-microphysical properties of smoke haze from Siberian forest fires in summer 2012. *International Journal of Remote Sensing*. 2014. Vol. 35. No.15, p. 5722–5741.
176. Rakhimov, R.F., Kozlov V.S., Panchenko M.V. et al., Properties of atmospheric aerosol in smoke plumes from forest fires according to spectronephelometer measurements. *Atmospheric and Oceanic Optics*. 2014. Vol. 27. No. 3, p. 275–282.
177. Smolyakov, B.S., Makarov V.I., Shinkorenko M.P. et al. Effects of Siberian wildfires on the chemical composition and acidity of atmospheric aerosols of remote urban, rural and background territories. *Environmental Pollution*. 2014. Vol.188, p. 8–16.
178. Tomshin, O.A., Protopopov A. V., Solovyev V.S. Study of atmospheric aerosol and carbon monoxide variations over forest fires. The contemporary problems of the Earth remote sensing. 2012. Vol. 27. No.7, p. 145–150 (in Russian).
179. Tomshin, O.A., Solovyev V.S. Studying of variations of atmospheric aerosol properties caused by large-scale forest fires in Central Yakutia (2002). *Atmospheric and Oceanic Optics*. 2014. Vol. 27. No. 3, p. 634–639 (in Russian).
180. Tomshin, O.A., Solovyev V.S. The impact of large-scale forest fires on atmospheric aerosol characteristics. *International Journal of Remote Sensing*, 2014. Vol. 35. No. 15, p. 5742–5749.
181. Chubarova, N.E., Gorbarenko E. V., Nezval' E.I., Shilovtseva O.A. Aerosol and radiation characteristics of the atmosphere during forest and peat fires in 1972, 2002, and 2010 in the region of Moscow. *Izvestiya. Atmospheric and Oceanic Physics*. 2011. Vol. 47. No 6, p. 729–738.
182. Gorchakov, G.I., Sviridenkov M.A., Emilenko A.S. et al. Optical and microphysical parameters of the aerosol in the smoky atmosphere of the Moscow region in 2010. *Doklady Earth Sciences*. 2011. Vol. 437. No. 2, p. 513–517.
183. Gorchakov, G.I., Semoutnikova E. G., Isakov A.A. et al. Moscow smoky haze of 2010. Extreme aerosol and gaseous air pollution in Moscow region. *Atmospheric and Oceanic Optics*. 2011. Vol. 24. No. 6, p. 452–458 (in Russian).

184. Gorchakova, I.A., Mokhov I.I. The radiative and thermal effects of smoke aerosol over the region of Moscow during the summer fires of 2010. *Izvestiya Atmospheric and Oceanic Physics*. 2012. Vol. 48. No. 5, p. 496–503.
185. Popovicheva, O., Kistler M., Kireeva E. et al. Physicochemical characterization of smoke aerosol during large-scale wildfires: Extreme event of August 2010 in Moscow. *Atmospheric Environment*. 2014. Vol. 96, p. 405–414.
186. Sitnov, S.A. Analysis of satellite observations of aerosol optical properties and gaseous species over Central District of Russian Federation in the period of abnormally high summer temperature and mass wild fires in 2010. *Atmospheric and Oceanic Optics*. 2011. Vol. 24. No. 7, p. 572–581 (in Russian).
187. Sitnov, S.A., Gorchakov G.I., Sviridenkov M.A. et al. Aerospace monitoring of smoke aerosol over the European part of Russia in the period of massive forest and peat bog fires in July–August of 2010. *Atmospheric and Oceanic Optics*. 2013. Vol. 26. No. 4, p. 265–280.
188. Konovalov, I.B., Beekmann M., Kuznetsova I.N. et al. Atmospheric impacts of the 2010 Russian wildfires: integrating modeling and measurements of an extreme air pollution episode in the Moscow region. *Atmos. Chem. Phys*. 2011. Vol. 11, p. 10031–10056.
189. Parshutkina, I.P., Sosnikova E.V., Grishina N.P. et al. Atmospheric aerosol characterization in 2010 anomalous summer season in the Moscow region. *Russian Meteorology and Hydrology*. 2011. Vol. 36. No. 6, p. 355–361.
190. Chubarova, N.E, Nezval' E.I., Sviridenkov M.A. et al. Smoke aerosol and its radiative effects during extreme fire event over Central Russia in summer 2010. *Atmos. Meas. Tech*. 2012. Vol. 5, p. 557–568.
191. Sitnov, S.A., Gorchakov G.I., Sviridenkov M.A., Karpov A.V.. Evolution and radiation effects of the extreme smoke pollution over the European part of Russia in the summer of 2010. *Doklady Earth Sciences*. 2012. Vol. 446. No. 2, p. 1197–1203.
192. Plakhina, I.N., Pankratova N.V., Makhotkina E.L. Spatial variations in the air turbidity factor above the European part of Russia under conditions of abnormal summer of 2010. *Izvestiya. Atmospheric and Oceanic Physics*. 2011. Vol. 47. No. 6, p. 708–713.
193. Sitnov, S.A. Aerosol optical thickness and the total carbon monoxide content over the European Russia territory in the 2010 summer period of mass fires: Interrelation between the variation in pollutants and meteorological parameters. *Izvestiya. Atmospheric and Oceanic Physics*. 2011. Vol. 47. No. 6, p. 714–728.
194. Shukurov, K.A., Mokhov I.I., Shukurova L.M. Estimate for radiative forcing of smoke aerosol from 2010 summer fires based on measurements in the Moscow region. *Izvestiya, Atmospheric and Oceanic Physics*. 2014. Vol. 50. No. 3, p. 256–265.
195. Isakov, A.A., Anikin P.P., Elokhov A.S., Kurbatov G.A. On characteristics of smokes of forest and peat fires in Central Russia in summer of 2010. *Atmospheric and Oceanic Optics*. 2011. Vol. 24. No. 6, p. 478–482 (in Russian).
196. Golovko, V.V., Koutzenogii K.P. *Atmospheric and Oceanic Optics*. 2011. Vol. 24. No. 6, p. 525–528 (in Russian).

197. Golovko, V.V., Koutzenogii K.P., Bizin M.A., Popova S.A. Components of atmospheric aerosol in the Novosibirsk region in summer. *Atmospheric and Oceanic Optics*. 2013. Vol. 26. No. 3, p. 196–202 (in Russian).
198. Golovko, V.V., Koutzenogii K.P., Istomin I.I. Agglomerate composition of pollen aerosol in the atmosphere of Novosibirsk. *Atmospheric and Oceanic Optics*. 2014. Vol. 27. No. 6, p. 553–559 (in Russian).
199. Gorchakov, G.I., Karpov A.V., Kopeikin V.M. et al. Study of the dynamics of saltating sand grains over desertified territories K.P., Istomin I.I. Determination of the mass of individual pollen grains of Siberian plants. *Doklady Earth Sciences*. 2013. Vol. 452. No. 2, p. 1067–1073.
200. Gorchakov, G.I., Karpov A.V., Sokolov A.V. Experimental and theoretical study of the trajectories of saltating sand particles over desert areas. *Atmospheric and Oceanic Optics*. 2012, Vol. 25, No. 6, p. 423–428.
201. Gorchakov, G.I., Kopeikin V.M., Karpov A.V. et al. The specific charge of saltation sand particles in arid territories. *Doklady Earth Sciences*. 2014b, Vol. 456. No. 2, p. 700–704.
202. Chkhetiani, O.G., Gledzer E.B., Artamonova M.S., Iordanskii M.A.. Dust resuspension under weak wind conditions: direct observations and model. *Atmos. Chem. Phys.* 2012. Vol. 12, p. 5147–5162.
203. Chubarova, N.Y., Sviridenkov M.A., Smirnov A., Holben B.N. Assessments of urban aerosol pollution in Moscow and its radiative effects. *Atmos. Meas. Tech.* 2011. Vol. 4, p. 367–378.
204. Kireeva, E.D., Popovicheva O.B., Timofeev M.A., Shonija N.K.. Physical–chemistry of carbonaceous particles from ship exhaust. *Atmospheric and Oceanic Optics*. 2011. Vol. 24. No. 6, p. 459–467 (in Russian).
205. Kurgansky, M.V. On the vertical lifting of dust in a convective unstable atmospheric boundary layer. *Izvestiya, Atmospheric and Oceanic Physics*. 2014. Vol. 50. No. 4, p. 337–342.
206. Afonin, S.V. An appraisal of the method of AOD retrieval over land according to MODIS satellite measurements in IR spectral range. *Atmospheric and Oceanic Optics*. 2011. Vol. 24. No. 6, p. 584–586.
207. Antokhin, P.N., Arshinova V.G., Arshinov M. Yu., et al. Large-scale studies of gaseous and aerosol composition of air over Siberia. *Atmospheric and Oceanic Optics*. 2014. Vol. 27. No. 3, p. 232–239 (in Russian).
208. Antonnikova, A.A., Korovina N.V., Kudryashova O.B., Akhmadeev I.R. Experimental investigation of aerosol transformation processes under ultrasonic impact. *Atmospheric and Oceanic Optics*. 2012. Vol. 25. No. 7, p. 650–652 (in Russian).
209. Astashkina, M.S., Beresnev S.A., Safatov A.S., Buryak G.A. About opportunities of trajectory analysis methods for estimation of bioaerosol characteristics in the south of Western Siberia. *Atmospheric and Oceanic Optics*. 2011. Vol. 24. No. 8, p. 711–716 (in Russian).
210. Bedareva, T.V., Sviridenkov M.A., Zhuravleva T.B. Retrieval of aerosol optical and microphysical characteristics according to data of ground-based spectral

measurements of direct and scattered solar radiation. Part 1. Testing of algorithm. *Atmospheric and Oceanic Optics*. 2013. Vol. 26. No. 1, p. 24–34.

211. Bedareva, T.V., Sviridenkov M.A., Zhuravleva T.B. Retrieval of aerosol optical and microphysical characteristics according to data from ground-based spectral measurements of direct and diffuse solar radiation. Part 2. Algorithm testing. *Atmospheric and Oceanic Optics*. 2013. Vol. 26. No. 2, p. 107–117.

212. Bedareva, T.V., Zhuravleva T.B. Retrieval of aerosol scattering phase function and single scattering albedo according to data of radiation measurements in solar almucantar: Numerical simulation. *Atmospheric and Oceanic Optics*. 2011. Vol. 24. No. 4, p. 373–384.

213. Izrael, Y.A., Zakharov V.M., Petrov N.N. et al. A field experiment on modeling the impact of aerosol layers on the variability of solar insolation and meteorological characteristics of the surface layer. *Russian Meteorology and Hydrology*. 2011. Vol. 36. No. 11, p. 705–711.

214. Kazadzis, S., Veselovskii I., Amiridis V. et al. Aerosol microphysical retrievals from precision filter radiometer direct solar radiation measurements and comparison with AERONET. *Atmos. Meas. Tech*. 2014. Vol. 7, p. 2013–2025.

215. Kouznetsov, R., Sofiev M. A methodology for evaluation of vertical dispersion and dry deposition of atmospheric aerosols. *Journal of Geophysical Research: Atmospheres*. 2012. Vol. 117, p. D01202.

216. Kozlov, V.S., Panchenko M. V., Tikhomirov A.B. et al. Influence of the relative air humidity on results of photoacoustic measurements of aerosol absorption in atmospheric air. *Atmospheric and Oceanic Optics*. 2011. Vol. 24. No. 4, p. 323–327 (in Russian).

217. Matvienko, G.G., Belan B. D., Panchenko M. V. et al. Instrumentation complex for comprehensive study of atmospheric parameters. *International Journal of Remote Sensing*. 2014. Vol. 35. No. 15, p. 5651–5676.

218. Mikhailov, E.F., Merkulov V. V., Vlasenko S. S. et al. Filter-based differential hygroscopicity analyzer of aerosol particles. *Izvestiya. Atmospheric and Oceanic Physics*. 2011. Vol. 47. No. 6, p. 747–759.

219. Poddubny, V.A., Nagovitsyna E. S. Retrieval of spatial field of atmospheric aerosol concentration according to data from local measurements: A modification of the method of back trajectory statistics. *Izvestiya. Atmospheric and Oceanic Physics*. 2013. Vol. 49. No. 4, p. 404–410.

220. Rublev, A.N., Gorchakova I.A., Udalova T.A. The effect that coarse particles have on estimates of both optical and radiation characteristics of dust aerosol. *Izvestiya. Atmospheric and Oceanic Physics*. 2011. Vol. 47. No. 2, p. 190–200.

221. Smirnov, A., Holben B. N., Giles D. M. et al. Maritime aerosol network as a component of AERONET — first results and comparison with global aerosol models and satellite retrievals. *Atmos. Meas. Tech*. 2011. Vol. 4, p. 583–597.

222. Suvorina, A.S., Veselovskii I.A., Korenskii M. Yu., Kolgotin A. V. Use of a linear estimation method in calculation of integral parameters of atmospheric aerosol from spectral measurements of its optical depth. *Atmospheric and Oceanic Optics*. 2014. Vol. 27. No. 3, p. 237–246.

223. Sviridenkov, M.A., Verichev K. S., Vlasenko S. S. et al. Retrieval of atmospheric aerosol parameters from data of a three-wavelength integrating nephelometer. *Atmospheric and Oceanic Optics*. 2014. Vol. 27. No. 3, p. 230–236.
224. Veretennikov, V.V., Men'shchikova S. S. Features of retrieval of microstructural parameters of aerosol from measurements of aerosol optical depth. Part I. Technique for solving the inverse problem. *Atmospheric and Oceanic Optics*. 2013. Vol. 26. No. 6, p. 473–479.
225. Veretennikov, V.V., Men'shchikova S. S. Features of retrieval of microstructural parameters of aerosol from measurements of aerosol optical depth. Part II. Inversion results. *Atmospheric and Oceanic Optics*. 2013. Vol. 26. No. 6, p. 480–491.
226. Veretennikov, V.V., Men'shchikova S.S., Kabanov D.M., Sakerin S.M. Optical-microphysical properties of atmospheric aerosol from SP-6 and CE-318 sun photometers data. *Atmospheric and Oceanic Optics*. 2014. Vol. 27. No. 11, p. 1006–1016 (in Russian).
227. Yegorov, A.D., Potapova I.A., Rzhonsnitskaya Y.B. et al. Atmospheric aerosol measurements and the reliability problem: new results. *International Journal of Remote Sensing*. 2014. Vol. 35. No. 15, p. 5750–5765.
228. Jaroslavtseva, T.V., Raputa V.F. Numerical reconstruction of fields of losses of volcanic ashes. *Atmospheric and Oceanic Optics*. 2011. Vol. 24. No. 6, p. 521–524 (in Russian).
229. Kutsenogii, K.P., Kutsenogii P.K., Levykin A.I. Modeling of generation of the size-spectrum of nano- and submicron aerosols. *Atmospheric and Oceanic Optics*. 2011. Vol. 24. No. 9, p. 743–753 (in Russian).
230. Belov, V.V., Beloborodov V.E., Kabanov D.M. On a possibility of forecasting the aerosol optical thickness of the atmosphere based on the measurements of a Cimel CE-318 radiometer. *Atmospheric and Oceanic Optics*. 2012. Vol. 25. No. 1, p. 80–86 (in Russian).
231. Panchenko, M.V., Kozlov V.S., Polkin V.V. et al. Retrieval of optical characteristics of the tropospheric aerosol in West Siberia on the basis of generalized empirical model taking into account absorption and hygroscopic properties of particles. *Atmospheric and Oceanic Optics*. 2012. Vol. 25. No. 1, p. 46–54 (in Russian).
232. Yurova, A. Yu., Paramonov A. V., Konovalov I. B. et al. Forecast of the intensity of thermal radiation and aerosol emission from forest fires at the Central European region. *Atmospheric and Oceanic Optics*. 2013. Vol. 26. No. 36, p. 203–207 (in Russian)
233. Khvorostyanov, V.I., Curry J.A. *Thermodynamics, Kinetics, and Microphysics of Clouds*. New-York: Cambridge University Press. 2014. 800 pp.
234. Arkhipov, V.A., Berezikov A. P., Trofimov V.F., Usanina A. S. Experimental study of the loss of the droplet shape stability in a skirling flow. *Atmospheric and Oceanic Optics*. 2012. Vol. 25. No. 12, p. 1034–1038. (in Russian)
235. Balin, Yu.S. Kaul B. V., Kokhanenko G. P., Penner I.E. Observations of specularly reflective particles and layers in crystal clouds. *Optics Express*, 2011. Vol. 19. No. 7, p. 6209–6214.
236. Burnashov, A.V., Konoshonkin A.V. Matrix of light scattering on a truncated plate-like droxtal preferably oriented in a horizontal plane. *Atmospheric and Oceanic Optics*. 2013. Vol. 26. No. 3, p. 194–200.

237. Gatebe, C., Kuznetsov A. D., Melnikova I. N. Cloud optical parameters from airborne observation of diffuse solar radiation accomplished in USA and USSR in different geographical regions. *International Journal of Remote Sensing*. 2014. Vol. 35. No. 15, p. 5812–5829.
238. Genya, M.J., Kuznetsov A. D., Melnikova I. N. Considering uncertainties and regularizing the solution of the inverse problem of cloud optics in shortwave spectral ranges. *The contemporary problems of the Earth remote sensing*. 2013. Vol. 10. No. 4, p. 175–187.
239. Grinin, A.P., Gor G. Yu., Kuni F.M. On the theory of aerosol particle growth: Non-steady transport problems. *Atmospheric Research*. 2011. Vol. 101. No. 3, p. 503–509.
240. Kalinin, N.A., Smorodin B. L. Unusual phenomenon of freezing rain in Perm krai. *Russian Meteorology and Hydrology*. 2012. Vol. 37. No. 8, p. 521–528.
241. Prigarin, S.M., Bazarov K. B., Oppel U.G. Looking for a glory in A-water clouds. *Atmospheric and Oceanic Optics*. 2012. Vol. 25. No. 4, p. 256–262.
242. Shavlov, A.V., Dzhumandzhi V.A., Romanyuk S. N. Spatially ordered structures of water drops in clouds. *Cryosphere of the Earth*. 2011. Vol. 25. No. 4, p. 52–54 (in Russian).
243. Shavlov, A.V., Sokolov I. V., Romanyuk S. N., Dzhumandzhi V.A. Spatially ordered water drops in atmospheric fog. *Cryosphere of the Earth*. 2014. Vol. 28. No. 1, p. 39–46.
244. Troshkin, D.N., Kabanov M. V., Pavlov V.E., Romanov A. N. Function of distribution of clouds' optical thickness over the West Siberian Plain. *Doklady Earth Sciences*. 2011, Vol. 436. No. 1, p. 113–116.
245. Gladkikh, V.A., Nevzorova I. V., Odintsov S. L., Fedorov V.A. Structure functions of air temperature over an inhomogeneous underlying surface. Part I. Typical forms of structure functions. *Atmospheric and Oceanic Optics*. 2014. Vol. 27. No. 2, p. 147–153.
246. Gladkikh, V.A., Nevzorova I. V., Odintsov S. L., Fedorov V.A. Structure functions of air temperature over an inhomogeneous underlying surface. Part II. Statistics of structure functions' parameters. *Atmospheric and Oceanic Optics*. 2014. Vol. 27. No. 2, p. 154–163.
247. Glazunov, A. V. Numerical simulation of stably stratified turbulent flows over an urban surface: Spectra and scales and parameterization of temperature and wind-velocity profiles. *Izvestiya, Atmospheric and Oceanic Physics*. 2014. Vol. 50. No. 4, p. 356–368.
248. Glazunov, A. V. Numerical simulation of stably stratified turbulent fluxes over flat and urban surfaces. *Izvestiya, Atmos. and Oceanic Physics*. 2014. Vol. 50. No. 3, p. 236–245.
249. Novitsky, M.A., Gaitandzhiev D. E., Mazurin N.F., Matskevich M. K. Turbulence characteristics in the coastal zone with breeze circulation. *Russian Meteorology and Hydrology*. 2011. Vol. 36. No. 9, p. 580–589
250. Novitsky, M.A., Mazurin N. F., Kulidzhanova L. K. et al. Vertical variability of turbulence characteristics during cold atmospheric front traveling, based on weather tower measurements in Obninsk. *International conference "Turbulence, atmosphere and climate dynamics"*, Moscow, 13–16 May, 2013. Abstracts. M. 2013, p. 36–37 (in Russian).
251. Strunin, A. M. Cloud water content effects on computing spectral characteristics of temperature fields and turbulent heat fluxes in the cumulus cloud zones as derived

from airborne observations. *Russian Meteorology and Hydrology*. 2013. Vol. 38. No. 7, p. 472–479.

252. Strunin, M. A. Measurements of turbulence in a cloudy atmosphere aboard an aircraft laboratory. Moscow, Publ. “Prist”, World of Measurements, No. 9, 2011, p. 9–19.

253. Strunin, M. A. Turbulence in a cloudy atmosphere (in and around clouds). An empirical model of turbulence in a cloudy atmosphere. Handbook of scientists and engineers-meteorologists. 2013a. M: DPS Ltd. 174 p (in Russian).

254. Ashabokov, B.A., Zalikhanov M. Ch., Tapaskhanov V.O. et al. About a condition of researches on the physics of thunderstorm clouds and active Influences on them. *Bulletin of Universities. Northern Caucasian region. Natural sciences*. 2012. No. 5, p. 43–45.

255. Tashilova A.A., Khuchunaev B.M. Regression analysis of atmospheric parameters, leading to the formation of different types of hail seed. *Bulletin of Kabardino-Balkaria scientific center of RAS*. 2011. No. 6, p. 107–115 (in Russian).

256. Kamalov, B.A. On mechanism of hail cloud modification by seeding. *Russian Meteorology and Hydrology*. 2011. Vol. 36. No. 9, p. 608–612.

257. Plusnin, S.D., Potapov E.I., Garaba I.A., Popova V.P. Forecast of convective storms evolution based on the analysis of their radar echo and wind hodograph in the troposphere in the moving coordinate system. *Russian Meteorology and Hydrology*. 2013. Vol. 38. No. 7, p. 465–471.

258. Doronin, A.P., Belevich M. V., Goncharov I. V. et al. Recommendations for the use of methods of convective cloudiness seeding for the applied problems solving. Proceedings of 23rd All-Russian interuniversity scientific and practical conference. Kazan. 16–28 May 2011. Kazan, 2011, p. 161–163 (in Russian).

259. Kozlov, V.N., Mazurov G. I., Akselevich V. I. Artificial regulation of heavy snowfalls over the cities. In: *Radar Meteorology and Weather Modification*. Saint-Petersburg: Roshydromet. 2012, p. 84–97 (in Russian).

260. Beryulev, G.P., Borisov Yu.A., Danelyan B. G. Major principles of development and optimal operation of drought control in Russia with rainfall augmentation. Proceedings of the International conference “Innovative methods of research in the atmospheric physics, hydrometeorology, ecology and climate change”. Stavropol, 2013, p. 17–19 (in Russian).

261. Koloskov, B.P., Korneev V.P., Shchukin G.G. Methods and instruments of clouds, precipitation and fog modifications. Saint-Petersburg: Russian State Hydrometeorological University. 2012, 343 p.

262. Mamuchiev, I.M., Kalov Kh.M. Numerical modeling of active influences on low stratiform clouds and fogs by artificial water droplets. Proceedings of Adygeya (Cherkessia) International Academy of Sciences. 2011. Vol. 13. No. 2, p. 111–116 (in Russian).

263. Mamuchiev, I. M. Estimated accounts for development of a method of dispersion of warm fogs by artificial drops of water. *Transactions of the Main Geophysical Observatory*. 2012. No. 566, p. 282–288 (in Russian).

264. Doronin, A.P., Makarov A.V., Sheremet’ev R.V., Kalov R. Kh. Development of recommendations on optimization of the use of methods and tools stratiform clouds seeding. *Bulletin of Kabardino-Balkaria scientific center of RAS*. 2011. No. 5, p. 57–65.

265. Pashkevich, M. Yu., Berezinskiy N.A., Berezinskiy I.N. et al. Results of natural experiments on translucence of «warm» stratiform cloud cover in foothill zone. *Geology and geophysics of South Russia*. 2012. No. 1, p. 50–58 (in Russian).
266. Krauss, T.W., Sin'kevich A.A., Burger R. et al. Investigation of the impact of dynamic factors on Cb cloud development in Saudi Arabia. *Russian Meteorology and Hydrology*. 2011. Vol. 36. No. 10, p. 643–652.
267. Krauss, T.W., Sin'kevich A.A., Ghulam A.S. Radar investigations of cloud merger. *Russian Meteorology and Hydrology*. 2012. Vol. 37. No. 9, p. 604–614.
268. Sin'kevich, A.A., Krauss T. W., Ghulam A. S., Kurov A. B. Investigation of high-depth cumulonimbus clouds characteristics after seeding to increase precipitation. *Russian Meteorology and Hydrology*. 2013. Vol. 38. No. 9, p. 587–597.
269. Vardanyan, A.A., Galechyan G.A. Flows of negative ions for stimulation of the precipitation. *International scientific journal for alternative energy and ecology*. 2012. No. 8, p. 86–90 (in Russian).
270. Avakyan, S.V. Radiooptic mechanism of natural and artificial influence on weather-climate characteristics. *Proceedings of the 10th International conference “Research, development and application of high technology in the industry”*. Saint-Petersburg. 2010. Vol. 2, p. 108–112 (in Russian).
271. Adzhiev, A. Kh., Mashukov Kh.Kh. Experiments on the acceleration of the formation and separation of bulk electric charges in stratiform clouds. *Bulletin of Kabardino-Balkaria scientific center of RAS*. 2011. No. 6, p. 64–68 (in Russian).
272. Sin'kevich, A.A., Krauss T. W., Efficiency of convective clouds seeding by crystallized reagents for precipitation increase. In: *Radar Meteorology and Weather Modification*. Saint-Petersburg: Roshydromet. 2012, p. 30–49 (in Russian).
273. Belyaeva, M.V., Drofa A. S., Ivanov V.N. Efficiency of stimulating precipitation from convective clouds using salt powders. *Izvestiya, Atmospheric and Oceanic Physics*. 2014, Vol. 49. No. 2, p. 154–161.
274. Koloskov, B.P., Korneev V.P., Petrov V.V. et al. Some results of activities on the improvement of weather conditions over metropolises. *Russian Meteorology and Hydrology*. 2011. Vol. 36. No. 2, p. 117–123.
275. Malkarova, A.M. Estimation of physical efficiency of hail protection accounting for changes in hail climatology. *Russian Meteorology and Hydrology*. 2011. Vol. 36. No. 6, p. 392–398.
276. Pastushkov, R.S. An experience in the use of basic MGO units for numerical modeling of Cb seeding with ice-forming particles. *Proceedings of 7th All-Russian conference on atmospheric electricity*. Saint-Petersburg, 24–28 September, 2012, p. 181–183.
277. Vladimirov, S.A., Pastushkov R. S. Numerical modeling of Cb seeding with hygroscopic particles. *Proceedings of 7th All-Russian conference on atmospheric electricity*. Saint-Petersburg, 24–28 September, 2012, p. 40–50.
278. Zhekamukhov, M.K., Abshaev A.M. Dispersion of crystallizing reagents by detonation method. Part I: Detonation product expansion and kinetics of critical-size embryo droplet formation. *Russian Meteorology and Hydrology*. 2012. Vol. 37. No. 7, p. 448–454.

-
279. Zhekamukhov, M.K., Abshaev A. M. Dispersion of crystallizing reagents by detonation method. Part II: Computation of condensation growth of embryo droplets and their further enlargement using the simplified Brownian coagulation scheme. *Russian Meteorology and Hydrology*. 2012. Vol. 37. No. 8, p. 529–536
280. Zhekamukhov, M.K., Abshaev A. M. Dispersion of crystallizing reagents by detonation method. Part III: Complex scheme of Brownian coagulation and formation of ice-forming particle spectrum *Russian Meteorology and Hydrology*. 2012. Vol. 37. No. 9, p. 615–623.
281. Dinevich, L.A., Ingel L. Kh., Khain A. Evaluation of ice-forming particles from round generators. *Modern high technologies*. 2013. No. 13, p.14–25 (in Russian).
282. Drofa, A.S., Eran'kov V.G., Ivanov V.N. et al. Experimental investigations of the effect of cloud-medium modification by salt powders. *Izvestiya, Atmospheric and Oceanic Physics*. 2014, Vol. 49. No. 3, p. 298–306.
283. Chastukhin A. V., Kim N. S., Korneev V. P. et al. Laboratory research of the action mechanisms of powdered reagents promising for clouds and fog seeding. *Proceedings of the International conference “Innovative methods of research in the atmospheric physics, hydrometeorology, ecology and climate change”*. Stavropol, 2013, p. 179–182.
284. Vatiashvili M.R. Influence of water phase transition on parameters of clouds and cloud systems, which develop under natural conditions and under seeding with ice-forming particles. In: *Radar Meteorology and Weather Modification*. Saint-Petersburg: Roshydromet. 2012, p. 162–177 (in Russian).

Dynamic Meteorology

M. V. Kurgansky¹, V. N. Krupchatnikov^{2,3}

¹A. M. Obukhov Institute of Atmospheric Physics RAS
kurgansk@ifaran.ru

²Siberian Regional Scientific Research
Hydrometeorological Institute

³Institute of Computational Mathematics
and Mathematical Geophysics SB RAS
vkrupchatnikov@yandex.ru

Introduction

Scientific work in the field of dynamical meteorology, which has been carried out by the Russian researchers in 2011–2014 and will be discussed in this review can be conditionally be related to the following topics: “General dynamics of the atmosphere”, “Large-scale processes and the weather forecast”, “Mesoscale processes”, “Turbulence in the boundary layer”, “Dynamical interaction between lower, middle and high atmosphere”, “Mathematical problems of climate and ecology”. The review structure follows mainly the previous review report over 2007–2010 (Lykossov and Krupchatnikov, 2012).

1. General dynamics of the atmosphere

During May 13–16, 2013 an International conference “Turbulence, Dynamics of Atmospheric and Climate” took place in Moscow, which was devoted to the memory of Academician A. M. Obukhov and was dealing to the research in the atmospheric physics, environment and climate. The organizers of the Conference were the A. M. Obukhov Institute of Atmospheric Physics, Russian Academy of Science (RAS), The Earth Science Section of RAS, RFBR — the Russian Foundation for Basic Research. Alexandr Mikhailovich Obukhov (05.05.1918–12.03.1989) is an outstanding scientist of the modern time, the creator together with Andrey Nikolaevich Kolmogorov of the small-scale turbulence theory and one of the creators, together with C.-G. Rossby, J. Charney, A. Eliassen and few others, of modern geophysical fluid dynamics, as a science. The Conference program included plenary reports of leading Russian scientists and there were also 124 oral and 34 poster talks in the framework of six separate Conference sections: Turbulence, Geophysical Fluid Dynamics, Dynamics of the Atmospheric and Climate System, Atmospheric Physics and Composition, Atmosphere-Ocean Interaction, Wave Propagation. The contributions presented contemporary achievements in the above mentioned areas of

science and their perspectives. The collection of the most important papers is published in (Turbulence, Dynamics of Atmospheric and Climate, 2014), and several papers, explicitly cited below in the current review, belong to this collection.

Publisher URSS (<http://www.URSS.ru>) publishes a series of books under the title “Sinergetics: from past to future.” In this book series a book of outstanding Russian scientist, Academician Golitsyn G. S. “Statistics and Dynamics of Natural Processes and Phenomena: Methods, Tools and Results” has been published (Golitsyn, 2013). The majority of processes in Nature are stochastic and described by probability distributions and their moments: mean values, variances, spectra and higher moments. Quite often, in certain intervals, their empirical distributions are power laws: small-scale turbulences, frequency-size distributions for earthquakes, volcanic eruptions or floods, cosmic rays spectrum and many others. The book describes study methods for such processes and explains the distribution shapes for the above processes on a single base. It is worth noting that for the last four processes it is done for the first time ever. Some general rules and models are proposed formulated by the author as “the rule of the fastest response of a system to an external forcing” and “the random walks in the momentum space”. From these positions the author reformulates some of his previous results such as similarity theory for atmospheric circulation, convection and turbulence in rotating fluids and many others. All this is illustrated by examples found in Nature. New results obtained by the author are related to the sea surface and air-sea interactions: energy cycle for the wind waves, eddy diffusion in their random field, some quantitative conditions for the origin and development of hurricanes, problems of galaxies and clusters evolution.

The classic chapter of general dynamics of the atmosphere is the dynamics of large-scale atmospheric processes, which is widely used in the theory of climate (e.g., in the frame of the theory of dynamical systems).

Various geometrical approximations for the rotating shallow water equations are considered in (Medvedev, 2013). The first approximation is a transformation from the equations on the ellipsoid to the equations on the sphere. The second approximation is to proceed from the equations on the sphere to the equations on the tangent plane or the surface. The approximate equations for all geometric approximations are obtained. The main requirement for constructing these approximations is a conservation of the Hamiltonian structure. This goal was achieved in two ways. First, because the metric tensor of the surface determines the Hamiltonian structure of the equations on it, so the first way was to appropriately choose the approximate equations, part of the complete system, which is associated with the corresponding expansion of the metric tensor. Second, it was observed that the Poisson bracket for the covariant components of the velocity

is almost independent of the Lamé coefficients, so the Hamiltonian contains the main dependence on the Lamé coefficients and all approximations can be reduced to the expansion of this Hamiltonian.

Dymnikov (2012) has estimated the dependence on Grashof number of the dimension of the attractor (generated by the two-dimensional equations of the dynamics of a viscous incompressible fluid on a rotating sphere) in cases where either the energy or the enstrophy cascade determines the dissipation scale.

The theory of chaotic dynamical systems gives many tools that can be used in climate studies. These tools include a procedure that involves an expansion in terms of unstable periodic orbits (UPOs). In (Gritsun, 2013), the idea of UPO expansion is applied to the simple atmospheric system based on the barotropic vorticity equation of the sphere. It is checked how well orbits approximate the system attractor, its statistical characteristics and PDF. The connection of the most probable states of the system with the least unstable periodic orbits is also analyzed.

Climate-system models use a multitude of parameterization schemes for small-scale processes. These should respond to externally forced climate variability in an appropriate manner so as to reflect the response of the parameterized process to a changing climate. Provided that the dynamics of the process in question is sufficiently stochastic, and that the external forcing is not too strong, the fluctuation–dissipation theorem (FDT) might be a tool to predict from the statistics of a system (e.g., the atmosphere) how an objectively tuned parameterization should respond to external forcing (e.g., by anomalous sea surface temperatures). In (Achatz et al., 2013) this problem is addressed within the framework of low-order (reduced) models for barotropic flow on the sphere, based on a few optimal basis functions and using an empirical linear subgrid-scale (SGS) closure. A reduced variant of quasi-Gaussian FDT (rqG-FDT) is used to predict the response of the SGS closure to anomalous local vorticity forcing. At sufficiently weak forcing, use of the rqG-FDT is found to systematically improve the agreement between the response of a reduced model and that of a classic spectral code for the solution of the barotropic vorticity equation.

Atmospheric convection is a fundamentally important mechanism responsible for the generation of kinetic energy of atmospheric motion, and several papers are devoted to its study.

Identification of key physical processes and mechanisms responsible for the spectral transfer of kinetic and available potential energy in a wide range of spatial scales (ranging from the general circulation of the atmosphere to the small-scale turbulence) is a fundamental problem of modern atmospheric physics and dynamic meteorology. Investigation of the spectral structure of the multi-scale atmospheric turbulence is conveniently carried out through the use of hierarchy of mathematical models of turbulence: a three-dimensional, mesoscale

and the quasi-two-dimensional, respectively. Glazunov et al., (2013) present some results of such research. With eddy-resolving (LES) model they study the thermal Rayleigh-Bénard convection in a doubly periodic channel with solid walls as an analog of multi-scale atmospheric turbulence. The “mesoscale” ratio of its horizontal to vertical dimensions ensured the existence of large-scale quasi-two-dimensional flow, whereas the size of the uniform computational grid of the tens of millions of grids made it possible to clearly reproduce the dynamics of small-scale three-dimensional turbulent component. Decomposition of studied turbulent flow into the barotropic and baroclinic components allowed proposing a scheme for the kinetic energy conversion in the system, which explains some of the spectral properties of the observed atmospheric turbulence.

Stationary convection in a rotating fluid uniformly heated from above and non-uniformly cooled from below has been studied analytically in the linear approximation by Ingel and Belyaeva (2011). As distinct from a number of previous works, the case of both stable background stratification and intense rotation around the vertical axis has been analyzed. One of the interesting properties of the solution found is that despite the stable stratification the temperature, pressure, and vertical velocity perturbations over the thermal inhomogeneities of the horizontal surface penetrate deep into the medium in the case of strong rotation (up to heights of the order of the horizontal scales of the inhomogeneities mentioned.) The ascending motions over the “warm spot” transport relatively cool fluid parcels upwards, so that beginning from a certain level a vast “cold” region can be formed, accompanied with the positive pressure deviation. This leads to the formation of the anticyclonic vortex perturbation.

Kalasnik and Chkhetiani (2013) considered the problem of convection in the horizontal fluid layer with a wavy lower boundary. It was shown that for the periodic temperature distribution with a certain phase shift given on the wavy boundary, a unidirectional horizontal flow arises in the fluid layer. The flow velocity linearly decreases with increase in altitude and depends on the relief distribution wavelength. There is an optimum wavelength (of the order of the layer thickness) at which the velocity reaches its maximum value. In Chkhetiani et al. (2013) the problem of stationary convective flows over a nonuniformly heated wavy surface is studied in the context of a simplified analytical model. It is shown that the horizontally periodic heating of such a surface can lead to a “thermal wind” effect, i.e., the generation of a uniform horizontal flow far from the surface.

The classical Rayleigh theory of convective instability of a viscous and heat conductive rotating atmospheric layer is generalized onto the case of water vapor phase transitions both for the precipitation convection (PC) (Shmerlin et al., 2012; Shmerlin and Kalashnik, 2013) and for the nonprecipitation (NPC) one (Shmerlin and Shmerlin, 2014). A principal difference is stated between moist

convection and dry Rayleigh convection, on the one hand, and PC and NPC, on the other hand. In particular, the instability region on the plane of model parameters turned out to generally consist of two sub-regions, in one of which the localized axisymmetric disturbances with a tropical cyclone (hurricane) structure have the highest growth rate. Depending on the anisotropy of turbulent mixing, the vortex scale changes from the scale of a single convective cloud (tornado) to the scale of a tropical cyclone. In case of PC the ascending motions on the axis of symmetry correspond to such disturbances, in case of NPC a spontaneous growth of localized vortices both with ascending and descending motions on the axis is possible. Under other parameters values in case of PC spatial periodic cloud structures (convective rolls or closed cloud cells) have the highest growth rate and in case of NPC — mesoscale systems of convective rolls or mesoscale cloud clusters with annular cloud structures.

Previous investigations using the numerical modeling of moist convection in the atmosphere found an interesting effect: clouds arising through the water vapor condensation shield partially the underlying surface and change its radiation balance. The vertical heat fluxes on the surface become horizontally inhomogeneous, that can exert a backward profound effect on the convection and dynamics of clouds, for example, a cloud “runs away from its own shadow”). The paper by Ingel (2014) is dedicated to the corresponding generalization of the classical Rayleigh problem on the convective instability of horizontal layer of a fluid. This generalization has as its objective to describe the effect mentioned above — the influence of partial surface shielding on convection. The results show that the given relatively small modification of the Rayleigh problem, taking into account the possibility of the horizontally shifted thermal response to the vertical motions, leads to qualitatively new results. There appears a new, easily realizable type of instability, for which the strengthening of disturbances moving horizontally is typical.

A statistical mechanism that explains the formation of probability distribution functions of thermals according to temperature fluctuations is considered by Vul'fson and Borodin (2012). In the proposed approach based on the Boltzmann–Jaynes variational method, a statistical ensemble of convective thermals is characterized by a class of stationary probability densities that depend on temperature fluctuations. It is assumed that the probability density functions of this class may depend on the potential energy, as well as on the available potential energy. For a class of stationary probability density functions, the entropy functional is defined to be an analogue of the Boltzmann H-entropy. The equilibrium distributions of thermals according to temperature fluctuations correspond to the most probable distributions that yield a maximum of the entropy functional. The exponential and normal distributions of thermals according to temperature fluctuation that are constructed using the variational method quite adequately

approximate field atmospheric observations, as well as the results of laboratory modeling.

The stratified two-component media (for example, salt marine water or wet air) can differ significantly by their general hydro-thermodynamic properties from “usual” fluids, whose density depends on temperature only. For example, temperature disturbances in such media can increase, in spite of hydrostatically stable stratification of density. The paper by Ingel and Kalashnik (2012) contains a review of some new physical mechanisms and phenomena found in the latest years: the unknown previously mechanisms of convective instability, hydrodynamic “memory” of two-component media, the possibility of temperature and admixture concentration breaks (jumps) formation, anomalous response of binary mixtures to mechanical and thermal forcing, effective “negative heat capacity”, etc.

A number of papers were devoted to the study of intense convective atmospheric vortices: tropical cyclones, tornadoes and dust devils.

In (Kalashnik and Kalashnik, 2011) analytical solutions to the equation of transfer of angular momentum are derived for several model streamfunction distributions imitating the TC radial circulation. The features of TC intensification are described on the basis of these solutions. In particular, for the TC typical steady radial circulation, cyclonic rotation in the axial zone of the vortex encompasses with time the entire troposphere. The low-level TC intensification is accompanied by an exponential growth of maximum tangential velocity and by shrinking of the radius of the maximum wind (vortex contraction). Numerical estimates are obtained which show that the Coriolis force plays a crucial role in TC cyclonic rotation. A rapid super-exponential growth of maximum vortex velocity is possible for a non-stationary (increasing) mass inflow. The influence of friction is also studied using a simple phenomenological model. In the frictional model it is found that for TC intensification the radial flow velocity at the lower level should be higher than a certain critical (threshold) value.

Yaroshevich and Ingel (2013) studied statistically diurnal variations in the maximum wind velocity in tropical cyclones, based on vast experimental material. They have found notable oscillations in the acceleration of rotation velocity (rate of variations in the maximum wind velocity), which are most pronounced in the periods of intensification and decay of the cyclones. The diurnal variations can differ notably in phase in different geographical conditions.

In Ingel (2014) attention is focused on a positive feedback that may play a significant role in intense vortices, such as tornadoes and, probably, tropical cyclones: namely the rotation suppresses turbulence which, in turn, may intensify rotation. Some simple models illustrate this phenomenon.

A class of exact solution of the gas dynamics equations with the linear dependence of the velocity components on the coordinates and a functional

arbitrariness in the density (entropy) distribution is constructed in Visseratin and Kalashnik (2014). Using this class of solution the characteristics are studied of acoustic oscillations occurring, when a swirling gas flow deviates from the steady cyclostrophic equilibrium regime, that is, the equilibrium between the pressure gradient and the centrifugal force. An expression for the fundamental oscillation frequency agreeing with the measurements is derived.

In Kurgansky et al. (2013) analyzed are large- and mesoscale atmospheric processes which preceded and accompanied the tornado formation on June 12, 2012 near Khanty-Mansiysk city (61°N) in West Siberia. Estimated are the possible trends in the nature of the atmospheric circulation over West Siberia accompanying the global warming during the 21st century which may contribute to a more regular tornado formation in such high-latitudinal regions, also due to the physiographic peculiarities of the region.

In Kurgansky (2012) theoretical predictions with regard to dust devil (apparent) angular size–frequency distribution are made and critically compared with Mars Exploration Rover (MER) Spirit optical observations. For an idealized horizontal viewing geometry one should expect that the number of dust devils having the apparent angular diameter greater than a given angle α is inversely proportional to α^2 . The actual dependency for Spirit dust devils is in between the inverse-squared and simple inverse laws, and close to the latter one for small and moderate angles α . It is emphasized that such a comparison can be considered as a benchmark for completeness and adequateness of dust-devil optical observations and correctness of competing analytical formulations for dust devil size–frequency distribution.

Intense atmospheric vortices are characterized by non-zero helicity of the velocity field. The following papers were devoted to the study of the dynamic aspects of helicity, which also have a general hydrodynamic value.

Based on results of direct numerical simulation of atmospheric flows, Levina and Montgomery (2011) proposed a helical scenario of tropical cyclogenesis and further vortex intensification. The main idea of the scenario consists in a specific topology of helical flows which is characterized by the linkage of vortex lines. Velocity fields resulting from a high resolution numerical simulation by the Regional Atmospheric Modeling System (RAMS) are used to calculate helical and other integral characteristics during a tropical cyclone formation. It is shown how non-zero mean helicity is generated by moist convective atmospheric turbulence, which implies a new flow topology with linked vortex lines. A possible role of vortical hot towers (VHTs) is discussed in generating the linkage.

Two results that are fundamentally different from what takes place in a dry atmosphere have been obtained by Kurgansky (2013) for adiabatic motions of unsaturated moist air: (1) the steady helical motion of moist air with collinear velocity and vorticity vectors everywhere is dynamically impossible; (2) the

spontaneous amplification (generation) of helicity in a moist air due to baroclinicity is dynamically and thermodynamically feasible. In the absence of helical flows passing through the boundary of the domain occupied by air flows, the difference between the values of integral helicity H at time instant t delaying at a small time interval from the initial instant t_0 (at which the instantaneous state of air motion is isomorphic either to a steady Beltrami flow or to an irrotational flow) and the initial value of H increases proportionally to $(t - t_0)^4$. The nonzero value of the proportionality factor is ensured by the difference in values of the Poisson ratio for dry air and water vapor, respectively.

Kurgansky (2014) discusses the general relationship between the concepts of helicity and potential vorticity in a compressible, rotating fluid. This paper also includes two sections that are based on materials which in the form, they are presented, have not been previously published in the literature. The first section deals with the formulation of Nambu brackets for two-component compressible media (moist air, and dusty dry air). The second section considers the question of the evolution of helicity in adiabatic motion of saturated moist air; concerning an unsaturated moist air to see Kurgansky (2013).

The self-similar relaxation of helicity in homogeneous turbulence has been considered in (Levshin and Chkhetiani, 2013) by taking into account integral invariants related to helicity. It has been shown that in addition to helical analogs of Loitsyanskii and Birkhoff-Saffman invariants, associated with the conservation laws of momentum and angular momentum, respectively, the new, unknown before, integral invariants for both helicity and energy are possible. Helicity always relaxes more rapidly than the energy. Its decay exponent is in the interval from $-3/2$ to $-5/2$ versus the interval from $-6/5$ to $-10/7$ for the energy.

Two distinct asymptotic solutions of the inviscid Boussinesq equations for a steady helical baroclinic Rankine-like vortex with prescribed buoyancy forcing are considered and critically compared in (Kurgansky, 2013). In both cases the relative distribution of the velocity components is the same across the vortex at all altitudes (the similarity assumption). The first vortex solution demonstrates monotonic growth with height of the vortex core radius, which becomes infinite at a certain critical altitude, and the corresponding attenuation of the vertical vorticity. The second vortex solution schematizes the vortex core as an inverted cone of small angular aperture. These idealized vortices are then embedded in a convectively unstable boundary layer; the resulting approximate vortex solutions have been applied to determine the maximum rotational velocity in vortices. The helicity budget of the vortex flow is analyzed in detail, where applicable.

Currently, there is a keen interest in a fundamental question on the possibility of a cyclone-anticyclone asymmetry, which is principally absent in the classical formulation, based on the use of the Charney–Obukhov equation for the quasi-geostrophic potential vorticity conservation.

It is stated in (Kalashnik, 2011) that cyclone–anticyclone asymmetry in a rotating fluid results in vortices with cyclonic rotation being attenuated more rapidly than vortices with anticyclonic rotation due to the Ekman bottom friction. To explain this effect, earlier authors invoked rather complex, averaged along the vertical, integral models with the parameterization of nonlinear friction. A simple analytical model, free of the procedure of formal averaging and based on a separate consideration of the equations for external flow in the inviscid region and internal flow in the boundary layer, is investigated in (Kalashnik, 2011). The corresponding equations are written in the so-called geostrophic momentum approximation. The nonlinear equation of the hyperbolic type for the tangential velocity, which describes the process of attenuation of an axisymmetric vortex, is obtained from the condition of total mass conservation. It was established that the concentration (compression) of anticyclonic vortices and the extension of cyclonic ones take place in the process of attenuation.

The manifestations of the cyclone-anticyclone asymmetry effect, which is observed in nature and in laboratory experiments with a rotating fluid, have been studied in (Kalashnik and Chkhetiani, 2014) from the standpoint of the vorticity evolution generalized equation. Under laboratory conditions, asymmetry is observed as a faster decay of cyclonic vortices as compared to anticyclonic ones. This effect has been analytically described based on the analysis of the vortex spot decay and of spatially periodic vortex lattice. It has been indicated that anticyclonic vortices compress and cyclonic ones expand when a lattice damps. Examples of exact solutions of the vorticity equation (describing, specifically, collapsing of an axisymmetric vortex core with anticyclonic vorticity) have been constructed. The effect of the Ekman friction on the interaction between singular vortices is discussed.

A series of studies on the generation of waves by moving sources and vortices has been carried out.

A general approach based only on the law of wave dispersion is proposed. It allows one to describe the phase structure of wave perturbations induced by moving localized sources. A simple analytic expression is obtained for the phase surfaces in the frameworks of the approach proposed. On the basis of this expression studied are the peculiarities of the phase patterns of the gravity–capillary waves, the structures of the wave traces in the ocean left by moving tropical cyclone (hurricane) and the systems of leeward waves in the Earth’s atmosphere (Svirkunov and Kalashnik, 2012, 2014). The phase pattern of inertia–gravity waves that form a wake in the ocean behind a moving hurricane is also investigated using a kinematic theory. In the framework of the two-layer ocean model, simple analytical expressions are obtained for phase surfaces (surfaces of the ridges and troughs of wave structure) and the dependence of the semi-angle of a wave cone on the speed of the hurricane is determined. It is shown that the

observed asymmetry of the wave wake in the horizontal plane may be related to inhomogeneity in the distribution of the Coriolis parameter with latitude (Kalashnik and Svirkunov, 2014).

In the gravity field, the rotating fluid possesses its own wave motion (inertia-gravity waves). In the presence of shear flows, these waves can be trapped (localized) within the shear layer. Within the framework of the linearized system of fluid dynamical equations Kalashnik (2011) constructed analytical solutions describing the structure of the trapped waves. The propagation and trapping of wave packets is investigated in the framework of the wave ray theory. The process of propagation and trapping of inertial gravity wave (IGW) packets in oceanic shear flows has also been studied in (Kalashnik, 2013) in the geometrical optics approximation (ray theory).

A linear problem of oscillations of an interface in a two-layer system, in which the upper layer is at rest and the lower layer has a constant velocity shear, is considered in (Kalashnik and Chkhetiani, 2014). The dynamic perturbations in the lower layer are represented as the sum of vortex and wave disturbances (disturbances with zero vorticity). It is shown that in the shear flow the evolution of the vortex disturbances with a non-smooth or a singular initial vorticity distribution can result in the resonant excitation of waves on the interface. The occurrence of the resonance corresponds to the coincidence of the oscillation frequencies of the perturbations of both classes. In the absence of hydrodynamic instability of the shear flow, the resonant excitation can be one of the main mechanisms of wave generation in two-layer systems.

A mechanism of internal gravity wave generation by eddy perturbations in a horizontal flow with a vertical shear has been investigated in (Kalashnik, 2014). It was assumed that a shear flow is localized in the atmospheric boundary layer with neutral stratification, over which there is a semi-bounded stratified layer moving at a constant velocity. It is shown that the propagation of vortex perturbations in the boundary layer is inevitably accompanied by wave generation. On the basis of a linearized system of hydrodynamic equations, an integro-differential equation is formulated for finding wave characteristics. A wave field excited by a vortex perturbation with an initial singular vorticity distribution is studied. Numerical estimates are obtained for the vertical energy flow density vector component characterizing the wave energy transport to the upper atmosphere.

Traditionally, important foci of research by dynamic meteorologists are the “shallow water model” and quasi-two-dimensional turbulence.

Laboratory measurements of decaying quasi-two-dimensional turbulence in thin fluid layers with various depths have been performed by Kostykin et al. (2012). It has been shown that decay at large Reynolds numbers corresponds to a non-linear bottom friction with the coefficient satisfying the law following from theoretical estimates, including the proportionality to $|K|^{1/4}$, where K is the Okubo-Weiss

function depending on the enstrophy and degree of ellipticity of vortices. It has been shown that the structure of the flow changes in the decay process.

The mechanisms and structural elements of an instability whose development results in the collapse of flow fragments have been studied in (Goncharov, 2011) in the frame of the Hamilton version of the “shallow water” 3D model on a slope. The study indicated that the 3D model differs from its 2D analog in a more varied set of collapsing solutions. In particular, the solutions describing anisotropic collapse, during which the area of a collapsing fragment in contact with the slope contracts into a segment rather than a point, exist together with the solutions describing radially symmetric (isotropic) collapse. The mechanisms of instability, whose development leads to the occurrence of the collapse (blow up) have been studied in the scope of the rotating shallow water flows with horizontal density gradient. Analysis shows that collapses in such models are initiated by the Rayleigh-Taylor instability and two scenarios are possible. Both the scenarios obeys a power law for the period of time remaining before the collapse, with indices -1 , -2 and $-2/3$, -1 for the isotropic and anisotropic collapses, respectively. The rigorous criterion of collapse is found on the base of integrals of motion (Goncharov, Pavlov, 2012, 2014).

Diffusion processes of various admixtures in geophysical media have been studied; cf. Golitsyn (2013).

The classical problem of heat transfer or tracer dispersion in a homogeneous medium has been thoroughly investigated. However, the actual detection of temperature perturbations or diffusion tracers is associated with the sensitivity of the measuring instrument, which has a threshold value. In view of this circumstance, Chkhetiani and Golitsyn (2014) analyze solutions for Green’s function (impulsive point source) and for the case of a constant perturbation source, which reveal the temporal behavior of the boundaries of instrumentally detected tracer spots and their life-times. Solutions are also analyzed with a coordinate dependent diffusion coefficient in the one dimensional case and for cylindrical symmetry.

In the problem of admixture diffusion on the sea surface in the presence of wind waves, it has been indicated that the potential flow is disturbed when viscosity in the wind-generated wave velocity field is taken into account. Modeling indicates that this allows a fluid particle to pass from one wave into another wave, as a result of which diffusion is maintained on the water surface. A distance between initially adjacent fluid particles increases in time, which is also evidence of diffusion. Observational data coincide with calculations if viscosity about turbulent, i.e., several $\text{cm}^2 \text{s}^{-1}$, is introduced. The study was performed because liquid particles do not go beyond a wave (i.e., diffusion is formally impossible) in the classical potential theory of sea waves (Golitsyn and Chkhetiani, 2014).

There are also papers on the general dynamics of the atmosphere, which can conditionally be classified as “Miscellaneous”.

In (Ingel, 2011) the classic Prandtl slope flow model is generalized to include nonlinear turbulent friction and rotation. Several general regularities are established. In particular, a universal expression for the mass flux along the slope and a relationship between the surface velocity components, both independent of the friction law, are obtained. The applicability of the model to describing katabatic winds on fairly large horizontal scales is discussed.

When heavy particles move in a shear flow, the drag depends on the Reynolds number and, hence, on the magnitude of the particle velocity relative to the medium. This leads to a nonlinear interaction between various components of motion. For example, when a particle precipitates in a horizontal air flow with vertical shear, it also acquires horizontal motion relative to air in addition to vertical motion. These two components of motion contribute to the hydrodynamic drag coefficient by affecting the Reynolds number and thereby influence each other. Steady motion of a particle in a flow with constant vertical shear is analyzed. Dimensionless criterion of significance of the nonlinear effect under consideration is determined. It is demonstrated that this effect can be significant in the near-surface atmospheric layer in the case of storm wind (Ingel, 2012).

For the first time in the literature, Ingel and Macosco (2014a, b) analytically calculated the linear disturbances induced by inhomogeneities of the gravity force field in a stratified rotating medium. The interaction of a geostrophic current with gravity force anomalies in the model considered here can lead to notable generation of velocity disturbances. The physical mechanisms of the generation of these disturbances have been studied.

2. Large-scale processes and the weather forecast

Problems, recently acquired greater urgency, are to study the mechanisms of extreme weather events, such as an extraordinary heat wave in the summer of 2010 over the European part of Russia.

In Shakina et al. (2011) quantitative characteristics are presented of weather in anomalously hot and dry summer of 2010 as caused by a blocking high of extraordinary intensity and life duration. The features of the blocking high are considered within a context of present-day concepts in climatology, genesis, mechanisms of maintaining the blocking highs, along with possibilities of their forecasting. As the main cause of the blocking high generation, nonlinear instability of the Rossby waves has been suggested, associated with intense energy exchange both with planetary waves and synoptic-scale eddies. The medium-range forecasting of the blocking highs, in the case of their absence in the initial fields, can be successful within projection of several days; the results are better in the case of ensemble forecasting than when single numerical models are

used. The blocking maintenance and the beginning of its decay can be successfully predicted within the medium-range time.

From the objective analysis data, the blocking criteria are calculated by Ivanova et al. (2011) for May to August 2010, 2002, and 2007, along with Hoskins quasi-vectors *E* and Eliassen-Palm fluxes. According to the blocking criteria by G. V. Gruza and by Tibaldi-Molteni, blocking at 500hPa is observed more frequently and during longer period, than the blocking as the Rossby wave breakdown at the dynamic tropopause (by Pelly-Hoskins criterion). The 2010 summer blocking was more long-living, reached higher latitudes and larger vertical extent than the blockings in 2002 and 2007. Energy supply from the synoptic eddies to the Rossby wave in all the cases could take place. In 2010 and 2002, the main “hot wave” in July-August was preceded by well-developed high in May, which contributed significantly to the development of subsequent summer drought.

Dynamic processes in the troposphere, i. e., wave trains, which could contribute to the blocking anticyclone (BA) formation and sustenance in the summer of 2010 over the European part of Russia, are investigated. In order to study these wave trains, three-dimensional Plumb vectors have been calculated and analyzed in Vargin et al. (2012). It is shown that, in June 2010, three wave trains propagated eastward in the troposphere over the Atlantic. The first two wave trains, having reached Europe, continued to propagate in eastern and southeastern directions. Only the third wave train, upon reaching Europe, continued to propagate toward the northeast and, on June 17–19, entered northwestern Russia. The anticyclone, which started to form on June 18 precisely in this region, subsequently developed into a stable BA observed over European Russia up to mid-August. The propagation direction of the wave trains could change due to the formation of a double structure of the zonal flow in the troposphere. The wave trains are revealed in the middle of June in regions with increased cloudiness over the northwestern part of the Atlantic Ocean and over the northwestern and northern parts of the central United States. Eastward propagating wave trains, which could contribute to the intensification of the corresponding BAs that brought anomalously high temperatures to European Russia, were also revealed in July and August of 2010 and 1972. The calculated 10-day backward trajectories are analyzed to determine the character of motions of air particles that penetrated into the anticyclone over the region of Moscow during the 2010 summer in the period of its development. Schneidereit et al., (2012) analyze the large-scale flow structure based on the ECMWF Re-Analysis Interim (ERA-Interim) data (1989–2010). The anomalous long-lasting blocking high over western Russia including the heat wave occurs as an overlay of a set of anticyclonic contributions on different time scales.

Detailed dynamic analysis of atmospheric blocking including in the summer of 2010 is given by Lupo et al. (2012, 2014a, b). Using NCAR-NCEP reanalysis

datasets, the climatological and dynamic character of blocking events for summer 2010 and a precursor May blocking event were examined. It was found that these events were stronger and longer lived than typical warm season events. Using dynamic methods, it was demonstrated that the July 2010 event was a synoptic-scale dominant blocking event; unusual in the summer season. An analysis of phase diagrams demonstrated that the planetary-scale did not become stable until almost one week after block onset. For all other blocking events studied here and previously, the planetary-scale became stable around onset. Analysis using area integrated regional enstrophy (IRE) demonstrated that for the July 2010 event, synoptic-scale IRE increased at block onset. This was similar for the May 2010 event, but different from case studies examined previously that demonstrated the planetary-scale IRE was prominent at block onset. During the 2010 summer, a severe drought impacted Western Russia, including regions surrounding Moscow and Belgorod (about 700 km south of Moscow). The drought was accompanied by high temperatures. Moscow recorded 37.8 °C (100°F) for the first time in over 130 years of record keeping. The excessive heat and humidity in Western Russia were the result of atmospheric blocking from June through mid-August. The NCAR-NCEP reanalyses were used to examine blocking in the Eastern European and Western Russia sector during the spring and summer seasons from 1970 to 2012. It was found that drier years were correlated with stronger and more persistent blocking during the spring and summer seasons. During these years, the Moscow region was drier in the summer and Belgorod during the spring seasons. In the Moscow region, the drier summers were correlated with transitions from El Niño to La Niña, but the opposite was true in the Belgorod region. Synoptic flow regimes were then analyzed and support the contention that dry years are associated with more blocking and El Niño transitions. The objective of (Mokhov et al., 2013) is to study variations in the characteristics of blockings with a lifetime of at least five days in the NH in 1969–2011. Also, possible variations in atmospheric blocking activity in the twenty-first century were analyzed by means of the model simulations under various anthropogenic scenarios. A more detailed analysis was performed for summer blockings in the Euro-Atlantic Region to estimate the risks and potential predictability of extremely long atmospheric blocking events. Hydrodynamic model of blocking formation, based on the fluid dynamical notion of singular vortices was proposed by Mokhov et al. (2013).

In (Shakina and Skriptunova, 2011) the method of the probabilistic forecast of precipitation on the basis of the output data of meso-scale models is offered (or global ones with high resolution). Similar approach can be used for the forecast of wind and other meteorological parameters. The method represents a variant of MOS-approach. On the basis of archive records about precipitation forecasts for a concrete model and of parallel station data on precipitation at each

square of the model grid, the spectrum of precipitation probabilities are obtained (with respect to intensity grades) for given gradation of predicted precipitation in the numerical model.

One of physical conclusions is that the grade of predicted precipitation in the model is not the most probable: as a rule, rainfall of the lower intensity grade is most probable. The review of a current state of knowledge of mechanisms and conditions of formation of the overcooled rainfall (causing sleet) and approaches to a problem of their forecasting is submitted. Algorithms of determination of rainfall type, i.e. differentiation of conditions of rainfall, snow, the freezing precipitation and ice grains are considered in details. Based on the example catastrophic sleet episode on December 25–26, 2010, a possibility of formation of the freezing rain and the freezing drizzle both in the presence of air layers with a positive temperature, and in their absence is shown. Possibility of the overcooled drops in a frontal cloudy system as a result of their transfer in the ascending warm air over a frontal inversion layer is discussed. In the course of rise and transformation this air acquires negative temperature (remaining warm in comparison with underlying and overlying layers). Such modification of “the classical mechanism” considering three-dimensional process (and not just stratification in a cloud over an observational point), generalizes the existing ideas of formation of the freezing rainfall (Shakina, etc., 2012).

Traditional research of various aspects of large-scale dynamics of the atmosphere was continued, including (but not being limited to) dynamics of atmospheric fronts, (dynamic) tropopause structure, etc.

Shakina, et al. (2014a, b) presented a review of quantitative characteristics of atmospheric frontogenesis as the process of changing of a vector of a horizontal temperature gradient (in magnitude and direction) in an individual air parcel. The review of the published results about calculations of components of a frontogenesis function F for particular processes according to real and model data are submitted. Calculations revealed the significance of frontogenesis as the cause of emergence of lows and highs on a high-level frontal zone, a meandering and intensification of jet streams, origin and evolution of cyclones. The main quantitative characteristics of a frontogenesis vector function are its projections onto the potential temperature isoline in an isobaric surface and onto a normal to this isoline. The first component describes the frontogenetic effect of rotation isotherms (rotational frontogenesis) and the second one is a measure of change of the modulus of a horizontal gradient of temperature (scalar frontogenesis). Preliminary results about calculations of frontogenesis characteristics for a case of large-amplitude wave on a high-level frontal zone with an intensive jet stream and deep stratospheric intrusion are presented. It is shown that descending of a tropopause on the cold side in an entrance of area of the maximum wind on almost straight section of a high-level frontal zone is caused mainly by a scalar

frontogenesis whereas the rotational frontogenesis plays the main role in the field with abrupt turn of isohypses, causing intense ascending of air on the warm side of frontal zone and descending on the cold side. Comparison of calculations for data of the objective analysis and output data of global semi-Lagrangian model of the atmosphere shows that the model qualitatively correctly reproduces the jet stream, the tropopause topography and the effects of frontogenesis, but quantitatively the forecast fields are considerably smoother.

A method of calculation of the tropopause slope on basis of data about its height presented on regular grid is proposed in (Ivanova, 2011). Based on NCEP2 reanalysis data over 1990–2007, the tilt angles of the tropopause are calculated by approximating it by different isoscalar surfaces of Ertel's potential vorticity in the latitude band 30–70°N.

To increase efficiency of regional models in analysis and forecast of global cyclonic activity the “seamless” algorithm of tracking of trajectories of cyclones of high latitudes with taking into account increasing resolution of regional model was proposed in (Shkolnik and Efimov, 2013). The structure of cyclonic activity depending on spatial resolution of models is investigated. Assessment of quality of model simulations and of reanalysis data for extreme cyclones, which study demands high temporal and spatial resolution, is given. Position of the polar front and its possible change over the European territory of Russia during the summer season are investigated, based on results of numerical climate modeling with the Main Geophysical Observatory regional climatic model for the midst of the XXI century. The simplest method of detection of the polar front on the synoptic map as loci of increased temperature gradients is considered. From model estimates, the polar front is more meridionally elongated compared with the climatological polar front specification by S. P. Khromov. Stability in position of the polar front during various climatological periods is revealed: in the middle of the XXI century it is possible to expect shift of area of the greatest gradients of temperature to the South by one degree relative to the position of similar area at the last decade of XX in (Cherenkova and the Shkolnik, 2012). Reaction of the polar atmosphere to reduction in the area and thickness of an ice cover in the Arctic and increase of oceanic surface temperature is investigated by means of atmospheric general circulation model given the boundary conditions (observation data of sea ice and temperature for the last three decades). Simulation results show that the reduction in the area of sea ice is the main factor of warming amplification in the Arctic. However, spatio-temporal distribution of warming is very non-uniform. To a large extent it is manifested in the fall and winter seasons and extends up to the height of 1 km in the areas of reduction or disappearance of sea ice. It is shown that increasing of ocean surface temperature also affects the Arctic warming. Global warming for the last decades was resulted by statistically significant changes in distribution of sea level pressure at and geopotential

heights in the polar region and midlatitudes in the fall, winter and spring. However, these changes are mainly caused by increase in ocean temperature, but not reduction in ice cover extent. None meaningful connections between anomalies of an ice cover in the Arctic and the time-evolution of perturbations of the synoptic-scale pressure field are found, which may contribute to the formation of cold weather regime during the Eurasian winter (Baydin and Meleshko, 2014). Influence was revealed of changes in ice cover over the Arctic on the atmospheric circulation and formation of anomalously cold weather over the Eurasian continent in the winter.

Papers by Akperov and Mokhov (2013) and Neu et al. (2013) are devoted to development of objective methods of assessment of cyclonic activity in extratropical latitudes.

The availability of observational data and the exponentially growing computational resources have together led to new approaches to resolve the withstanding problems of geophysical data assimilation. In the context of earth sciences, the temporal as well as spatial variability is an important and essential feature of data about the oceans and the atmosphere, capturing the inherent dynamical, multiscale, chaotic nature of the systems being observed. This has led to development of mathematical methods that blend such data with computational models of the atmospheric and oceanic dynamics — in a process called data assimilation — with the aim of providing accurate state estimates and uncertainties associated with these estimates.

In the following papers (Gorin and Tsyrlunikov, 2011; Tsyrlunikov and Gorin, 2013; Masutani et al., 2013; Klimova, 2011; Klimova, 2012; Klimova, etc., 2014) the description is given of new technologies of data assimilation on the basis of the known methods used in problems of a weather forecast.

Advanced Microwave Sounding Unit A (AMSU-A) observation-error covariances are objectively estimated by comparing satellite radiances with radiosonde data in (Gorin and Tsyrlunikov, 2011). Significant horizontal, inter-channel, temporal, and inter-satellite correlations are found. Besides, cross correlations between satellite and forecast (background) errors (largely disregarded in practical data assimilation) proved to be far from zero. The directional isotropy hypothesis is found to be valid for satellite error correlations. Dependencies on the scan position, the season, and the satellite are also checked. Bootstrap simulations demonstrate that the estimated covariances are statistically significant. The estimated correlations are shown to be caused by the satellite errors in question and not by other (non-satellite) factors.

In predictability experiments with simulated model errors (ME) and the COSMO model, reproducibility of ME from finite-time model-minus-observed tendencies is studied. It is found that in 1-h to 6-h tendencies, ME appear to be too heavily contaminated by noises due to, first, initial errors and, second, trajectory

drift as a result of ME themselves. The resulting reproducibility error is far above the acceptable level. The conclusion is drawn that the accuracy and coverage of current routine observations are far from being sufficient to reliably estimate ME (Tsyrlunikov and Gorin, 2013).

The Arctic is recognized as one of the key areas of the globe, both in terms of its sensitivity to climate change, and by the increasing economic activity that is expected with the opening up of Arctic areas in a warming climate. In addition, Arctic weather can have important influences in winter cold outbreaks of air which can affect Northern Hemisphere countries as far south as the subtropics with serious economic implications. Therefore, a revised assessment of Arctic satellite and surface observation capabilities and requirements is warranted, especially given the Arctic surface and upper air network is sparse. Observing System Simulation Experiments (OSSEs) are a powerful tool to assess added value of planned or hypothetical observing systems for weather analysis and prediction. The paper (Masutani et al., 2013) reviews the current state of OSSE science with respect to the Arctic, and provides lines of investigation for the future, with a focus on weather and air quality observations in the Arctic. Recommendations are based on perceived observation gaps in the Arctic, and the experience gained by the World Weather Research Programme — The Observing Systems Research and Predictability Experiments/Polar Prediction Project (WWRPTHORPEX/PPP) and the broader OSSE scientific community.

Observations are one of the major factors influencing result of data assimilation. Additional sources of observations, such as, for example, the data of airplanes recently have appeared. In this connection there was a problem of execution of additional observations for improvement of result of data assimilation. Such observations in the literature are named « adaptive observations » or « targeting observations ». In (Klimova, 2011) approaches to an estimation of areas of additional observations for increase of accuracy of the analysis and the forecast in data assimilation procedure are considered. The technique of planning of the observations network, using ensemble Kalman filter is offered. Results of numerical experiments on estimation of proposed algorithm properties with the use of barotropic quasi-geostrophic model are presented.

In (Klimova, 2012) sub-optimal algorithm for data assimilation based on the ensemble Kalman filter (EnKF) is proposed. An advantage of the algorithm is that it does not require an additional calculation of the ensemble of perturbations that corresponds to the analysis-error covariance matrix. With this algorithm it is calculated automatically. The operation count of the algorithm is close to that of the Local Ensemble Transform Kalman Filter (LETKF), but its formulas are different from those of LETKF.

The paper (Klimova et al., 2014) outlines the currently accepted approaches to solving the problem of data assimilation for the environment, based on the

ensemble Kalman filter. Along with the approximate description of the estimation error covariances using ensemble forecasts, on the basis of the control theory it is proposed to use sub-optimal algorithms in which the probability averaging is replaced by time-averaging, assuming the ergodicity of the forecast errors. An application of the assimilation algorithm, based on this approach to data on passive gas components in the atmosphere over the Siberian region and to the problem of simulating processes in the ocean is considered in the examples given in this article.

Results of use of three methods of calibration of ensembles in relation to the probabilistic monthly forecast of ground air temperature with weekly specification for the territory of Northern Eurasia are presented in (Mirvis et al., 2012). Considered are: nonparametric calculation of probabilities with correction of shift (NPKS), parametrical calculation with correction of shift and a standard deviation (PKSS), and also calculation of probabilities on the basis Bayesian model averaging. It is shown that for close results the calibration on the basis of the PKSS-VMA methods has clear advantage over the NPKS method.

Martynova et al., (2014) considered realization of forecast weather system (preprocessing, assimilation of data, the forecast and postprocessing) on the basis of the atmospheric WRF-ARW model for calculation of a weather forecast in the Siberian region. Verification scores of WRF as compared with those of the NCEP global model are provided. The obtained results allow to draw a conclusion that during a summer season short-term forecasts based the WRF-ARW model have some advantage in comparison with the global model, and during the winter period the global weather forecasting model has small advantage.

Objectives of the study by Zdereva et al. (2011) included development of computer-assisted calculation scheme for the air temperature forecasting over points of Western Siberia region based on atmospheric hydrodynamic fields. Methodological approaches to the task solution are described. The main difference with previous investigations is using the Group Method of Data Handling (GMDH) in production of stable solutions, and DW algorithm for selection of information signs. Original samples are arranged in accordance with year periods with account for seasonal variability of the temperature. Clustering of working samples within seasons was performed by dividing the latter in accordance with changes in pressure and temperature fields at the AT-850 level. Threshold was presented by a sign of expected pressure and temperature trends (daily difference) at a majority of 25 points surrounding the station. Eventually, GMDH equations were derived for every station of the studied region separately for minimum and maximum air temperatures.

In Kurzke et al. (2012) a quasi-geostrophic model of Southern Hemisphere's wintertime atmospheric circulation with horizontal resolution T21 has been coupled to a global ocean circulation model with a resolution of $2^\circ \times 2^\circ$ and

simplified physics. This simplified coupled model reproduces qualitatively some features of the first and the second EOF of atmospheric 833 hPa geopotential height in accordance with NCEP data. The variability patterns of the simplified coupled model have been compared with variability patterns simulated by four complex state-of-the-art coupled CMIP5 models. The simplified model exhibits skill in reproducing essential features of decadal and multi-decadal climate variability in the extratropical Southern Hemisphere. Notably, 800 yr long coupled model simulations reveal sea surface temperature fluctuations on the timescale of several decades in the Antarctic Circumpolar Current region.

The results of first experiments in mesoscale ensemble weather prediction in the Russian Federation, using the non-hydrostatic atmospheric model COSMO-RU (horizontal resolution — 14 km) are presented in (Alferov and Rivin, 2011).

The paper (Vilfand et al., 2011) presents a brief history of the development of numerical short-range limited-area weather forecast in Siberia under the guidance of academician G. I. Marchuk. Because of the need, for the numerical weather prediction, of the data on the lateral boundaries of the area of integration, the current state of global prediction models and their future development in 2011–2012 are shortly discussed. Analogous information on limited-area weather forecast models is given, too. In the rest part of the paper the current state of the COSMO-RU system of short-range weather forecast is characterized.

3. Mesoscale processes

An actual problem of modern “dynamic mesoscale meteorology” is the study of dynamic processes in the Arctic, particularly with regard to the interaction of the atmosphere with the ocean covered with ice.

In (Chechin et al., 2013) a nonhydrostatic model (NH3D) is used for idealized dry quasi 2-D simulations of Arctic cold-air outbreaks using horizontal grid spacings between 1.25 and 60 km. Despite the idealized setup, the model results agree well with observations over Fram Strait. It is shown that an important characteristic of the flow regime during cold-air outbreaks is an ice-breeze jet (IBJ) with a maximum wind speed exceeding often the large-scale geostrophic wind speed. According to the present simulations, which agree very well with those of another nonhydrostatic mesoscale model (METRAS), the occurrence, strength, and horizontal extent L of this jet depend strongly on the external forcing and especially on the direction of the large-scale geostrophic wind relative to the orientation of the ice edge. It is found that coarse-resolution runs underestimate the strength of the jet. This underestimation has important consequences to the surface fluxes of heat and momentum, which are also underestimated by about 10–15% on average over the region between the ice edge and 120–180 km downstream. Our results suggest that a grid spacing of about $L/7$ is required (about

10–30 km) to simulate the IBJ strength with an accuracy of at least 10%. Thus, the results of large-scale models as well might contain uncertainties with regard to the simulated IBJ strength which would influence the energy budget in a large region along the marginal sea ice zones.

A hierarchy of parametrizations of the neutral 10 m drag coefficients over polar sea ice with different morphology regimes is derived in (Lüpkes et al., 2012) on the basis of a partitioning concept that splits the total surface drag into contributions of skin drag and form drag. The new derivation, which provides drag coefficients as a function of sea ice concentration and characteristic length scales of roughness elements, needs fewer assumptions than previous similar approaches. It is shown that form drag variability can explain the variability of surface drag in the marginal sea ice zone (MIZ) and in the summertime inner Arctic regions. In the MIZ, form drag is generated by floe edges; in the inner Arctic, it is generated by edges at melt ponds and leads due to the elevation of the ice surface relative to the open water surface. It is shown that an earlier fit of observed neutral drag coefficients is obtained as a special case within the new concept when specific simplifications are made which concern the floe and melt pond geometry. Due to the different surface morphologies in the MIZ and summertime Arctic, different functional dependencies of the drag coefficients on the sea ice concentration result. These differences cause only minor differences between the MIZ and summertime drag coefficients in average conditions, but they might be locally important for atmospheric momentum transport to sea ice. The new parametrization formulae can be used for present conditions but also for future climate scenarios with changing sea ice conditions.

Realistic modeling of polar sea ice dynamics and atmospheric processes over sea ice needs a detailed representation of the near-surface atmospheric fluxes of momentum. In (Lüpkes et al., 2013) parametrizations of neutral drag coefficients mostly used in different general circulation models are compared with a recently developed parametrization including the impact of sea ice morphology. The new parametrization, using the sea ice and melt pond fraction as governing parameters, accounts for the effect of form drag caused by edges at leads, melt ponds, and floes. Based on remote sensing data of ice and melt pond fraction, it is shown that during Arctic summer the traditionally used drag coefficients differ from the new ones by a factor 0.5–1.2. The geographic distribution of drag coefficients obtained from both parametrizations is very different. Differences are due to a nonlinear and non-monotonic dependence of drag coefficients on sea ice concentration in the new parametrization.

Another area of interest of specialists in dynamical meso-meteorology is the dynamics of the tropical atmosphere and in particular of tropical cyclones.

Diagnostic, prognostic and quasi-predictive calculations of movement of the tropical cyclones (TC) within hydro-mechanical model (GMM) are carried out.

The model contains the parameters characterizing TC and its interaction with the large-scale current called the leading stream (LS), which are constants for a given TC. By the diagnostic and quasi-predictive calculations are meant those ones in which during the whole life time of TC the objective analysis data of the speed of LS, and also of intensity and radial structure of TC are used. It is shown that in the diagnostic mode GMM rather correctly describes displacement of TC. The GMM parameters (constants for each TC) rather correctly can be determined for the pre-forecast period: average errors of quasi-forecasts for northwest part of the Pacific Ocean are 217, 272, 258, 257, 267 km for 3, 4, ... 7 days, respectively. Season-averaged TC forecast errors of GMM in 2011, by taking into account errors of forecasts in an extra tropical zone, are 397, 457, 574 km for 3, 4, 5 days, respectively. This corresponds to the level of errors of official US forecasts and is slightly less than errors of the most developed dynamic forecast methods, at least, for earliness of forecast of 4 and 5 days (Shmerlin and Shmerlin, 2011, 2012, 2014).

In recent papers (Ingel and Petrova, 2011, 2012) it is reported about some new approaches to research on the tropical cyclones (TC) dynamics, to modeling and forecasting of their intensity, and also about active impacts on them. Much attention is paid to recent progress in studying of the influence of natural and anthropogenic aerosols on TC. It has been shown, by using observational data and numerical modeling results, that this influence can be essential. In particular, observations show that when TCs approach continents, their interaction with a continental aerosol considerably influences the lightning activity in TC. This is probably due influence of the aerosol on microphysics of cloudy systems of TC, which affects also dynamics of tropical cyclones. Studies suggest that lightning activity can be used as a predictor of changes of intensity of TC, and artificial addition of aerosol into cloudy systems on the periphery of hurricanes can reduce their intensity.

Transformation of tropical into extra tropical cyclones during 1970–2012, including tendencies of changes of this process, was investigated in (Mokhov, et al., 2014).

In a number of recent papers the suggestions to affect the meso-meteorological processes are discussed by regulation of radiation balance of air and creation of artificial cloudy formation. It is suggested, in particular, to affect the weather during the periods of extreme temperatures of ground air over the cities for the purpose of reduction of harmful and dangerous consequences of such episodes. In (Ingel, 2013) estimates of amplitudes of meso-scale circulation which can arise at such influences are made. It is shown that negative feedbacks are associated with such circulations, which are important to account for when evaluating the expected effects.

Kizhner et al. (2013) and Starchenko A. (2013) presented the results of numerical modeling of weather conditions around Bogashevo airport and the city

of Tomsk obtained by means of meso-scale Weather Research & Forecasting (WRF) model. The main attention is paid to a choice of the parametrization of microphysical processes adequate for conditions of Western Siberia, for the purpose of obtaining reliable forecast of intense rainfall. Comparison of forecasted and observed precipitation and cloudiness data was done, which showed ability model to predict rainfall and the phenomena, dangerous to aircrafts. The best results were yielded by application of parametrization of microphysics of the ETA model. The micro-scale meteorological model was developed for calculation of a detailed wind situation in airport vicinities taking into account the influence of buildings of various heights, existing vegetation areas and heterogeneity of the underlying surface. The results of mathematical modeling help to define structure of a flow in locations of airfield meteorological stations for the purpose of a preliminary estimate of extent of influence of closely located airport buildings on the accuracy of measurements, and also to reveal effect of wind shear at small heights on flight characteristics of an aircraft landing or taking-off.

Strong gusty winds are observed during the cold season at the southern slopes of the Caucasus between the towns of Anapa and Novorossiysk when the pressure gradient is directed approximately normally to the Caucasus ridge, i.e. from north-east to south-west. The forecast of extreme wind (bora) in the Novorossiysk using the COSMO-Ru model with 7.0 km and 2.2 km grid cells developed at the Hydrometeorological Centre of Russia is discussed in (Blinov et al., 2013). A detailed analysis of prognostic fields is performed. It was shown that the model is good in simulating the spatial and temporal structure of the wind field and other meteorological fields.

Sharp weather contrasts and high spatiotemporal variability are typical for the region of the Sochi-2014 Winter Olympic Games. The complex mountain terrain and the intricate mixture of marine subtropical and Alpine conditions make the weather forecasting in this region extremely challenging. The complexity of the Sochi region stimulates the development of high-resolution mesoscale modeling as a backbone of the Olympic meteorological services. Presented are the main branches of the current research in this area carried out in the Hydrometeorological Centre of Russia (Kiktev et al., 2013).

4. Turbulence in the boundary layer

Advanced theory of geophysical turbulence has been developed including revision of the very concept of stably stratified turbulence, and novel turbulence-closure method has been proposed for modelling the atmosphere and hydrosphere (Zilitinkevich et al., 2007, 2008, 2009, 2013) that have led to the following major results: (i) The concept of critical Richardson number, conventionally perceived as the boundary between turbulent and laminar regimes, is

applicable only to the low Reynolds number flows. (ii) In the very large Reynolds number flows typical of geophysics and astrophysics, turbulence is maintained by the velocity shear up to the strongest observed stratification. (iii) In this case, the critical Richardson number remains a boundary but between the two principally different turbulent regimes: the familiar strong-mixing turbulence with basically similar eddy viscosity K_M and eddy conductivity K_H , and the earlier unknown weak-mixing turbulence, wherein the turbulent Prandtl number K_M/K_H sharply increases with increasing Richardson number. These results are important for meteorology, oceanography and prospectively astrophysics: The research community have received novel, physically grounded method (the Energy-and Flux-Budget turbulence closure) for modelling very stably stratified turbulent flows dominating 90% of the atmosphere and hydrosphere, and the Universe.

New results by S. S. Zilitinkevich and his co-authors on the study and modeling of turbulence in the atmospheric boundary layer are also contained in the papers (Esau et al., 2011; Baklanov et al., 2011; Zilitinkevich et al., 2012; Zilitinkevich, 2012; Troitskaya et al., 2012; Baklanov et al., 2012; Esau et al., 2012; Esau et al., 2013a; Hellsten and Zilitinkevich, 2013; Esau et al., 2013b; Troitskaya et al., 2013a, b; Anisimov et al., 2013; Druzhinin et al., 2013; Lappalainen et al., 2014; Troitskaya et al., 2014).

When the turbulence emerges in a stably stratified flow, the internal gravity waves, are typically generated, which are able to transfer energy from the source. Internal waves generated by turbulence observed in different setups: in layers with a shift in the leeward side of the relief, in the turbulence behind bars, etc. Problems of describing intermittent turbulence in a stably stratified geophysical flow, the role of turbulent diffusion processes in the generation of intermittent turbulence, buoyancy effect of internal waves and turbulent flows on the pulse, are still the center of attention of researchers. Understanding these processes and the creation of appropriate turbulence models is important for modeling the dynamics of weather and climate.

Specific features of the turbulent transfer of the momentum and heat in stably stratified geophysical flows, as well as possibilities for including them into RANS turbulence models, are reviewed by Vasil'ev et al. (2011). The momentum (but not heat) transfer by internal gravity waves under conditions of strong stability is, for example, one such feature. Laboratory data and measurements in the atmosphere fix a clear dropping trend of the inverse turbulent Prandtl number with an increasing gradient Richardson number, which must be reproduced by turbulence models. Ignoring this feature can cause a false diffusion of heat under conditions of strong stability and lead, in particular, to noticeable errors in calculations of the temperature in the atmospheric boundary layer. Therefore, models of turbulent transfer must include the effect of the action of buoyancy and internal gravity waves on turbulent flows of the momentum. Such a strategy of

modeling the stratified turbulence is presented in the review by a concrete RANS model and original results obtained during the modeling of stratified flows in the environment. Semi-empirical turbulence models used for calculations of complex turbulent flows in deep stratified bodies of water are also analyzed. This part of the review is based on the data of investigations within the framework of the large international scientific Comparative Analysis and Rationalization of Second-Moment Turbulence Models (CARTUM) project and other publications of leading specialists. The most economical and effective approach associated with modified two-parameter turbulence models is a real alternative to classical variants of these models. A class of test problems and laboratory and full-scale experiments used by the participants of the CARTUM project for the approbation of numerical models are considered.

Some changes in the eddy mixing in the atmospheric boundary layer (ABL) are investigated in (Kurbatskii and Kurbatskaya, 2012) with the use of the mesoscale RANS turbulence model. It is found that the behavior of parameters of the eddy turbulence mixing is in compliance with the recently obtained data of laboratory and atmospheric measurements. In particular, the flow Richardson number (Ri_f) during the transient flow to a strongly stable state can behave non-monotonically, growing with the increasing gradient Richardson number (Ri) to the state of saturation at a certain gradient Richardson number ($Ri \cong 1$), which separates two different turbulent regimes: the regimes of *strong mixing* and *weak mixing*. An analysis of the energetics based on the balance equations of kinetic and potential turbulence energies shows, in particular, that the weak mixing ($Ri > 1$) is quite capable of transferring momentum. This phenomenon can be explained not only by the fact that the flow is sustained by propagating internal waves, which effectively transfer momentum under strong stratification conditions, but also by the fact that turbulence permanently arises in the free atmosphere and in the deep ocean at $Ri \gg 1$.

The flow structure and statistical features of a turbulent stable stratified boundary layer are studied in (Kurbatskii and Kurbatskaya, 2013) by using the Reynolds-averaged Navier-Stokes (RANS) scheme of turbulence, which takes into account the influence of internal gravity waves. The possibility of the RANS description of intermittent turbulence both near the surface and above the surface in the vicinity of the low-level jet flow formed above the boundary layer is analyzed. The role of turbulent diffusion (third-order statistical moments) in intermittent turbulence generation is discussed. Numerical results are demonstrated to agree with results of LES modeling and actual observations. Intermittency of turbulent kinetic energy both near the surface and above this surface in the vicinity of the low-level jet flow is revealed.

Direct measurements of eddy diffusivities for momentum K_m and heat K_h by Doppler radar and by a radio acoustic sounding system in the upper troposphere

and lower stratosphere were used in (Kurbatskii and Kurbatskaya, 2014) to examine the applicability of three Reynolds-averaged Navier-Stokes (RANS) schemes of stratified turbulence in the environment: the E-e turbulence scheme modified for stratified flows, the algebraic two-parameter E-e Reynolds-stress scheme, and the three-parameter E-e- $\langle\theta^2\rangle$ turbulence scheme. All turbulence parameters — the turbulent kinetic energy (E), the dissipation rate (ϵ), and vertical profiles of potential temperature (atmospheric stability) and mean wind velocity — were derived from direct measurements for all three turbulence schemes. It is shown that the profile of the vertical diffusivity of momentum (K_m) obtained from the three-parameter RANS turbulence scheme agrees well with its directly measured analog. The profile of K_m calculated by the two-parameter turbulence schemes fits measurements rather qualitatively.

The paper by Ingel (2011b) is adjacent to papers on the theory and modeling stably stratified boundary layers. It considers a nonlinear analytical model of the water surface adjacent air layer. In the model, the effect of spray droplets on turbulent exchange is taken into account through their effect on density stratification. To close the system of equations, a semi-empirical turbulence theory in the Kolmogorov–Monin form is used. Unlike previous publications, an alternative closure scheme that seems more appropriate is used. A version is also proposed for generalizing the model onto the case where heavy admixture particles (spray droplets) make a dominant contribution to the average density of a medium. This model allows a general analytical solution that, in principle, describes nonlinear effects such as a decrease in the effective friction and “self-closure” of the heavy admixture in the near-surface layer because of turbulence suppression due to the strengthening of stratification stability. As the current data show, however, the intensity of spray production is probably insufficient to explain the recently discovered phenomenon of the aerodynamic drag decrease (saturation) in storm winds.

Some results of “large-eddy” simulation of flows in a neutral and stable-stratified boundary layer over a flat and very rough (due to urban development) surfaces are described in the following papers.

Computations of turbulent flows over surfaces with explicitly specified roughness elements that imitate an urban built-up area have been performed in (Glazunov, 2014a) using a large-eddy simulation (LES) model. Results are presented for neutral stratification. Some statistics of the flow over an inhomogeneous surface are compared with those over a flat surface. Results of spectral analysis performed to identify characteristic length scales are discussed. A relation is established between the Prandtl mixing length and the turbulence scale defined through the cospectrum-weighted-mean wave number. Values of the roughness parameter and displacement height are determined for three different configurations of objects on the surface. Analogous simulations were performed for stably

stratified turbulent flows (Glazunov, 2014b). A method of conducting numerical experiments allowing turbulent flows with specified values of the Obukhov scale L to reach a quasi-steady state at the surface has been proposed. It has been shown that, to calculate both temperature and wind-velocity profiles over such objects, one can use the same universal dependences that are used for a flat surface. It has been found that stable stratification does not affect the roughness parameter z_0 and the displacement height D .

Work was carried out to study atmospheric convection, convective transport of impurities and convective structures in the boundary layer.

Using a high-resolution LES numerical model, Glazunov and Dymnikov (2013) calculated the turbulent thermal convection for high ratios of horizontal and vertical sizes of the computational domain (26: 26: 1). The natural analog of the simulated process is the atmospheric planetary boundary layer (PBL) growing with height beneath stably stratified overlying air layers and over a horizontally homogeneous heated surface under a weak average wind. Glazunov and Dymnikov (2013) obtained the spectral distributions of variances of fluctuations in potential temperature and velocity components in ranges corresponding to scales from a few tens of meters to a few tens of kilometers. They found energetically significant segments of the spectrum of large-scale fluctuations in the potential temperature for which the power dependences $S \sim k^{-1/3}$ and $S \sim k^{-4/3}$ are satisfied with good accuracy. The characteristic spatial scales of horizontal fluctuations in velocity and temperature were calculated, and a dependence of these scales on the height of the growing convective PBL was obtained. The characteristic features of large-scale distributions in terms of the self-similarity of the growing boundary layer behavior are discussed.

Kurgansky et al. (2011) report on field observations in January 2009 (austral summer) of atmospheric dust devils in the northern part of the Atacama Desert in South America ($\approx 20^\circ\text{S}$). An extremely high level of dust-devil activity over the study site has been observed, dependent on local meteorological conditions. A high correlation was found between the dust-devil frequency of occurrence and the Obukhov length scale, L , calculated from meteorological gradient measurements, with a clear tendency for this frequency to increase with decreasing $-L$. The upper threshold values of $-L \approx 20\text{--}30$ m, and the 2-m mean wind speed, $V_2 \approx 8\text{ m s}^{-1}$, for dust-devil occurrence have been found, but the minimal V_2 threshold was not observed. Parallel routine meteorological measurements enabled us to calculate the main constituents of the surface energy balance, to obtain direct estimates of the surface albedo ($\alpha \approx 0.21$ at the solar noon) and to summarize the local conditions.

Chkhetiani et al. (2012) describe the results of the direct observations of fine scale mineral dust aerosol carried out over extensive sand areas in desertified lands of Kalmykia in 2007, 2009 and 2010 under conditions of weak wind and

strong heating of the surface with near absence of saltation processes. Measurements show that the fine mineral dust aerosol in the chosen region constitutes a considerable fraction of the entire air aerosol in the atmospheric surface layer (in terms of both the number of particles and their mass). Data of fine aerosol mass concentrations are treated on the basis of physical model estimates obtained for fluid dynamic parameters in the viscous thermal boundary layer near the ground surface. The deviations of mass concentrations from background are linked to temperature drop in the thermal layer near the surface and the value of friction velocity.

A model for the density Q of vertical mass flux of sand (dust) in the convective atmospheric boundary layer as a function of the number density N of convective elements (including vortices), friction velocity u^* , and vertical (turbulent) buoyancy flux B is proposed in (Kurgansky, 2014). It is shown that the flux Q is proportional to the product of the square root of B and the sixth power of u^* . This finding is consistent with empirical dependences reported in the literature. We discuss two methods for experimentally determining density N when the lifting of dust occurs, mainly due to (terrestrial and Martian) dust devils.

A brief review of published observations of methane fluxes to the atmosphere from bogs and lakes in the permafrost zone is presented in (Stepanenko et al., 2011). A one-dimensional model developed by the authors for methane generation, transport, and sink in the ground-water body system and coupled to a hydro-thermodynamic model of a water body is described. The results of calibrating this model against available observations of methane emission from the thermokarst Shuchi Lake in northeastern Siberia are discussed.

5. Dynamical interaction between the troposphere, middle and high atmosphere

This section presents the contributions, where dynamic coupling between the different layers of the atmosphere is investigated, or focuses on the dynamics of the upper atmosphere, but from the point of view of experts in dynamic meteorology.

The major sudden stratospheric warming (SSW) in the beginning of January 2013 led to considerable temperature growth in the polar stratosphere (up to 60 K at ~44 km altitude), to mean zonal wind reversal, to the split of the stratospheric polar vortex, and to a change in the temperature and dynamic regimes of the mesosphere and lower thermosphere. Using the data of reanalysis and ground based spectrometric and satellite observations, the changes in thermodynamic parameters related to the SSW and expanding from the troposphere to the lower thermosphere are analyzed (Vargin and Medvedeva, 2014). An intensification of

wave activity fluxes from the troposphere to the stratosphere is revealed a week before the SSW over East Siberia and China. It is shown that wave trains propagating eastwards in the upper troposphere could contribute to the intensification of an anticyclone over the northeast Atlantic Ocean a week before the SSW. In its turn, such intensification has led to the split of the stratospheric polar vortex into two parts during the SSW.

Two-dimensional direct numerical simulation of nonlinear acoustic-gravity waves (AGW) from the surface of the Earth to the thermosphere have been carried out in (Gavrilov and Kshevetskii, 2013). Gavrilov and Kshevetskii (2013, 2014) developed a similar three-dimensional model. Three-dimensional algorithm for solving the hydrodynamic equations based on the finite-difference analogue of the fundamental conservation laws. Using this model, they calculated the spread of non-linear decaying AGV into the upper atmosphere from moving horizontally periodic structures of the vertical velocity at the surface, which are used as sources of AGV in the model (Gavrilov and Kshevetskii, 2014a). It is shown that after activation of the wave source initial impulse of acoustic and very long-wavelength gravitational waves arises, which in a few minutes can reach heights of more than 100–200 km. Dissipation of this initial pulse produces a significant secondary heating and induced by wave of mean wind at altitudes above 200 km. This may affect the distribution of AGV and increase vertical temperature gradients, horizontal velocity and increase dissipation of the wave at the bottom of the secondary flow induced by wave, helping its spread downward. Calculations demonstrate significant differences from existing analytical theory of AGW in conditions of considerable unsteadiness, dissipation and nonlinear waves (Gavrilov and Kshevetskii, 2014b). Numerical simulation of nonlinear AGV helps to better understand the details of the dynamic and thermal influence of waves propagating from the troposphere to the middle and upper atmosphere. In addition, the direct numerical simulation of AGW is a useful tool for testing parameterizations simplified wave effects in the atmosphere.

Gavrilov and Koval (2013) proposed a parameterization of the dynamic and thermal effects of stationary orographic gravity waves (OGA) generated by orography. It was included in the general circulation model middle and upper atmosphere (MMUA) to study the sensitivity of the general circulation of the atmosphere at altitudes ranging from the troposphere up to the thermosphere to the effects of the OGA propagating from the troposphere. Gavrilov et al. (2013) examined changes in atmospheric circulation under conditions of change of generation and propagation of OGA in different seasons. It has been shown that during the solstice basic dynamic and thermal effects of the OGA are created in the middle atmosphere winter hemisphere, where, in particular, changes in the amplitudes of planetary waves from the impact of the OGA can reach up to 50% (Gavrilov et al., 2013). During the equinoxes OGA effects are more evenly

distributed between the northern and southern hemispheres. Gavrilov et al. (2014) carried out numerical modeling of general circulation in the troposphere and stratosphere and investigated the influence that propagating upward OGA, exert on the meridional and vertical velocity. It is shown that taking into account the dynamic and thermal effects of these waves in the numerical model causes changes in the meridional circulation and the associated ozone fluxes up to 20–30% at the altitudes of the ozone layer maximum.

On the basis of empirical monthly-mean data on oscillation parameters of a horizontal component of wind velocity of the diurnal and semidiurnal migrating tides the altitude-latitude distributions of oscillation parameters of the vertical velocity component of diurnal and semidiurnal tides in the mesosphere and the lower thermosphere (80–100 km) has been calculated (Portnyagin et al., 2011; Merzlyakov et al., 2012). Source data are obtained from results of satellite observations of the mesosphere and lower thermosphere in the range of heights of 90–120 km and of results of ground-based sounding of this area by a radio meteor method and method of partial reflections in the range of heights of 80–100 km. Characteristic feature of the obtained empirical distributions of amplitude of a vertical velocity component of daily tides is existence of three areas of the increased values of amplitude: in the vicinity of the equator, in the vicinity of 30°N latitude and in the vicinity of 30°S which occur during all seasons.

In (Suvorov and Pogoreltsev, 2011) on the basis of modeling using general circulation model of middle and upper atmosphere the relative role of distributed sources in the atmosphere non-migrating tides are investigated. It is shown that in the winter, when the stationary planetary waves (SPW) in the stratosphere are well developed, the main contribution to the generation of non-migrating tides makes the nonlinear interaction between the migrating tides and SPW with zonal wave number 1. Accounting for climate distributions of longitudinal inhomogeneities of ozone in the model leads to additional sources of non-migrating tides caused by non-uniform longitudinal daily variations of solar heating of the atmosphere. The contribution of these sources can be comparable to the contribution from the nonlinear interaction during weak SPW-activity in the stratosphere.

Based on the analysis and reanalysis data and numerical simulation results, the variability of dynamic processes in the stratosphere is studied. It includes the studies of climate variability of the timing of the spring alteration of stratospheric circulation (Savenkov et al., 2012). It is shown that in recent decades a shift of the timing of the spring adjustment to later dates is seen, indicating on a weakening of the planetary wave activity in the last months of winter in the Northern Hemisphere. The influence of the normal atmospheric modes (NAM) on the incidence and intensity of sudden stratospheric warming events (SSW) is considered (Pogoreltsev et al., 2014). It was found that accounting for parameterization NAM in general circulation model permits more correctly reproduce

the intra-seasonal variability of dynamic regime of the stratosphere. It is also noted that the conditions for the development of the SSW are more favorable during the eastern phase of the quasi-biennial oscillation.

The paper by Kulyamin and Dymnikov (2013) presents a new global three-dimensional model of the Earth thermosphere (for altitudes from 90 to 500 km) with a high spatial resolution. The model uses simple approximations for calculation of solar radiation and ion-neutral interaction. A detailed description of the algorithm is presented. It is shown that the model represents the main features of the general thermospheric circulation with a satisfactory accuracy.

Kulyamin and Dymnikov (2014) present a coupled troposphere-stratosphere-mesosphere and ionosphere D-layer model (for altitudes 0–90 km). It is based on three-dimensional atmospheric general circulation model with a hybrid vertical coordinate. Five-component model is taken as photochemical presentation of the D layer. The properties of the differential formulation are studied; an efficient semi-implicit numerical scheme is developed. On the basis of presented coupled model the role of the thermodynamic characteristics of the neutral atmosphere in the formation of D-layer is investigated.

6. Mathematical problems of climate and ecology

The main tool in the study of the climate system as a whole, and the processes occurring in it is a mathematical (numerical) modeling, based on a hierarchy of models — from global, which are based on the model of the general circulation of the atmosphere and ocean, to the multi-scale modeling of geophysical turbulence. It is discussed in (Dymnikov et al. 2012).

The book (Lykosov et al., 2012) presents fundamentals of mathematical modeling for solving problems of physics of climate system, methods of finite difference approximation and the concomitant basic numerical algorithms. Supercomputing technology of numerical model implementation are discussed. As an illustration of the described approach the following tasks are considered: simulation of viscous incompressible fluid in domains with complex geometry, the problem of large-eddy simulation of dynamics of geophysical boundary layers, the problem of modeling of regional characteristics of atmospheric circulation, the problem of reproducing the current climate and the evaluation of its possible future changes. The book is intended for specialists in the field of the sciences of Earth's climate system, teachers, graduate students, and can be used as a textbook for students of natural science disciplines.

The monograph (Gordov et al., 2013) considers the current level of state in information technologies for monitoring and modeling of climate change and its impacts on the environment. Described in detail is a computational geo-informational web-based platform to work with “geo-tied” climate data. The monograph

presents an overview of current and of expected future climate changes and their consequences. The current situation with informational-computing resources for monitoring and modeling of climate processes is shown. Detailed analysis is presented of modern computing and information technology to work with “geotied” data and also a method to combine the capacity of computationally-GIS and Web 2.0 approaches, which is implemented in a web platform for processing, visualization and analysis of large data archives “Climate”. This book presents first results of studies of climate change and its impacts on the territory of Siberia, obtained through the platform “Climate”. The book is intended for specialists in meteorology, climatology, computer science and applied mathematics, as well as graduate and undergraduate students in related disciplines.

In the book “Models and methods in the problem of interaction between the atmosphere and hydrosphere: Tutorial” (Eds. Dymnikov et al.) lecture materials are presented on the problem of interaction between the atmosphere and hydrosphere, as an outcome of the Young Scientist School — International Conference on Computational Information Technologies for Environmental Sciences, held in Petrozavodsk from August 25 to September 5, 2013. Lectures are presented in the form of textbook chapters, which address issues such as the role of the ocean in the observed and possible future climate variability; models and methods used in the problems of large-scale air-sea interaction; models and methods used in the problems of large-scale air-sea interaction; the problem of data assimilation in models of ocean circulation and sea; short-period response of upper ocean to atmospheric forcing; the sensitivity of climate models with respect to small perturbations; regional and local aspects of the interaction between the atmosphere and hydrosphere (lakes and climate, wind waves on the oceans and seas, hydrological processes on land); computational and informational technologies for the analysis of climate change and game-theoretic model of coordination in the problem of control of marine bioresources. The final chapter presents the results obtained by students of the school workshop on climate change modeling. This book will be useful for specialists in the field of earth sciences, computer science and applied mathematics and students of relevant specialties.

Observations of atmospheric conditions and processes in urban areas is fundamental to the understanding of the interaction between the surface of the city (which is, by definition, an anthropogenic surface) and weather conditions, to knowledge about the weather and air quality in the city at any time, to the ability to forecast the weather and air quality in the city and provide important information to end users (this decision makers — the city authorities, public utilities, health care, education and others.). With the growth of the urban population, this modeling trend based on dynamic models of the atmosphere and chemical transport models, is becoming increasingly important.

In (Bart et al., 2011) an approach is proposed that allows using a one-dimensional meteorological model and transport model to predict the impurities air quality over the urbanized area. A characteristic feature of the method is the use of medium-term weather forecast data from the global model of RF Hydrometeorological Center. Impurity transport model is implemented on supercomputers, which allows obtaining the forecast in short terms.

In (Kelyashova and Tokarev, 2011) graphical and statistical analysis of space-time series (2005–2008, 10 stations) of eleven pollutant concentrations over Novosibirsk city was performed. Conventional statistical estimations of the dispersion decomposition along the axes of multidimensional matrix of observation data were obtained. Evident violations of statistical homogeneity, stationarity, and ergodicity of data, unrelated to weather conditions, were shown. Contributions of long-term trends, seasonality, and spatial inhomogeneity within the megalopolis to the total dispersion of different pollutant concentrations were assessed. In conclusion, possible mechanisms of elevated pollutant concentration formation and dispersion within the megalopolis without an imperative predominant role of weather conditions are discussed.

Analysis and forecast of weather conditions that affect the concentration of atmospheric pollutants in a metropolis, is presented in (Zdereva and Tokarev, 2011). Logical decision rules for 1–3 day forecasting of the excess of individual pollutant's MAC (maximum allowable concentration) were built based on Novosibirsk observation data archive for 2005–2008 (10 stations, 11 pollutants) and synchronous data in the GRIB points. The complex of methodological measures for detection of fine structure of latent and poor statistical links was accepted, balanced criterion for derivation of tree of the DW algorithm solutions was developed, and the forecast method and technology ready for operational testing were obtained. Feasibility of probabilistic approach to derivation of logical trees enables a correction of obtained decision rules without repeated training by means of the choice of truncation criterion values.

Methods of calculating the emission of pollutants from forest fires, designed to adjust the input to the simulation of the propagation of atmospheric pollutants, are applied to cases of fires in the center of the European Russia in August 2010 (Surkova et al., 2014). It allows one to estimate the appropriate emission factor, and with the known (or assumed) fire area and duration, to model the spread of a fire plume taking into account the physical and chemical transformation of pollutants in the atmosphere. Numerical experiments are performed using the chemical transport model COSMO-Ru7-ART. Verification of the results demonstrates the ability of the model to calculate realistic plume shape and values for the concentration of pollutants in the surface layer.

This review would not be possible without the participation and support of a large number of Russian scientists.

References

1. Achatz U., Löbl U., Dolaptchiev S. I., Gritsun A. Fluctuation-dissipation supplemented by nonlinearity: a climate-dependent subgrid-scale parameterization in low-order climate models // *Journal of the Atmospheric Sciences*. 2013. T. 70. № 6. C. 1833–1846.
2. Akperov M. G., Mokhov I. I. Estimates of the sensitivity of cyclonic activity in the troposphere of extratropical latitudes to changes in the temperature regime // *Izvestiya. Atmospheric and Oceanic Physics*. 2013. Vol. 49. № 2. P. 113–120.
3. Alferov D. Yu., Rivin G. S. The mesoscale weather forecast COSMO-RU system: the ensemble forecast // *Proceedings of Hydrometcentre of Russia*. 2011. Vol. 346. P. 5–16.
4. Anisimov S. V., Mareev E. A., Shikhova N. M., Shatalina M. V., Galichenko S. V., Zilitinkevich S. S. Aeroelectric structures and turbulence in atmospheric boundary layer// *Non-linear Proc. in Geophys.* 2013. 20, 819–824 (DOI: 10.5194/npg-20-819-2013).
5. Baklanov, A. A., Grisogono, B., Bornstein, R., Mahrt, L., Zilitinkevich, S. S., Taylor, P., Larsen, S. E., Rotach, M. W., and Fernando, H. J. S., 2011: The nature, theory, and modeling of atmospheric planetary boundary layers. *Bull. Amer. Meteorol. Soc.*, February 2011, 123–128.
6. Baklanov A. A., Bondur V. G., Klaic Z. B., Zilitinkevich S. S. Integration of geospheres in Earth systems: modern queries in environmental physics//*Geofizika*. 2012. V. 29, No. 1, 1–4.
7. Bart A. A., Belikov D. A., Starchenko A. V. Supercomputer-based mathematical model for air quality prediction in the urban area // *Vestnik Tomskogo Gosudarstvennogo Universiteta. Matematika i Mekhanika* 2011, Number 3(15), Pages 15–24.
8. Baydin A. V., Meleshko V. P. Reaction of the atmosphere over high and moderate latitudes on the reduction of area of sea ice and increase of the sea surface temperature // *Meteorologiya i Gidrologiya*. 2014. No. 6. P. 5–18 (in Russian).
9. Blinov D. V., Perov V. L., Peskov B. E., Rivin G. S. Extreme bora of February 7–8, 2012, in the area of Novorossiysk and its forecast with the COSMO-Ru model // *Journal “Vestnik MSU”, ser. 5, geography*. 2013. No 4, P. 36–43.
10. Chechin D. G., Lüpkes C., Repina I. A., Gryanik V. M. Idealized dry quasi 2-D mesoscale simulations of cold-air outbreaks over the marginal sea ice zone with fine and coarse resolution//*Journal of Geophysical Research: Atmospheres*. 2013. VOL. 118, 1–27, doi:10.1002/jgrd.50679.
11. Cherenkova E. A., Shkolnik I. M. Possible location of the polar front over the Eastern European Plain in the middle of the 21 Century // *Izvestiya, Atmospheric and Oceanic Physics*. 2012. Vol. 6, pp. 17–22.
12. Chkhetiani O. G., Gledzer E. B., Artamonova M. S., Iordanskii M. A. Dust resuspension under weak wind conditions: direct observations and model *Atmos. Chem. Phys.*, 12, 5147–5162, 2012, www.atmos-chem-phys.net/12/5147/2012/ doi:10.5194/acp-12-5147-2012.
13. Chkhetiani, O. G., Golitsyn, G. S. Detection and dispersion of diffusion tracer spots and their life times // *Doklady Mathematics*. 2014. Vol. 89, No. 2, pp. 245–249.

14. Chkhetiani, O.G., Kalashnik, M.V., Ingel, L.K. Generation of thermal wind over a nonuniformly heated wavy surface. *Izvestiya, Atmospheric and Oceanic Physics*. 2013. Vol. 49. Issue 2, pp. 121–127.
15. Druzhinin O.A., Ostrovsky L.A., Zilitinkevich S.S. The study of the effect of small-scale turbulence on internal gravity waves propagation in a pycnocline//*Nonlin. Processes Geophys.* 2013. 20, 1–11. doi:10.5194/npg-20–1–2013.
16. Dymnikov V.P. The dimension of an attractor generated by equations of 2D viscous noncompressible liquid dynamics on a revolving sphere // *Doklady Earth Sciences*. 2012, Vol. 447, Issue 2, pp. 1349–1350.
17. Dymnikov V.P., Lykosov V.N., Volodin E.M. Modeling climate and its changes: current problems // *Herald of the Russian Academy of Sciences*. 2012. Vol. 82. № 2, pp. 111–119.
18. Esau I.N., Zilitinkevich, S.S., Djolov G., Rautenbach C.J. deW., 2011: A micro-meteorological experiment in the atmospheric boundary layer in Highveld Region. *IOP Conf. Series: Earth and Environmental Science* 13, 012011 (8 pp), doi:10.1088/1755–1315/13/1/012011.
19. Esau I., Luhunga P., Djolov G., Rautenbach C.J. deW., Zilitinkevich S. Links between observed micro-meteorological variability and land use patterns in Highveld Priority Area of South Africa//*Meteorology and Atmospheric Physics*. 2012. V. 118, Issue 3, 129–142 (DOI: 10.1007/s00703–012–0218–4).
20. Esau, I., Davy, R., Outten, S., Tyuryakov, S., Zilitinkevich, S., Structuring of turbulence and its impact on basic features of Ekman boundary layers // *Non-linear Proc. in Geophys.* 2013. 20, 589–604 (doi:10.5194/npg-20–589–2013).
21. Esau I.N., Wolf T., Miller E., Repina I.A., Troitskaya Yu.I., Zilitinkevich S.S. The analysis of results of remote sensing monitoring of the temperature profile in lower atmosphere in Bergen (Norway) // *Russian Meteorology and Hydrology*. 2013. Vol. 38, pp. 715–722.
22. Gavrilov N.M., Kshevetskii S.P. Numerical modeling of propagation of breaking nonlinear acoustic-gravity waves from the lower to the upper atmosphere // *Advances in Space Research*, 2013. Vol. 51, № 7. P. 1168–1174.
23. Gavrilov N.M., Kshevetskii S.P. A study of propagation of nonlinear acoustic-gravity waves in the middle and upper atmosphere by means of numerical modeling // *Russian Journal of Physical Chemistry B*. 2013, Vol. 7, Issue 6, pp. 788–794.
24. Gavrilov N.M., Kshevetskii S.P. Three-dimensional numerical simulation of nonlinear acoustic-gravity wave propagation from the troposphere to the thermosphere // *Earth, Planets and Space*, 2014. Vol. 66, № 1. P. 88
25. Gavrilov N.M., Kshevetskii S.P. Verifications of the nonlinear numerical model and polarization relations of atmospheric acoustic-gravity waves // *Geoscientific Model Development Discussions*, 2014. Vol. 7, P. 7805–7822.
26. Gavrilov N.M., Kshevetskii S.P. Numerical modeling of the propagation of nonlinear acoustic-gravity waves in the middle and upper atmosphere // *Izvestiya, Atmospheric and Oceanic Physics*. 2014, Vol. 50, Issue 1, pp. 66–72.

27. Gavrilov N. M., Koval' A. V. Parameterization of mesoscale stationary orographic wave forcing for use in numerical models of atmospheric dynamics // *Izvestiya Atmospheric and Oceanic Physics*. 2013, Vol. 49, Issue 3, pp. 244–251.
28. Gavrilov N. M., Koval A. V., Pogoreltsev A. I., Savenkova E. N. Numerical modeling influence of inhomogeneous orographic waves on planetary waves in the middle atmosphere. // *Advances in Space Research*, 2013. Vol. 51, № 11. P. 2145–2154.
29. Gavrilov N. M., Koval' A. V., Pogorel'tsev A. I., Savenkova E. N. Numerical simulation of the response of general circulation of the middle atmosphere to spatial inhomogeneities of orographic waves // *Izvestiya, Atmospheric and Oceanic Physics*. 2013, Vol. 49, Issue 4, pp. 367–374.
30. Gavrilov N. M., Koval' A. V., Pogorel'tsev A. I., Savenkova E. N. Numerical simulation of the influence of stationary mesoscale orographic waves on the meridional circulation and ozone fluxes in the middle atmosphere // *Geomagnetism and Aeronomy*. 2014. Vol. 54(3), pp. 381–387.
31. Glazunov A. V. Numerical modeling of turbulent flows over an urban-type surface: Computations for neutral stratification // *Izvestiya, Atmospheric and Oceanic Physics*. 2014. Vol. 50, Issue 2, pp. 134–142.
32. Glazunov A. V. Numerical simulation of stably stratified turbulent flows over flat and urban surfaces // *Izvestiya, Atmospheric and Oceanic Physics*. 2014, Vol. 50, Issue 3, pp. 236–245.
33. Glazunov A. V., Dymnikov V. P. Spatial spectra and characteristic horizontal scales of temperature and velocity fluctuations in the convective boundary layer of the atmosphere // *Izvestiya. Atmospheric and Oceanic Physics*. 2013. Vol. 49. Issue 1, pp. 33–54.
34. Glazunov A., Dymnikov V., Kulyamin D., Lykossov V. Mathematical modeling of the spectral structure of atmospheric turbulence // "Turbulence, Dynamics of Atmosphere and Climate". Collected papers of International Conference devoted to the memory of Academician A. M. Obukhov / Eds. G. S. Golitsyn, I. I. Mokhov, S. N. Kulichkov, M. V. Kurgansky, O. G. Chkhetiani. Moscow: GEOS, 2014, pp. 17–18 (In Russian).
35. Golitsyn G. S. Statistics and Dynamics of Natural Processes and Phenomena: Methods, Tools, Results. Series "Synergetics: from Past to Future". Krasand Publ., Moscow. 2012. 400 pp.
36. Golitsyn, G. S., Chkhetiani, O. G. Effect of viscosity on admixture horizontal diffusion in the wind-wave field // *Izvestiya, Atmospheric and Oceanic Physics*. 2014. Vol. 50. Issue 6, pp. 547–553.
37. Goncharov V. P. Structural elements and collapse regimes in 3D flows on a slope // *Journal of Experimental and Theoretical Physics*. 2011, Vol. 113, Issue 4, pp. 714–721.
38. Goncharov V. P., Pavlov V. I. Blow-up instability in shallow water flows with horizontally-nonuniform density // *JETP Letters*. 2012, Vol. 96, Issue 7, pp. 427–431.
39. Goncharov V. P., Pavlov V. I. Structural elements of collapses in shallow water flows with horizontally nonuniform density // *Journal of Experimental and Theoretical Physics*. 2013, Vol. 117, Issue 4, pp. 754–763.
40. Gordov E. P., Lykossov V. N., Krupchatnikov V. N., Okladnikov I. G., Titov A. G., Shul'gina T. M. Computing and information technologies of monitoring and modeling

of climate change and its impacts. — Novosibirsk: Nauka Publ., Siberian branch, 2013, 199 pp. (in Russian).

41. Gorin V.E., Tsyulnikov M.D. Estimation of multivariate observation-error statistics for AMSU-A data // *Monthly Weather Review*. 2011. Vol. 139, pp. 3765–3780.

42. Gritsun A. Statistical characteristics, circulation regimes and unstable periodic orbits of a barotropic atmospheric model // *Philosophical Transactions: Mathematical, Physical and Engineering Sciences (Series A)*. 2013. T. 371. № 1991, pp. 20120336–20120336.

43. Hellsten A., Zilitinkevich S. Role of convective structures and background turbulence in the dry convective boundary layer // *Boundary-Layer Meteorol.* 2013. 149, 323–353 (DOI 10.1007/s10546-013-9854-6).

44. Ingel L. Kh. Toward a nonlinear theory of katabatic winds // *Fluid Dynamics*. 2011, Vol. 46, Issue 4, pp. 505–513.

45. Ingel L. Kh. On the effect of spray on the dynamics of the marine atmospheric surface layer in strong winds // *Izvestiya, Atmospheric and Oceanic Physics*. 2011, Vol. 47, Issue 1, pp. 119–127.

46. Ingel L. Kh. Nonlinear interaction between two components of motion upon precipitation of a heavy particle in a shear flow // *Technical Physics*. 2012, Vol. 57, Issue 11, pp. 1585–1588.

47. Ingel L. Kh. Towards estimates of the effectiveness of active impacts aiming at the control of surface air temperature extremes // *Meteospektr*. 2013. № 2. P. 128–131 (In Russian).

48. Ingel L. Kh. On some generalization of the Rayleigh problem on a convective instability // *Universal Journal of Applied Mathematics*. 2014. V. 2. N 1. P. 24–28. DOI: 10.13189/ujam.2014.020104.

49. Ingel L. Kh. On a positive-feedback mechanism in intense atmospheric vortices // *Izvestiya, Atmospheric and Oceanic Physics*. 2014, Vol. 50, Issue 1, pp. 61–65.

50. Ingel L. Kh., Belyaeva M. V. Toward the theory of convection in a rotating stratified medium over a thermally inhomogeneous horizontal surface // *Journal of Engineering Physics and Thermophysics*. 2011. Vol. 84, No. 4, pp. 820–826.

51. Ingel L. Kh., Kalashnik M. V. Nontrivial features in the hydrodynamics of seawater and other stratified solutions. *Physics–Uspekhi*. 2012. V. 55. No. 4. P. 356–38.

52. Ingel L. Kh., Macosco A.A. The theory of atmospheric disturbances induced by gravity field inhomogeneities // *Doklady Earth Sciences*. 2014a, Vol. 455, Issue 2, pp. 454–458.

53. Ingel L. Kh., Macosco A.A. On atmospheric disturbances related to the gravity field inhomogeneities // *International Conference MSS-2014 “Wave transformation, coherent structures and turbulence”*/ Moscow. November 2014. Collected papers. M.: LENAND. 2014b. P. 239–244 (In Russian).

54. Ingel L. Kh., Petrova L.I. New approaches to the prediction of tropical cyclones intensity and active influences on them. *Meteospektr*. 2011. No. 3. P. 106–113. (In Russian).

55. Ingel L. Kh., Petrova L.I. Tropical cyclones: new ideas // *Priroda*. 2012. № 5. P. 27–35. (In Russian).

56. Ivanova A.R. The tropopause slope as a characteristic of its deformation // *Russian Meteorology and Hydrology*. 2011. Vol. 36, Issue 2, pp. 82–90.
57. Ivanova A.R., Shakina N.P., Skriptunova E.N., Bogaevskaya N.I. Comparison of dynamical episodes of the blocking anticyclone of the summer 2010 with earlier episodes. In: “Analysis of conditions for anomalously weather over the Russian territory in summer 2010”. 2011. Triada Ltd. Pp. 65–71 (in Russian).
58. Kalashnik M.V. Distribution and trapping of inertia-gravity waves in a rotating fluid shear flows // *Herald of N.I. Lobachevsky State University of Nizhny Novgorod*. 2011. № 4 (3). *Fluid Dynamics*. P. 818–819. (In Russian).
59. Kalashnik M.V. The effect of cyclone–anticyclone asymmetry at small Rossby numbers // *Izvestiya, Atmospheric and Oceanic Physics*. 2011, Vol. 47, Issue 4, pp. 439–444.
60. Kalashnik M.V. Propagation and trapping of inertial gravity waves in shear flows (ray theory) // *Izvestiya, Atmospheric and Oceanic Physics*. 2013, Vol. 49, Issue 2, pp. 217–228.
61. Kalashnik M.V. Generation of internal gravity waves by vortex disturbances in a shear flow // *Izvestiya, Atmospheric and Oceanic Physics*. 2014, Vol. 50, Issue 6, pp. 638–647.
62. Kalashnik M.V., Chkhetiani O.G. Generation of the mean flow in the fluid layer with a nonuniformly heated wavy boundary // *Fluid Dynamics*. 2013, Vol. 48, Issue 2, pp. 163–178.
63. Kalashnik M.V., Chkhetiani O.G. The nonlinear decay of vortex flows in a rotating fluid // *Doklady Earth Sciences*. 2014, Vol. 456, Issue 2, pp. 769–774.
64. Kalashnik M.V., Chkhetiani O.G. Wave generation on an interface by vortex disturbances in a shear flow // *Fluid Dynamics*. 2014, vol. 49, No. 3, pp. 384–394.
65. Kalashnik M.V., Kalashnik A.M. Analytical model of the intensification of a tropical cyclone // *Izvestiya, Atmospheric and Oceanic Physics*. 2011, Vol. 47, Issue 6, pp. 766–779.
66. Kalashnik M.V., Svirkunov P.N. On the wave wake behind a moving hurricane // *Izvestiya, Atmospheric and Oceanic Physics*. 2014, Vol. 50, Issue 3, pp. 278–283.
67. Kelyashova R.E., Tokarev V.M. Analysis of time series of atmospheric pollutants in the city of Novosibirsk // *Proceedings of Siberian Regional Scientific Research Hydrometeorological Institute*. 2011. Issue 106. P. 159–167.
68. Kiktev D.B., Astakhova E.D., Blinov D.V., Zaripov R.B., Murav'ev A.V., Rivin G.S., Rozinkina I.A., Smirnov A.V., Tsyrunnikov M.D. Development of forecasting technologies for meteorological support of the Sochi-2014 Winter Olympic Games // *Russian Meteorology and Hydrology*, 2013, Vol. 38, No. 10, pp. 653–660.
69. Kizhner L.I., Barashkova N.K., Akhmetshina A.S., Bart A.A., Starchenko A.V. Forecast of precipitation in the area of Bogashevo airport using the WRF model // *Atmospheric and Oceanic Optics*. 2014. Vol. 27, Issue 2, pp. 187–194.
70. Klimova E.G. The use of ensemble Kalman filter for the planning of adaptive observations // *Russian Meteorology and Hydrology*. 2011, Vol. 36, Issue 8, pp. 511–519.
71. Klimova E. A suboptimal data assimilation algorithm based on the ensemble Kalman filter // *Quarterly Journal of the Royal Meteorological Society*. 2012. v. 138, p. 2079–2085. DOI:10.1002/qj.1941.

72. Klimova E. G., Platon G. A., Kilanova N. V. Development of environmental data assimilation system based on the ensemble Kalman filter // *Computational Technologies*. 2014, Vol. 19, № 3, pp. 27–37 (In Russian).
73. Kostykin S. V., Khapaev A. A., Yakushkin I. G. On the decay law of quasi-two-dimensional turbulence // *Journal of Experimental and Theoretical Physics Letters (JETP Letters)*. 2012. Vol. 95. № 10. P. 515–520.
74. Kulyamin D. V., Dymnikov V. P. A three-dimensional thermosphere general circulation model // *Geliogeofizicheskie issledovaniya*. 2014. № 7 (7). P. 15–42. (In Russian).
75. Kulyamin D. V., Dymnikov V. P. Modeling of the general circulation of troposphere-stratosphere-mesosphere with inclusion of the stratospheric d-layer // *Geliogeofizicheskie issledovaniya*. 2014. № 10 (10). P. 5–44.
76. Kurbatskii A. F., Kurbatskaya L. I. On the eddy mixing and energetics of turbulence in a stable atmospheric boundary layer // *Izvestiya, Atmospheric and Oceanic Physics*, 2012, Vol. 48, No. 6, pp. 595–602.
77. Kurbatskii A. F., Kurbatskaya L. I. RANS modelling of intermittent turbulence in a thermally stable stratified boundary layer // *Journal of Applied Mechanics and Technical Physics*, Vol. 54, No. 4, pp. 561–571, 2013.
78. Kurbatskii A. F., Kurbatskaya L. I. Modeling the eddy transport of momentum and heat: Comparison with direct measurements in free atmosphere // *Izvestiya, Atmospheric and Oceanic Physics*, 2014, Vol. 50, No. 4, pp. 369–376.
79. Kurgansky M. V. Statistical distribution of atmospheric dust devils // *Icarus*. 2012. Vol. 219. P. 556–560.
80. Kurgansky M. V. Simple models of helical baroclinic vortices // *Procedia IUTAM*. 2013, Vol. 7, P. 193–202.
81. Kurgansky M. V. On helical vortex motions of moist air // *Izvestiya, Atmospheric and Oceanic Physics*, 2013, Vol. 49, No. 5, pp. 479–484.
82. Kurgansky M. V. On the vertical lifting of dust in a convective unstable atmospheric boundary layer // *Izvestiya, Atmospheric and Oceanic Physics*, 2014, Vol. 50, No. 4, pp. 337–342.
83. Kurgansky M. V. Relationship between helicity and potential vorticity in a compressible rotating fluid // *Turbulence, Dynamics of Atmosphere and Climate. Collected papers of International Conference devoted to the memory of Academician A. M. Obukhov / Eds. G. S. Golitsyn et al. Moscow: GEOS, 2014, pp. 119–130 (In Russian)*.
84. Kurgansky M. V., Chernokulsky A. V., Mokhov I. I. The tornado over Khanty-Mansiysk: An exception or a symptom? // *Russian Meteorology and Hydrology*, 2013, Vol. 38, No. 8, pp. 539–546.
85. Kurgansky M. V., Montecinos A., Villagran V., Metzger S. M. Micrometeorological conditions for dust-devil occurrence in the Atacama Desert // *Boundary-Layer Meteorol.* 2011. V. 138. P. 285–298.
86. Kurzke H., Kurgansky M. V., Dethloff K., Handorf D., Erxleben S., Olbers D., Eden C., Sempf M. Simulating Southern Hemisphere extra-tropical climate variability with an idealised coupled atmosphere-ocean model // *Geosci. Model Dev.*, 2012. V. 5, p. 1161–1175.

87. Lappalainen H.K., Petäjä T., Kujansuu J., Kerminen V.-M., Shvidenko A., Bäck J., Vesala T., Vihma T., de Leeuw G., Lauri A., Ruuskanen T., Lapshin V.B., Zaitseva N., Glezer O., Arshinov M., Spracklen D.V., Arnold S.R., Juhola S., Lihavainen H., Viisanen Y., Chubarova N., Chalov S., Filatov N., Skorokhod A., Elansky N., Dyukarev E., Esau I., Hari P., Kotlyakov V., Kasimov N., Bondur V., Matvienko G., Baklanov A., Mareev E., Troitskaya Y., Ding A., Guo H., Zilitinkevich S., Kulmala M. Pan-Eurasian Experiment (PEEX) — A research initiative meeting the grand challenges of the changing environment of the northern Pan-Eurasian Arctic-boreal areas// *Geography, Environment and Sustainability*. 2014. V. 7. No. 2, 13–48.

88. Levina G.V., Montgomery M.T. Helical scenario of tropical cyclone genesis and intensification // 13th European Turbulence Conference (ETC13) IOP Publishing Journal of Physics: Conference Series. 2011 Vol. 318, 072012 doi:10.1088/1742–6596/318/7/072012.

89. Levshin A.O., Chkhetiani O.G. Decay of helicity in homogeneous turbulence // *JETP Letters*. 2014, Vol. 98, Issue 10, pp. 598–602.

90. Lupo A.R., Mokhov I.I., Akperov M.G., Chernokulsky A.V., Athar H. A dynamic analysis of the role of the planetary- and synoptic-scale in the summer of 2010 blocking episodes over the European part of Russia // *Advances in Meteorology*. 2012. V. 2012. P. 584257.

91. Lupo A.R., Hubbart J.A., Mokhov I.I., Akperov M., Chendev Y.G., Lebedeva M.G. Studying summer season drought in Western Russia // *Advances in Meteorology*. 2014a. V. 2014. P. 942027.

92. Lupo A.R., Colucci S.J., Wang Y., Mokhov I.I. Large-scale dynamics, anomalous flows, and teleconnections // *Advances in Meteorology*. 2014b. V. 2014. P. 207413.

93. Lüpkes, C., Gryanik V.M., Hartmann J., Andreas E.L. A parametrization, based on sea ice morphology, of the neutral atmospheric drag coefficients for weather prediction and climate models// *J. Geophys. Res.* 2012 V. 117, D13112, doi:10.1029/2012JD017630.

94. Lüpkes C., Gryanik V.M., Rösel A., Birnbaum G., Kaleschke L. Effect of sea ice morphology during Arctic summer on atmospheric drag coefficients used in climate models// *Geophysical Research Letters*. 2013. VOL. 40, 446–451, doi:10.1002/grl.50081.

95. Lykosov V.N. Book review: *Statistics and Dynamics of Natural Processes and Phenomena: Methods, Instrumentation, and Results* (by G.S. Golitsyn). — *Izvestiya AN. Fizika Atmosfery i Okeana*, 2014, Vol. 50, No. 1, pp. 126–128 (In Russian).

96. Lykosov V.N., Glazunov A.V., Kulyamin D.V., Mortikov E.V., Stepanenko V.M. *Supercomputer Modelling in Physics of the Climate System: Manual*. — Moscow University Publishing, 2012, 408 p.

97. Lykosov V.N., Krupchatnikov V.N. Some directions in the development of dynamic meteorology in Russia in 2007–2010. — *Izvestiya, Atmospheric and Oceanic Physics*, 2012, v. 48, No. 3, pp. 255–271.

98. Martynova Yu., Zaripov R., Krupchatnikov V., Petrov A. Estimation of the quality of atmospheric dynamics forecasting in the Siberian region using the WRF-ARW mesoscale model // *Russian Meteorology & Hydrology*. 2014, Vol. 39 Issue 7, p. 440.

99. Masutani M., Garand L., Lahoz W., Riishøjgaard L.-P., Andersson E., Rochon Y., Tsyrlunikov M., McConnell J., Cucurull L., Xie Y., Ishii S., Grumbine R., Brunet G., Woollen J. S., Sato Y. Observing System Simulation Experiments: Justifying new Arctic Observation Capabilities. — U. S. Department of Commerce, National Oceanic and Atmospheric Administration, National Weather Service, National Centers for Environmental Prediction Office Note 473, 2013, 20 pp.
100. Medvedev S.B. The geometrical approximation for the rotating shallow water equations // *Computational technologies*. 2013. V. 18. № 1. P. 45–64.
101. Merzlyakov E. G., Portnyagin Yu.I., Solov'eva T. V., Pogoreltsev A. I., Suvorova E. V. Altitude-latitude structure of the vertical wind component of the migrating diurnal tide in the range of heights from 80 to 100 km // *Izvestiya, Atmospheric and Oceanic Physics*. 2012, Volume 48, Issue 2, pp. 174–184.
102. Mirvis V. M., Lvova T. Yu., Meleshko V. P., Matyugin V. A. Calibration of probabilistic surface air temperature forecast based on the MGO atmospheric GCM ensemble runs. *Proceeding of MGO*. 2012. V. 566. P. 7–25.
103. *Models and Methods in the Problem of Atmosphere-Hydrosphere Interaction: Tutorial* / Eds. V.P. Dymnikov, V.N. Lykossov, E.P. Gordov. — Tomsk: Publ. House Tomsk State Univ., 2014, 524 pp. (in Russian).
104. Mokhov I. I., Akperov M. G., Prokofyeva M. A., Timazhev A. V., Lupo A. R., Le Treut H. Blocking in the Northern Hemisphere and Euro-Atlantic region: estimates of changes from reanalysis data and model simulations // *Doklady Earth Sciences*. 2013. T. 449. № 2. P. 430–433.
105. Mokhov I. I., Chefranov S. G., Chefranov A. G. Interaction of global-scale atmospheric vortices: modeling based on Hamiltonian dynamic system of antipodal point vortices on rotating sphere // *Procedia IUTAM Ser. "IUTAM Symposium on Waves in Fluids: Effects of Nonlinearity, Rotation, Stratification and Dissipation"* 2013. P. 176–185.
106. Mokhov I. I., Dobryshman E. M., Makarova M. E. Transformation of tropical cyclones into extratropical: the tendencies of 1970–2012 // *Doklady Earth Sciences*. 2014. V. 454. № 1. P. 59–63.
107. Neu U., Akperov M. G., Mokhov I. I., Bellenbaum N., Pinto J. G., Ulbrich S., Benestad R., Blender R., Fraedrich K., Caballero R., Hanley J., Coccozza A., Reale M., Dacre H. F., Feng Y., Wang X. L., Grieger J., Schuster M., Ulbrich U., Gulev S. et al. IM-ILAST: A community effort to intercompare extratropical cyclone detection and tracking algorithms // *Bulletin of the American Meteorological Society*. 2013. Vol. 94. № 4. P. 529–547.
108. Pogoreltsev A. I., Savenkova E. N., Pertsev N. N. Sudden stratospheric warmings: the role of normal atmospheric modes // *Geomagnetism and Aeronomy*. 2014, Vol. 54, Issue 3, pp. 357–372.
109. Portnyagin Yu.I., Merzlyakov E. G., Solov'eva T. V., Pogorel'tsev A. I., Suvorova E. V., Mukhtarov P., Pancheva D. Height-latitude structure of the vertical component of the migrating semidiurnal tide in the upper mesosphere and lower thermosphere region (80–100 km) // *Izvestiya, Atmospheric and Oceanic Physics*. 2011, Vol. 47, Issue 1, pp. 108–118.

110. Savenkova, E.N., Kanukhina A. Yu., Pogoreltsev A.I., Merzlyakov E.G. Variability of the springtime transition date and planetary waves in the stratosphere//*Journal of Atmospheric and Solar-Terrestrial Physics*. 2012. V. 90–91. P. 1–8, doi:10.1016/j.jastp.2011.11.001.
111. Schneider A., Schubert S., Vargin P., Lunkeit F., Zhu X., Peters D., Fraedrich K. Large scale flow and the long-lasting blocking high over Russia: Summer 2010 // *Monthly Weather Review*. 2012. Vol. 140. P. 2967–2981.
112. Shakina N.P., Ivanova A.R., Komarov N.I. Present-day concepts of atmospheric frontogenesis. Part 1. Theoretical ideas // *Russian Meteorology and Hydrology*. 2014a, Vol. 39, Issue 10, pp. 639–649.
113. Shakina N.P., Ivanova A.R., Komarov N.I. Present-day concepts of atmospheric frontogenesis. Part 2. Some results of computation from the real data // *Russian Meteorology and Hydrology*. 2014b, Vol. 39, Issue 11, pp. 713–726.
114. Shakina N.P., Ivanova A.R., Birman B.A., Skriptunova E.N. Blocking: conditions of summer 2010 and the present state-of-art of investigation. In “Analysis of anomalous weather conditions over the territory of Russia in summer 2010”. 2011. Triada Ltd, pp. 6–21 (In Russian).
115. Shakina N.P., Khomenko I.A., Ivanova A.R., Skriptunova E.N. Origination and forecasting of freezing precipitation: review and some new results // *Proceedings of Hydrometcentre of Russia*. 2012. Vol. 348. P. 130–161. (In Russian).
116. Shakina N.P., Skriptunova E.N. Diagnosis and forecasting of the probability spectra of precipitation rate ranges // *Russian Meteorology and Hydrology*. 2011, Vol. 36, Issue 8, pp. 499–510.
117. Shkolnik I.M., Efimov S.V., Cyclonic activity in high latitudes as simulated by a regional atmospheric climate model: added value and uncertainties // *Environ. Res. Lett.* 2013, 8. 045007 (12 pp.).
118. Shmerlin B. Ya., Kalashnik M. V., Shmerlin M. B. Convective instability of a water-vapor-saturated atmospheric layer. The formation of localized and periodic cloud structures // *Journal of Experimental and Theoretical Physics*. 2012. V. 115. № 6. P. 1111–1127.
119. Shmerlin B. Ya., Kalashnik M. V. Rayleigh convective instability in the presence of phase transitions of water vapor. The formation of large-scale eddies and cloud structures // *Physics — Uspekhi*. 2013. V. 56. № 5. P. 473–485.
120. Shmerlin B. Ya., Shmerlin M. B. The use of hydromechanical model for description of movement of tropical cyclones // *Herald of N.I. Lobachevsky State University of Nizhny Novgorod*. 2011. № 4 Part 2. N.I. Lobachevsky State University of Nizhny Novgorod Press, 2011, pp. 564–566 (In Russian).
121. Shmerlin B. Ya., Shmerlin M. B. A hydromechanical model of movement of tropical cyclones // *Current problems in remote sensing of the Earth from space* 2012. T. 9. № 2. C. 243–248 (In Russian).
122. Shmerlin B. Ya., Shmerlin M. B. Forecast of movement of tropical cyclones (TC) with the use of a hydromechanical model (HMM) // *International Conference MSS-2014 “Wave transformation, coherent structures and turbulence”*/ Moscow. November 24–27, 2014. Collected papers. M.: LENAND. 2014. P. 268–273 (In Russian).

123. Shmerlin B. Ya., Shmerlin M. B. Convective instability of cloud media // International Conference MSS-2014 “Wave transformation, coherent structures and turbulence”/ Moscow. November 24–27, 2014. Collected papers. M.: LENAND. 2014. P. 262–267 (In Russian).
124. Starchenko A. V., Danilkin E. A., Nuterman R. B., Terenteva M. V. Application of a microscale meteorological model for studying the airflow pattern above the airport runway // *Vestn. Tomsk. Gos. Univ. Mat. Mekh.*, 2013, No 5(25), P. 91–101.
125. Stepanenko V. M., Machul’skaya E. E., Glagolev M. V., Lykossov V. N. Numerical modeling of methane emissions from lakes in the permafrost zone // *Izvestiya, Atmospheric and Oceanic Physics*. 2011, Vol. 47, No. 2, pp. 252–264.
126. Surkova G., Blinov D., Kirsanov A., Revokatova A., Rivin G.. Simulation of spread of air pollution plumes from forest fires with the use of COSMO-Ru7-ART chemical-transport model // *Atmospheric and Oceanic Optics*, 2014, Vol. 27, N3, p. 268–274.
127. Suvorova E. V., Pogoreltsev A. I. Modeling of nonmigrating tides in the middle atmosphere // *Geomagnetism and Aeronomy*. 2011, Vol. 51, Issue 1, pp. 105–115.
128. Svirkunov P. N., Kalashnik M. V. Phase patterns of waves from localized sources moving relative a stratified rotating medium (Moving Hurricane, Orographic Obstacle) // *Doklady Physics*. 2012, Vol. 57, Issue 12, pp. 474–478.
129. Svirkunov P. N., Kalashnik M. V. Phase patterns of dispersive waves caused by moving localized sources // *Physics Uspekhi*. 2014. Vol. 57, Issue 1, pp. 80–91.
130. Troitskaya Y. I., Druzhinin O., Zilitinkevich S. Direct numerical simulation of a turbulent wind over a wavy water surface // *J. Geophys. Res.* 2012. 117, C00J05, doi:10.1029/2011JC007789, 16 pp.
131. Troitskaya Yu. I., Ezhova E. V., Zilitinkevich S. S. Momentum and buoyancy exchange in a turbulent air boundary layer over a wavy water surface. Part 1. A harmonic wave// *Non-linear Proc. in Geophysics*. 2013. 20, 825–839 (DOI:10.5194/npg-20–825–2013).
132. Troitskaya Yu. I., Ezhova E. V., Sergeev D. A., Kandaurov A. A., Vaidakov G. A., Vdovin M. I., Zilitinkevich S. S. Momentum and buoyancy exchange in a turbulent air boundary layer over a wavy water surface. Part 2. Wind wave spectra // *Non-linear Proc. in Geophysics*. 2013. 20, 841–856 (DOI: 10.5194/npg-20–841–2013).
133. Troitskaya Yu. I., Sergeev D. A., Druzhinin O., Kandaurov A. A., Ermakova O. S., Ezhova E. V., Esau I., Zilitinkevich S. Atmospheric boundary layer over steep surface waves//*Ocean Dynamics*. 2014. 64, 1153–1161 (DOI 10.1007/s10236–014–0743–4).
134. Tsyrlunikov M. and Gorin V. Are atmospheric-model tendency errors perceivable from routine observations? // *COSMO Newsletter N13*, 2013.
135. Turbulence, Dynamics of Atmospheric and Climate. Collected papers of International Conference devoted to the memory of Academician A. M. Obukhov / Eds. G. S. Golitsyn, I. I. Mokhov, S. N. Kulichkov, M. V. Kurgansky, O. G. Chkhetiani Moscow: GEOS, 2014, 697 pp (In Russian).
136. Vargin P. N., Luk’yanov A. N., Gan’shin A. V. Investigation of dynamic processes in the period of formation and development of the blocking anticyclone over European Russia in summer 2010 // *Izvestiya, Atmospheric and Oceanic Physics*. 2012. Vol. 48, Issue 5, pp. 476–495.

137. Vargin P.N., Medvedeva I.V. Temperature and Dynamical Regimes of the Northern Hemisphere Extratropical Atmosphere during Sudden Stratospheric Warming in Winter 2012–2013 // *Izvestiya, Atmospheric and Oceanic Physics*, 2015, Vol. 51, No. 1, pp. 12–29.
138. Vasil'ev, O.F. Voropaeva, and A.F. Kurbatskii. Turbulent Mixing in Stably Stratified Flows of the Environment: The Current State of the Problem (Review) // *Izvestiya, Atmospheric and Oceanic Physics*, 2011, Vol. 47, No. 3, pp. 265–280.
139. Vilfand R.M., Rivin G.S., Rozinkina I.A. Modern operational systems for limited-area numerical weather forecast // *SibNIGMI Proceedings*. 2011. Issue 106, p.5–12.
140. Visheratin K.N., Kalashnik M.V. Nonlinear acoustic oscillations in swirling gas flows // *Fluid Dynamics*. 2014. Vol. 49, Issue 4, pp. 530–539.
141. Vul'fson A.N., Borodin O.O. Boltzmann-Jaynes variational method and the temperature distribution of thermals in the turbulent convective atmospheric surface layer // *Izvestiya, Atmospheric and Oceanic Physics*. 2012, Vol. 48, Issue 6, pp. 603–609.
142. Yaroshevich M.I., Ingel L. Kh. Diurnal variations in the intensity of tropical cyclones // *Izvestiya, Atmospheric and Oceanic Physics*. 2013, Vol. 49, Issue 4, pp. 375–379.
143. Zdereva M. Ya., Tokarev V.M. Analysis and forecast of weather conditions affecting the concentration of atmospheric pollutants in a megalopolis // *Proceedings of Siberian Regional Scientific Research Hydrometeorological Institute*. 2011. Issue 106. P. 152–158.
144. Zdereva M. Ya., Tokarev V.M., Vinogradova M.V. Automated forecast of air temperature with training by the method of a group account of arguments // *Proceedings of Siberian Regional Scientific Research Hydrometeorological Institute*. 2011. Issue 106. P. 143–151.
145. Zilitinkevich S.S., 2012: The Height of the Atmospheric Planetary Boundary layer: State of the Art and New Development — Chapter 13 in “National Security and Human Health Implications of Climate Change”, edited by H.J.S. Fernando, Z. Klaić, J.L. McKulley, NATO Science for Peace and Security Series — C: Environmental Security (ISBN 978-94-007-2429-7), Springer, 147–161.
146. Zilitinkevich S.S. Atmospheric Turbulence and Planetary Boundary Layers. 2013. Fizmatlit, Moscow, 248 pp. (in Russian).
147. Zilitinkevich S.S., Elperin T., Kleorin N., Rogachevskii I., Esau I.N. A hierarchy of energy- and flux-budget (EFB) turbulence closure models for stably stratified geophysical flows // *Boundary-Layer Meteorol.* 2013. 146, 341–373 (DOI: 10.1007/s10546-012-9768-8).
148. Zilitinkevich S.S., Tyuryakov S.A., Troitskaya Yu. I., Mareev E.A. Theoretical models of the height of the atmospheric boundary layer and turbulent entrainment at its upper boundary // *Izvestiya, Atmospheric and Oceanic Physics*. 2012. Vol. 48, No. 1, pp. 133–142. DOI: 10.1134/S0001433812010148.

Middle Atmosphere

A. A. Krivolutsky, A. A. Kukoleva

Central Aerological Observatory

krivolutsky@mail.ru kuan-2012@yandex.ru

The review presents the main results of Russian research in the area of the middle atmosphere (10–100 km) in the period 2011–2014. The following questions were considered: numerical modeling of the composition and dynamics of the atmosphere under various perturbations on its lower and upper boundaries; the calculations of climate change; the monitoring data on the composition and thermodynamic regime of the atmosphere. The active impact is described on the middle atmosphere by powerful HF radiation from the surface of the Earth.

Key words: composition of the middle atmosphere, numerical modeling, climate, atmospheric ozone, dynamic of the atmosphere, the stratosphere, the mesosphere.

1. Introduction

The region of the middle atmosphere (MA), the height of 10–100 km, is actively studied over the last years thanks to the development of satellite observations a network and numerical models. Thermodynamic processes in MA are largely determined by the photochemistry of atmospheric ozone. The ozone concentration depends on the atmospheric composition (the concentrations of the connection group NO_y, HO_x, aerosol, etc.), and on the solar radiation variations, on the corpuscular fluxes of solar and galactic cosmic rays. The O₃ concentration changes causes the relevant changes in temperature and dynamics of the middle atmosphere, the variations of solar radiation spectral composition that penetrating to the troposphere. To understand the causes of the variations of the atmosphere in General is needed about the connections between chemistry, photochemistry and atmospheric dynamics occurring in different layers.

2. Study long-term changes in the composition and mode of the atmosphere

2.1. Some problems of climate research

Existing problems of climate modeling are discussed in several papers [1–7]. In [1] author presented the issues of the monitoring system of main climate-forming factors (greenhouse gases, ozone, aerosol, water vapor) in the middle

atmosphere of the Earth. The block diagram of monitoring introduced and described as concept, which is implemented in the form of information-analytical system. Some materials are presented about the latitudinal distribution of ozone, about his long-term dynamics of change and on the relationship of ozone and methane in the lower stratosphere.

The Authors [2] discuss the problems which are of main importance for understanding the origin of climate changes in XX century and basic physical processes responsible for these changes. The possible role of solar activity in the Earth's climate changes in the past and future is considered. As shown, physical mechanisms which can provide for solar variability effect on weather and climate come to controlling the energy flux from the Earth to space. A special emphasis is given to mechanism of solar activity effect on climatic characteristics of the troposphere through the atmospheric electricity. The authors consider peculiarities of the response of thermal and dynamic regimes of the ocean and atmosphere to solar activity changes processes in the atmosphere, ocean, and cryosphere. The authors also show and discuss the results of analysis of regularities and peculiarities of the troposphere and ocean surface temperature (OST) response to both isolated heliogeophysical disturbances and to long-term changes of solar and geomagnetic activity.

In [3] one can find a brief review of the studies of the atmosphere sensitivity as the climate system to external forcing. Among the factors were considered: a radiative forcing (forcing, RF), the potential global warming potential (GWP) and the recently proposed global temperature potential (GTP). These values are widely used not only in research but also in the number of economic and political assessments of the effects of the factors shaping the climate and climate change (increase in greenhouse gases, aerosols, etc.). There are new indexes that require to compute quantitative information about the characteristics of the climate system components — current and anticipated — in standard periods: 20, 100 and 500 years. Calculations of some these values require the consideration of changes in the rate of energy exchange between the atmosphere and underlying surface (ocean) in the periods indicated. This factor leads to the consideration of a more General problem of sensitivity analysis of the climate system to external (radiation) exposure and its response to impact conditions for “stationary” (equilibrium) and non-stationary “greenhouse” climate.

2.2. Numerical modeling of geoengineering impacts on the atmosphere

Model [4, 5] was used to assess the effects of hypothetical geoin-generic impacts to mitigate global warming [6, 7].

General circulation model of the atmosphere and ocean was developed in the INM RAS and was named INMCM (Institute of Numerical Mathematic Climate Model, version 3.0, version 4).

The resolution of the model: $5 \times 4^\circ$ in longitude and latitude and 39 vertical levels up to a height of 90 km, the model includes the block of the General circulation of the atmosphere and ocean, as well as the block describing the chemistry of the atmosphere. In the chemical unit takes into account the variability of 74 trace gases of the atmosphere, directly or indirectly affect the photochemical change in the concentration of ozone. The reaction of oxygen, hydrogen, nitrogen, chlorine, bromine and sulphur were considered. The carbon cycle was considered, including the evolution of the carbon of plants, soils, the ocean and the atmosphere.

Atmospheric transport of chemically active impurities is carried out using the calculated dynamic block wind speeds. The chemical reactions rate are measured using the temperature obtained from the circulation model. The calculated ozone concentrations are used to calculate the velocity of the radiant heating of the atmosphere, and the methane and water vapor concentration were used to calculate the atmosphere cooling in the circulation unit. To account for heterogeneous processes discusses the formation and evolution of polar stratospheric clouds. The interaction between chemical and dynamic blocks is described in detail in [5]. The time step in a dynamic block is 5 minutes. In the ocean model resolution is $1 \times 0.5^\circ$ in longitude and latitude and 40 vertical levels. The time step is 2 hours. At each step, the boundary conditions and exchange between the atmosphere and the ocean are taken into account. The processes also were calculated occurring in the cryosphere, an Earth surface, including vegetation.

The various scenarios were considered with emission in the stratosphere H_2S , which is transformed into sulfate aerosol and increases the reflection of solar radiation by the Earth's atmosphere. The most effective scenarios was the one that ensured maximum drop of the globally averaged surface temperature. In that scenario the emission of sulfur-containing compounds occurs near the equator at a height of 22–24 km. The authors examined the equilibrium distribution of sulphate aerosol, the temperature change at the Earth's surface and at various altitudes, changes in precipitation, ozone concentrations and primary production of plants as a result of geoengineering impacts. In [7] the calculations model results are presented. The scenario assumed the geoengineering stabilizing of the global temperature at level $+2^\circ\text{C}$ relative to the average temperature at the twentieth century. Previously, the temperature rise was calculated due to the greenhouse effect. A Geoengineering impact was began in the form of H_2S injection into the stratosphere as the threshold temperature reaching a value $+2^\circ\text{C}$.

It is shown that geoengineering temperature stabilization during the twenty-first century may be in the range $+(2 \pm 0,11)^\circ\text{C}$. The 4,5 MT S injection in the

H₂S form will be annually needed to stabilize the temperature by the end of the XXI century. The specific efficiency of the method will be about 0.09 °C/MT aerosol.

It was found that the stabilization of global average precipitation intensity is not achieved with the stabilization of global temperature. The maximum influence of aerosol is implemented in the Equatorial zone, where its mass in the atmosphere will reach to 0.074 g/m² by the end of the twenty-first century.

The temperature fields characteristics and precipitation are compared with ones for two cases: in the absence of temperature stabilization and in the geoengineering application. It is shown that the use of the climate geoengineering will greatly reduce the temperature anomalies for most of the regions. The effect of the rapid global temperature increase is evaluated during sudden of geoengineering impacts. The modeling results are described in the case of gradual decreasing of the impacts intensity. In this case the negative effect will be smoothed.

2.3. Assessment of changes in ozone and atmospheric dynamics in the XXI century

In [8] a three-dimensional chemistry-climate model SOCOL was used for assessment of ozone and atmospheric dynamics changes during the XXI century. The model performed four numerical experiment in the “time section” conditions for 1980, 2000, 2050 and 2100.

Boundary conditions, including the temperature of the ocean surface, sea ice parameters, the concentration of greenhouse and ozone-depleting gases have been established for these calculations in accordance with the IPCC scenario “A1B” and the WMO scenario — A1. The statistically significant cooling of modeling stratosphere was obtained: at 4–5 K for 2000–2050, and 3–5 K for 2050–2100.

The temperature of the lower atmosphere increases during the twenty-first century by 2–3 K. The warming of the troposphere provides a significant increase of planetary scale wave activity at the tropopause level. This leads to a substantial increase in the flow of Eliassen-Palma and its divergence in the middle and upper model the stratosphere. Thus there is a weakening of the zonal circulation intensity and strengthening of the meridional residual circulation, especially in the winter and spring of each hemisphere. These dynamic changes decrease concentrations of ozone-depleting gases and accelerate the growth of O₃ outside of the tropics. Thus, by 2050, the total ozone value in middle and high latitudes very close to her modeling level in 1980, and the “ozone hole” in Antarctica is populated. According to modeling the “overreduction” of the ozone layer happens in 2100 in middle and polar latitudes of both hemispheres. In the tropics the ozone layer is recovering much more slowly, reaching the level of 1980 only to 2100 yr.

3. The complex studies of the atmosphere using observation data and numerical methods

3.1. Numerical modeling of the General circulation of the middle atmosphere response on spatial heterogeneity orographic waves

In [9] the interaction of orographic waves and the General circulation of the atmosphere is simulated. Orographic waves was induced by the topography of the earth's surface. The following results are obtained: polarization ratios for stationary mesoscale orographic waves (SOW); the formula for calculating the total vertical flux of wave energy; the formula of the vertical profile of the horizontal vibration amplitude of velocity taking into account the rotation of the atmosphere; the full expression for the wave of heat flow; the acceleration of middle flow and heat created by the SOW.

Characteristics of the SOW propagation from the Earth's surface to heights of the lower thermosphere are calculated.

Obtained by the authors [9] parameterization of dynamical and thermal effects of stationary orographic waves are included in a three-dimensional nonlinear model of the General circulation of the middle and upper atmosphere. The model is developed based on the model COMMA-LIM (Cologne Model of the Middle Atmosphere — Leipzig Institute for Meteorology) [10, 11]. As the lower boundary conditions are used climatic distribution of geopotential height and temperature.

The latitudinal and vertical distribution of the temperature in the troposphere and lower stratosphere are used in the model. Ones are derived from these reanalysis models: NCEP/NCAR (National Centre of Environmental Prediction / National Centre for Atmospheric Research), UK Met Office (United Kingdom Meteorological Office). Stationary planetary waves with wave numbers 1–3 are considered. One were derived from the UK Met Office model.

Model results realistically reproduce the location and intensity of jet streams in the troposphere, which is necessary for correct modeling of the occurrence of orographic waves.

On the upper and the lower boundary of the vertical mass flux was supposed equal to zero. The lower boundary condition is imposed through the perturbation of the geopotential on the Earth's surface due to tidal fluctuations. It is shown that a SOW can have a significant impact on the circulation and thermal regime of the middle and upper atmosphere.

The atmospheric circulation sensitivity is considered during SOW generating and propagating at different seasons. As shown SOW have a major dynamic and thermal effects on the middle atmosphere of the winter hemispheres during the

solstices periods. Change of the zonal circulation velocity, called a SOW, can reach 30% in these regions. The impact of SOW is distributed more evenly between the Northern and Southern hemispheres in the periods of the equinoxes. The relative speed changes of the zonal circulation can be 10% in the middle atmosphere.

The SOW effect on the meridional and vertical RMS-velocity is investigated in [11, 12]. It is necessary to consider atmosphere rotation in mathematical ratios for orographic waves when calculating the vertical profile of the heat inputs and wave accelerations using stationary orographic waves. According to the results of calculations orographic waves create significant heat (up to 10–15/day at altitudes of 50 km), and average accelerations of flow (up to 20 m/s²/day). One can greatly affect the overall circulation, planetary waves and thermal regime of the middle atmosphere.

Accounting for orographic waves leads to changes in the vertical ozone flux (10–15%) generated by the General circulation of the atmosphere at altitudes from 20 to 60 km. The dynamic and thermal effects of these waves leads to changes in the meridional circulation and related ozone flux according to modeling [12]. The corresponding changes of the vertical ozone flux generated by the General circulation of the atmosphere, amounted to 10–15% at altitudes from 20 to 60 km, reaching 20–30% at the altitude of maximum ozone layer.

A numerical modeling algorithm for the vertical distribution and destruction of nonlinear acoustic-gravity waves (AGW) from the ground to the upper atmosphere is briefly described in [13]. Monochromatic variations of vertical velocity at the earth's surface are used as the source of AGW in the model.

The algorithm used to solve the hydrodynamic equations was based on three-dimensional finite-difference analogues of the basic conservation laws. This approach allows to select the physically correct generalized wave solutions of the hydrodynamic equations. Numerical simulation is carried out in the field heights from the ground surface to 500 km. Vertical profiles of the background temperature, density, coefficients of molecular viscosity and thermal conductivity are defined by standard models of the atmosphere. The calculations are performed for different amplitudes of the wave source at the lower boundary. The amplitude of the AGV increasing with height, and the waves can break down in the middle and upper atmosphere.

3.2. Study of tidal phenomena in the middle atmosphere

On the heights of the mesosphere and lower thermosphere tidal fluctuations are the strongest regular perturbations, which affect daily and seasonal variations in temperature, composition, and dynamic mode.

In [14, 15] altitudinal and latitudinal distribution of diurnal tide were calculated for the vertical wind speed component in the mesosphere and lower thermosphere (80–100 km). The monthly average variations of the horizontal wind speed component due to the diurnal migrating tide were used.

The used data were obtained from the results of satellite observations of the mesosphere and lower thermosphere in the altitude range 90 to 120 km. The ground sounding results of this area by radiometry method and the method of partial reflections in the altitude range of 80–100 km were used. The numerical simulation of the migrating diurnal tide was made. The global circulation model of the middle and upper atmosphere was used for the calculations. The calculation results compared of the observed semidiurnal temperature variations from the satellite. It is shown that different models give good agreement of the distribution parameters semidiurnal oscillations within the errors of the values. The distribution of semidiurnal fluctuations parameters of the vertical wind was received. Their feature is the presence of the high-latitude regions of local maximum values of the amplitudes. Overall, at altitudes of about 90 km and above semidiurnal fluctuations of vertical wind exceed in amplitude the prevailing vertical wind.

In [15] it is shown that the models give good agreement of the distribution of the parameters of the migrating diurnal tide. Revealed the presence of three regions of high values of the amplitude of the vertical component of wind velocity in the vicinity of the equator and latitudes 30°N and 30°S, which are observed in all seasons. The maximum value of vibration amplitude of the vertical components of the wind velocity of approximately 0.1 m/sec. Evaluate the divergence of the flow of Eliassen Palma give the value of about 10 m s⁻¹ day⁻¹.

3.3. Study of the sudden stratospheric warmings (SSW)

Despite the winter stratospheric warming were discovered in 1952, they are still not fully understood. Accumulated data over more than a half-century period indicates an important role of the SSW in the formation of thermodynamic characteristics in the troposphere, in the stratosphere, and even in the upper atmosphere and ionosphere.

The paper [16] analyses disturbances of the Earth's middle atmosphere temperature regime associated with sudden stratospheric warmings observed over West, East Siberia and Russian Far East in January–February of 2008–2010. The analysis rests on data on vertical temperature distribution in the upper troposphere and stratosphere obtained from lidar measurements over Tomsk, Yakutsk and Paratunka, the Kamchatka Krai. For the complex analysis of the spatial-temporal temperature distribution in the middle atmosphere, the lidar measurement

data are exploited along with satellite data on temperature acquired by “Aura” Microwave Limb Sounder (MLS). This paper addresses regional effects of sudden stratospheric warmings over the Asian region of Russia in the longitudinal sector of $\sim 85\div 160^\circ$ E during winters of 2008–2010. During the development of the SSW in high-altitude temperature profiles appear several maximums, pronounced stratopause and the mesopause was absent. Region of elevated temperature in stratopause (maximum warming reached $70\text{--}80^\circ$) was expanded to tens of kilometers or more and down to heights of about 25 km. In General, there was satisfactory agreement between the data of measurements of the altitude distribution of stratospheric temperatures lidar and satellite methods.

The authors of [17] on the basis of calculations using the model of the General circulation of the middle and upper atmosphere studied the role of normal atmospheric modes in the occurrence and development of sudden stratospheric warming (SSW). Analysis of the influence of the phase of the quasi-biennial oscillation on the extratropical dynamics of the stratosphere showed that during the East phase of these oscillations, the situation for the occurrence of events more favourable SSW, and the events themselves SSW more intense in comparison with the Western phase. It is concluded that the normal atmospheric modes may be detected in the temperature field at altitudes of the mesopause using ground optical method measurements.

In [18] the results of long-term radiation observations of hydroxyl and the atmospheric system of molecular oxygen, the temperature of the hydroxyl near the mesopause were used. The intensity of the night and the variability of these parameters were investigated during winter sudden stratospheric warming. For hydroxyl considered band (6–2), $\lambda = 834.4$ nm, for molecular oxygen — band A(0–1), $\lambda = 864.5$ nm. The epoch superposition method shows the activity growing of internal gravity waves in the mesopause region for several days after the SSW.

A correlation between the standard deviation of the temperature due to the tides, and prevailing zonal wind was received in [19]. The SSW induced changes of the temperature gradient affect dramatically the SSW propagation. Planetary waves carry out spatial and temporal modulation of SSW propagation. SSW, in turn, transfer momentum and energy to the average current, changing and affecting planetary and tidal waves.

In [20] a weak (minor) stratospheric warming event and transition of the stratosphere to the background thermal regime observed in 2011 is analyzed in comparison with the preceding (major) warming event observed from January 22 till January 29, 2010. During this period, the temperature in the stratopause at some nights increased up to $+30^\circ\text{C}$, and the tropopause height decreased to 37–38 km. In February, the temperature noticeably decreased; its positive deviation from the average monthly value was observed in the altitude range below

40 km. The stratopause reached record low altitudes of 23–25 km. In April, the vertical temperature profile approached that, described by the CIRA-86 model. For the warming event in 2011, dynamic events occurred in January. Thus, a sharp temperature change was observed on January 14, when in accordance with lidar and satellite data, the stratopause height decreased to 32–35 km, and the temperature deviation reached 42–45 K. On January 15, from the data of lidar measurements, the stratopause height was smeared (it extended from 30 to 37 km), and from the data of satellite observations, it decreased by 31 km. In the subsequent months in February–April, the vertical temperature profile was stabilized with transition to the background state.

In [21] the results of joint ground-based measurements of vertical structures of ozone and temperatures with the use microwave and lidar technical equipment during stratospheric warming are presented. During winter warming (December 2012 — January 2013) appreciable variations of ozone concentration and temperature in the middle atmosphere are registered. Changes of ozone concentration at height levels from 25 to 60 km increased by 1.5–2 times, the amplitude of their oscillations thus has considerably increased. The peak of a positive deviation of temperature from its monthly average value reached 70 K at a height of 30 km. Daily ozone oscillations at a height of 60 km, connected with sunset and sunrise, were about 30%.

Sudden stratospheric warming which is important element in the dynamics of climate system and impacts weather anomalies in the troposphere. In [22] the temperature in the stratosphere is compared with the characteristics of circulation in the troposphere and stratosphere in the winters of 2008/09 and 2012/13. It is found that SSW is associated with increased stationary orographic waves. Blocking anticyclones in the troposphere are destroyed for 15–20 days before the onset of SSW. Distribution of torsional oscillations in the stratosphere from the low-latitude area contributed to the development of the SSW.

3.4. The study of the Earth atmosphere quasi-biennial oscillation

The quasi-biennial oscillation (QBO) — a well-known interannual atmospheric variability, mechanisms of their formation have not been completely found out — an example of high-frequency quasi-regular variability of an atmosphere (and climate) of the Earth on interannual scales. There is the review [23] of researches devoted to the history of discovery of QBO zone wind in the stratosphere of the Earth and the identification of mechanisms of their formation, and also there are described the observational data of the quasi-biennial oscillations of various characteristics of the atmosphere — the data of ground-based observations obtained in the form of local measurements. There is the review of the

results of the numerical and laboratory models of QBO, there are described mechanisms of formation of QBO and the theoretical models, which are unable to generate similar to a realistic oscillations. There are discussed on the relationship between the QBO and the meridional atmospheric circulation, the tropical convection, the activity of tropical cyclogenesis. There are presented characteristics of the waves forced at lower layers of the tropical stratosphere and help to drive the QBO in the appendix

In [24] tested the hypothesis of Holton and Tan [25] consists in the fact that oscillation of Equatorial stratospheric wind change the terms vertical and meridional propagation of planetary waves in the extratropical regions. This may be the cause of the quasi-biennial oscillation in middle and polar latitudes. The estimates of the atmospheric wave activity are made to verify the hypothesis of the Holton-Tan. This assessments are made for the Northern hemisphere winter during different phases of the quasi-biennial oscillation of Equatorial stratospheric zonal wind. The evaluation showed that a higher level of wave activity expected in the Eastern Equatorial phase of the QBO, was characteristic only for the establishment period of the winter circulation. In late winter a higher level of wave activity observed during the West phase of the FTC, which contradicts the hypothesis of the Holton-tan. In late winter a higher level of wave activity observed during the West phase of the QBO, which contradicts the hypothesis of the Holton-Tan. A small but noticeable differences in the level of wave activity in the lower troposphere suggests that the cause of the quasi-biennial cyclicity of wave activity in the middle latitudes at all height can be fluctuations of synoptic processes between the predominantly zonal and meridional circulation forms.

The authors of [26] note the changes of the vertical structure of the Equatorial wind in the stratosphere during the QBO cycle. They demonstrate a clear connection with the seasons. The lowering mode of the East wind from the average in the lower stratosphere has always fixed period — a stagnation. The East wind lower bound in different QBO is located at different height in the range from ~22 to ~26 km In each individual QBO. One was practically constant throughout the period of stagnation. Stagnation always begins on the solstice (in June-July or December-January). The resumption of descent after stagnating always begins near the vernal equinox in March-April or September-October. Consequently, the duration of stagnation varies discretely, and in different cycles may be equal to one, three or five seasons (three, nine or fifteen months, respectively). If the period, QBO defined as the interval between the starting moments of successive stages of stagnation, it must also change discretely and may be equal to 24, 30 or 36 months. The many atmospheric phenomena that affect the Earth's climate depend on a QBO phase. The prediction of the QBO evolution need. Established seasonal patterns allow to forecast the QBO development, its duration and moments of change of phases of a cycle.

The paper [27] analyzed the pattern of the quasi-biennial oscillation of the total ozone and ozone concentrations at separate altitudinal levels in the stratosphere over Arctic territory and Tomsk according to data of TOMS satellite instrumentation. The correlation coefficient between TO changes and variations in equatorial zonal wind for the period of 1996–2013 is statistically insignificant. The average springtime (over March–April) values of ozone concentration and zonal wind mostly show the correlation in the interval of $-0.23 \div -0.26$. The time series of the mixing ratio, composed for separate altitudinal levels over the period of 2005–2013, exhibit quasi-biennial oscillation, which takes shape at heights of ~ 30 km and weakens in overlying regions. The correlation dependence between the ozone mixing ratio and the equatorial zonal wind index most distinctly manifests itself in the Western Hemisphere and is more complex in the Eastern Hemisphere.

3.5. The interaction of the stratosphere and troposphere

This paper [28] covers the question of stratosphere-troposphere exchange in 2007–2009 in transitional ocean — continent zone by means of lidar measurements of vertical ozone distribution. The simultaneous analysis of vertical ozone distribution, meteo and wind field parameters shows that stratosphere-troposphere exchange over the Vladivostok is caused primarily by tropopause folds, which are formed due to stratospheric air movements from north to south and then into the troposphere southwest from cyclones. In this case, positive trend of ozone concentration and decrease of air humidity in upper troposphere occurs when polar air masses forms polar jet in the vicinity of subtropical jet. Hence, the location of kernels of both jets becomes unstable and breaks down a tropopause inversion layer, that leads to possibility of stratospheric air intrusions into the troposphere in the area of mutual influence of jet streams.

Two possible mechanisms of stratospheric control for concentration and dynamics of ozone in troposphere through stratosphere are considered in [29]. The first is carried out through modulation by the general contents of ozone in a stream of ultra-violet radiation in troposphere and starting up here photochemical processes. The second mechanism acts through direct carry from the stratosphere of ozone, triggering the photolysis and the initiation of the same processes of generation of ozone, but already in troposphere. It is shown, that in area of Tomsk both management mechanisms manifest themselves by stratospheric ozone of its ground concentration. Thus, management through an ultra-violet stream determines the amplitude modulation, and carrying from stratosphere to troposphere, the time one.

3.6. Studies of the Solar-terrestrial relations

The condition of the middle and upper Earth atmosphere is determined by the action of solar electromagnetic radiation, corpuscular fluxes (protons from solar flares, eruptions of relativistic electrons), galactic cosmic rays.

In [30] changes in neutral composition, thermal and dynamic atmosphere conditions during periods of the Sun disturbances were discussed. The impact on the atmosphere of the solar corpuscular fluxes, electromagnetic radiation, galactic cosmic rays, relativistic electron precipitations is considered. An overview of the basic results in the field of measurements and calculations of ionization of the atmosphere. It is shown the effect of these factors leads to 1) direct destruction of the ozone dissociating UV radiation with $\lambda < 3068 \text{ \AA}$; 2) the formation of chemical substances that affect the global balance of ozone: sources of ozone atomic oxygen under the action of $\lambda < 2424 \text{ \AA}$ and sinks of ozone (compounds like NO_x and HO_x). The observation and model calculation results of changes in neutral composition of the atmosphere during the period of disturbances, thermal and dynamic response were presented. The review concluded the action mechanisms of charged particles in earth's atmosphere below 100 km require further research.

Authors [31] have compared composition changes of NO, NO₂, H₂O₂, O₃, N₂O, HNO₃, N₂O₅, HNO₄, ClO, HOCl, and ClONO₂ as observed by the Michelson Interferometer for Passive Atmospheric Sounding (MIPAS) on Envisat in the aftermath of the "Halloween" solar proton event (SPE) in late October 2003 at 25–0.01 hPa in the Northern Hemisphere (40–90 N) and simulations performed by the following atmospheric models: the Bremen 2-D model (B2dM) and Bremen 3-D Chemical Transport Model (B3dCTM), the Central Aerological Observatory (CAO) model, FinROSE, the Hamburg Model of the Neutral and Ionized Atmosphere (HAMMONIA), the Karlsruhe Simulation Model of the Middle Atmosphere (KASIMA), the ECHAM5/MESSy Atmospheric Chemistry (EMAC) model, the modeling tool for SOLar Climate Ozone Links studies (SOCOL and SOCOLi), and the Whole Atmosphere Community Climate Model (WACCM4). The large number of participating models allowed for an evaluation of the overall ability of atmospheric models to reproduce observed atmospheric perturbations generated by SPEs, particularly with respect to NO_y and ozone changes. We have further assessed the meteorological conditions and their implications for the chemical response to the SPE in both the models and observations by comparing temperature and tracer (CH₄ and CO) fields. Simulated SPE-induced ozone losses agree on average within 5% with the observations. Simulated NO_y enhancements around 1 hPa, however, are typically 30% higher than indicated by the observations which are likely to be related to deficiencies in the used ionization rates, though other error sources related to the models'

atmospheric background state and/or transport schemes cannot be excluded. The analysis of the observed and modeled NO_y partitioning in the aftermath of the SPE has demonstrated the need to implement additional ion chemistry (HNO_3 formation via ion-ion recombination and water cluster ions) into the chemical schemes. An overestimation of observed H_2O_2 enhancements by all models hints at an underestimation of the OH/HO₂ ratio in the upper polar stratosphere during the SPE. The analysis of chlorine species perturbations has shown that the encountered differences between models and observations, particularly the underestimation of observed ClONO_2 enhancements, are related to a smaller availability of ClO in the polar night region already before the SPE. In general, the intercomparison has demonstrated that differences in the meteorology and/or initial state of the atmosphere in the simulations cause a relevant variability of the model results, even on a short timescale of only a few days.

The results of 3D numerical simulation are presented in [32]: temperature changes, wind speed and composition in the altitude range up to 130 km caused by 1) the influence of high energy protons during the solar flares, and 2) the change in the spectral composition of Solar radiation in 23 of CSA .

In the simulation the following models are used: three-dimensional numerical photochemical model of the middle atmosphere and troposphere, the global circulation model of the troposphere, middle atmosphere and lower thermosphere. The interaction between 30 chemical components is considered in photochemical block of the model. This block includes 73 chemical reactions, 38 photodissociation reactions. The time step 100, the rate of dissociation was calculated in an hour. The range of heights — 0–88 km, step — 2 km; step in latitude 5° , the longitude is 10° .

The global circulation model CHARM (developed versions of the COMMA), it contains more advanced radiation units, taking into account the radiative transfer in the presence of clouds and aerosol, also this model has a more detailed spatial resolution: a height step — 1 km (range 1–135 km), longitude step — 11.5° , latitude step — 10° . The model includes the molecular viscosity, turbulence, ion friction.

In [32] the effect of solar proton event (SPE) 28.11.2003 on the composition of Earth's atmosphere is considered. Calculations of the atmosphere ionization rate were carried out using the block AIMOS [33]. One based on the measurements of the fluxes of solar protons and relativistic electrons and presented in [34]. The investigation showed the absence of zonal homogeneity in ionization rates distribution due to, firstly, the magnetic pole shift, and, secondly, the polar caps expansion into the lower latitudes during geomagnetic disturbances.

Changes in temperature and wind speed were obtained using the model of the General circulation of the atmosphere based on early calculated ozone changes during SPE28.11.2003. The results showed a very large period of NO_y influence

to ozone concentration after SPE ending. This duration of effect is associated with a long lifetime NO_y formed by SPE. The effect on the ozone intensifies after the end of polar night. The analysis of the respective temperature changes in the atmosphere showed the most cooling (5 K) in summer in the stratosphere due to the destruction of ozone in the high latitudes (75 N). The results showed the small temperature decrease in the troposphere and increase in the mesosphere.

The calculations show the corresponding changes of the zonal wind speed in the Northern polar latitudes (75 N). The zonal wind speed increases up to (2–4 m/s) in spring and autumn period in the upper stratosphere. The zonal wind speed weakened in the troposphere in autumn (a year after SPE). In the southern hemisphere (72.5 S) the zonal wind changes is negligible. This is a consequence of the seasonal insolation differences between the Northern and southern hemispheres during the related period.

The atmosphere composition response to the solar radiation variation in 23 CSA is presented in [32]. According to the observation data the declining phase of 23 CSA was very long and the UV solar irradiance was extremely low. The modeling was made using the UV spectral irradiance values about 2 times smaller than in previous cycles. In the numerical scenarios the characteristics of the internal stationary gravity waves were set for the lower boundary. According to the modeling results the temperature increasing was about 2 K in the mesosphere and up to 20 K in the thermosphere.

Studies of the temperature response and the zonal wind response showed a wavy structure along the circle of latitude: alternation of positive and negative deviations. The temperature variation amplitude was about 5 K in the troposphere and stratosphere. The wind variations were with amplitude up to 1 m/s.

The author [35] investigated the 11-year CSA influence on the ozone content in the stratosphere and lower mesosphere. For this the data of satellite measurements (instruments SBUV/SBUV2) in 1978–2003 were used, and methods of spectral, cross-spectral and regression analysis were applied. The high coherence between the ozone concentration and the level of solar activity is received.

In most of the middle atmosphere ozone varies were approximately in phase with the solar cycle. In areas of significant gradients of the ozone mixing ratio, the phase shift between ozone and solar fluctuations can be considerable (up to $\pi/2$). This shift appears to be caused by dynamic processes.

The maxima of ozone sensitivity to the 11-year solar cycle is observed above the stratopause (50–55 km), in the middle stratosphere (35–40 km) and lower stratosphere (below 25 km). The maximum changes of ozone in the solar cycle, up to 10% or more, occurred in the winter and spring in the polar regions.

In [36] effects of the Pinatubo volcano eruption and variations of solar activity on stratospheric O_3 and NO_2 are estimated, using data of satellite measurements of ozone concentration by SBUV/SBUV-2 instruments and results of

ground-based measurements of the column NO_2 content in the NDACC. The NO_2 decrease related to the Pinatubo eruption is within 19–23% at different stations, the NO_2 decrease in the Southern hemisphere (SH) is on the whole something larger than in the Northern hemisphere (NH). The decrease in O_3 concentration in the NH extratropical lower stratosphere ($\sim 10\%$) is, on the contrary, much larger than in the SH. Maximal decrease in ozone concentration is noted in the neighbourhood of 10 hPa level (32 km) at 10–15°S. The effect of the 11-year solar cycle in stratospheric ozone is approximately symmetrical about the equator. Altitude maxima of the O_3 response to the solar cycle are noted at altitudes of 50–55, 35–40, and below 25 km. The changes in O_3 concentration in these layers are usually within several percents. Essential interhemispheric difference is noted in the NO_2 response to the 11-year solar cycle. The NO_2 content at most of SH stations is usually lower during the phase of maximum than during the phase of minimum of solar activity. The NO_2 content at the low- and mid-latitude stations of the NH is often larger during a solar activity maximum compared to that during its minimum. NO_2 changes related to the solar cycle are usually within 5%.

The authors [37] investigate the influence of the solar and galactic cosmic rays variations on the duration of elementary SYNOPTIC processes (ESR) in the Atlantic-European sector of the Northern hemisphere. It is found that the bursts of solar cosmic rays (SCR) increase the duration of the ESP related to Western and meridional atmospheric circulation forms. Forbush decrease of galactic cosmic rays (GCR) is accompanied by an increase in the ESP duration of the meridional atmospheric circulation form. The duration of the Western and Eastern forms ESP reduces. The assumption is made that the observed changes in the ESP duration are caused by the short-period variations of cosmic rays in the intensity of cyclonic processes in middle and high latitudes. With the regeneration of cyclones in the South-Eastern coast of Greenland after bursts of the SCR and the development of a blocking anticyclone over the North-East Atlantic, Europe and Scandinavia during Forbush-decreases of GCR. The influence of the short-period variations of cosmic rays in the intensity of cyclonic processes in middle and high latitudes were established. One affect the ESP duration.

The author [38] analyzed the relation between the total ozone variations in Arosa and international index numbers of sunspots R_i for a period 1932–2009. Until the 1970s, the phase of maximum ozone variations lagged behind variations in solar activity by about 2.5–2.8 years, and in the future was ahead for about 1.5 years. The assumption is made that in the period from mid 60's to mid 70-ies of the quasi-decadal total ozone oscillation in the middle Northern latitudes were close to resonance with the oscillations of solar activity. The characteristic attenuation time of the 10-year fluctuations in total ozone was estimated. The global distribution of the phases and amplitudes of the quasi-decadal

oscillations of total ozone were studied for the period 1979–2008, according to satellite measurements. The phase of maximum quasi-decadal oscillations of total ozone first occurs in Northern temperate and high latitudes and coincides with the end of the growth phase of the 11-year solar activity cycle. In the tropics the phase of maximum oscillations lag 0.5–1 year. The maximum phase lag close to 40–50°S is about 2 years. The approximation of the O₃ variation latitudinal phase was made for the quasi-decadal periods.

Nitrogen oxides, produced as a result of ionizing proton impacts, have long lifetimes and substantially affect the ozone balance. Photochemical models give an increased production level of nitrogen oxides during solar proton flares. The authors [39, 40] were analyzed observational data from satellite UARS HALOE for ozone, NO, and temperature of the atmosphere after the solar proton event 14 July 2000. The relaxation time of nitric oxide (NO) was estimates for the mesosphere in the polar Northern latitudes using these data. The usage of an increased NO production effectiveness value (molecule number per each ion pair) during increased ionization of the atmosphere in models can be among the causes. This value has been estimated based on satellite observational data for height 60–80 km. The period of the proton event of July 14, 2000, has been considered. Data on the solar proton fluxes and the composition of the atmosphere have been used. Different methods the following value is obtained: (1.21+0.17) mol/ions pair and (0.88+0.10) mol/ions. The NO production effectiveness, obtained when the observational data were analyzed, was much smaller than the value obtained previously theoretically. The causes of these differences should be studied additionally.

In [41] shows the main results obtained over the past 60 years in the areas of research radiation the upper atmosphere. Considered nocturnal, crepuscular and diurnal conditions at altitudes above 80 km, and Discusses their relationship to other areas of atmospheric and solar processes.

4. The composition and temperature of the atmosphere from observation data

4.1. The results of measurements of ozone, NO₂ and temperature in the middle atmosphere

In [42] according to the European database ERA-40 and ERA Interim for the period 1958–2007, the models were created for average global temperature, concentration of air, ozone and water vapor, zonal and meridional winds in the altitude 0–45 km. The values of the parameter time series were represented as sum of the harmonic, trend and fluctuation components. A comparative analysis of the obtained model parameters was made. The relation between average global

ozone concentration with solar activity was found. The authors suggested a relationships physical mechanism of O₃ content and solar activity.

In the article [43] the used lidar characteristics are prepresented. The lidar sounding of the ozone height distribution are analyzed together with the data of weather stations located along the 132 Meridian. A comparison of the ozone height distribution over the Primorye and Japan in the winter is made. The established analysis showed a relationship between the subtropical jet stream and the ozone height distribution layer structure and the tropopause. It is found that region of a local maximum of the ozone height distribution above the tropopause situates at the top of the tropopause inversion layer. The width of this region depends on the distance to the core of the subtropical jet streams. It is found that in the winter, when there is a high frequency of overlap of the two tropopause, a local minimum of ozone in the lower stratosphere, corresponds to the height position of the local minimum of the squared frequency of Brent Vaisala. It is suggested that the formation of the local maximum ozone and tropopause inversion layer may be due to mixing processes in the layer of contact between the stratospheric and tropospheric circulation cells near the core of the subtropical jet streams.

In [44], IAP RAS, a comparison of the results of ground-based measurements of NO₂ at Zvenigorod scientific station and satellite measurements EOS-Aura (OMI). Comparison of the data of the satellite when it passes over the station revealed that the mean difference values of “uncontaminated” aerosol (mainly stratospheric) part of the total NO₂ content for the entire term of joint observations coincide within the errors of measurements.

However, the content of NO₂ satellite data in the summer less than the values obtained from ground-based observations, and more of them in the winter. High correlation between ground and satellite data are largely attributable to NO₂ annual variations. The correlation decreases when comparing the data by months. In General, there was considerable discrepancy between the values of the NO₂ content in the vertical column of the troposphere according to OMI data and ground-based measurements. The correlation between satellite and ground data, weak overall for the year, increases in winter and spring.

The correlation coefficient between ground-based and satellite data “uncontaminated” part of the total NO₂ content increases, and the correlation coefficient between the data of tropospheric NO₂ content decreases with clouds cover increase. The correspondence between quasi-regular seasonal variations of the OMI data and ground data is noted. However, annual variations of tropospheric NO₂ satellite data does not match the phase of the annual course in ground-based measurements. Anomaly of NO₂ in late March-early April 2011, caused by the gulfs of stratospheric air from the Arctic ozone “hole”, is clearly manifested in the results of ground-based measurements at the Zvenigorod station. But one is not revealed in OMI data.

In [45] the regular observation results of NO_2 content are received from solar IR radiation data in the atmosphere in the St. Petersburg region are presented. This data are received using a high spectral resolution spectrometer. Information on variations in the total NO_2 content in the stratosphere in 2009–2011 obtained from analysis of the absorption spectra of the multiplet $\text{NO}_2 \sim 2915 \text{ cm}^{-1}$. The accuracy of these data are evaluated by comparison with independent ground-based and satellite measurements. The parameters of the stratospheric NO_2 seasonal cycle are estimated. Accumulated data set of measurements in the infrared region allowed to identify the component of daytime photochemical growth of NO_2 in the stratosphere and to estimate its speed.

In [47] errors in lidar measurements of the air density in the middle atmosphere are analyzed. A lidar was placed onboard the ISS. A solid-state Nd:YAG-laser, operating at the 3rd and 4th harmonics with wavelengths of 355 and 266 nm, was used as a lidar transmitter. Calculations were performed for the lidar with reasonable parameters: pulse energy of 0.4 (355 nm) and 0.2 J (266 nm), pulse repetition frequency of 20 Hz, accumulation time of 60 s, radius of the receiving mirrors of 0.3 and 0.5 m, field of view of the receiving telescope of 1 and 0.1 mrad, filter bandwidth of 0.5, 1, and 10 nm, and spatial resolution of 1 km. The results showed that radiation at a wavelength of 355 nm can cover altitude range, on average, from 75 km at night and from 55 km in the daytime to 10 km depending on the parameters of the lidar with 10% measurement errors (calculations were not carried out below 10 km). When operating with radiation at 266 nm for 10% measurement error, the sensing range can be expanded to the upper mesosphere at 90 km and penetrate deeper into the atmosphere to 38 km. Thus, the use of two harmonics allows the altitude range of air density measurements from the ISS to be expanded from 90 km down to the troposphere.

4.2. Investigation of ozone loss occurred in the Arctic in spring 2011

An unprecedented ozone loss occurred in the Arctic in spring 2011 [48, 49]. The details of the event are revisited from the twice-daily total ozone and NO_2 column measurements of the eight SAOZ/NDACC (Système d'Analyse par Observation Zénithale/Network for Detection of Atmospheric Composition Changes) stations in the Arctic. In [49] significant negative anomalies of nitrogen dioxide were detected on the basis of results obtained from the ground-based spectrometric measurements of the stratospheric NO_2 content in Tomsk (West Siberia) and Zhigansk (East Siberia) [49]. It is shown that the total ozone depletion in the polar vortex reached 38% (approx. 170 DU) by the end of March, which is larger than the 30% of the previous record in 1996. Aside from the long

extension of the cold stratospheric NAT PSC period, the amplitude of the event is shown to be resulting from a record daily total ozone loss rate of 0.7% after mid-February, never seen before in the Arctic but similar to that observed in the Antarctic over the last 20 yr. This high loss rate is attributed to the absence of NO_x in the vortex until the final warming, in contrast to all previous winters where, as shown by the early increase of NO₂ diurnal increase, partial renoxification occurs by import of NO_x or HNO₃ from the outside after minor warming episodes, leading to partial chlorine deactivation.

Negative anomalies of NO₂ were accompanied by anomalies of total ozone content (TOC), temperatures, and heights of the isobaric surfaces in stratosphere. The analysis of the transport atmospheric trajectories and horizontal TOC distribution [49] demonstrated that the stratospheric NO₂ content decrease was caused by the transport of stratospheric air from low TOC area. Vertical NO₂ profiles in Tomsk show that, most probably, some contribution to the negative anomalies in the early spring of 2011 brought by denitrification of the polar stratosphere in ozone hole area.

According to [50] the annual average ozone concentration over entire territory of Russia in 2011 was significantly less than in the previous decade. Total ozone deficit achieved to approximately 140 D.U. in the polar vortex in the spring of 1997 and 2011. Over land area of greatest deficit in common with-holding of ozone was observed over the Northern coast of Eastern Siberia. This unprecedented reduction of ozone, apparently, was the result of extreme weather conditions and is not related to climate change.

The conditions of formation of spring ozone anomalies in the Arctic and Antarctic are compared in [51]. It is shown that the distinction between polar ozone anomalies is due to a significant difference in the velocity and stability of the southern and northern polar vortices, as well as to the Antarctica's Mount Erebus volcano, which is the powerful source of HCl. The paper describes the nature of its volcanogenic activity and the mechanism of the volcanogenic gas emissions transport to the Antarctic stratosphere.

The cause of the absence of renoxification and thus of high loss rate, is attributed to a vortex strength similar to that of the Antarctic but never seen before in the Arctic [51]. The total ozone reduction on 20 March was identical to that of the 2002 Antarctic winter, which ended around 20 September, and a 15-day extension of the cold period would have been enough to reach the mean yearly amplitude of the Antarctic ozone hole. However there is no sign of trend since 1994, either in PSC (polar stratospheric cloud) volume (volume of air cold enough to allow formation of PSCs), early winter denitrification, late vortex renoxification, and vortex strength or in total ozone loss. The unprecedented large Arctic ozone loss in 2011 appears to result from an extreme meteorological event and there is no indication of possible strengthening related to climate change.

The paper [52] studies the temperature, humidity, and ozone anomalies, recorded in March 2011 by the TOMS satellite instrumentation in the stratosphere of Arctic latitudes. Their relation to the decrease in the ozone concentration over Tomsk in April 2011 is analyzed. It is hypothesized that the Arctic phenomena are the result of the competition between the meridional ozone transport from tropical ozone reservoir in winter season and the subsequent ozone loss due to heterogeneous reactions on the surfaces of particles in polar stratospheric clouds, while the midlatitude phenomena are caused by synoptic-scale export of the ozone-depleted humid Arctic air masses.

4.3. Measurements of the stratospheric aerosol

In the work [53–60] methods and results of the stratospheric aerosol concentration measuring were considered.

The article [53] gives the analysis of volcanogenic disturbances of the stratosphere since 1979 till 2008 and their impact on the long-term changes of the ozonosphere. It is shown that volcanogenic aerosol disturbance of the stratosphere was the principle regulator of the behavior of the ozonosphere during this period.

In [54] the behavior of the vertical aerosol structure (profiles of the ratio of the coefficients of the backward total and molecular scattering) in the height interval 30–80 km is analyzed from the results of lidar observations in Kamchatka over the period from October 2007 through December 2009. The data obtained revealed a regular two layer aerosol structure in this height range with the maxima of the ratio of the scattering coefficients in the upper stratosphere at heights 35–50 km and in the mesosphere at heights of 60–75 km, as well as a relation between seasonal variations in the aerosol stratification and the circumpolar vortex affecting dynamic processes in the atmosphere of midlatitudes. The procedure of including the aftereffect of the Hamamatsu M825901 PEM, which influences the error in the calculation of the ratio of scattering coefficients, is described.

In [55] the basic results on lidar sounding of the vertical aerosol structure in the upper troposphere and stratospheric over Tomsk for the period 2008–2009 are given. Results of modernized lidar complex are shown. The observations of volcanic and background aerosol, executed by the modern lidar complex are presented. Seasonal features of aerosol stratification in the upper troposphere and a stratosphere over Tomsk, revealed earlier, are confirmed. Dynamics of transfer of the eruptive aerosol from volcanic eruptions in islands of Aleutian and Kuril chains is traced over Western Siberia. Isolated cases of the appearance of an aerosol layer in the troposphere from Eyyafyatlayokudl are also reported.

In [56] The clearly expressed maxima of aerosol scattering were reported in Tomsk in January, 2010, from lidar observations in stratosphere at altitudes from

14 to 24 km. Calculations of back trajectories of air mass transfer to Tomsk demonstrated that enhanced aerosol scattering was directly related to air mass cooling for 6–12 h before its occurrence over Tomsk in the regions below thresholds for polar stratospheric cloud formation. The calculated back trajectories demonstrated that the polar stratospheric clouds registered in Tomsk at altitudes of 16–24 km could be formed over the Scandinavian mountains, and the clouds at altitudes of 11–14 km could be formed over mountain ridges of Polar Ural Mountains and Novaya Zemlya Archipelago. The presence of the stratospheric aerosol of synoptic scales in these regions in January, 2010 was confirmed by the data of CALIOP satellite lidar.

In [57] the observations results of aerosol disturbances in the stratosphere in the second half of 2011 are presented. The observations were performed at stations of CIS lidar network CIS-LiNet in Minsk (53.9°N; 27.60°E), Tomsk (56.5°N; 85.0°E), and Vladivostok (43.0°N; 131.9°E). Based on the lidar measurement data at the sensing wavelengths of 353, 355, and 532 nm, an increased aerosol content was observed in the lower stratosphere up to altitudes of 18 km from June–July and practically until the end of 2011. A well-defined and temporally stable aerosol layer was observed until October 2011 in the altitude range 13–17 km. An increased aerosol content in the lower stratosphere was observed until January 2012. The trajectory analysis of air mass transport in the stratosphere on the basis of NOAA HYSPLIT MODEL with the use of CALIPSO satellite data shows that the observed increased aerosol content was due to the transport of eruption products of Grimsvötn volcano (May 21, 2011, Iceland: 64.4°N; 17.3°W).

The paper [58] analyzes experimental data on variations of vertical-temporal structure of aerosol, which were obtained using lidar complex of the small station of high-altitude atmospheric sensing (SSHAS) IAO SB RAS for the period 2010–2011. A characteristic feature of this period was almost no volcanic activity with emissions to the stratosphere. This made it possible to study the behavior of the vertical structure of the background aerosol in the stratosphere on a monthly basis for certain nights during two years. The analysis of the results revealed differences in the vertical stratification of aerosol between 2010 and 2011. For 2010, the aerosol loading was maximal in January up to heights of 30 km, it diminished starting from February until almost no decrease in March–August, and showed a steady growth since September. In 2011, the aerosol loading of the stratosphere was more intense and longer-term. For instance, the height of the extension of the aerosol component reached 40 km in January–March, and the aerosol was absent in the stratosphere within three months (May–July).

In [59] the results of joint ground-based measurements of vertical structures of ozone and temperatures with the use microwave and lidar technical equipment are presented. The importance of similar observations in the studying of the

influence of various disturbances on ozone layer is discussed. The comparative analysis of the received results with satellite MLS/AURA data and with model profiles are given.

In [60] the problem of determining microphysical characteristics of stratospheric aerosol according to data of lidar sensing at wavelengths of 355 and 532 nm is considered. A priori information about the aerosol spectra obtained from balloon and aircraft measurements was used. The spectra mode structure was analyzed. Its relation to the integral microphysical characteristics of the aerosol was analysed. It is shown that the contribution of two aerosol modes (background and volcanic) to the aerosol integral characteristics is commensurate. This fact complicates using of the traditional method of model evaluations. The use of statistical nature optical models is more effective. This method is based on approximating the dependencies between the defined integral of the aerosol characteristics and the measured lidar optical characteristics. The correlation between aerosol characteristics (the area, volume, effective particle size the lidar ratio at 355 nm) and the absolute values of backscatter coefficients at wavelengths of 355 or 532 nm is established. The error of determining the integral characteristics of the aerosol by using the developed model is estimated. The performance of the model is demonstrated on real data of lidar sensing of stratospheric aerosol.

5. Active impact experiment on the lower ionosphere from the earth's surface

Recently developed methods of studying the state of the atmosphere based on the anthropogenic impact on the atmosphere by powerful SW radiation. The radiation is generated by a special heating stands ("Sura" in Russia, Tromse, Norway, HAARP in the US). This stands can provide heating of electrons in the ionospheric plasma by powerful radio emission. The authors of [61, 62] describes the active impacting experiment on the ionosphere by powerful HF radiation from the Earth's surface.

Results of experiments on the modification of the lower ionosphere, which were held on March 27–28, 2011 at the pumping stand "Sura" (FSSI RRI), located near p. Vasilsursk in the Nizhny Novgorod region. The parameters of the created disturbance are measured. The purpose of this experiment was to determine the influence of powerful radio on the content of mesospheric ozone. In March 2009, during the similar measurements the response of mesospheric ozone to heating of the lower ionosphere by powerful HF radio waves was recorded.

Stand "Sura" radiated at the angle of 12° from the Zenith to the South powerful radio waves at a frequency of 4.3 MHz. The reception of the thermal radiation in the middle atmosphere on the frequency 110836.04 MHz was carried out

using two identical mobile microwave ozonometers [62]. Using tow device the vertical ozone distribution at altitudes between 22 and 60 km with a temporal resolution of 15 minutes are received. The measurements of the thermal radiation spectra were performed by the calibration method using two “black body” standards: with the boiling point of liquid nitrogen temperature and with the ambient temperatures.

The decrease in the intensity of thermal radiation of the atmosphere in the line of ozone on average 12% was measured. The ozonometer antenna was oriented at an angle of 70°. The decrease in the intensity of radiation by 2% was measured using device, that received radiation from the modified field (antenna is oriented at an angle of 12 degrees). At maximum radiated power decrease of the ozone line intensity was on average by 7%. According to measurement data the vertical ozone distribution were estimated. The calculation showed that the lower ionosphere heating leads to the decrease of the mesospheric ozone content at altitudes around 60 km on average 20%. The ozone is recovering with the end of the artificial exposure. The authors explain this effect by the excitation as a result of heating of internal gravity waves in the mesosphere and his influence on the mesospheric ozone variation.

The theoretical analysis results of the radial distribution of electron temperature are presented In [63]. The field of the lower ionosphere heated by powerful short-waves radiation. It is obtained that the effective radius of the heating r_{eff} at fixed height may significantly differ from the characteristic radius of a flare of the ionosphere by radio waves at this height a .

The effective radius r_{eff} can be both less and more a . Boundary heating ($r = r_{\text{eff}}$) characteristic radial scale change T_e less than the corresponding magnitude of change of the square of the amplitude of the electric field radiation. The dependence of this effect on the magnitude of the amplitude itself is missing. Thus, the formation of such a boundary is relatively strong T_e gradient is quite General property of the heating of the lower ionosphere by powerful SW radiation.

Conclusions

In this brief review the main results of the works of Russian scientists who conducted in 2011–2014 and published in peer-reviewed journals are presented. Most of them is a logical continuation of the previously initiated research and covers the chemistry, atmospheric dynamics, technical problems and the results of measurements of atmospheric composition. More detailed work can be accessed by contacting the list of references.

References

1. Izrael Y.A., Anokhin Y.A., Gruza G.V., Ivanov V.N., Egorov V.I., Kruchenitskii G.M., Savchenko A.V., Petrov N.N. Development and some results of functioning of system of monitoring of key climate forcing in the middle atmosphere. *Meteorology and hydrology*. 2013. No. 7. P. 5–14.
2. Kovalenko V.A., Zherebtsov G.A. Influence of solar activity on climate change // *Optics of atmosphere and ocean*. 2014. T. 27. No. 02. P. 134–138.
3. Karol, I. L., Kiselev A.A., frokiss V. A. The Indices of the factors, influencing multi-scale climate change *Izvestiya an. Physics of atmosphere and ocean*. 2011. T. 47. No. 4. P. 451–466.
4. Volodin E.M., Diano Marina N. And., Gusev A.V. Play modern climate using a coupled model of the General circulation of the atmosphere and ocean INMCM4.0 // *Izv. Physics of atmosphere and ocean*. 2010. V. 46. No. 4. P. 448–466.
5. Galin V. Ya., Smyshlyaev S.P., E.M. Volodin Joint Chemicalisation model of the atmosphere // *Izv. Physics of atmosphere and ocean*. 2007. T. 43. No. 4. P. 437–452.
6. Volodin E.M., Kostrykin S.V., A. Ryaboshapko, A. G., Modeling of climate change due to the introduction of sulfur-containing substances in the stratosphere // *Meteorology and hydrology*. 2011. T. 47. No. 4. P. 467–476.
7. Y.A. Izrael, E.M. Volodin, Kostrykin S.V., Revokatova A.P., A.G. Ryaboshapko the Possibility of geoengineering the stabilization of global temperature in the twenty-first century using stratospheric aerosols and to evaluate possible negative consequences // *Meteorology and hydrology*. 2013. No. 6. P. 9–23
8. Zubov V.A., Rozanov E.V., Rozanov, V. I., Egorova T.A., Kiselev A.A., Karol I.L., Smuts V. Modeling of global changes of ozone and atmospheric dynamics in the twenty-first century using a chemistry-climate model SOCOL // *FAO*. 2011. V. 47 No. 3. P. 330–342.
9. Gavrillov N.M. Koval V.A. Parameterization of the impact of mesoscale stationary orographic waves for use in numerical models of atmospheric dynamics. *Izvestiya ran. Physics of atmosphere and ocean*. 2013. V. 49. No. 3. P. 271–278.
10. Gavrillov N.M. Koval V.A., A.I. Pogoreltsev, E. Savenkova N. Numerical modeling of the response of the General circulation of the middle atmosphere on spatial heterogeneity orographic waves // *proceedings of RAS. Physics of atmosphere and ocean*. 2013. V. 49. No. 4. P. 401–409.
11. Koval V.A. The influence of orographic waves on the General circulation and the transport of ozone in the atmosphere. The dissertation on competition of a scientific degree of candidate of Phys.m.N. St. Petersburg state University. 2011. 104 S. HAC RF 25.00.29, Physics of atmosphere and hydrosphere.
12. Gavrillov N.M., Koval A., A.I. Pogoreltsev, E. Savenkova N. Numerical simulation of the influence of stationary mesoscale orographic waves on the meridional

circulation and the flow of ozone in the middle atmosphere // *Izv. Geomagnetism and Aeronomy*. 2014 Vol. 54 No. 3. S. 412 DOI: 10.7868/S0016794014030055.

13. Gavrilov N.M. The S.P. Krewetki Numerical modeling of the propagation of nonlinear acoustic-gravity waves in the middle and upper atmosphere // *Izv. Physics of Atmosphere and Ocean*. 2014. T. 50. No. 1 Pp. 76–82.

14. Portnyagin, Y. I., Merzlyakov E. G., Solov'eva T. V., Pogoreltsev A. I., Suvorova E. V., P. Mukhtarov, D. Pancheva. Altitudinal and latitudinal structure of the vertical wind components migrating semidiurnal tide in the upper mesosphere and lower thermosphere (80–100 km) *Izvestiya. Atmospheric and Oceanic Physics*. 2011. T. 47. No 1. P. 108–118.

15. Merzlyakov, E. G., Portnyagin, Y. I., Solov'eva T. V., A. I. Pogoreltsev, E. V. Suvorov. Altitudinal and latitudinal structure of the vertical wind components migrating diurnal tide in the altitudes of 80–100 km. // *Izvestiya ran. Physics of atmosphere and ocean*. 2012. T. 48. No. 2. P. 195–206.

16. Kurkin V.I., Chernigovskaya M.A., Marichev V.N., Nikolashkin S.V., Bychkov V.V. Peculiarities of manifestation of winter sudden stratospheric warming in the period 2008–2010 over the regions of Siberia And the Russian Far East according to lidar and satellite measurements of temperature // *Solar-terrestrial physics*. Vol. 17 (2011). Pp. 166–173.

17. Pogoreltsev, A. I., Savenkova E.N., Pertsev N.N. Sudden stratospheric warming: the role of atmospheric mod // *news of Academy of Sciences of Geomagnetism and Aeronomy*. 2014. T. 54. No. 3. S. 387 DOI: 10.7868/S0016794014020163.

18. Perminov, V. I., Pertsev N.N. The behavior of emissions and temperature of the mesopause during stratospheric warming events based on observations at mid-latitudes // *Izv. Geomagnetism and Aeronomy*. 2013. T. 53. No. 6. P. 827–832. DOI: 10.7868/S0016794013060102.

19. Pertsev N.N., Andreev A.B., Merzlyakov E.G., Perminov V.I. Mesospheric-thermospheric manifestations stratospheric warming: the joint use of satellite and ground-based measurements // *Modern problems of remote sensing of the Earth from space*. 2013. T. 10. No. 1. P. 93–100.)

20. Marichev V.N. Study of the peculiarities of manifestation of winter stratospheric warming over Tomsk according to lidar measurements of temperature in 2010–2011. // *Optics of atmosphere and ocean*. 2011. T. 24. No. 12. Pp. 1041–1046.

21. Marichev V.N., Matvienko G.G., Lisenko A.A., Bochkov D. A., Kulikov Yu. Yu., Krasilnikov A.A., Ryskin V.G., Demkin V.M. Microwave and optical observations of ozone and temperature in the middle atmosphere during stratospheric warming in Western Siberia. // *Optics of atmosphere and ocean*. 2014. T. 27. No. 01. P. 46–52.

22. Kochetkova O.S., Mordvinov V.I., Rudnev M.A. Analysis of factors affecting the occurrence of stratospheric warming. // *Optics of atmosphere and ocean*. 2014. T. 27. No. 08. P. 719–727.

23. G. R. Khairullina, Astafyeva N. M. The quasi-biennial oscillation in the Earth's atmosphere. Overview: supervision and formation mechanisms: establishment of the Russian Academy of Sciences space research Institute (IKI), Moscow. 2011. 60.

24. Devyatova E. V., Mordvinov V. I. Quasi-biennial oscillation of wind in the low-latitude stratosphere and wave activity of the atmosphere in winter in the Northern hemisphere // proceedings of the Russian Academy of Sciences. Physics of Atmosphere and Ocean. 2011. Tom: 47. No: 5 Pp. 608–621.

25. Holton J. R., Tan H. The influence of the equatorial Quasi-Biennial Oscillation on the global circulation at 50 mb // J. Atmos. Sci. 1980. V. 37. No. 10. R. 2200–2208.

26. Gabis I. P., Troshichev O. A. Quasi-biennial oscillation in the Equatorial stratosphere: seasonal changes in patterns of wind, the discreteness of the cycle period and the forecast duration // Izv. Geomagnetism and Aeronomy. 2011. T. 51. No. 4, Pp. 508–519.

27. Bazhenov O. E. Study of the quasi-biennial periodicity of the total content and concentration of ozone at high levels over the Arctic and Tomsk according to satellite instrument TOMS // Optics of atmosphere and ocean. 2014. T. 27. No. 12. Pp. 1074–1078.

28. Pavlov A. N., Stolyarchuk S. Y., Smirko K. A., Bukin O. A. Lidar studies of the variability of the vertical distribution of ozone under the influence of the processes of stratosphere-troposphere exchange in the far East // Optics of atmosphere and ocean. 2012. Vol. 25. No. 09. P. 788–795.

29. The Antokhin P. N., Belan B. D. Regulation of the dynamics of tropospheric ozone through the stratosphere // Optics of atmosphere and ocean. 2012. Vol. 25. No 10. P. 890–895.

30. Krivolutsky A. A. Repnev A. I. Impact of space energetic particles on the Earth's atmosphere (a review) // Izv. Geomagnetism and Aeronomy. T. 52. No. 6. S. 723–754.

31. Funke B. A. Baumgaertner, M. Calisto, T. Egorova, C. H. Jackman, J. Kieser, A. Krivolutsky, M. Lopez-Puertas, D. R. Marsh, T. Reddmann, E. Rozanov, S.-M. Salmi, M. Sinnhube, G. P. Stiller, P. T. Verronen, S. Versic, T. von Clarmann, T. Y. Vyushkova, N. Wieters and J. M. Wissing Composition changes after the “Halloween” solar proton event: the High Energy Particle Precipitation in the Atmosphere (HEPPA) model versus MIPAS data intercomparison study // Atmos. Chem. Phys. 2011. V. 11. P. 9089–9139, www.atmos-chem-phys.net/11/9089/2011/ doi:10.5194/acp-11-9089-2011.

32. Krivolutsky A. A., Cherepanova, L. A., M. Vissing, G. R. Zakharov, Vuchkov T. Y. three-Dimensional numerical simulation of temperature changes, wind and chemical composition of Earth's atmosphere, caused by Solar activity // Solar-terrestrial physics. 2012. Vol. 21. P. 37–45.

33. Wissing, J. M., Kallenrode M.-B. Atmospheric ionization Module Osnabruck (AIMOS): A 3D model to determine atmospheric ionization by energetic charged particles from different populations // Ibid. 2009. V. 114. A06104. Doi:10.1029/2008JA013884.

34. Krivolutsky A. A., Remnev A. I., Vuchkov T. Yu, M. Wassing Effects of space plasma on the ozonosphere of the Earth // Solar-terrestrial physics. 2011. Vol. 17. P. 153–160.

35. Gruzdev A. N. Evaluation of the influence of the 11-year solar activity cycle on the ozone content in the stratosphere // *Izv. Geomagnetism and Aeronomy*. 2014. Vol. 54 No. 5. S. 678. DOI: 10.7868/S0016794014040178.
36. Gruzdev A. N. Assessment of the effects of the eruption of mount Pinatubo in the stratospheric content of O₃ and NO₂ taking into account variations in the level of solar activity. *Optics of atmosphere and ocean*. 2014. T. 27. No. 6. P. 506.
37. Artamonova, I. V., S. V. Veretenenko The influence of variations of solar and galactic cosmic rays on the duration Macrokinetics processes // *Geomagnetism and Aeronomy*. 2013. T. 53. No. 1. P. 5–9.
38. Viscerating K. N. The phase relation between quasidegenerate fluctuations of total ozone and the 11-year cycle of solar activity // *Geomagnetism and Aeronomy*. 2012. T. 52. No. 1. P. 94–102.
39. Kukoleva A. A., Krivolutsky A. A. evaluation of the efficiency of formation of NO molecules in a period of solar proton flares 14.07.2000 on satellite data // *Saik-2012. Solar-terrestrial physics*. 2012. Vol. 21. P. 51–57.
40. Kukoleva A. A. and Krivolutskii A. A. Analysis of Variations in the Nitrogen Oxide Content in the Polar Atmosphere of the Northern Hemisphere during the Solar Proton Flare of July 14, 2000, Based on the UARS Satellite Data // *Geomagnetism and Aeronomy*, 2013, Vol. 53, No. 8 (Issue), pp. 932–936. DOI 10.1134/S0016793213080136 <http://link.springer.com/journal/11478/53/8/page/1>.
41. Semenov A. I., Chufs N. N., Devyatova E. V., Mordvinov V. I. Radiation of the upper atmosphere — sensitive indicator of solar-terrestrial processes. the results of 60 years of age (review) *Geomagnetism and Aeronomy*. 2011. T. 51. No. 4. P. 429–443.
42. Belorukov V. I., Glazkov V. N., Fedorov V. V. Analysis of time series of the global mean values of the thermodynamic and circular parameters of the atmosphere, ozone and water vapor // *Izv. Physics of atmosphere and ocean*. 2011. T. 47. No. 1. P. 67–76.
43. Bukin O. A., Nguyen Xuan Anh, Pavlov A. N., Stolyarchuk, S. Y., Smirko K. A. Effect of jet streams on the vertical ozone distribution and characteristics tropopause inversion layer in the far East. *Physics of atmosphere and ocean*. 2011. T. 47. No. 5. P. 610–618.
44. Gruzdev A. N., Elokhov S. A. New results data validation measurements of NO₂ with OMI on the basis of these measurements at the Zvenigorod scientific station // *The Study of Earth from space*. 2013 No. 1 P. 16.
45. Ionov D. V., M. A. Kshevetskaya, Yu. M. Timofeev, A. V. Poberovskii the NO₂ Content in the stratosphere according to ground-based measurements of solar IR radiation // *proceedings of RAS. Physics of atmosphere and ocean*. 2013. V. 49. No. 5. P. 519–529.
46. Gavril'eva G. A., P. P. Ammosov, Koltovskij I. Comparison of ground-based and satellite measurements of atmospheric temperature in the mesopause region at high

latitude region of Eastern Siberia. // *Izv. Geomagnetism and Aeronomy*. T. 51. No. 4. 2011. P. 563–569.

47. Marichev V.N., Bochkov, D.A. Lidar measurements of air density in the middle atmosphere. Part 2. Modeling potential sensing in the UV region of the spectrum. // *Optics of atmosphere and ocean*. 2013. T. 26. No. 08. P. 701–704.

48. Pommereau J.-P., F. Goutail, F. Lef evre, A. Pazmino, C. Adams, V. Dorokhov, P. Eriksen, R. Kivi, K. Stebel, X. Zhao, M. van Roozendael. Why unprecedented ozone loss in the Arctic in 2011? Is it related to climate change? // *Atmos. Chem. Phys.* 2013. V. 13. 5299–5308, www.atmos-chem-phys.net/13/5299/2013/ doi:10.5194/acp-13–5299–2013.

49. Ageyev, V., Grishaev M.V., Gruzdev A.N., Elokhov A.S., Salnikov N. With. Anomalies of the stratospheric NO₂ content over Siberia, associated with the Arctic ozone hole 2011 // *Optics of atmosphere and ocean*. 2014. T. 27. No. 1. 40–45.

50. Zvyagintsev A.M., Kuznetsov G.I., Kuznetsov I.N. Anomalies of ozone in spring over Russia // *Meteorology And Hydrology*. 2013. No. 5 Pp. 5–13.

51. Zuev V.V., Zueva N.E., Savelieva E.S. Specificity of formation of the Antarctic and Arctic ozone anomalies. // *Optics of atmosphere and ocean*. 2014. T. 27. No. 05. P. 407–412.

52. Bazhenov O.E. evaluation of the effect of humidity and temperature in the stratosphere on the occurrence of ozone anomalies in the spring of 2011 in the Arctic and the Northern territory of Russia. // *Optics of atmosphere and ocean*. 2012. Vol. 25. No. 07. P. 589–593.

53. Zuev V.V., Zueva N.E. Volcanic perturbations of the stratosphere is the main regulator of long-term behavior of the ozonosphere in the period from 1979 to 2008 // *Optics of atmosphere and ocean*. 2011. T. 24. No. 01. Pp. 30–34.

54. Bychkov V.V., A] A. S., Shevtsov B.M., Marichev V.N., Novikov P.V. Cheremisin A.A. Seasonal patterns of occurrence of aerosol scattering in the stratosphere and mesosphere of Kamchatka on the results of lidar observations in 2007–2009 *Izv. Geomagnetism and Aeronomy*. 2011. T. 47. No. 5. P. 603–609.

55. Marichev V.N., Samokhvalov I.V. Lidar observations of volcanic aerosol layers in the stratosphere of Western Siberia in 2008–2010 // *Optics of atmosphere and ocean*. 2011. T. 24. No. 03. P. 224–231.

56. Cheremisin A.A., Marichev V.N., Novikov P.V. Transfer of polar stratospheric clouds from the Arctic to Tomsk in January 2010 // *Optics of atmosphere and ocean*. 2013. T. 26. No. 02. P. 93–99.

57. Dolgii S.I., Burlakov V.D., Makeev, A. P., Nevzorov A.V., Smirko K.A., Pavlov A.N., Stolyarchuk, S. Y., Bukin O.A., A.P. Tchaikovsky, F.P. Osipenko, D.A. Trifonov Aerosol disturbance of the stratosphere since the eruption of the Grímsvötn volcano (Iceland, may 2011) based on data from observational stations lidar network CIS,

CIS-LiNet in Minsk, Tomsk, and Vladivostok. // Optics of atmosphere and ocean. 2013. T. 26. No. 07. P. 547–552.

58. Marichev V.N. Investigation of the variability of the vertical structure of the background aerosol in the stratosphere over Tomsk-based lidar observations in 2010–2011 // Optics of atmosphere and ocean. 2012. Vol. 25. No. 11. P. 976–984.

59. Marichev V.N., Matvienko G. G., Lisenko A. A., Ilusic V. Yu., Kulikov Yu. Yu., Krasilnikov A. A., Ryskin V. G., Bychkov V. V. First results of a comprehensive experiment on the sounding of the middle atmosphere at optical and millimeter wavelengths (over Tomsk). // Optics of atmosphere and ocean. 2012. Vol. 25. No. 12. P. 1091–1095.

60. Korshunov V. A., Subochev D. S. About the definition of the parameters of stratospheric aerosol according to the two-wavelength lidar sounding. // Proceedings Of The Russian Academy Of Sciences. Physics of atmosphere and ocean. 2013. V. 49. No. 2. P. 196.

61. Kulikov Yu. Yu., Frolov V. L., Grigor'ev G. I., V. M. Demkin, Komrakov G. P., Krasilnikov A. A., Ryskin V. G., the Response of mesospheric ozone to heating of the lower ionosphere by powerful HF radio waves Volume: 53 issue: 1 Year: 2013 Pages: 102 DOI: 10.7868/S0016794013010112.

62. Krasilnikov A. A., Y. Y. Kulikov, V. G. Ryskin, etc. a New small microwave Spectroradiometer-ozonometer. Instruments and experimental techniques. 2011. No. 1. P. 127–133.

63. Alpatov V. V., badin, V. I., I. A. Grebnev, Deminov M. G., Faermark D. S. Effective radius of the heating of the lower ionosphere by powerful HF radiation // proceedings of

64. RAS. Geomagnetism and Aeronomy. 2012. T. 52. No. 46. Pp. 832–836.

Ozone

N. F. Elansky

A. M. Obukhov Institute of Atmospheric Physics RAS
n.f.elansky@mail.ru

1. Tropospheric ozone

1.1. Observations

The Russian network for monitoring the surface ozone concentration (SOC) has insignificantly changed over the past four years. The background stations mentioned in the previous reports [*Elansky, 2009; Elansky, 2012*] — the Kislovodsk High-Altitude Scientific Station (KHASS) and the Lovozero, Mondy, and Vyatskie Polyany stations as well — continued to carry out regular observations. A scientific station located in the Karadag Nature Reserve did not stop operating after the Crimea joined Russia [*Lapchenko and Zvyagintsev A.M., 2014*]. The SOC was regularly measured from 300-m towers in Obninsk (Kaluga oblast, NPO Taifun) and Zotino (Krasnoyarsk krai, Obukhov Institute of Atmospheric Physics, Russian Academy of Sciences). All background stations are equipped with regularly calibrated network instruments of the same type [*Aref'ev et al., 2013; Heimann et al., 2014*]. A regional network of stations for surface-ozone observations has been set up in the Tomsk region [*Arshinov et al., 2007; Arshinov et al., 1999*]. At present, four stations are operating: the Fonovyi and Berezorechka background stations, a base experimental complex (BEC) located in the natural zone of Tomsk, and a tropospheric ozone research (TOR) station. Russian chemiluminescent ozone analyzers of the 3–02P are used at the Fonovyi, BEC, and TOR stations. A TEI-49 ultraviolet ozonometer has been installed at the Berezorechka station. In order to measure the SOC, at the Fonovyi and BEC stations, air samples are collected at heights of 10 and 30 m, which makes it possible to estimate vertical air flows. At the TOR and Berezorechka stations, air samples are collected at heights of 5 and 10 m, respectively. At all these stations, the concentration of ozone is continuously measured at an interval of 1 h.

Unfortunately, the SOC monitoring system has been developing slowly in urbanized regions. The state network of stations for monitoring atmospheric pollution, which includes about 240 Russian cities, does not carry out full-scale SOC observations. Basically, SOC measurements are occasionally performed at stations that are few in number [*Bezuglaya and Smirnova, 2008*]. A current system for monitoring atmospheric pollution operates in Moscow. This system includes about 35 stations, however, SOC measurements are outside the scope of

its main tasks [Mosecomonitoring website. <http://www.mosecom.ru/air/air-to-day/>]. Continuous once-a-minute measurements of the surface concentration of ozone, its precursors (CO, NO, NO₂, and NMHC), and other atmospheric components were performed at the Ecological Station of the Obukhov Institute of Atmospheric Physics, Russian Academy of Sciences (ES IAP RAS) [Elansky et al., 2011a; 1 Elansky et al., 2011b; Elansky et al., 2015]. This ES IAP RAS is located on the territory of the Meteorological Observatory of Moscow State University (MSU.) Regular observations were carried out also in Tomsk, Ulan-Ude, and St. Petersburg [Elansky, 2009; Belan, 2012; Zayakhanov et al., 2013b].

Changes in the composition of the atmosphere and in the state of ecosystems and climate have given impetus to more active field, marine, and aircraft observations of tropospheric ozone in Russia, which are usually carried out within the framework of international programs. Among the most important projects is the sounding of tropospheric ozone from boards the AN-30, TU-134, and AN-2 aircraft laboratories (Institute of Atmospheric Optics, Siberian Branch, Russian Academy of Sciences (IAO SB RAS)). Such flights were performed in the monitoring regime in a region located to the south of Novosibirsk, and episodic large-scale observations covered the entire Siberian region, including the Arctic [Antokhin et al., 2012a; Anokhin et al., 2011; Matvienko et al., 2014; Berchet et al., 2013; Antokhin et al., 2012b]. The transcontinental observations of the composition of the atmosphere over Russia from a mobile railroad laboratory (TROICA experiments) were completed in 2010 [Elansky et al., 2009b]. However, a large body of obtained data on surface ozone and its precursors are still under treatment and analysis.

The vertical distribution of ozone in the troposphere and lower stratosphere was measured using ozonesondes launched by the Central Aerological Observatory (CAO) and the IAO SB RAS [Dorokhov et al., 2013; Dorokhov et al., 2014] and a lidar (Tomsk, IAO SB RAS). This lidar sounding within a height range of 5–16 km was based on the method of differential absorption and scattering at wavelengths of 241/341 nm [Burlakov et al., 2010; Dolgii, 2012; Burlakov et al., 2013]. Satellite observational data on ozone were used in solving many problems. In particular, a station for receiving satellite information has started to operate at the IAO SB RAS [Arshinov et al., 2013a; Arshinov et al., 2014a; Arshinov et al., 2014b].

Instruments and methods for measuring ozone have been improved. A semiconductor ozonometer developed at the Karpov Institute of Physical Chemistry is unique. This compact instrument was compared to standard network gas analyzers and yielded good results [Obvintseva et al., 2014]. This instrument was efficiently used in studying the interaction of ozone with different materials. It was shown, in particular, that fine-fiber filters based on polystyrene and

polysulfone are an efficient respiratory protective device against ozone [Belikov et al., 2013; Obvintseva et al., 2011].

1.2. Distribution and Variability

The longest (since 1989) SOC observations in Russia have been carried out at the KHASH located at a height of 2070 m (Northern Caucasia) [Senik I. and Elansky, 2011]. The rapid SOC decrease 1.53 ± 0.14 ppb·yr⁻¹ observed from 1989 to 1996 had slowed down by 2006, and, in recent years, the SOC trend has been close to zero. The obtained data series reflects changes that occurred in the industries of the countries of the former Soviet Union in the 1990s and the influence of large-scale atmospheric processes on the long-range transport of ozone and its precursors, vertical mixing, and radiation regime in the troposphere.

The distribution of the concentrations of ozone and nitrogen oxides over northern Eurasia within the latitudinal belt 48–58° N according to observational data obtained from board the mobile railroad laboratory running between Moscow and Vladivostok (1995–2008 TROICA experiments) is analyzed in [Pankratova et al., 2011]. The characteristic features of their background distribution is an increase in the concentration of O₃ (especially in spring 1.05 ± 0.02 ppb/10°) and a decrease in the concentrations of NO and NO₂ in the eastern direction. The photochemical formation of ozone in Siberia is, on the whole, inactive. Noticeable increases in the surface concentration of ozone are associated with biomass combustion, long-range (transboundary) transport of its precursors, and an active stratosphere–troposphere exchange in the east of the continent. Both daily and seasonal variations in the concentrations of ozone and nitrogen oxides in the atmosphere over Siberia significantly differ from those observed at background stations in high-altitude and coastal zones. A high stability of the atmospheric boundary layer (ABL) in the boreal-forest zone results in their intensive dry precipitation onto the land surface.

Regular observations of O₃, CO, NO_x, greenhouse gases, and other atmospheric components have regularly been observed at the Zotino background station (central Siberia) since 2007. The time variability of the SOC is determined by natural atmospheric processes [Vasileva et al., 2011; Skorokhod, 2013]. The influence of anthropogenic factors is episodically manifested. The characteristic feature of the annual SOC cycle is a clearly pronounced maximum in April. During this period, the most intensive stratosphere–troposphere exchange is observed as well as the activation of meridional transport, which is associated with the collapse of the circumpolar vortex. The annual variability of the SOC is low—the 90th percentile does not exceed 52 ppb. If air flows with biomass-combustion products arrive, the concentration of ozone may increase up to 80 ppb as

in the case of extreme fires in 2012. An analysis of the sensitivity of the SOC to anthropogenic forcing shows its correlation with the direction of transport: when clean-air flows arrive from both northern and eastern directions, the SOC is lower, and the SOC is noticeably higher when polluted-air flows arrive from both southern and south-western regions of Siberia [Vasileva *et al.*, 2011; Engvall Stjernberg A.-C. *et al.*, 2012]. The results of a joint analysis of observational data obtained at the Zotino station, in the TROICA experiments, and from board an aircraft laboratory showed that the Siberian region is characterized by an abnormally high vertical gradient of ozone [Engvall Stjernberg A.-C. *et al.*, 2012]. Its low concentrations in the surface air are due to weak mixing in the boundary layer of the boreal atmosphere and its intense dry under the conditions of long and powerful surface temperature inversions. The averaged (over individual regions of Siberia) rates of the dry deposition of ozone are given in [Berezina *et al.*, 2014]. Calculations were performed on the basis of the 1996–2008 observational ozone and radon-222 data obtained from board the mobile railroad laboratory [Berezina *et al.*, 2013]. These results supported the conclusion (see [Engvall Stjernberg A.-C. *et al.*, 2012]) that, on the whole, in Siberia, the sinks of ozone predominate over its sources that are due to the transport of its precursors from both southern and western directions (Europe, Central and Eastern Asia).

The results of SOC observations carried out at stations in the Tomsk region made it possible to reveal differences between ozone regimes in background and urban areas [Arshinov *et al.*, 2013c]. Both annual and daily SOC variations obtained at the background Berezorechka and Fonovyi stations slightly exceed those obtained at the Zotino station. The largest amplitude of SOC variations is observed in winter at a short distance from Tomsk (BEC). This amplitude becomes approximately the same for all the four stations during the warm period. Throughout the year, the monthly mean concentrations of ozone at a height of 30 m are higher than those at a height of 10 m under both background and urban conditions. The diurnal dynamics of the vertical distribution of ozone in the atmospheric boundary layer over the Berezorechka station was studied using observations from board the AN-2 aircraft [Antokhin *et al.*, 2013a]. During intensive turbulent exchange, the descending fluxes of ozone due to its transport from the free troposphere were recorded in the upper boundary layer and its ascending fluxes due to its generation with participation of its precursors were recorded in the lower boundary layer. When polluted air masses arrive in a region of observations, a noticeable diurnal cycle of ozone is observed in the atmospheric boundary layer due to its generation during daylight hours. In the presence of clouds, the vertical distribution of ozone may noticeably vary [Arshinov *et al.*, 2013]. The CO concentration increased, on average, by 14 ppb and the ozone concentration decreased by 11–15 ppb were observed inside clouds. The excess of CO and the deficit of ozone are different in clouds of different types. On the

basis of data obtained from board the aircraft, the influence of cloudiness on both regional and global balances of ozone was estimated. Vertical ozone profiles obtained in aircraft experiments were compared to those retrieved from IASI satellite data. The absolute differences between the aircraft and satellite concentrations of ozone amount to 3–18 ppb at a height of 0.5 km and 8–38 ppb at a height of 7 km [Arshinov et al., 2013a; Arshinov et al., 2014a; Arshinov et al., 2014b].

The results of the 2008–2012 observations of the SOC in the Karadag Nature Reserve located in the coastal zone of the Black Sea are given by Lapchenko and Zvyagintsev A.M (2014). The mean values of the SOC and its seasonal and daily variations suggest that the influence of regional pollution is weak. The maximum hourly means observed during hot days in summer did not exceed 90 ppb. The concentrations of the main ozone precursors CO and NO_x are close to their background values.

The results of the 2004–2010 observations of the SOC in Obninsk [Aref'ev et al., 2013] show that the influence of anthropogenic factors on the state of regional atmosphere increases. The yearly mean SOC increased by 45% over the period of measurements. The maximum hourly mean concentration of ozone 110 ppb was recorded in the summer of 2010 under the conditions of smoke generation over European Russia. The results of regular meteorological observations from the 300-m tower show a close relation of increased and decreased hourly mean SOCs with the presence of surface temperature inversions.

Long-term variations in both daily mean and maximum daily SOCs, which were recorded at eight stations in Germany and estimated in [Zvyagintsev and Tarasova, 2011], make it possible to compare both background and regional characteristics of the SOC variability, which were obtained in Russia, to those obtained in Europe. The trends of monthly mean SOCs in Germany vary from 0 to 10% over a period of 10 years, and the trends of maximum daily SOCs are smaller, on average, by 1.5 times. A noticeable portion of such trends is associated with long-term variations in temperature, humidity, and transport direction, and taking into account these variations noticeably changes the estimates of ozone trends.

1.3. Ozone in cities

The content of ozone in the surface air layer over cities depends on photochemical processes, in which NO, NO₂, CO, and volatile organic compounds have a dominant role. Therefore, measurements of the surface concentration of ozone are accompanied by measurements of its precursors. The time variability of the SOC and its distribution over cities are affected by meteorological conditions that determine the radiation regime, the processes of transport and

accumulation of pollutants in the atmospheric surface layer and their dry and wet deposition. These characteristics of the atmospheric composition and state are monitored in Moscow at the ES IAP RAS and the MSU Meteorological Observatory. Summary results obtained from the 2002–2012 measurements of ozone and its precursors are given in [Elansky *et al.*, 2015]. Changes in the infrastructure of Moscow and, first and foremost, both quantitative and qualitative changes in the system of motor transport were accompanied by an increase in the SOC ($1\% \text{ yr}^{-1}$) and a decrease in the concentration of NO. The content of NO₂ remained almost unchanged. The features of both annual and diurnal variations in the concentrations of O₃, NO, NO₂, CO, and SO₂ are also analyzed in [Elansky *et al.*, 2015]. Observations of the vertical stratification of the ABL, which were carried out simultaneously with sodar measurements of the wind profile, made it possible to study the relation between gas concentrations and wind velocity. A weekly cycle is pronounced in the time variability of ozone and its precursors. The diurnal cycle of these gases is different for different days of the week [Elansky *et al.*, 2012a; Trifanova *et al.*, 2013].

Observations carried out at the MSU Meteorological Observatory yield a detailed pattern of variations in the meteorological characteristics of the urban atmosphere, which affect the SOC [Chubarova *et al.*, 2014; Yeremina *et al.*, 2014]. A significant temperature trend was obtained from the results of the 1954–2013 measurements ($+0.041^\circ\text{C yr}^{-1}$). From 1967 to 2012, the rate of temperature increase became faster and amounted to $+0.067^\circ\text{C yr}^{-1}$. In Moscow, both meteorological parameters and the chemical composition of precipitation changed over this measurement period. Observational data on the composition and state of the atmosphere, which were obtained at the ES IAP RAS and the Moscow Ecological Monitoring (MEM) network, made it possible to make the air-quality indices for Moscow more accurate [Elansky, 2014]. The calculated indices of air pollution showed that Moscow is one of the world's six cleanest megacities with a population of over 12 million. The emissions of CO from the Moscow megacity were also estimated in [Elansky, 2014].

An analysis of multiyear observational data (obtained at the MEM network) on the surface concentration of CO revealed its significant weekly cycle [Sitnov and Adiks, 2014], which is most clearly pronounced in the center of Moscow, where the signal swing amounts to 32%. The year-to-year (1994–2000) reproducibility of the cycle, its seasonal dependence, and the features of its manifestation at different times of the day were studied [Sitnov and Adiks, 2014]. The Moscow megacity affects NO₂ content in the troposphere retrieved from satellite data obtained with an OMI spectrometer [Sitnov, 2011a]. The mean multiyear spatial distribution of tropospheric NO₂ reveals the sources of urban-air pollution, the main of which is the eastern suburban zone of the megacity ($8.1 \cdot 10^{15} \text{ mol cm}^{-2}$). Its minimum content ($2.0 \cdot 10^{15} \text{ mol cm}^{-2}$) is noted in the north-western zone

of Moscow. The tropospheric content of NO_2 over Moscow decreased with a rate of $-7.2 \cdot 10^{14} \text{ mol cm}^{-2} \text{ yr}^{-1}$ from 2004 to 2009 [Sitnov, 2011a]. A significant weekly cycle is also pronounced in its time variability (the signal swing reaches 35%) [Sitnov and Adiks, 2013]. The weekly cycles of the tropospheric content of NO_2 were also revealed from OMI data obtained over other megacities. Its within-cycle variations range from 14% over Cairo and Jakarta to 64% over Los Angeles [Sitnov and Adiks, 2013].

The total content of CO in a vertical column has been observed in Moscow since 1974. Since the main portion of CO is concentrated in the lower troposphere, the variability of its total content reflects the pollution of Moscow's air basin. The 1986–2008 period, during which the infrastructure of Moscow rapidly changed, is considered in [Rakitin et al., 2011; Wang Pu-Cai et al., 2014; Golitsyn et al., 2015]. Despite the fact that the number of cars increased by a factor of five, the content of CO in the atmosphere over the city decreased due to the replacement of old cars by up-to-date car models and a rapid reduction of industrial production in Moscow in the 1990s. Variations in the concentrations of CO over Moscow and over Beijing (in which similar measurements were performed) were compared. The CO content in the atmosphere over Beijing is significantly higher than that over Moscow. But, unlike Moscow, in Beijing, a significant portion of CO is due to regional sources. A slight decrease in the concentration of CO has been noted in Beijing in the last decade, which is associated with gas supply to both residential and industrial sectors.

It is evident that urban agglomerations affect mainly the atmospheric boundary layer. Therefore, the proposed in [Ivanov and Postylyakov, 2010; Postylyakov et al., 2014] methods for measuring the integral contents of NO_2 and formaldehyde (HCHO) in this layer are of great importance. Their contents are retrieved from observations of scattered radiation in the visible and UV spectral regions, respectively. In this case, such observations can be carried out under both cloudy and cloudless conditions with errors of 5–25% (NO_2) and 5–40% (HCHO), which depend on the surface albedo, the state of cloudiness, and other observation conditions. Observational data on these (important for the photochemistry of ozone) components, which have been obtained in the last several years in Moscow and at the Zvenigorod Scientific Station (ZSS) located at a distance of 53 km to the south-west of the center of Moscow, are given in [Postylyakov et al., 2014; Kanaya et al., 2014]. Such observational data were used in estimating the volume of NO_2 emissions from different sources [Ivanov et al., 2012]. In particular, the amount of NO_2 emitted by the Moscow motor transport was estimated at 88 kt/yr. On the basis of observational data obtained at the ZSS and six other stations, the time variability of NO_2 in the ABL over different regions of Asia was studied and satellite NO_2 data were validated [Pinardi et al., 2014]. A stereophotographic method was developed to determine

the cloudiness height, which is important for validation [Andreev *et al.*, 2014a; Andreev *et al.*, 2014b].

Regular SOC observations have been carried out at the TOR station in Tomsk since 1992. The results of an analysis of this longest urban SOC series for Russia are generalized in [Belan, 2012; Arshinov *et al.*, 2011; Arshinov *et al.*, 2013d]. The diurnal cycle of the concentration of ozone is characteristic of urban conditions: with its maximum in the afternoon and minimum in the morning. Its diurnal cycle is more pronounced during the warm season. In October–November, its secondary night maximum, which may exceed its daytime maximum, is often observed. Four time periods with characteristic annual cycles of the SOC are pronounced in its long-term variability. The 2000–2012 observational data obtained in Ulan-Ude (another city in Siberia) yield the similar features of the diurnal and seasonal cycles of the SOC [Zayakhanov *et al.*, 2013b]. However, since Ulan-Ude is significantly smaller than Tomsk and there were no rapid changes in its infrastructure during the observation period, the annual cycle of ozone in Ulan-Ude is close to the background one with its clearly pronounced maximum within the spring–summer period.

Studying the features of both spatial and temporal variations in the SOC in the atmosphere over Russian cities was one of the objectives of the TROICA experiments [Elansky *et al.*, 2009b; Elansky *et al.*, 2012b]. Along the Trans-Siberian railroad route between Moscow and Vladivostok, the mobile laboratory passed through 110 cities. Over the 1996–2008 period, it passed through each of these cities 22 times in different seasons and at different times of the day. The measurement interval was 10 s. The mean concentrations of ozone and its precursors in different seasons for large (500 000 residents), medium (50 000–500 000 residents), and small (19 000–50 000 residents) cities are given and compared to their values for the background conditions in [Elansky and Lavrova, 2014]. The averaged (over each group of cities) daily cycles of the gases for different seasons are also analyzed. The mean SOC distribution over the cities during both cold and warm seasons was first described. The character of such a distribution is close to the heat-island structure studied in detail in [Elansky and Lavrova, 2012]. The distribution of ozone and other trace gases was obtained for the Moscow megacity in the course of the 1995–2010 experiments due to frequent passages through the megacity in different directions [Elansky N. F. *et al.*, 2014]. The level of the air pollution of Moscow is low (when compared to other megacities) due to a good natural ventilation of this megacity located on a plain. Lower ozone concentrations imply that the intensity of photochemical processes in the atmosphere over Moscow, the northernmost megacity in the world, is relatively low. The zone of Moscow's influence extends for a distance of 150–200 km and covers the atmospheric layer up to a height of 300–400 m. This relatively

small extension of Moscow's plume, which is determined from the concentrations of NO_x and CO_x , is due to their small (for a megacity) emissions, because Moscow is fully supplied with gas and there are almost no large industrial enterprises [Elansky, 2014]. According to [Makarova et al., 2011], the plume from St. Petersburg, in which main enterprises continued to operate after the crisis in the 1990s, propagates for a distance of over 300 km. It is evident that this is the result of its location farther to the north and a higher mean wind velocity in the atmospheric surface layer.

1.4. Ozone under the extreme conditions of 2010

The summer of 2010 was anomalously hot in European Russia (ER). This was caused by a blocking anticyclone of unusually high intensity and duration (from June 18 to August 19). Such hot weather resulted in the occurrence of both forest and peatbog fires. The maximum spread of fires was noted on July 27–29. On these days, the area of fires in ER amounted to 3000 km² [Lokoshchenko et al., 2014]. This unique situation resulted in changes in the composition of the regional atmosphere [Sitnov S.A., 2011b; Sitnov S.A., 2011d; Sitnov, 2011c]. The content of CO in a vertical air column over ER reached $7.2 \cdot 10^{18}$ mol cm⁻², which exceeded its mean multiyear values by 3.5 times. The tropospheric content of NO_2 in the vicinity of intense-fire clusters increased up to $8.9 \cdot 10^{18}$ mol cm⁻². The air quality rapidly deteriorated in cities. The evaporation of combustive-lubricating materials, paints, lacquers, and other substances increased. The products of biomass combustion arrived in cities. The presence of a dense aerosol haze led to powerful and long surface-temperature inversions and to the formation of favorable conditions for the accumulation of trace gases in the surface air layer [Lokoshchenko et al., 2014]. In [Lokoshchenko et al., 2014] the variations of SOC and other gases for Moscow (ES IAP RAS) were shown. The maximum hourly concentrations of O_3 , NO, NO_2 , and CO reached 134.2, 175.9, 214.7, and 15800 ppb, respectively. These maxima were recorded on August 4–7, when a dense aerosol haze hung over Moscow. The concentrations of ozone and its precursors also increased before the products of biomass combustion arrived in Moscow's air basin. The rate of increase in the concentration of ozone amounted to 0.48 ± 0.09 ppb-day⁻¹ during this period. In this case, the weekly cycle of ozone with its maximum and NO_x minimum on Sundays was clearly pronounced. Variations in the integral content of trace gases in a vertical air column within the boundary layer weakly correlated with those in their surface concentrations. The contribution made by the long-range transport of biomass-combustion products to their integral content was more significant than that made by temperature inversions.

The SOC maximum exceeding 100 ppb was noted in summer 2010 in Obninsk [Tereb *et al.*, 2013]. Such increased ozone concentrations are associated with high contents of CO, NO_x, and the sum of hydrocarbons in air masses arrived from regions of forest and peatbog fires. Variations in the contents of ozone, NO_x, CO, and PM10 in the atmosphere over Moscow, Kiev, and Crimea in summer 2010 are analyzed in [Zvyagintseva *et al.*, 2011a; Zvyagintseva *et al.*, 2011b]. In Moscow increased concentrations of ozone and aerosol on August 4–9 reached values hazardous to the health of people. The number of additional cases of mortality due to an increase in the maximum permissible concentrations of ozone and PM10 was estimated for Moscow. The air quality in Kiev and Crimea, which were almost not affected by the fires of summer 2010, mainly remained satisfactory.

Some important methodical approaches to the recording of extreme CO concentrations in a vertical atmospheric column are considered in [Yurganov *et al.*, 2011]. A comparison of CO data obtained in summer 2010 from satellite observations and ground-based measurements taken in Moscow and at the ZSS showed their significant disagreement. On some days, the satellite concentrations of CO were lower by 2–3 times due to the fact that the amount of CO in the surface air layer was not taken into account. It is proposed to introduce corrections for CO concentrations retrieved on the basis of observations with the AIRS, MOPITT, and IASI satellite instruments. At the same time, attention is focused on significant disagreements between CO concentrations retrieved from satellite observational data, if different methods are used [Fokeeva *et al.*, 2011].

2. Stratospheric ozone layer

2.1. Total content

The network including 28 ozonometric stations equipped with M-124 filter ozonometers (Voeikov Main Geographical Observatory (MGO)) continues operating in Russia. These ozonometers are calibrated using Dobson spectrophotometer No.108, which regularly participates in the intercalibrations. Each of these stations has three instruments which provide continuous measurements. Measurement data are transferred to the World Ozone and Ultraviolet Radiation Data Center (WOUDC, www.woudc.org) and the results of an analysis of the current state of the ozone layer are regularly published in the journal “Meteorology and Hydrology” and in annual reports on the state of environment, which are issued by the Russian Federal Service for Hydrometeorology and Environmental Monitoring (Rosgidromet) [Shalamyansky, 2013]. In 2008–2014, an automated UV ozone spectrometer (UVOS) was under development, and its production started in 2014 [Dorokhov *et al.*, 2014]. This instrument makes it possible to measure the total ozone content (TOC) within a range of 100–600

DU and the spectral composition of UV radiation within a range of 290–400 nm under any weather conditions. In 2015, such spectrometers are to be installed at the ozonometric stations.

In 2011–2014, the KHASS, Obninsk, and Tomsk stations equipped with Brewer spectrophotometers continued carrying out TOC observations. Data obtained at these stations are also regularly transferred to the WOUDC. In 2012, these instruments were calibrated using the mobile standard of Brewer spectrophotometer No. 17 [Arshinov *et al.*, 2013a]. The daily measurements of the NO₂ content in a vertical atmospheric column, which is closely related to the TOC and is necessary for studying variations in the state of the ozone layer, are taken at the KHASS, Tomsk, and ZSS stations [Gruzdev and Elokhov, 2011; Arabov *et al.*, 2012; Ivlev *et al.*, 2013]. The TOC is regularly measured with an IR-Fourier spectrometer (IRFS) at the Petergof station in the vicinity of St. Petersburg [Virolainen *et al.*, 2011; Virolainen *et al.*, 2013]. A comparison between TOC data obtained in 2009–2012 with the aid of the IRFS and other instruments (M-124, Dobson spectrophotometer, and OMI) showed only a slight disagreement (2.5–4.5%). On the basis of the results of this comparison, the conclusion was drawn that it is possible to use the IRFS for validating satellite TOC data. TOC data were first obtained with an IR multichannel scanning device (MSU-GS) installed aboard the Russian satellite Elektro-L No.1 [Kramchaninova and Uspenskii, 2013]. The results of an analysis of retrieved TOC data for some observation periods in 2011–2013 showed that, using this device and developed algorithms, it is possible to monitor the fields of ozone with high spatial and temporal resolutions.

The quality of observational TOC data obtained at the Russian network of stations was estimated in [Izrael *et al.*, 2014]. It was concluded that the accuracy of filter instruments is insufficient for diagnosing the long-term trends of ozone. Disagreements are also noted in ozone-trend data obtained with spectral instruments, however, in this case, one should take into account the fact that these instruments are installed in regions remotely located from one another. At the same time, a rather dense network of filter instruments makes it possible to analyze the spatial distribution of the TOC. The TOC anomalies observed in the atmosphere over Russia during a period of over 50 years are discussed in [Zvyagintsev *et al.*, 2013a]. Ozone deficiencies during a month and more were observed over northern Eurasia in 1995–1997 and 2011. All these anomalies were associated with the behavior of the circumpolar vortex which was unusually deep, stable, and long, and this resulted in a rapid decrease in stratospheric temperature in the high latitudes. The TOC losses in the circumpolar vortex during the springs of 1997 and 2011 amounted to 140 DU. During the winter–spring period, under the influence of the transport of air masses from the arctic stratosphere, the region of decreased ozone content extended to the middle latitudes. Anomalously low TOC values were recorded in Obninsk and Tomsk [Ivlev *et al.*,

2013b; Bazhenov, 2014]. These ozone anomalies were accompanied by a decrease in the stratospheric content of NO₂. At the ZSS, in late March 2011, the content of NO₂ decreased by 40% with respect to its mean value for this time of the year [Gruzdev and Elokhov, 2012; Gruzdev and Elokhov, 2013]. Record negative NO₂ anomalies (30% decrease) were observed during the 2011 winter–spring period in Tomsk and Zhigansk [Ageyeva et al., 2014]. In all cases, a rapid decrease in the TOC and NO₂ was accompanied by a decrease in air temperature and in the heights of isobaric surfaces in the stratosphere [Bazhenov, 2011; Bazhenov, 2012].

A close relation between ozone and NO₂ in the atmosphere is also manifested in the response of the latter to variations in solar activity and atmospheric circulation. A unique 30-year data series on the NO₂ content in the entire atmospheric vertical column, which was obtained from direct solar-radiation measurements at the KHASS station from 1979 to 2008, is given in [Arabov et al., 2012]. Its analysis revealed the characteristic features of the time variability of the total content of NO₂, which are associated with the 11-year solar-activity cycle, volcanic eruptions, quasi-biennial oscillations of tropical circulation, and the El Niño effect. These features quantitatively differ from those revealed from measurements of the stratospheric content of NO₂ according to solar radiation scattered in the zenith (NDAAC data).

TOC variations exceeding 100 DU may occur during a day. Such situations were analyzed on the basis of observational data obtained in 2009 [Ivanova, 2011] and 2009–2011 [Ivanova, 2013]. It was shown that a rapid increase (decrease) in the TOC is unambiguously associated with a descent (ascent) of the tropopause position. The recurrence of such situations throughout the year amounts to 0.25–0.27% of the total sample. Some of such situations were noted to be related to a sudden stratospheric warming.

2.2. Vertical ozone distribution

Over the past four years, the system for monitoring the vertical ozone distribution (VOD), on the whole, has remained unchanged. Ozonesondes were occasionally launched mainly in winter [Dorokhov et al., 2013; Dorokhov et al., 2014]. Both microwave (Moscow and Nizhny Novgorod) and lidar (Tomsk) soundings were continuously carried out. Instruments and methods for sounding were significantly improved. A new-generation mobile automated microwave spectroradiometer was developed. This instrument makes it possible to obtain data on the VOD within a height range of 20–60 km during 15–20 min. A more accurate algorithm for retrieving vertical profiles was also developed. This algorithm combines the Tikhonov regularization method and the method of statistical regularization [Solomonov et al., 2011]. A multiyear data series on the VOD over

Moscow was used to study the influence of circulation systems and processes, such as large-scale vortices, waves, and sudden stratospheric warmings, on the ozone layer. New methodical approaches to the solution of these problems and obtained results are given in [Solomonov et al., 2011; Solomonov et al., 2012a; Solomonov et al., 2012b; Kropotkina et al., 2013; Solomonov et al., 2014]. During the winter period, planetary waves with the wavenumbers $n = 1, 2$ dominate in the stratosphere, in latitude 69° N. At $n = 2$, the polar vortex was often shifted towards Moscow, and its frequent occurrence in the atmosphere over Moscow made it possible to obtain new data on its intensity and sizes and on the structure of the VOD inside this vortex and at its borders. Thus, when the vortex passed over Moscow in the winter of 2010, the concentration of ozone at a height of 30 km increased from 54 to 92 ppm [Solomonov et al., 2012b].

The state of stratosphere rapidly changes during sudden stratospheric warmings. Such warmings, especially the major warmings of 2001 and 2013, strongly affected the VOD, and the character of these VOD variations is described in [Solomonov et al., 2011; Kulikov et al. 2013]. The VOD during the formation and existence of the ozone anomaly of winter–spring 2011 is analyzed in detail in [Solomonov et al., 2012b]. In late March – early April, an approximately 30% decrease in the content of ozone over Moscow was observed throughout almost the entire middle and upper stratosphere. Decreased ozone concentrations in the upper stratosphere were regularly observed also outside the polar-vortex zone. It was shown in [Solomonov et al., 2012a] that such VOD variations occur during the exchange of air masses characterized by their different compositions and temperatures.

The results of long-term measurements of the VOD with a microwave spectroradiometer over Nizhny Novgorod are given in [Ryskin et al., 2012]. The characteristic features of its variability are emphasized. Variations in the VOD structure and temperature in the middle atmosphere are analyzed in detail. The microwave sounding increases its informativeness in combination with lidar observations. Such experiments carried out in Tomsk are described in [Marichev et al., 2014; Kulikov et al., 2014; Marichev et al., 2012]. During the December 2012 – January 2013 stratospheric warming, the content of ozone at heights of 25–60 km increased by 1.5–2 times [Marichev et al., 2014]. In this case, the amplitude of daily variations significantly increased (up to 30% at a height of 60 km). According to lidar observations, the maximum deviation of air temperature from its monthly mean reached 70° K at a height of 30 km. This major warming was associated with the fact that circulation in the upper stratosphere over western Siberia reversed the direction of its transport from west to east. Similar situations (but with weaker variations) were observed from December 2013 to February 2014 [Kulikov et al., 2014].

In addition to the influence of natural factors on the content of ozone in the mesosphere, of some interest is the possibility of artificial impact on ozone with

the aid of powerful short-wave radiation. Such experiments were carried out using the “Sura” heating stand [Kulikov *et al.*, 2012; Kulikov *et al.* 2013; Kulikov and Frolov, 2013]. The radiation power amounted to 100 MW. Ozone-layer disturbances at heights of 50–90 km were measured using the method of ground-based microwave radiometry. On the basis of the results obtained in these experiments, a new physical phenomenon was revealed — the intensity of the microwave radiation of the mesosphere within the ozone line decreases when the ionosphere changes its state under the influence of powerful short-wave radiation.

Observational VOD data obtained with the SBUV/SBUV2 satellite instruments in 1978–2003 were used to estimate the effect of the 11-year cycle of solar activity on the content of ozone in the stratosphere and mesosphere [Gruzdev, 2014a]. A high coherence was revealed between the content of ozone and the level of solar activity on the solar-cycle scale. Maximum heights for the sensitivity of ozone to the 11-year cycle of solar activity were noted for the upper (50–55 km), middle (35–40 km), and lower (below 25 km) stratospheres. Maximum variations (up to 10%) in the content of ozone were noted for spring and summer in the polar regions. The content of NO₂ in the stratosphere also varies under the influence of the 11-year cycle of solar activity [Schmidt *et al.*, 2013]. There are interhemispheric differences in its variations (up to the change of sign). These variations do not exceed 5%. Taking into consideration the 11-year cycle made it possible to specify the effect of the Pinatubo eruption products on ozone and NO₂ [Gruzdev, 2014b]. In the response of ozone, there are two layers with its decreased concentration: 25–32 km within the latitudinal zone 50° S–40° N and 18–25 km within higher latitudes in both hemispheres. A maximum 22% decrease in the concentration of ozone was observed at heights of about 32 km within 10°–15° S. The decrease in the content of NO₂ amounted to 23–33% in the middle latitudes.

The influence of the subtropical jet stream (SJS) on the VOD is estimated in [Bukin *et al.*, 2011]. Data obtained from lidar sounding along the meridian of longitude 132° E, which crosses the SJS active region, were also analyzed. The VOD is locally maximum above the tropopause in the upper tropopause inversion layer and the VOD is minimum in the lower stratosphere. It is assumed that the local maximum and the inversion layer are formed due to the superposition of the stratospheric and tropospheric cells of circulation in the vicinity of the SJS axis.

2.3. Numerical simulation

A method for calculating the atmospheric emissions of ozone precursors from natural fires has been developed for three-dimensional chemical transport models [Konovalov *et al.*, 2011; Berezin *et al.*, 2013; Berezin *et al.*, 2013]. The key

features of this method are the use of daily maxima of the intensity of IR radiation from fires according to satellite data and the assimilation (by such a model) of ground-based measurement data on atmospheric pollution. This method has successfully been tested in comparing model data on the composition of the atmosphere over Russia with data obtained from ground-based and satellite measurements. The model study of the evolution of ozone and its precursors in Russian regions with natural fires in summer 2010 has been conducted [Konovalov *et al.*, 2012]. A current chemical transport model and the developed method for calculating the amount of pollutants emitted by fires were used. It was revealed that an increase in the rate of the formation of ozone in a smoke plume, which is caused by increased concentrations of its precursors, is fully compensated due to the fact that the flux of solar radiation is attenuated by smoke aerosol [Berezin *et al.*, 2013]. It was first shown that heterogenic reactions on the surface of smoke aerosol may result in significant ozone losses in the atmospheric surface layer [Konovalov *et al.*, 2012].

The model study of the transboundary transport of anthropogenic pollutants from China to the Far East region of Russia has been conducted [Kuznetsova *et al.*, 2013]. It was found that the transboundary transport of anthropogenic pollutants may cause repetitive events with increased O_3 and NO_x concentrations in the atmosphere over southern Khabarovsk krai. The results of both trajectory and synoptic analyses showed that the occurrence of such events is caused mainly by the transport of air masses from north-eastern China in the forefront of continental cyclones [Kuznetsova *et al.*, 2013].

The distribution of the concentrations of ozone and its precursors (CO and NO_x) over Siberia was numerically simulated using the GEOS-chem global transport model [Shtabkin and Moiseenko, 2014]. The results of this simulation adequately reproduce the measured (in Zotino) concentrations of these gases, and this favors the view that the photochemical system in the boreal zone of Eurasia is homogeneous [Heimann *et al.*, 2014; Engvall Stjernberg A.-C. *et al.*, 2012]. Natural fires significantly contribute to the tropospheric content of ozone, and their contribution dominates over that made by both long-range and regional transports of anthropogenic pollutants.

The air quality has been estimated and predicted for the Moscow region using both WRF ARW and CHIMERE models [Zaripov *et al.*, 2011]. Different configurations of the prediction system, which differ in spatial resolution and a method of specifying boundary conditions, have been considered. An empirical model for predicting the daily mean concentrations of ozone on the basis of a neural net has been developed for the Tomsk region [Antokhin *et al.*, 2013b]. The neuronet approach has proved more efficient when compared to models based on multiple linear regression and autoregression. This approach makes it possible to describe up to 70% of the total variance of mean value and 50% of the variance of rms deviation.

The seasonal dependence, time intermittency, and nonlinearity of both ozone and temperature responses to 27-day solar activity have been revealed using the HAMMONIA chemistry climate model [Gruzdev *et al.*, 2014]. The response sensitivity in the extratropical latitudes may be higher in winter than in summer, which implies that the role of atmospheric circulation may be important. This assumption is supported by results given in [Schmidt *et al.*, 2013], where 27-day variations in geopotential and its zonal harmonics were revealed.

The SOCOL three-dimensional chemistry climate model was used for estimating variations in ozone and atmospheric dynamics in the 21st century [Zubov *et al.*, 2011; Ozolin *et al.*, 2011]. The model yielded a statistically significant stratospheric cooling of 4–5 K for 2000–2050 and 3–5 K for 2050–2100. The temperature of the lower atmosphere increases by 2–3 K by 2100. Tropospheric warming and intensified wave activity lead to a decrease in zonal circulation and an increase in meridional residual circulation. Due to such dynamic changes and decreased concentrations of ozone-depleting gases, the rate of increase in the content of ozone outside the tropics increases. Here, by 2050, the TOC is retrieved almost to its level of 1989. In the tropics, the ozone layer is retrieved significantly slower and reaches its level of 1980 only by 2100. Both individual and combined effects of all factors that affect the ozone layer were studied in [Zubov *et al.*, 2013a]. In the first half of the 21st century, the TOC in the middle and high latitudes of both hemispheres is retrieved mainly due to a decrease in the concentrations of ozone-depleting compounds. In the second half of this century, in both tropical and extratropical regions of the Northern Hemisphere, ocean-temperature variations and sea ice play the most important role. Greenhouse gases affect the ozone layer mainly in the upper and lower stratospheres of the high latitudes of the Southern Hemisphere. The lower tropical stratosphere in the Northern Hemisphere depends, to a considerable degree, on the temperature of the ocean surface.

A strategy for slowing climate change, which is alternative to that for reducing anthropogenic CO₂ emissions, was proposed in [Karol *et al.*, 2013]. Reduced emissions of methane, hydrofluorocarbons, and aerosols (first and foremost, carbon-black aerosols) and decreased ozone generation in the atmospheric boundary layer may also noticeably affect the environment and climate. The sources and destruction mechanisms of these substances in the atmosphere are discussed, their emissions and the degree of their influence on climate are estimated, and recommendations as to how to decrease such emissions are given. An important aspect of the problem of changes in climate and atmospheric ozone is their influence on the regime of UV radiation and the production of vitamin D in the human body. On the basis of both SOCOL and FASTRT(uvspec) models, processes affecting variations in the flux of UV radiation incident on the land surface are studied in [Zubov *et al.*, 2013b]. Possible UV-radiation variations are estimated for the 21st century.

3. Conclusions

In 2011–2014, a team of Russian researchers continued to study atmospheric ozone. Noticeable achievements are associated with studying processes that determine the spatiotemporal variability of ozone and its precursors (CO and NO_x) in the atmosphere over northern Eurasia. These studies were, to a considerable extent, initiated by the start of work on the implementation of the Pan-Eurasian Experiment (PEEX) [Lappalainen et al., 2014]. A certain achievement in the area of observations of ozone and other atmospheric components was the development of a YaK-42D aircraft laboratory equipped with current instruments (CAO). This aircraft laboratory successfully stood the test in 2014. At the same time, for lack of financing, the Danki and Shepelevo background stations stopped operating and, in 2010, the TROICA international experiments were completed. The unique mobile railroad laboratory was dismantled, and two specialized railway cars were mothballed. In the last two years, there has been some progress towards the development of a system for the space monitoring of ozone and other important components of the atmosphere. In 2014, the first experiments were carried out to validate satellite atmospheric-sounding data. Great expectations are related to an increase in the state support of young professionals in the area of atmospheric investigations.

References

1. Ageyeva V. Yu., Grishaev M. V., Gruzdev A. N., Elokhov A. S., Salnikova N. S. Anomalies of stratospheric NO₂ content over Siberia related to the Arctic ozone hole 2011 // *Atmospheric and oceanic optics*. 2014. V. 27. No 1. P. 40–45.
2. Andreev M. S., Chulichkov A. I., Medvedev A. P., Postlyakov O. V. Estimation of cloud base height using ground-based stereo photography: Method and first results // *Proc. SPIE*. 2014a. V. 9242. 924219. 1–7. doi: 10.1117/12.2069824.
3. Andreev M. S., Chulichkov A. I., Emilenko A. S., Medvedev A. P., Postlyakov O. V. Estimation of cloud height using ground-based stereophotography: Methods, error analysis and validation // *Proc. of SPIE*. 2014b. V. 9259. 92590N. 1–6. doi: 10.1117/12.2069800.
4. Anokhin G. G., Antokhin P. N., Arshinov M. Yu., Barsuk V. E., Belan B. D., Belan S. B., Davydov D. K., Ivlev G. A., Kozlov A. V., Kozlov V. S., Morozov M. V., Panchenko M. V., Penner I. E., Pestunov D. A., Sikov G. P., Simonenkov D. V., Sinitsyn D. S., Tolmachev G. N., Filipov D. V., Fofonov A. V., Chernov D. G., Shamanaev V. S., Shmargunov V. P. OPTIK Tu-134 aircraft laboratory // *Atmospheric and oceanic optics*. 2011. V. 24. No 9. P. 805–816
5. Antokhin P. N., Arshinov M. Yu., Belan B. D., Davydov D. K., Zhidovkin E. V., Ivlev G. A., Kozlov A. V., Kozlov V. S., Panchenko M. V., Penner I. E., Pestunov D. A., Simonenkov D. V., Tolmachev G. N., Fofonov A. V., Shamanaev V. S.,

Shmargunov V. P. Optik-É AN-30 aircraft laboratory: 20 years of environmental research // Atmospheric and Oceanic Technology. 2012a. V. 29. No 1. P. 64–75.

6. Antokhin P. N., Arshinov M. Yu., Belan B. D., Belan S. B., Davydov D. K., Kozlov A. V., Krasnov O. A., Pestunov D. A., Praslova O. V., Fofonov A. V., Inoue Gen., Machida Toshinobu., Maksutov Shamil. Shamil., Shimoyama Ko., Sutoh H. An-2 aircraft investigation of air composition in the atmospheric boundary layer // Atmospheric and oceanic optics. 2012b. V. 25. No 08. P. 714–720.

7. Antokhin P. N., Arshinova V. G., Arshinov M. Yu., Belan B. D., Belan S. B., Davydov D. K., Kozlov A. V., Krasnov O. A., Praslova O. V., Rasskazchikova T. M., Savkin D. E., Tolmachev G. N., Fofonov A. V. Diurnal dynamics of ozone vertical distribution in the atmospheric boundary layer near Tomsk city // Atmospheric and oceanic optics. 2013a. V. 26. No 8. P. 665–672.

8. Antokhin P. N., Belan B. D., Savkin D. E., Tolmachev G. N. The comparison of different methods of statistical prediction of diurnal dynamics in the ground ozone concentration // Atmospheric and oceanic optics. 2013b. V. 26. No 12. P. 1082–1089.

9. Arabov A. Ya., A. N. Borovskii, N. F. Elansky, A. S. Elovkov, I. A. Senik, and V. V. Savinyk. Nitrogen Dioxide in the North Caucasus Atmosphere: 30 Years of Observations // Doklady Earth Sciences. 2012. V. 446. No 1. P. 1121–1126. doi: 10.1134/S1028334X12090176.

10. Aref'ev V. N., F. V. Kashin, L. I. Milekhin, V. L. Milekhin, N. V. Tereb, and L. B. Upenek Concentration of Surface Ozone in Obninsk, 2004–2010 // Izvestiya, Atmospheric and Oceanic Physics. 2013. V. 49. No 1, P. 66–76. doi: 10.7868/S0002351513010021.

11. Arshinov M. Yu., Belan B. D., Davydov D. K., Kovalevskii V. K., Plotnikov A. P., Pokrovskii E. V., Sklyadneva T. K., Tolmachev G. N. Automatic station for monitoring of minor gases constituents in the atmospheric air // Meteorology and Hydrology. 1999. No 3. P. 110–118.

12. Arshinov M. Yu., Belan B. D., Davydov D. K., Ivlev G. A., Kozlov A. V., Pestunov D. A., Pokrovskii E. V., Tolmachev G. N., Fofonov A. V. Sites for monitoring of greenhouse gases and gases oxidizing the atmosphere // Atmospheric and oceanic optics. 2007. V. 20. No 1. P. 45–53.

13. Arshinov M. Yu., Belan B. D., Inoue G., Machida T., Tolmachev G. N., Fofonov A. V. Results of long-term monitoring of the ozone vertical distribution in the Siberian troposphere derived from airborne measurements // Proceedings of the Second “Tropospheric Ozone” Workshop on Tropospheric ozone changes: Observations, state of understanding, and model performances, 11–14 April. 2011. Toulouse, France. P. 60–64.

14. Arshinov M. Yu., Afonin S. V., Belan B. D., Belov V. V., Gridnev Yu. V., Davydov D. K., Machida Toshinobu., Nedelec Ph., Paris J.-D., Fofonov A. V. Comparison of satellite and aircraft measurements of gas composition in troposphere above the South of West Siberia // Atmospheric and oceanic optics. 2013a. V. 26. No 9. P. 773–782.

15. Arshinov M. Yu., Belan B. D., Nédélec P., Paris J.-D., Sia F., Tolmachev G. N., Fofonov A. V. The peculiarities of gases species distribution in clouds. Do we need to use them in the models // Solar — Terrestrial Physics. 2013b. V. 23. P. 115–119.

16. Arshinov M. Yu., Belan B. D., Davydov D. K., Savkin D. E., Sklyadneva T. K., Tolmachev G. N., Fofonov A. V. Mesoscale distinctions in ozone concentrations in the

surface air of the Tomsk region (2010–2012) // Proc. The 3-th international meeting-seminar. Moscow. HMC. 2013c. 11 p. <http://cao-rhms.ru/oom/meeting.html>.

17. Arshinov M. Yu., Belan B.D., Davydov D.K., Savkin D.E., Sklyadneva T.K., Tolmachev G.N., Fofonov A.V. Long standing monitoring of ozone in the Tomsk environs // Proc.of the 2-th international meeting — seminar. Moscow. IGP RAN. 2013d. P. 38–49.

18. Arshinov M. Yu., Afonin S.V., Belan B.D., Belov V.V., Gridnev Yu.V., Davydov D.K., Nédélec P., Paris J.-D., Fofonov A.V. Comparison between Satellite Spectrometric and Aircraft Measurements of the Gaseous Composition of the Troposphere over Siberia during the Forest Fires of 2012 // *Izvestiya, Atmospheric and Oceanic Physic*. 2014a. V. 50. No 9. P. 916–928. doi: 10.1134/S0001433814090047.

19. Arshinov M. Yu., Afonin S.V., Belan B.D., Belov V. V., Gridnev Yu.V., Davydov D.K., Nédélec P., Paris J.-D., Fofonov A.V. Comparison between Satellite Spectrometric and Aircraft Measurements of the Gaseous Composition of the Troposphere over Siberia during the Forest Fires of 2012 // *Earth Investigations from Space*. 2014b. No 1. C. 72–84.

20. Bazhenov O.E. Long-term trends of variations in total ozone content according to data of ground-based (Tomsk: 56.48 N, 85.05 E) and satellite measurements // *Atmospheric and oceanic optics*. 2011. V. 24. No 9. P. 770–774.

21. Bazhenov O.E. Assessing the effects of humidity and temperature in the stratosphere on the occurrence of ozone anomaly in spring of 2011 in Arctic and over northern territory of Russia // *Atmospheric and oceanic optics*. 2012. V. 25. No 7. P. 589–593

22. Bazhenov O.E. Study of the quasi-biennial oscillation of total ozone and ozone concentrations at individual altitude levels over Arctic and Tomsk according to data of TOMS satellite instrumentation // *Atmospheric and oceanic optics*. 2014. V. 27. No 12. P. 1074–1078.

23. Bezuglaya, E. Yu., Smirnova T.V. Air of cities and its changes // St. Petersburg, Asterion Publisher. 2008. 254 p.

24. Belan B.D. Tropospheric ozone // *Palmarium Academic Publishing*. Saarbrücken, Germany, 2012. 552 c.

25. Berchet A., Paris J.-D., Ancellet G, Law K.S., Stohl A., Nédélec P, Arshinov M. Yu., Belan B.D. and Ciais P. Tropospheric ozone over Siberia in spring 2010: remote influences and stratospheric intrusion // *Tellus. B*. 2013. V.65. 19688. <http://dx.doi.org/10.3402/tellusb.v65i0.19688>.

26. Belikov I.B., Obvintseva L.A., Tsyrkina T.B., Sukhareva I.P., Dmitrieva M.P., Zhernikov K.V., Avetisov A.K. Automatized gas measuring devices on the basis of semiconductor sensors // Proc. of Conference of young specialists on hydrometeorology and monitoring of the environment. 2013 June 4–6. Obninsk. P. 345–348.

27. Berezina E.V., Elansky N.F., Moiseenko K.B., Belikov I.B., R.A. Shumsky, A.N. Safronov, and C. A.M. Brenninkmeijer. Estimation of nocturnal 222Rn soil fluxes over Russia from TROICA measurements // *Atmos. Chem. Phys*. 2013. V. 13. 11695–11708. doi: 10/5194/acp-13-11695-2013.

28. Berezina E.V., Elansky N.F., Moiseenko K.B., Safronov A.N., Skorokhod A.I., Lavrova O.V., Belikov I.B., Shumsky R.A. Estimation of biogenic CH₄ and CO₂ emissions and dry deposition of O₃ using Rn-222 measurements in TROICA expeditions // *Izvestiya, Atmospheric and Oceanic Physics*. 2014. V. 50. No 6. P. 583–594. doi: 10.1134/S000143381406005X.

29. Burlakov V.D., Dolgii S.I., Makeev A.P., Nevzorov A.V., Kharchenko O.V., Romanovskii O.A. Lidar of differential absorption for sounding of ozone in the up troposphere — low stratosphere // *Instruments and Experimental Technique* 2010. No 5. P. 121–124.
30. Burlakov V.D., Dolgii S.I., Makeev A.P., Matvienko G.G., Nevzorov A.V., Soldatov A.N., Romanovskii O.A., Kharchenko O.V., Yakovlev S.V. Lidar technologies for remote sensing of atmospheric parameters. // *Atmospheric and oceanic optics*. 2013. V. 26. No 10. P. 829–837.
31. Borovski A.N., Dzhola A.V., Elokhov A.S., Grechko E.I., Postilyakov O.V., Kanaya Y. First measurements of formaldehyde integral content at Zvenigorod Scientific Station // *Int. J. of Remote Sensing*. 2014. 35:15. 5609–5627. doi:10.1080/01431161.2014.945011.
32. Bukin O.A., Nguen Suan An, Pavlov A.N., Stolyarchuk S. Yu, Shmirko, K.A. Effect that jet streams have on the vertical ozone distribution and characteristics of tropopause inversion layer in the far east region // *Izvestiya, Atmospheric and Oceanic Physics*. 2011. V. 47. No 5. P. 610–618. doi: 10.1134/S0001433811050021.
33. Berezin E.V., Konovalov I.B., Gromov S.A., Beekmann M.3, Schulze E.D. The Model Study Of The Wildfire Impact On The Spatial Distribution Of Deposition Of Sulfur And Nitrogen Compounds In Siberia // *Meteorology and Hydrology*. 2013. V. 38. No 11. P. 750–758. doi: 10.3103/S1068373913110046.
34. Chubarova N.E., Nezval' E.I., Belikov I.B., Gorbarenko E.V., Eremina I.D., Zhdanova E. Yu, Korneva I.A., Konstantinov P.I., Lokoshchenko M.A., Skorokhod A.I., Shilovtseva O.A. Climatic and environmental characteristics of Moscow megapolis according to the data of the Moscow State University Meteorological Observatory over 60 years // *Meteorology and Hydrology*, Allerton Press Inc. 2014. T. 39. No 9. P. 602–613.
35. Dorokhov V., Yushkov V., Makshtas A., Ivlev G., Tereb N., Savinykh V., Shepelev D., Nakajima H., McElroy C.T., Tarasick D., Goutail F., Pommereau J.-P., Pazmino A. Brewer, SAOZ and Ozonesonde Observations in Siberia // *Atmosphere-Ocean*. 2013. V. 51. No 3. doi: 10.1080/07055900.2013.830078.
36. Dorokhov V., Arshinov M. Yu., Balugin N.V., Belan B.D., Fofonov A.V., F. Goutail, Ivlev G.A., Lykov A.D., Makshtas A., Nakajima H., Pazmino A., Pommereau J.-P., Shepelev D.V., Simonenkov D.V., Yushkov V.A. Ozone profile observations in Siberia in 2014 // *EGU General Assembly 2014*, Vienna 27 April-03 May 2014. *Geophysical Research Abstracts*. V. 16. EGU2014–2306, 2014.
37. Dorokhov V.M., Ivlev G.A., Privalov V.I., Shalamyansky A.M. Technical equipment of ground-based stations for total ozone measurements in Russia and prospects of modernization // *Atmospheric and oceanic optics*. 2014. V. 27. No 3. P. 250–257.
38. Dolgii S.I. Laser gas analyzers: Use of optic-sonic method and method of differential absorption and scattering // LAP LAMBERT Academic Publishing. ISBN: 978-3-8484-0113-0. 2012. 113 p.
39. Elansky N.F. Russian Studies of the Atmospheric Ozone in 2003–2006 // *Izvestia, Atmospheric and Oceanic Physics*. 2009. V. 45. No 2. P. 207–220.
40. Elansky N.F., Belikov I.B., Berezina E.V., Brenninkmeijer C.A. M., Buklikova N.N., Crutzen P.J., Elansky S.N., Elkins J.V., Elokhov A. S., Golitsyn G.S., Gorchakov G.I., Granberg I.G., Grisenko A.M., Holzinger R., Hurst D.F., Ageev A.I., Kozlova A.A., Kopeikin V.M., Kuokka S., Lavrova O.V., Lisitsyna L.V., Moeseenko K.B.,

Oberlander E.A., Obvintsev Yu. I., Pankratova N.V., Postilyakov O.V., Putz E., Romashkin P.A., Safronov A.N., Shenfeld K.P., Skorokhod A.I., Shumsky R.A., Tarasova O.A., Turnbull J.C., Vartiainen E., Weissflog L., Zhernikov K.V. Atmospheric composition observations over Northern Eurasia using the mobile laboratory: TROICA experiment // 2009. ISTC publ. Moscow. 73 p. <http://www.ifaran.ru/troica/biblio/troica-en.p>.

41. Elansky N.F., Mokhov I.I., Belikov I.B., Berezina E.V., Elokhov A.S., Ivanov V.A., Pankratova N.V., Postilyakov O.V., Safronov A.N., Skorokhod A.I., and Shumsky R.A. Gas Composition of the Surface Air in Moscow during the Extreme Summer of 2010 // *Doklady Earth Sciences*. 2011a. V. 437. No 1. P. 357–362.

42. Elansky N.F., Mokhov I.I., Belikov I.B., Berezina E.V., Elokhov A.S., Ivanov V.A., Pankratova N.V., Postilyakov O.V., Safronov A.N., Skorokhod A.I., and Shumskii R.A. Gaseous Admixtures in the Atmosphere over Moscow during the 2010 Summer // *Izvestiya, Atmospheric and Oceanic Physics*. 2011b. V. 47. No 6. P. 672–681. doi: 10.1134/S000143381106003X.

43. Elansky N.F. Russian Studies of Atmospheric Ozone in 2007–2011 // *Izvestiya, Atmospheric and Oceanic Physics*. 2012. V. 48. No. 3. P. 281–298. doi: 10.1134/50001433812030024.

44. Elansky N.F., Lokoshchenko M.A. and Trifanova A.V. Weekly course of minor atmospheric gases in Moscow // In: *Proceedings of the 8th International Conference on Air Quality — Science and Application*. Athens, Greece, 19–23 March 2012a, CD-version. P. 793–796.

45. Elansky N.F., Belikov I.B., Lavrova O.V., Skorokhod A.I., Shumsky R.A., Brenninkmeijer C.A.M. and Tarasova O.A. Chapter 8. Train-Based Platform for Observations of the Atmospheric Composition (TROICA Project) P. 175–196 // In “*Air Pollution-Monitoring, Modelling and Health*”. Ed. Mukesh Khare ISBN: 978-953-51-0424-7, Publisher: In Tech. 2012b. 386 p. doi: 10.5772/1801.

46. Elansky N.F., Lavrova O.V. Corresponding Member of the RAS I.I. Mokhov, and A.A. Rakin. Heat Island Structure over Russian Towns Based on Mobile Laboratory Observations // *Doklady Earth Sciences*. 2012. V. 443. No 1. P. 420–425. doi: 10.1134/S1028334X12030245.

47. Elansky N. Air quality and CO emissions in the Moscow megacity // *Urban Climate*. 2014. V. 8. 2014. P. 42–56. <http://dx.doi.org/10.1016/j.uclim.2014.01.007>.

48. Elansky N.F., Lavrova O.V. Minor Gases Species in the Atmosphere of Russian Cities from Mobile Laboratory Measurements (TROICA Experiments // *Doklady Earth Sciences*. 2014. V. 459. No 2. P. 1603–1608. doi: 10.1134/S1028334X14120149.

49. Elansky N.F., Lavrova O.V., Rakin A.A., Skorokhod A.I. Anthropogenic Disturbances of the Atmosphere in Moscow Region // *Doklady Earth Sciences*. 2014. V. 454. No 2. P. 158–162. doi: 10.1134/S1028334X14020020.

50. Elansky. N.F., Lokoshchenko M.A., Trifanova A.V., Belikov I.B., Skorokhod A.I. On Contents of Trace Gases in the Atmospheric Surface Layer over Moscow // *Izvestiya, Atmospheric and Oceanic Physics*. 2015. V. 51, No 1. P. 30–41. doi: 10.1134/S000143381501003X.

51. Engvall Stjernberg A.-C., Skorokhod A., Paris J.-D., Elansky N., Nédélec P., and A. Stohl. Low concentrations of near-surface ozone in Siberia // *Tellus B*2012. V. 64. 11607. doi: 10.3402/tellusb.v64i0.11607.

52. Fokeeva E. V., Safronov A. N., Rakitin V. S., Yurganov L. N., Grechko E. I., Shumskii R. A. Investigation into the Impact of the 2010 July – August Fires on Carbon Monoxide Atmospheric Pollution in Moscow and Its Surrounding Areas // *Izvestiya, Atmospheric and Oceanic Physics*. 2011. V. 47. No 6. P. 682–698.
53. Golitsyn G. S., Grechko E. I., Genchen Wang, Pusai Wang, Dzhola A. V., Emilenko A. S., Kopeikin V. M., Rakitin V. S., Safronov A. N., Fokeeva E. V. The investigation of CO and aerosols atmospheric pollution in Moscow and Beijing // *Izvestiya, Atmospheric and Oceanic Physics*. 2015. V 51. No 1. P. 1–11. doi: 10.1134/S0001433815010041.
54. Gruzdev A. N., Elokhov A. S. Variability of stratospheric and tropospheric nitrogen dioxide observed by visible spectrophotometer at Zvenigorod, Russia // *International Journal of Remote Sensing*. 2011. V. 32. No 11. P. 3115–3127.
55. Gruzdev A. N., Elokhov A. S. Negative anomaly of the stratospheric NO₂ content over Zvenigorod at the end of March and beginning of April 2011 // *Doklady Earth Science*. 2012. V. 448. No 1. P 126–130. doi: 10.1134/S1028334X12100078.
56. Gruzdev A. N., Elokhov A. S. New results of the validation of NO₂ abundance measurement data obtained with OMI instrument on the basis of Zvenigorod scientific station measurements // *Earth Investigations from Space*. 2013. No 1. P. 16–27.
57. Gruzdev A. N. Estimate of the effect of the 11-year solar activity cycle on the ozone content in the stratosphere // *Geomagnetism and Aeronomy*. 2014a. V. 54. No 5. P. 633–639. doi: 10.1134/S0016793214040161.
58. Gruzdev A. N. Estimation of the Pinatubo volcano eruption effect on stratospheric O₃ and NO₂, taking into account variations of solar activity // *Atmospheric and oceanic optics*. 2014b. V. 27. No 6. P. 506–514.
59. Gruzdev A. N., Schmidt H., Brasseur G. P. Analysis of the effects of the 27-day solar cycle on the atmospheric dynamics calculated by a 3-D chemistry-climate model // XX International symposium «Optics of the Atmosphere and Ocean. Atmospheric Physics», 23–27 June 2014, Novosibirsk. Proceedings. 2014. P. D249-D252.
60. Heimann M., Schulze E.-D., Winderlich J., Andreae M. O., Chi X., Gerbig C., Kolle O., Kubler K., Lavric J., Mikhailov E., Panov A., S. Park, C. Rodenbeck, and A. Skorochod. The Zotino Tall Tower Observatory (ZOTTO): Quantifying Large Scale Biogeochemical Changes in Central Siberia // *Nova Acta Leopoldina*. 2014. V. 117. No 399. P. 51–64.
61. Ivanov V. A., O. V., Postlylyakov. Estimation of integral NO₂ content in atmospheric boundary layer using observations of scattered in zenith radiation // *Atmos. and ocean. optics*. 2010. V. 3. No 6. P. 471–475.
62. Ivanov V. A., Elokhov A. S., Postlylyakov O. V. On the possibility of estimating the volume of NO₂ emissions in cities using zenith spectral observations of diffuse solar radiation near 450 nm // *Atmos. and Ocean Optics*. 2012. V. 2. No 6. P. 539–543.
63. Ivanova A. R. Dynamics of the tropopause for the cases of sharp changes in total ozone at the midlatitudes of the northern hemisphere // *Meteorology and hydrology*. 2011. T. 36. No 6. C. 362–370.
64. Ivanova A. R. Interconnection of dynamics of the extra tropical tropopause and the total ozone variations in 2009–2011 rr. // *Proceedings of the Hydrometcenter. Moscow*. 2013. V. 350. P. 175–194.

65. Ivlev G.A., Belan B.D., Dorokhov V.M., Tereb N.V. Spectral observations of the total ozone content variation in Obninsk and Tomsk in 2011 and 2012 // *Atmospheric and oceanic optics*. 2013a. V. 26. No 4. P. 325–331.
66. Ivlev G.A., Belan B.D., Dorokhov V.M. Dynamics of solar UV-B and UV-A radiations in Tomsk during ozone anomaly in spring, 2011 // *Atmospheric and oceanic optics*. 2013b. V. 26. No 11. P. 995–1004.
67. Izrael Yu.A., L.M. Belokrinitskaya, I.V. Dvoret'skaya, I.V. Dvoret'skaya, V.M. K.A. Ivanov, Dorokhov, G.M. Kruchenitskii, D.V. Shepelev, T.A. Yusipov. Comparison of ground-based and satellite measurements of total ozone // *Meteorology and Hydrology*. 2014. V. 39. No 6. P. 420–430.
68. Kanaya Y., Irie H., Takashima H., Iwabuchi H., Akimoto H., Sudo K., Gu M., Chong J., Kim Y.J., Lee H., Li A., Si F., Xu J., Xie P.-H., Liu W.-Q., Dzhola A., Postylyako, O., Ivanov V., Grechko E., Terpugova S., Panchenko M. Long-term MAX-DOAS network observations of NO₂ in Russia and Asia (MADRAS) during the period 2007–2012: instrumentation, elucidation of climatology, and comparisons with OMI satellite observations and global model simulations // *Atmos. Chem. Phys.* 14. 7909–792. doi:10.5194/acp-14-7909-2014, 2014.
69. Karol I.L, Kiselev A.A., Genikhovich E.L, Chicherin S.S. Reduction of short-lived atmospheric pollutant emissions as an alternative strategy for climate-change moderation // *Izvestiya, Atmospheric and Oceanic Physics*. 2013. V. 49. No 5. P. 461–478. doi: 10.1134/S0001433813050058.
70. Konovalov I.B., M. Beekmann, I.N. Kuznetsova, A. Yurova, and A.M. Zvyagintsev. Atmospheric impacts of the 2010 Russian wildfires: integration modelling and measurements of an extreme air pollution episode in the Moscow Region // *Atmospheric Chemistry and Physics*. 2011. V. 11. No 19. P. 10031–10056.
71. Konovalov I.B., Beekmann M., D'Anna B., George C. Significant light induced ozone loss on biomass burning aerosol: Evidence from chemistry-transport modeling based on new laboratory studies // *Geophysical Research Letters*. 2012. V. 39. L17807. doi:10.1029/2012GL052432.
72. Konovalov I.B., Berezin E.V., Ciais P., Broquet G., Beekmann M., Hadji-Lazarro J., Clerbaux C., Andreae M.O., Kaise, J.W., Schulze E.-D. Constraining CO₂ emissions from open biomass burning by satellite observations of co-emitted species: a method and its application to wildfires in Siberia // *Atmospheric Chemistry and Physics*. 2014. V. 14. P. 10383–10410.
73. Kramchaninova E.K, Uspenskii A.B. Monitoring of total ozone content in the atmosphere from the Russian geostationary meteorological satellite Electro-L // *Earth Investigations from Space*. 2013. No 2. P. 12–17.
74. Krasilnikov A.A., Y.Y. Kulikov, V.G. Ryskin, V.M. Demkin, L.M. Kukin, V.L. Michaylovskiy, V.N. Shanin, M.Z. Sheyner, V.A. Shumilov, A.M. Shchitov. New mobile microwave spectroradiometer — ozonometer // *Instruments and Experimental Technique*. 2011. No 1. P. 127–133.
75. Kropotkina E.P., Solomonov S.V., Rozanov S.B., Ignatyev A.N., Lukin A.N. // Peculiarities of altitude ozone distribution over Moscow in 2011–2013 from

millimeter-wave observations // International symposium “Atmospheric Radiation and Dynamics” ISARD-2013, Proceedings, 24–27 June 2013, S.-Petersburg. 2013. P. 137–138.

76. Kulikov Yu.Yu., G.I. Grigoriev, A.A. Krasilnikov, V.L. Frolov // Variations of mesosphere microwave emission by modification of the lower ionosphere by powerful HF radio waves // *Izvestiya. High Schools — Radiophysics*. 2012. T 55. No 1–2. P. 57–65.

77. Kulikov Yu.Yu., V.L. Frolov, G.I. Grigoriev, V.M. Demkin, G.P. Komrakov, A.A. Krasilnikov, V.G. Ryskin. Response of the mesospheric ozone on lower ionosphere heating by powerful HF radio waves // *Geomagnetism and Aeronomy*. 2013. V. 53. No 1. P. 102–109.

78. Kulikov Yu.Yu., V.L. Frolov. Influence is artificial the indignant ionosphere on mesospheric ozone // *Chemical Physics*. 2013. V. 32. No 11. P. 26–30.

79. Kulikov Yu.Yu., D.A. Bochkovsky, V.N. Marichev, V.G. Ryskin. Experimental studies of ozone and temperature variations in the stratosphere over Tomsk by the methods of microwave and lidar sensing // *Proc. of SPIE* V. 9292. P. 92925C-1–92925C-4, 2014. doi: 10.1117/12.2075520.

80. Kuznetsova I. N., Glazkova A. A., Kononov I. B., Berezin E. V., Beekmann M., Schulze E. D. Estimation of transboundary transport contribution to the air pollution in the far east region using the chemistry transport model // *Meteorology and Hydrology*. 2013. V. 38. No 3. P. 150–158. doi: 10.3103/S1068373913030023.

81. Lapchenko V.A., Zvyagintsev. Surface ozone in Crimea // *Space and Time*. 2014. V. 16, No 2. C. 254–257.

82. Lokoshchenko M.A., Elansky N.F., Trifanova A.V. Meteorological conditions influence on the air pollution in Moscow // *M. Vestnik RANS*. 2014. V. 14. No 1. P. 64–67.

83. Lappalainen H., Petäjä T., Kujansuu J., Kerminen V., Shvidenko A., Bäck J., Vesala T., Vihma T., de Leeuw G., Lauri A., Ruuskanen T., Lapshin V., Zaitseva N., Glezer O., Arshinov M., Spracklen D.V., Arnold S.R., Juhola S., Lihavainen H., Viisanen Y., Chubarova N., Chalov S., Filatov N., Skorokhod A., Elansky N., Dyukarev E., Esau I., Hari P., Kotlyakov V., Kasimov N., Bondur V., Matvienko G., Mareev A. Baklanov E., Troitskaya Y., Ding A., Guo H., Kulmala M., Zilitinkevich S. Pan Eurasian Experiment (PEEX) — a research initiative meeting the grand challenges of the changing environment of the northern pan-eurasian arctic-boreal areas // *Geography. Environment. Sustainability*. 2014. No 2. P. 14–48.

84. Mosecomonitoring website. <http://www.mosecom.ru/air/air-today/>.

85. Matvienko G. G., Belan B. D., Panchenko M. V., Sakerin S. M., Kabanov D. M., Tuechinovich S. A., Turchinovich Yu.S., Eremina T.A., Kozlov V.S., Terpugova S.A., Pol'kin V.V., Yausheva E. P., Chernov D. G., Odintsov S. L., Burlakov V. D., Sinita L. N., Arshinov M. Yu., Ivlev G.A., Savkin D.E., Fofonov A.V., Gladkikh V.A., Kamarin A. P., Belan D.B., Grishaev M.V., Belov V.V., Afonin S.V., Balin Yu.S., Kokhanenko G.P., Penner I.E., Samoilova S.V., Antokhin P.N., Arshinova V.G., Davydov D.K., Kozlov A.V., Pestunov D.A., Rasskazchikova T.M., Simonenkov D.V., Sklyadnaya T.K., Tolmachev G.N., Belan S.B., Shmargunov V.P., Voronin B.A., Serdyukov V.I., Polovtseva E.R., Vasil'chenko S.S., Tikhomirova O.V., Smirnov S.V., Makarova M.V., Safatov A.S., Kozlov A.S., Malyshev S.B., Maksimova T.A. Combined Experiment on

Measurement of Atmospheric Parameters on May 22 of 2012 in Tomsk // *International Journal of Remote Sensing*. 2014. V. 35. N. 15. P. 5651–5676.

86. Makarova M. V., Rakitin A. V., Ionov, D. V., Poberovskii A. V. Analysis of variability of the CO, NO₂, and O-3 contents in the troposphere near St. Petersburg // *Izvestiya, Atmospheric and Oceanic Physics*. 2011. V. 47. No 4. P. 468–479. doi: 10.1134/S0001433811040074.

87. Marichev V. N., G. G. Matvienko, A. A. Lisenko, V. Yu. Iljushik, B. B. Bychkov. First results of an integrated experiment on sounding the middle atmosphere in optical and millimeter wavelength ranges (over Tomsk) // *Atmospheric and Oceanic Optics*. 2012. V. 25. No 12. P. 1091–1095.

88. Marichev V. N., G. G. Matvienko, A. A. Lisenko, D. A. Bochkovky, Y. Y. Kulikov, A. A. Krasilnikov, V. G. Ryskin, V. M. Demkin. Microwave and optical observation of ozone and temperature of the middle atmosphere during stratosphere warming at Western Siberia // *Atmospheric and Oceanic Optics*. 2014. V. 27. No 1. P. 46–52.

89. Obvintseva L. A., Tsyorkina T. B., Shepelev A. D., Sukhareva I. P., Dmitrieva M. P., Avetisov A. K. FP (Petryanov's Filters) materials in ozone-containing environment // *Proc. of The Eighth Petryanov Readings*. Moscow, June 28–30. 2011. P. 93–107.

90. Obvintseva L. A., Tsyorkina T. B., Sukhareva I. P., Belikov I. B., Avetisov A. K. Response features of the gas sensor resistive in flow mode // *Journal «Nauchnoe Priborostroenie (Scientific Instrumentation)»*. 2014. V. 24. Issue 3. PP. 32–41.

91. Ozolin Yu. E., Karol I. L., Kiselev A. A. The model estimation of the chemical component of global ozone layer in 1970–2050 under anthropogenic impact. // In: *Contribution of Russia in the International Polar Year 2007/08*. Volume: «Meteorological and geophysical Investigations». 2011. P. 187–198.

92. Pankratova N. V. Elansky N. F., Belikov I. B., Lavrova O. V., Skorokhod A. I., Shumsky R. A. Ozone and Nitric Oxides in the Surface Air over Northern Eurasia According to Observational Data Obtained in TROICA Experiments // *Izvestiya, Atmospheric and Oceanic Physics*, 2011. V. 47. No 3. C. 313–328. doi: 10.1134/S0001433811030108.

93. Postilyakov O. V., A. N. Borovski. Measurements of formaldehyde total content using DOAS technique: a new retrieval method for overcast // *Proc. of SPIE*. V. 9259, 925918.1–7, 2014, doi: 10.1117/12.2069595.

94. Postilyakov O. V., A. N. Borovski, A. V. Dzhola, A. S. Elokhov, E. I. Grechko, Y. Kanaya. Measurements of formaldehyde total content in troposphere using DOAS technique in Moscow Region: preliminary results of 3 years observations // *Proc. SPIE*. 2014. V. 9242. 92420T. 1–7. doi:10.1117/12.2069824.

95. Pinardi G., M. Van Roozendaal, J.-C. Lambert, J. Granville, F. Hendrick, F. Tack, H. Yu, A. Cede, Y. Kanaya, H. Irie, F. Goutail, J.-P. Pommereau, A. Pazmino, F. Wittrock, A. Richter, T. Wagner, M. Gu, J. Remmers, U. Friess, T. Vlemmix, A. Piters, N. Hao, M. Tiefengraber, J. Herman, N. Abuhassan, R. Holla, D. Balis, N. Kouremeti, J. Kujanp, J. Chong, O. Postilyakov, J. Ma. GOME-2 total and tropospheric NO₂ validation based on zenith-sky, direct-sun and multi-axis DOAS network observations // *Proc. EUMETSAT Meteorological Satellite Conference (EMSC2014)*, 22–26 September 2014, Geneva, Switzerland.

96. Rakitin V.S., E.V. Fokeeva, E.I. Grechko, A.V. Dzhola, R.D. Kuznetsov Variations of the Total Content of Carbon Monoxide over Moscow Megapolis // *Izvestiya, Atmospheric and Oceanic Physics*. 2011. V. 47. No 1. P. 59–66. doi: 10.1134/S0001433810051019.
97. Ryskin V.G., I.I. Zinchenko, A.A. Krasilnikov, Y.Y. Kulikov, V.I. Nosov, T.O. Orozobakov, A.T. Orozobakov, B.B. Sayakbaeva. Stratospheric ozone distribution. features from the results of simultaneous ground-based microwave measurements in Nizhni Novgorod and Kyrgyzstan // *Meteorology and Hydrology*. 2012. V. 37. No 10. P. 659–665. doi: 10.3103/S1068373912100032.
98. Senik I. and N. Elansky, The peculiarities of inter-annual variability of surface ozone at Kislovodsk high mountain station (Northern Caucasus) // Second tropospheric ozone workshop “Tropospheric ozone changes: observations, state of understanding and model performances” Eds. Martin G. Schultz and Valérie Thouret. GAW Report 199. 2011. P. 152–156. http://www.wmo.int/pages/prog/arep/gaw/documents/GAW_199_14_Oct_web.pdf.
99. Skorokhod A. I. Main results of atmospheric reactive gases observations at ZOTTO in 2007–2013 // International ZOTTO workshop “The response of northern Eurasian ecosystems to global climate change: from observations to forecasting” Krasnoyarsk, Russia, 16–22 September. Book of abstracts, ISBN978–5–903055–36–4. 2013. P. 22.
100. Sitnov S.A. Analysis of satellite observations of the tropospheric NO₂ content over the Moscow region // *Izvestiya, Atmospheric and Oceanic Physics*. 2011a. V. 47. No 2. P. 166–185. doi: 10.1134/S0001433811010129.
101. Sitnov S.A. Satellite monitoring of atmospheric gaseous species and optical characteristics of atmospheric aerosol over the European part of Russia in April–September 2010 // *Doklady Earth Sciences*. 2011b. V. 437. No 1. P. 368–373. doi: 10.1134/S1028334X11030081.
102. Sitnov S.A. Aerosol optical thickness and the total carbon monoxide content over the European Russia territory in the 2010 summer period of mass fires: Interrelation between the variation in pollutants and meteorological parameters // *Izvestiya, Atmospheric and Oceanic Physics*. 2011c. V. 47. No 6. P. 714–728. doi: 10.1134/S0001433811060156.
103. Sitnov S.A. Analysis of satellite observations of aerosol optical properties and gaseous species over Central District of Russian Federation in the period of abnormally high summer temperature and mass wild fires in 2010 // *Atmospheric and oceanic optics*. 2011d. V. 24. No 7. P. 572–581.
104. Sitnov S.A., Adiks J.G. Weekly cycles in tropospheric NO₂ content over urban regions // *Atmospheric and oceanic optics*. 2013. V. 26. No 6. P. 500–509.
105. Sitnov S.A., Adiks T.G. Weekly variability of surface CO concentrations in Moscow // *Izvestiya, Atmospheric and Oceanic Physics*. 2014. V. 50. No 2. P. 160–178. doi: 10.1134/S000143381402011X.
106. Shalamyansky A. M. Conception of ozone and air masses of the Northern Hemisphere interaction // *Proc. MGO*. 2013. V. 568. C. 173–195.
107. Solomonov S.V., K.P. Gaikovich, E.P. Kropotkina, S.B. Rozanov, A.N. Lukin, A.N. Ignat'ev. Remote sensing of atmospheric ozone at millimeter waves // *Radiophysics and Quantum Electronics*. 2011. V. 54. No 2. P. 102–109. doi:10.1007/s11141–011–9274–8.

108. Solomonov S. V., E. P. Kropotkina, A. N. Ignat'ev, A. N. Lukin, S. B. Rozanov. Study of ozone concentration variations in the upper stratosphere using millimeter wave spectroscopy methods // *Bulletin of the Lebedev Physics Institute*, ISSN: 1068–3356. 2012a. V. 39. No 3. P. 65–71. doi:10.3103/S1068335612030013.
109. Solomonov S. V., E. P. Kropotkina, S. B. Rozanov, A. N. Ignat'ev, A. N. Lukin. Features of the altitude-time distribution of ozone over Moscow during the strong ozone depletion in spring 2011 and during the stratospheric warming in 2010 according to observations at millimeter wavelengths // *ISSN 1068–3356. Bulletin of the Lebedev Physics Institute*. 2012b. V. 39. No 10. P. 277–283. doi: 10.3103/S1068335612100016.
110. Solomonov S. V., E. P. Kropotkina, S. B. Rozanov, A. N. Ignat'ev, A. N. Lukin. Variations of the Vertical Ozone Distribution over Moscow during Sudden Stratospheric Warming in Winter 2012–2013 // *ISSN1068–3356, Bulletin of the Lebedev Physics Institute*. 2014. V. 41. No 3. P. 56–62. doi: 10.3103/S1068335614030026.
111. Schmidt H., J. Kieser, S. Misios, and A. N. Gruzdev. The atmospheric response to solar variability: Simulations with a general circulation and chemistry model for the entire atmosphere. In: *Climate and Weather of the Sun-Earth System (CAWSES): Highlights from a priority program*. Ed. F.-J. Luebken Springer. Dordrecht. The Netherlands. 2013. P. 585–604.
112. Shtabkin Y. A., K. B. Moiseenko, Seasonal variations of O₃, CO and NO_x near-surface concentration in central Siberia: ZOTTO observations and model simulation, ENVIROMIS-2014 works compilation, Tomsk, Russia. 2014. P. 35–37.
113. Trifanova A. V., Lokoshchenko M. A., Elansky N. F. Weekly course of minor atmospheric gases in Moscow // In: *Abstracts of the XVII All-Russian school-conference of young scientists "Air composition. Atmospheric Electricity. Climatic processes."* Nizhny Novgorod, Russia, 23–25 September 2013, publishing by Institute of Applied Physics. 2013. P. 53–54.
114. Tereb N. V., L. I. Milekhin, V. L. Milekhin, V. D. Gniledov, D. R. Nechaev, L. K. Kulizhnikova, and V. V. Shirotov. Surface Ozone Values in Anomalous Summer 2010 Measured in Obninsk // *Meteorologiya and Gidrologiya*. 2013. V. 38. No 5. P. 304–312. doi: 10.3103/S1068373913050026.
115. Vasileva A. V., Moiseenko K. B., Mayer J.-C., Jurgens N., Panov A., Heilmann M., Andreae M. O. Assessment of the regional atmospheric impact of wildfire emissions based on CO observations at the ZOTTO tall tower station in central Siberia // *J. Geophys. Res.* 2011. V. 116. D07301. doi:10.1029/2010JD014571.
116. Virolainen, Ya. A., Timofeev Y. M., Ionov D. V., Poberovskii A. V., Shalamyan-skii A. M. Ground-based measurements of total ozone content by the infrared method // *Izvestiya, Atmospheric and Oceanic Physics*. 2011. V. 47. No 4. P. 480–490.
117. Virolainen, Ya. A., Timofeev Y. M., Poberovskii A. V. Comparison of the satellite and ground based total ozone observations // *Earth Investigations from Space*. 2013. No 4. P. 83–91.
118. Wang Pu-Cai, Georgy S. Golitsyn, Wang Geng-Chen, Evgeny I. Grechko, Vadim S. Rikitin, Ekaterina V. Fokeeva, and Anatoly V. Dzhola Variation Trend and Characteristics of Anthropogenic CO Column Content in the Atmosphere over Beijing and Moscow // *Atmospheric and Oceanic Science Lett.* 2014. V. 7. No 3. P. 243–247.

119. Yurganov L. N., V. Rakitin, A. Dzhola, T. August, E. Fokeeva, M. George, G. Gorchakov, E. Grechko, S. Hannon, A. Karpov, L. Ott, E. Semutnikova, R. Shumsky, and L. Strow, Satellite- and ground-based CO total column observations over 2010 Russian fires: accuracy of top-down estimates based on thermal IR satellite data // *Atmos. Chem. Phys.* 2011. V. 11. P. 7925–7942. doi:10.5194/acp-11-7925-2011.
120. Yeremina I. D., Chubarova N. E., Alexeeva L. I., Surkova G. V. Acidity and chemical composition of summer precipitation within the Moscow region // *Vestnik MGU. Series 5. Geography.* 2014. No 5. P. 3–11.
121. Zaripov R. B., Kuznetsova I. N., Konovalov I. B., Belikov I. B., Zvyagintsev A. M. WRF ARW and CHIMERE models for numerical forecasting of surface ozone concentration // *Meteorology and Hydrology.* 2011. V. 36. No 4. P. 249–257. doi: 10.3103/S1068373911040054.
122. Zvyagintsev A. M., Tarasova O. A. Trends of surface ozone concentrations in Germany and their connections with changes in meteorological variables // *Meteorology and Hydrology.* 2011. V. 36. No 4. P. 258–264. doi: 10.3103/S1068373911040066.
123. Zvyagintsev A. M., Blum O. B., Glazkova A. A., Kotelnikov S. N., Kuznetsova I. N., Lapchenko V. A., Lesina E. A., Miller E. A., Miliayev V. A., Popikov A. P., Semutnikova E. G., Tarasova O. A., Shalygina I. Yu. Anomalies of trace gases in air of the European part of Russia and Ukraine in summer, 2010 // *Atmospheric and oceanic optics.* 2011a. V. 24. No 7. P. 582–588.
124. Zvyagintsev A. M., Blum O. B., Glazkova A. A., Kotelnikov S. N., Kuznetsova I. N., Lapchenko V. A., Lezina E. A., Miller E. A., Milyayev V. A., Popikov A. P., Semutnikova E. G., Tarasova O. A., Shalygina I. Y. Air pollution over European Russia and Ukraine under the hot summer conditions of 2010 // *Izvestiya, Atmospheric and Oceanic Physics.* 2011b. V. 47. No 6. P. 699–707. doi: 10.1134/S0001433811060168.
125. Zvyagintsev A. M., Kuznetsov G. I., Kuznetsova I. N. Ozone Anomalies in Spring Over Russia // *Meteorologiya and Gidrologiya.* 2013a. V. 38. No 5. P. 297–303. doi: 10.3103/S1068373913050014.
126. doi: 10.3103/S1068373913050014.
127. Zayakhanov A. S., Zhamsueva G. S., Tsydyppov V. V., Bal'zhanov T. Results of surface ozone monitoring in the atmosphere over Ulan-Ude // *Meteorology and Hydrology.* 2013. V. 38. No 12. P. 846–852. doi: 10.3103/S1068373913120066.
128. Zubov V. A., Rozanov E. V., Rozanova I. V., Egorova T. A., Kiselev A. A., Karol I. L., Schmutz W. Modelling of the global ozone changes and atmospheric dynamics in XXI-century using chemistry-climate model “SOCOL” // *Izvestiya, Atmospheric and Oceanic Physics.* 2011. V. 47. No 3. P. 330–342.
129. Zubov V., Rozanov E., Egorova T., Karol I., Schmutz W. Role of external factors in the evolution of the ozone layer and stratospheric circulation in 21st century // *Atmos. Chem. Phys.* 2013a. V. 13. P. 4697–4706.
130. www.atmos-chem-phys.net/13/4697/2013/doi:10.5194/acp-13-4697-2013.
131. Zubov V. A., Rozanov E. V., Karol I. L., Egorova T. A., Kiselev A. A., Ю. Э. Озолин. Modelling of changes of UV solar radiation necessary for vitamin D in XXI century // *S.-Peterburg. MGO. Proc.* 2013b. V. 568. P. 118–136.

Planetary Atmospheres

O. I. Korablev

Space Research Institute RAS
Moscow Institute of Physics and Technology

The report of the Commission on Planetary atmospheres of the Russian National Geophysical Committee for XXV General Assembly of International Union of Geophysics and Geodesy (Prague, 28.06–7.07.2015) summarizes the investigations in the field of planetary atmospheres in Russia for the period of 2011–2014.

1. Introduction

The National report of the Commission on Planetary atmospheres of the Russian National Geophysical Committee includes studies completed in 2011–2014. With regards to the previous period the number of published papers in the field of meteorology and atmospheres of planets of the Solar System has significantly increased. There are a number of reasons. As previously [Korablev et al., 2009, 2012], a significant share of the results has been obtained at ESA Mars Express and Venus Express spacecraft, carrying instruments with Russian participation. Mars Express is operational in the Mars orbit for more than 12 years, and the observations are being continued. The Venus Express spacecraft has ended its mission in January 2015, the last science observation has been carried out in November 2014, after almost 9 year of successful operation. A huge dataset has been accumulated. Parallel investigations of the two terrestrial planets have stimulated a number of theoretical, and synthesis works in the frame of comparative planetology.

On the other hand, the consolidation of efforts in the field of planetary atmospheres in Russia has benefited from two events. First, the Presidium of Russian Academy of Sciences has supported the Programme “Fundamental problems of research and exploration in the Solar System” led by Academician L. M. Zelenyi. One part of the Programme is dedicated to atmospheres and climate of planets (coordinators O. I. Korablev and V. I. Shematovich). Second, the Ministry of Science and Education of Russia in 2011 (on the second wave of “megagrants”) has granted to MIPT, in cooperation with IKI to create a Laboratory of high-resolution infrared spectroscopy of planetary atmospheres led by V. A. Krasnopolsky.

The current report of the Commission on Planetary atmospheres of the National Geophysical Committee includes exclusively the result published in refereed literature. The increased number of publications has imposed a certain selection. We group the result following planets, and we have now introduced a special section on

comparative studies of atmospheres of planets and their satellites. New methods and instruments for the studies of planetary atmospheres are also included.

2. Mars

2.1. Hydrological Cycle

The measurements of water vapor in the Martian atmosphere, which are carried out regularly from the spacecraft, are important for understanding the hydrological cycle of the planet: Formation of clouds, transfer of water, status of the icy polar caps. Water vapor, a small condensable specie, is a good indication of the global thermal regime of the planet. The longest series of homogeneous observations is published after the measurements with SPICAM instrument, operating onboard Mars Express [Trokhimovsky et al., 2015]. Long-term monitoring of water vapor on Mars and comparison of different observations, including Viking and Mars Express orbiters, in the same water vapor absorption band and processed in the same manner demonstrate the stability of water vapor on the timescale of several tens of years. SPICAM/Mars Express measuring the waver vapor is the acousto-optic (AOTF) spectrometer, which has been criticized for putative spectral leakage, or stray light, to be responsible for underestimation of water amount measured by SPICAM. Laboratory calibrations of the spare SPICAM unit have demonstrated high fidelity of the AOTF measurements [Korablev et al., 2013].

Only a few measurements of the vertical distribution of water vapor have been available until recently. Limb radiometer at Mars Reconnaissance Orbiter (MRO), specifically dedicated for profiling, has only completed its mission for the aerosol and atmosphere density profiles: The channel dedicated to water vapor is not operational. Solar occultation's with SPICAM/Mars Express allowed to fill the gap, providing extensive dataset of water profiles for different seasons and geographic locations [Maltagliati et al., 2013]. Maltagliati et al. [2011] has provided evidence that the H_2O at 30–40 km is supersaturated. The observed supersaturation is significantly higher than that known in the terrestrial atmosphere. The supersaturated state allows water to travel higher, than the hygropause (saturation level), where it becomes involved in active meridional transport.

2.2. Aerosol

Bimodal aerosol distribution in the atmosphere of Mars has been determined and characterized. A small fraction of the Martian dust has been suspected since long time, explaining well the UV and visible measurements from orbiters and

astronomy observations. In turn they are basically incompatible with surface observations. Solar occultation observed by SPICAM/Mars Express simultaneously in 200–300 nm and 1–1.7 μm ranges allowed to detect the bimodal distribution unambiguously. The particle radii are 0.04–0.07 μm for the small mode and 0.7–0.8 μm for the large mode. This is the first direct evidence of presence of two different particle modes in the atmosphere of Mars [Fedora et al., 2014]. This study has employed a numerical model of aerosol microphysics [Burlakov and Rodin, 2012].

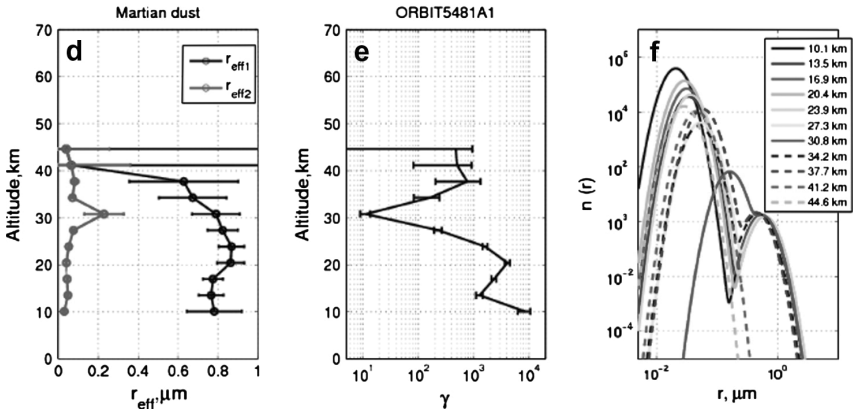


Fig 1. Bimodal distribution of Martian dust. A typical evolution with the altitude from solar occultation by SPICAM/Mars Express [Fedorova et al., 2014]

2.3. Dayglow and Nightglow

Dayglow and Nightglow of $\text{O}_2(a^1\Delta_g)$ at 1.27 μm was studied using ground-based astronomy and spacecraft observations.

The Mars $\text{O}_2(a^1\Delta_g)$ nightglow has been predicted long ago, but first detected in polar regions of Mars by OMEGA/Mars Express. The oxygen atoms are formed at the dayside, transported to the nightside by meridional Hadley circulation, and recombine at 50–60 km. The nightglow has been also observed by SPICAM/Mars Express in 2010. Seven profiles were retrieved in the Southern polar region. The profiles peak at 42–50 km, and their line intensity is 0.24–0.45 MR. After the discovery the corresponding OMEGA channel stopped working, while SPICAM has acquired a large number of observations, awaiting analysis [Fedorova et al., 2012]. An attempt to detect the nightglow from ground-based observations has resulted in upper limit of 40 kern A prolonged ground-based

monitoring of the O₂ dayglow during three Mars years allowed to detect interannual variations in the season of L_S ≈ 15, 65, и 110°. The variations of ~20% are detected during Northern spring and summer [Krasnopolsky 2013].

O₂(a¹Δ_g) dayglow and its connection to water distribution was studied using limb observations by SPICAM/Mars Express [Guslyakova et al. 2014]. Gravity waves were detected in the O₂ 1.27-μm patterns and compared to meteorological model. The most likely reason is the surface topography [Altieri et al., 2012].

Also, variations of temperature and CO mixing ratio at 50 km were studied from ground-based observations of the CO dayglow at 4.7 μm on Mars [Krasnopolsky 2014].

2.4. Other Minor Constituents

A search for methane and other minor constituents was performed in ground-based observations performed with CSHELL spectrometer at NASA IRTF in 2006 and 2009. The 2006 data (L_S = 10°) revealed ~10 ppb of methane in the latitude range 45°S ... 7°N (Mariners Vallis), and ~3 ppb elsewhere. In 2009 the upper limit for methane was 8 ppb. The results are consistent with detections by Mumma et al. [2009] in 2006, and are smaller than PFS/Mars Express mapping. The search for ethane in the 2977 cm⁻¹ band resulted in an upper limit of 0.2 ppb. This new upper limit does not contribute to solving the problem of methane origin on Mars. A repeated analysis of TEXES data to search for SO₂ has confirmed the previous upper limit of 0.3 ppb. The very low limit on SO₂ suggests the volcanic source of methane on Mars is insignificant given the similarity of volcanic degassing on terrestrial planets [Krasnopolsky, 2012].

3. Venus

3.1. Composition of the Atmosphere

Ozone was detected in the Venus atmosphere by SPICAV/Venus Express. Occultations of stars at the night side of the planet allowed detection of ozone in the Hartley band at 260 nm by UV spectrometer SPICAV. The ozone layer is located at ~100 km. Retrieved vertical profiles show volume concentrations of 10⁷–10⁸ molec.cm⁻³. The ozone content is consistent with photochemical model predictions, and with recent detection of OH by VIRTIS/Venus Express, which can be formed as O₃+H → O₂+OH*. The spatial distribution of ozone revealed no significant features but the absence of ozone in the antisolar point. The same is observed for OH, that suggests prevailing chemistry over dynamics in forming its distribution. A possible mechanism of ozone destruction in the antisolar point

is the reaction with chlorine radical $O_3 + Cl \rightarrow O_2 + ClO$. This suggests similarity with terrestrial atmosphere [Montmessin et al., 2011].

Dayside observations Venus by the high spectral resolution channel of VIR-TIS/Venus Express have been used to measure the altitude of the cloud tops and the water vapor abundance at this level. CO_2 and H_2O bands between 2.48 and 2.60 μm are analyzed to determine the cloud top altitude and water vapor abundance near this level. At low latitudes ($\pm 40^\circ$) the mean water vapor abundance is 3 ± 1 ppm and the cloud top altitude is 69.5 ± 2 km. Poleward from middle latitudes the cloud top altitude gradually decreases down to 64 km, while the average H_2O abundance reaches its maximum of 5 ppm at 80° of latitude with a large scatter from 1 to 15 ppm. The calculated mass percentage of the sulfuric acid solution in cloud droplets of mode 2 ($\sim 1 \mu m$) particles is in the range 75–83%. No systematic correlation of the dark UV markings with the cloud top altitude or water vapor has been observed [Cottini et al., 2012].

Sulfur dioxide is a million times more abundant in the atmosphere of Venus than that of Earth, possibly as a result of volcanism on Venus within the past billion years. A tenfold decrease in sulfur dioxide column density above Venus's clouds measured by the Pioneer Venus spacecraft during the 1970s and 1980s has been interpreted as decline following an episode of volcanogenic upwelling from the lower atmosphere. Using the data of SPICAV/Venus Express the sulfur dioxide column density above Venus's clouds is found to decrease by an order of magnitude between 2007 and 2012. This decline is similar to observations during the 1980s (Fig 2). A strong latitudinal and temporal variability in sulfur dioxide column density is observed that is consistent with supply fluctuations from the lower atmosphere. Episodic sulfur dioxide injections to the cloud tops may be caused either by periods of increased buoyancy of volcanic plumes, or, in the absence of active volcanism, by long-period oscillations of the general atmospheric circulation. The 30-year observational record from Pioneer Venus and Venus Express confirms that episodic injections of sulfur dioxide above the clouds recur on decadal timescales, suggesting a more variable atmosphere than expected [Marcq et al., 2011; 2013].

New measurements of sulfur dioxide (SO_2) and monoxide (SO) in the atmosphere of Venus by SPICAV/SOIR instrument onboard Venus Express orbiter provide ample statistics to study the behavior of these gases above Venus' clouds. Improved calibration of SOIR has been applied [Vandael et al., 2013]. Vertical profiles result from solar occultations in the absorption ranges of SO_2 (190–230 nm, and at 4 μm) and SO (190–230 nm). The dioxide is detected by the SOIR spectrometer at the altitudes of 65–80 km in the IR and by the SPICAV spectrometer at 85–105 km in the UV. The monoxide's absorption was measured only by SPICAV at 85–105 km. We analyzed 39 sessions of solar occultation, where boresights of both spectrometers are oriented identically, to provide complete

vertical profiling of SO_2 of the Venus' mesosphere (65–105 km). Two distinct SO_2 layers are detected. In the lower layer SO_2 mixing ratio is within 0.02–0.5 ppmv. The upper layer is also conceivable from microwave measurements [Belyaev et al., 2012].

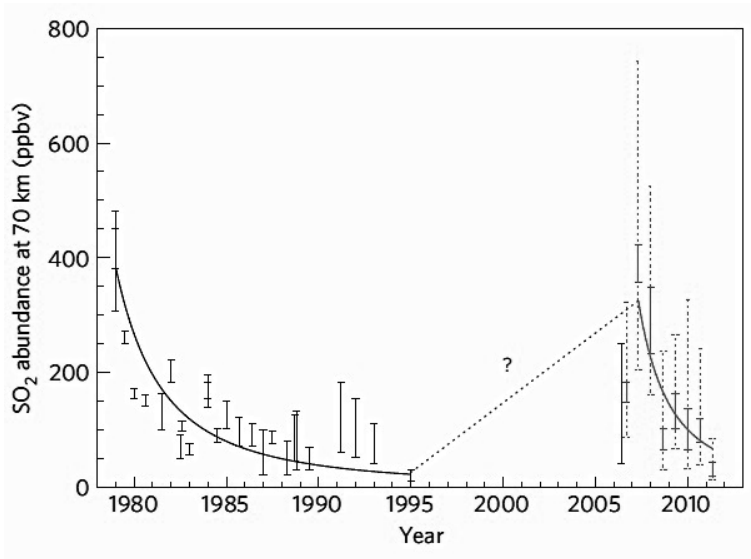


Fig. 2 More than thirty years of SO_2 measurements at Venus's cloudtop. Black stands for Pioneer Venus and other previously published measurements. Red stands for the 8-month moving average of SPICAV/Venus Express retrievals [Marcq et al., 2013]

Ground-based observations of the D/H ratios in H_2O , HCl , and HF on Venus has been carried out using the CSHELL spectrograph at NASA IRTF. The retrieved D/H ratios are: $(\text{D}/\text{H})\text{HF}$ is 420 ± 200 times that in the Standard Mean Ocean Water (SMOW); $(\text{D}/\text{H})\text{H}_2\text{O} = 95 \pm 15$ times SMOW; $(\text{D}/\text{H})\text{HCl} = 190 \pm 50$ times SMOW [Krasnopolsky et al., 2013].

Observations of the 1.10- and 1.18- μm nightside windows by the SPICAV-IR instrument aboard Venus Express [Korablev et al., 2012] were analyzed to characterize the various sources of gaseous opacity and determine the H_2O mole fraction in the lower atmosphere of Venus. Different approximations of line profile models are analyzed and an empirical lineshape is suggested. An additional continuum opacity is required to reproduce the variation of the 1.10- and 1.18- μm radiances with surface elevation as observed by the VIRTIS-M/Venus Express. Also different CO_2 and H_2O line lists are compared; a lack in CDSD

database, which provide significant opacity in Venus' deep atmosphere, is found. A composite line list that best reproduces the observations is suggested. It is shown that HDO brings significant absorption at 1140–1190 nm. The retrieved a water vapor mole fraction at 5–25 km is 30–5+10 ppmv. Combined with previous measurements in the 1.74- and 2.3- μm windows, this result provides strong evidence for a uniform H_2O profile below 40 km, in agreement with chemical models [Bezard et al., 2012].

3.2. Modeling of Atmospheric Chemistry

A photochemical model of the nighside Venus atmosphere was modified to account for the recent detection of ozone by SPICAV/Venus Express. The model includes more details regarding spectroscopy and chemistry of OH. The computed chlorine species, Cl_2 , ClO and ClNO_3 at 80–90 km is above 1 ppb, and the possibility of their detection is discussed. The modeled layer of ozone is consistent with SPICAV observations. Ignoring chlorine chemistry allows to reproduce the altitude and the density in the O_3 peak, but results in unrealistic content of ozone of $4 \times 10^8 \text{ cm}^{-3}$ at 80 km [Krasnopolsky 2013].

To explain the pronounced difference between Venus Express and ground-based microwave observations, a photochemical model of Venus atmosphere covering the attitude range of 47–112 km was updated. The H_2O profile is computed by the model. The main feature of the Venus photochemistry is the forming of H_2SO_4 in a narrow layer near the upper cloud deck leading to a significant decrease of SO_2 and H_2O content above the clouds. The SO_2 and H_2O transport through the bottleneck determines the chemical composition above clouds and its variations. It is shown that the observed variability of the composition of the mesosphere can be explained by small changes in atmospheric dynamics around the cloud layer, and does not require any volcanic activity [Krasnopolsky 2012]. A chemical-kinetic model of the Venus lower atmosphere has been modified to include the S_4 cycle, and other improvements to be consistent with recent mesosphere [Krasnopolsky 2012] model. The lower atmosphere chemistry is mainly driven by sulfur, but also involves chlorine compounds [Krasnopolsky 2013].

Venus Express measurements of the vertical profiles of SO and SO_2 in the middle atmosphere of Venus provide an opportunity to revisit the sulfur chemistry above the middle cloud tops (~ 58 km). A 1-D photochemistry-diffusion model was used to simulate the behavior of the whole chemical system including oxygen-, hydrogen-, chlorine-, sulfur-, and nitrogen-bearing species. A sulfur source is required to explain the SO_2 inversion layer above 80 km. The evaporation of the aerosols composed of sulfuric acid or polysulfur above 90 km could provide the sulfur source [Zhang et al., 2012].

3.3. Emissions

The CO dayglow at 4.7 μm on Venus has been observed using the long-slit high-resolution spectrograph CSHELL at NASA IRTF with a resolving power of 4×10^4 . The CO (1–0) dayglow is optically thick, its intensity weakly depends on the CO abundance and it proves poorly accessible for diagnostics of the Venus atmosphere. Six observed lines of the CO dayglow at the hot (2–1) band show a significant limb brightening typical of an optically thin airglow. Vertical intensities of the CO (2–1) band corrected for viewing angle and the Venus reflection are constant at 3.3 MR in the latitude range of $\pm 50^\circ$ at a solar zenith angle of 64° . Rotational temperatures of the CO (2–1) dayglow should reflect ambient temperature near 111 km. The observed temperatures are slightly higher on the south with a mean value of 203 K [Krasnopolsky, 2014].

The EUV spatially-resolved dayglow spectra obtained at 0.37 nm resolution by the UVIS instrument during the Cassini flyby of in 1999 are analyzed. Emissions from OI, OII, NI, Cl and CII and CO have been identified and their disc average intensity has been determined. The O, N(2) and CO densities are compared to the empirical VTS3 model [Gerard et al., 2011].

A model of the $\text{O}_2(a^1\Delta_g)$ nightglow limb profiles perturbed by the action of gravity waves propagating in the Venus' upper atmosphere is considered. The observational data are from VIRTIS/Venus Express. A high variability observed in the shape of the nightglow limb profiles between 80 and 120 km, often characterized by the presence of a double peak, suggests the occurrence of the gravity waves. A well-known theory used to study terrestrial density fluctuations induced by propagation of gravity waves is used. The retrieved vertical wavelengths and amplitudes of the waves at ~ 100 km are 7–16 km and 3–14% respectively. Temperature fluctuations exceed 40% at higher altitudes (115–120 km) thus inducing either wave breaking or dissipation. Intrinsic horizontal phase velocities are expected to vary between 32 and 85 m s^{-1} [Altieri et al., 2014].

3.3. Clouds

A glory has been observed recently by Venus Express orbiter. Glory is an optical phenomenon that poses stringent constraints on the cloud properties. It is possible to constrain two properties of the particles at the cloud tops (about 70 km altitude) which are responsible for a large fraction of the solar energy absorbed by Venus: A very accurate estimate of the cloud particles size of 1.2 μm with a very narrow size distribution, and the refractive index higher than that of sulfuric acid previously proposed for the clouds composition. Assuming that the species contributing to the increase of the refractive index is the same as the

unknown UV absorber, it is possible to constrain the list of candidates: Either small ferric chloride (FeCl_3) cores inside sulfuric acid particles or elemental sulfur coating their surface. Both species have been suggested in the past as candidates for the as yet unknown UV absorber [Markiewicz et al., 2014].

Since the discovery of ultraviolet markings on Venus, their observations have been a powerful tool to study the morphology, motions and dynamical state at the cloud top level. The cloud top morphology has been monitored by the Venus Monitoring Camera (VMC) on Venus Express mission. The camera acquires images in four narrow-band filters centered at 365, 513, 965 and 1010 nm with spatial resolution from 50 km at apocentre to a few hundred of meters at pericentre. The VMC experiment provides a significant improvement in the Venus imaging as compared to the capabilities of the earlier missions. The VMC observations revealed multiple morphology structures and provides an unprecedented dataset [Titov et al., 2012].

The cloud top structure on Venus was studied by joint analysis of the data from VIRTIS and the atmospheric temperature sounding by the Radio Science experiment (VeRa) onboard Venus Express. The cloud top altitude and aerosol scale height are derived by fitting VIRTIS spectra at 4–5 μm with temperature profiles taken from the VeRa radio occultation. A gradual descent of the cloud top from 67.2 ± 1.9 km in low latitudes to 62.8 ± 4.1 km at the pole and decrease of the aerosol scale height from 3.8 ± 1.6 km to 1.7 ± 2.4 km is observed. These changes correlate with the mesospheric temperature field. In the cold collar and high latitudes the cloud top position remarkably coincides with the sharp minima in temperature inversions suggesting importance of radiative cooling in their maintenance. This behavior is consistent with the earlier observations. Spectral trend of the cloud top altitude derived from a comparison with the earlier observations in 1.6–27 μm wavelength range is qualitatively consistent with sulfuric acid composition of the upper cloud and suggests that particle size increases from equator to the pole [Lee et al., 2012].

3.4. Structure and Dynamics

Six years of continuous monitoring of Venus by European Space Agency's Venus Express orbiter provides an opportunity to study dynamics of the atmosphere our neighbor planet. Venus Monitoring Camera (VMC) on-board the orbiter has acquired the longest and the most complete so far set of Venus UV images. These images enable a study the cloud level circulation by tracking motion of the cloud features. Total number of wind vectors derived is 45,600 for the manual tracking and 391,600 for the digital method. This allowed to determine the mean circulation, its long-term and diurnal trends, orbit-to-orbit

variations and periodicities. In low latitudes the mean zonal wind at cloud tops (67 ± 2 km) is about 90 m/s with a maximum of about 100 m/s at 40–50°S. Poleward of 50°S the average zonal wind speed decreases with latitude. The corresponding atmospheric rotation period at cloud tops has a maximum of about 5 days at equator, decreases to approximately 3 days in middle latitudes and stays almost constant poleward from 50°S [Khatuntsev et al., 2013].

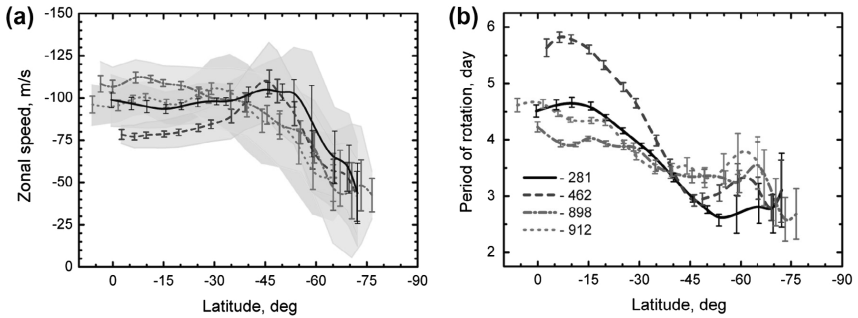


Fig. 3 Latitudinal profiles of zonal wind (a) and corresponding rotation periods (b) determined by cloud tracking for several individual orbits [Khatuntsev et al., 2013]

The dynamics of Venus' mesosphere (60–100 km altitude) was investigated using data acquired by the radio-occultation experiment VeRa on board Venus Express. VeRa provides vertical profiles of density, temperature and pressure between 40 and 90 km of altitude with a vertical resolution of few hundred meters of both the Northern and Southern hemisphere. Pressure and temperature vertical profiles were used to derive zonal winds, the cyclostrophic balance, which applies well on slowly rotating planets with fast zonal winds, like Venus and Titan. The main features of the retrieved winds are a midlatitude jet with a maximum speed up to 140 ± 15 m s⁻¹ which extends between 20°S and 50°S latitude at 70 km altitude and a decrease of wind speed with increasing height above the jet. Cyclostrophic winds show satisfactory agreement with the cloud-tracked winds derived from the VMC/ Venus Express UV images, although a disagreement is observed at the equator and near the pole due to the breakdown of the cyclostrophic approximation [Piccailli et al., 2012].

The average fields of the Venus atmosphere are derived from the nighttime observations in the 1960–2350 cm⁻¹ spectral range by VIRTIS-M/Venus Express. These fields include: (a) the air temperatures in the 1–100 mbar pressure range (~85–65 km above the surface), (b) the altitude of the clouds top, and (c) the average CO mixing ratio. At the lowest altitudes probed by VIRTIS (~65 km),

air temperatures are strongly asymmetric around midnight, with a pronounced minima at 3LT, 70°S. Moving to higher levels, the air temperatures first become more uniform in local time (~75 km), then display a colder region on the evening side at the upper boundary of VIRTIS sensitivity range (~80 km). The cloud effective altitude increases monotonically from the South Pole to the equator. However, the variations observed in night data are consistent with an overall variation of just 1 km, much smaller than the 4 km reported for the dayside. The cloud altitudes appear slightly higher on the evening side. Both observations are consistent with a less vigorous meridional circulation on the nightside of the planet. Carbon monoxide is not strongly constrained by the VIRTIS-M data. However, average fields present a clear maximum of 80 ppm around 60°S, well above the retrieval uncertainty [Grassi et al., 2014].

The mechanisms of the global circulation in the atmosphere of Venus have been studied with the use of numerical models. To calculate the heating/cooling of the atmosphere due to absorption/emission of electromagnetic radiation under initially weak and strong superrotation of the atmosphere, the complete system of gas dynamics equations in the relaxation approximation was considered. Heating parameters, at which the modeled zonal superrotation velocity turned out to be close to the observed one, have been found. High mountains on Venus induce a substantial increase of the vertical component of the wind speed and noticeably influence the global distribution of the horizontal wind at above 80 km, while its effect below 60 km is weak. [Mingalev et al., 2012, 2015].

Large-scale and small scale turbulence in the atmosphere of Venus is studied theoretically and using the experimental data including those acquired with the Venus Express spacecraft. The atmospheres of the Earth and Venus are compared, allowing to conclude that there is a inverse spectral flux of energy in the atmosphere of Venus, as in the terrestrial atmosphere, which participates in generating the superrotation of the atmosphere [Izakov, 2012, 2013].

4. Outer Planets and Their Satellites

Far ultraviolet spectral observations have been made with the Hubble Space Telescope in the time-tag mode with the Space Telescope Imaging Spectrograph (STIS) long slit allowing to build up the first spectral maps of the FUV Jovian aurora. The results are confirmed with modeling [Gerard et al., 2014].

Observational data on hydrocarbons, nitriles, and ions on Titan are compared with predictions of the photochemical model. Uncertainties of the observed abundances and differences between the data from different instruments and observing teams are comparable with the differences between the observations and the model results. Formation of haze by polymerization of hydrocarbons and nitriles and recombination of heavy ions is calculated along with condensation

of various species near the tropopause. Overall deposition forms a layer of 300 m thick for the age of the Solar System, and nitrogen constitutes 8% of the deposition. The model reproduces the basic observational data and adequately describes basic chemical processes in Titan's atmosphere and ionosphere [Krasnopolsky 2014]

5. Comparative studies of the atmospheres of planets and their satellites

5.1. Planetary boundary layer

Different aspects of planetary boundary layer described in the shallow-water approximation are studied in the frame of a finite-volume numerical method [Karelsky et al., 2012, 2013; Karelsky, Petrosyan, 2013; Chernyak et al., 2013].

A model for the density of vertical mass flux of dust in the convective atmospheric boundary layer as a function of the density of convective elements, including vortices, friction velocity, and vertical buoyancy is proposed. Two methods for experimentally determining the density of convecting elements are discussed, optical, as observations by Mars Exploration Rover (MER) camera in Gusev crater on Mars [Kurgansky 2012], and using a number of detecting stations placed perpendicular to the dominating wind vector. The results are validated using field observations [Kurgansky 2014].

Observations of fine mineral dust aerosol (0.15–15 μm) were carried out in Kalmykia in 2007, 2009, and 2010 under conditions of weak wind and strong heating of the surface, in the absence of saltation processes. These results show that the fine mineral dust aerosol (0.15–0.5 μm) contributes considerably to the total aerosol content. The problem of stationary convective flows over a nonuniformly heated wavy surface is studied in the context of a simplified analytical model. It is shown that the horizontally periodic heating of such a surface can lead to a “thermal wind” effect, i.e., the generation of a uniform horizontal flow far from the surface. Estimations for Mars conditions are suggested [Chkhetiani et al., 2012, 2013].

A review on the boundary layer of Mars is published [Petrosyan et al., 2011].

5.2. Outer Atmospheres and Escape

The processes of kinetics and transport of hot oxygen and hydrogen atoms in the transition (from the thermosphere to the exosphere) region of the upper Martian atmosphere are studied. It is shown that the exosphere is populated with a significant number of suprathermal oxygen atoms with kinetic energies ranging

up to the escape energy of 2 eV, i.e., the hot oxygen Martian corona is formed [Gröllner et al. 2012; Krauss et al., 2012]. The transfer of energy from hot oxygen atoms to thermal hydrogen atoms creates an additional nonthermal flux of atomic hydrogen escaping from the Martian atmosphere [Shematovich 2013].

The escape of hot O and C atoms from the present Martian atmosphere during low and high solar activity conditions has been studied with a Monte-Carlo model. The results yield a total loss rate of hot oxygen of $2.3\text{--}2.9 \times 10^{25} \text{ s}^{-1}$. The total loss rates of carbon are found to be 0.8 and $3.2 \times 10^{24} \text{ s}^{-1}$ for low and high solar activity, respectively. Depending on solar activity, the obtained carbon loss rates are up to ~ 40 times higher than the CO_2^+ ion loss rate inferred from ASPERA-3/Mars Express observations. Finally, collisional effects above the exobase reduce the escape rates by about 20–30% with respect to a collisionless exosphere [Gröllner et al. 2014].

The effect of the weak magnetic field on the escape processes from Mars and Venus is considered. The solar wind helium may be a significant source of neutral helium in the Martian atmosphere. The precipitating particles also transfer mass, energy, and momentum. To investigate the transport of He^{2+} in the upper atmosphere of Mars, the direct simulation Monte Carlo method to solve the kinetic equation was applied. The calculated upward fluxes of He, He^+ , and He^{2+} fluxes are compared to ASPERA-3/Mars Express measurements. If the induced magnetic field is ignored the precipitating He^{2+} ions are not backscattered by the Martian upper atmosphere. An assumed 20 nT horizontal magnetic field, a typical field measured by Mars Global Surveyor results in 30%–40% of the energy flux being backscattered. The induced magnetic field plays therefore a crucial role in the transport of charged particles in the upper atmosphere of Mars and determines the energy deposition of the solar wind [Shematovich et al., 2013].

Isolated events of proton and alpha particle precipitation in the Venusian atmosphere were recorded with the use of the ASPERA-4/Venus Express spacecraft. Using a Monte Carlo simulation method for calculation of proton and alpha particle precipitations in the Venusian atmosphere, reflected and upward particle fluxes have been found. Only a vanishing fraction of protons and alpha particles are backscattered to the Venusian exosphere when neglecting the induced magnetic field and under conditions of low solar activity. Accounting for the induced field drastically changes the situation: the backscattered by the atmosphere energy fluxes increase up to 44% for the horizontal magnetic field $B = 20 \text{ nT}$, measured for Venus, for the case of precipitating protons, and up to 64%, for alpha particles. The reflected energy fluxes increase to about 100% for both protons and alpha particles as the field grows to 40 nT, i.e., the atmosphere is protected against penetration of solar wind particles [Shematovich et al., 2014].

A number of other studies dedicated to dissipation of planetary atmospheres, including in-depth consideration of hydrodynamic escape were conducted

[Lammer et al., 2011, 2012ab; Erkaev et al., 2013, 2014, 2015; Kislyakova et al., 2013; Schaufelberger et al., 2012; Shematovich et al., 2014]

5.3. Other Issues on Comparative Studies

Actual state and perspectives of the observations of the planetary atmospheres in the ultraviolet range of wavelengths are discussed. The following hot problems of the planetary astronomy in the UV wavelength range are formulated: (i) UV observations of hot coronas of the terrestrial planets; (ii) formation and morphology of the rarefied H_2O^- , O^{2-} and O-dominant atmospheres of the icy satellites in the giant planet systems; formation and evolution of the neutral gas clouds in the giant planet systems; (iii) studies of the extended hydrogen coronae of the transit-exoplanets formed due to the stellar UV and plasma wind forcing. The mathematical models such as the Monte Carlo model for the electron, proton, and heavy-ion precipitation into the planetary atmospheres were also discussed. Such models are currently used to calculate the excitation rates of the atmospheric UV emissions and will be used for the interpretation of the expected UV observations of the planetary atmospheres with the space observatory World Space Observatory-Ultraviolet (WSO-UV) [Shematovich 2011].

Imaging spectrometers are highly effective instruments for investigation of planetary atmospheres. They deliver the information on both the compositional and the spatial distribution, allowing simultaneous study of chemistry and dynamics in the atmospheres of Venus and Mars. Recent results about the $\text{O}_2(\text{a}^1 \text{---} \text{X}^3\Sigma_g^-)$ night and day glows, obtained by VIRTIS/Venus Express and OMEGA/Mars Express respectively, the imaging spectrometers currently in orbit around Venus and Mars [Migliorini et al., 2011].

6. Methods and Instruments

A number of investigation related to CO_2 atmospheres were conducted. A new version of the CO_2 spectral line database CDS-2013 is created [Tashkun, Perevalov, 2011, 2013]. Experimental and theoretical studies of high-resolution CO_2 spectrum in the ranges of 1.18, 1.10 and 0.87 μm , used for modeling of Mars and Venus spectra is conducted. CDS parameters are updated [Petrova et al., 2013]. New isotopologue line lists of HD^{18}O , HD^{17}O and HD^{16}O in the wavenumber range 5600–12600 cm^{-1} for Venus atmosphere studies are compiled [Lavrentieva and Voronin 2013; Lavrentieva et al., 2014, 2015]. The parameters of methane lines broadening by CO_2 in the range of 5550–6140 cm^{-1} are measured [Lyulin et al., 2014]. The analysis and identification of new isotopologue

CO₂ bands detected in the Venus atmosphere by SOIR/Venus Express is conducted [Robert et al., 2013].

The modeling of high-resolution spectra of methane isotopologues ¹²CH₃D (at 900–5000 cm⁻¹) and measurements of ¹²CH₄ (at 4800–5300 cm⁻¹) is performed [Nikitin et al., 2014]. Line broadening of ro-vibrational lines of CH₃CN by N₂, and with self-broadening and their temperature dependence is investigated [Dudaryonok et al., 2015 ab].

The kinetics of electron-excited oxygen and CO molecules in the atmospheres of Venus and Mars is studied [Kirillov, 2013, 2014 ab].

The update of the principal spectroscopic databases, HITRAN and GEISA has been conducted with participation of Russian scientists [Rothman et al., 2014; Jacquinet-Husson et al., 2011].

A method to study the internal gravity waves using the vertical profiles of temperature, density or the square of buoyancy in the atmosphere of a planet is suggested. The method is validated using radiozonde measurements in the terrestrial stratosphere. The method allows to identify “discrete” (narrow-spectrum) wave events in the atmospheres of the Earth, Venus and Mars and to determine the characteristics of the internal gravity waves [Gubenko et al., 2011, 2015].

The so-called shadow method used to estimate the optical depth of the Martian atmosphere and the albedo of the surface from the differences in brightness between shadowed and sunlit regions observed from an orbiter is described and evaluated. The method is validated using high-resolution HiRISE/MRO images, and optical depth measured by the Opportunity rover [Hoekzema et al., 2011; Petrova et al., 2012].

The atmospheric chemistry suite (ACS) package for sensitive measurements of minor atmospheric gases, and the monitoring of the atmospheric thermal state is a part of the Russian contribution to the ExoMars ESA-Roscosmos mission. ACS consists of three separate infrared spectrometers. The near-infrared (NIR) channel is a versatile spectrometer for the spectral range of 0.7–1.6 μm with a resolving power of ~20,000. The instrument employs the principle of an echelle spectrometer with an AOTF as a preselector. NIR will be operated in nadir, in solar occultations, and possibly on the limb. Scientific targets of NIR on Mars are the measurements of water vapor, aerosols, and dayside or nightside airglows. The mid-infrared (MIR) channel is a cross-dispersion echelle instrument dedicated to solar occultation measurements in the range of 2.2–4.4 μm targeting the resolving power of 50,000. MIR is dedicated to sensitive measurements of trace gases, in particular methane. The thermal infrared channel (TIRVIM) is a 2-inch double pendulum Fourier-transform spectrometer for the spectral range of 1.7–17 μm with apodized resolution varying from 0.2 to 1.6 cm⁻¹. TIRVIM is primarily dedicated to the monitoring of atmospheric temperatures and aerosol states in nadir [Korablev et al., 2014]. The instrument inherits design solution of

previously developed instruments for Phobos-Grunt mission [Korablev et al., 2012, 2013].

7. Conclusion

As previously, many of the research on planetary atmospheres completed in 2011–2014 are related to Venus Express and Mars Express missions. Mars Express will continue its operations, as planned at present, until 2018. In the meanwhile, the launch of the national planetary project Phobos Grunt in 2011 turned a complete disaster. A new mission with planned serious atmosphere, climate and meteorology studies, and with a key Russian involvement is ExoMars. ExoMars consists of two launches, the 2016 with Trace Gas Orbiter, and the entry and descent demonstrator, and the 2018 with a Rover, and a stationary long-living science platform. All proposals for a Venus mission, national, or with Russian involvement [Vorontsov et al., 2011; Wilson et al, 2012] are not being implemented so far. The lack of national space programs have not prevented from consolidation of efforts in the field of planetary atmospheres in Russia. The number of publications is growing, and the studies become more synergetic. The planetary astronomy, almost forgotten is coming back.

Many studies included in the current Report were supported by the Programme No22 of the Presidium of Russian Academy of Sciences and the Grant of the Russian Government No11.G34.31.0074. The author is grateful to Svetlana Gulyakova for the help in preparation of the Report.

References

1. Altieri, F., Migliorini, A., Zasova, L., Shakun, A., Piccioni, G., Bellucci, G., 2014. Modeling VIRTIS/VEX O₂(a₁Δg) nightglow profiles affected by the propagation of gravity waves in the Venus upper mesosphere. *Journal of Geophysical Research (Planets)* 119, 2300–2316.
2. Altieri, F., Spiga, A., Zasova, L., Bellucci, G., Bibring, J.-P., 2012. Gravity waves mapped by the OMEGA/MEX instrument through O₂ dayglow at 1.27 μm: Data analysis and atmospheric modeling. *Journal of Geophysical Research (Planets)* 117, CiteID E00J08.
3. Belyaev, D., Montmessin, F., Bertaux, J., Mahieux, A., Fedorova, A., Korablev, O., Marcq, E., Yung, Y., Zhang, X., 2012. Vertical profiling of SO₂ and SO above Venus' clouds by SPICAV/SOIR solar occultations. *Icarus* 217, 740–751.
4. Bézard, B., Fedorova, A., Bertaux, J.-L., Rodin, A., Korablev, O., 2011. The 1.10- and 1.18-μm nightside windows of Venus observed by SPICAV-IR aboard Venus Express. *Icarus* 216, 173–183.

5. Burlakov, A. V., Rodin, A. V., 2012. A one-dimensional numerical model of H₂O cloud formation in the Martian atmosphere. *Solar System Research* 46, 18–30.
6. Chernyak, A. V., Karelsky, K. V., Petrosyan, A. S., 2013. Simple waves and the Riemann problem in compressible shallow water flows. *Physica Scripta Volume T 155*, 4041.
7. Chkhetiani, O. G., Gledzer, E. B., Artamonova, M. S., Iordanskii, M. A., 2012. Dust resuspension under weak wind conditions: direct observations and model. *Atmospheric Chemistry & Physics* 12, 5147–5162.
8. Chkhetiani, O. G., Kalashnik, M. V., Ingel', L. K., 2013. Generation of thermal wind over a nonuniformly heated wavy surface. *Izvestiya Atmospheric and Oceanic Physics* 49, 121–127.
9. Cottini, V., Ignatiev, N. I., Piccioni, G., Drossart, P., Grassi, D., Markiewicz, W. J., 2012. Water vapor near the cloud tops of Venus from Venus Express/VIRTIS day-side data. *Icarus* 217, 561–569.
10. Dudaryonok, A. S., Lavrentieva, N. N., Buldyreva, J. V., 2015. CH₃CN self-broadening coefficients and their temperature dependences for the Earth and Titan atmospheres. *Icarus* 250, 76–82.
11. Dudaryonok, A. S., Lavrentieva, N. N., Buldyreva, J. V., 2015. N₂-broadening coefficients of CH₃CN rovibrational lines and their temperature dependence for the Earth and Titan atmospheres. *Icarus* 256, 30–36.
12. Erkaev, N. V., Lammer, H., Elkins-Tanton, L. T., Stökl, A., Odert, P., Marcq, E., Dorfi, E. A., Kislyakova, K. G., Kulikov, Y. N., Leitzinger, M., Güdel, M., 2014. Escape of the martian protoatmosphere and initial water inventory. *Planetary and Space Science* 98, 106–119.
13. Erkaev, N. V., Lammer, H., Odert, P., Kulikov, Y. N., Kislyakova, K. G., 2015. Extreme hydrodynamic atmospheric loss near the critical thermal escape regime. *Monthly Notices of the Royal Astronomical Society* 448, 1916–1921.
14. Erkaev, N. V., Lammer, H., Odert, P., Kulikov, Y. N., Kislyakova, K. G., Khodachenko, M. L., Güdel, M., Hanslmeier, A., Biernat, H., 2013. XUV-Exposed, Non-Hydrostatic Hydrogen-Rich Upper Atmospheres of Terrestrial Planets. Part I: Atmospheric Expansion and Thermal Escape. *Astrobiology* 13, 1011–1029.
15. Fedorova, A. A., Lefèvre, F., Guslyakova, S., Korablev, O., Bertaux, J. L., Montmessin, F., Reberac, A., Gondet, B., 2012. The O₂ nightglow in the martian atmosphere by SPICAM onboard of Mars-Express. *Icarus* 219, 596–608.
16. Fedorova, A. A., Montmessin, F., Rodin, A. V., Korablev, O. I., Määttänen, A., Maltagliati, L., Bertaux, J. L., 2014. Evidence for a bimodal size distribution for the suspended aerosol particles on Mars. *Icarus* 231, 239–260.
17. Gérard, J.-C., Bonfond, B., Grodent, D., Radioti, A., Clarke, J. T., Gladstone, G. R., Waite, J. H., Bisikalo, D., Shematovich, V. I., 2014. Mapping the electron energy in Jupiter's aurora: Hubble spectral observations. *Journal of Geophysical Research (Space Physics)* 119, 9072–9088.
18. Gerard, J. C., Hubert, B., Gustin, J., Shematovich, V. I., Bisikalo, D., Gladstone, G. R., Esposito, L. W., 2011. EUV spectroscopy of the Venus dayglow with UVIS on Cassini. *Icarus* 211, 70–80.

19. Grassi, D., Politi, R., Ignatiev, N.I., Plainaki, C., Lebonnois, S., Wolkenberg, P., Montabone, L., Migliorini, A., Piccioni, G., Drossart, P., 2014. The Venus nighttime atmosphere as observed by the VIRTIS-M instrument. Average fields from the complete infrared data set. *Journal of Geophysical Research (Planets)* 119, 837–849.
20. Groller, H., Lammer, H., Lichtenegger, H.I.M., Pflieger, M., Dutuit, O., Shematovich, V.I., Kulikov, Y.N., Biernat, H.K., 2012. Hot oxygen atoms in the Venus night-side exosphere. *Geophysical Research Letters* 39.
21. Gröller, H., Lichtenegger, H., Lammer, H., Shematovich, V.I., 2014. Hot oxygen and carbon escape from the martian atmosphere. *Planetary and Space Science* 98, 93–105.
22. Gubenko, V.N., Kirillovich, I.A., Pavelyev, A.G., 2015. Characteristics of internal waves in the Martian atmosphere obtained on the basis of an analysis of vertical temperature profiles of the Mars Global Surveyor mission. *Cosmic Research* 53, 133–142.
23. Gubenko, V.N., Pavelyev, A.G., Salimzyanov, R.R., Pavelyev, A.A., 2011. Reconstruction of internal gravity wave parameters from radio occultation retrievals of vertical temperature profiles in the Earth's atmosphere. *Atmospheric Measurement Techniques* 4, 2153–2162.
24. Guslyakova, S., Fedorova, A.A., Lefèvre, F., Korablev, O.I., Montmessin, F., Bertaux, J.L., 2014. O₂(a¹Δ_g) dayglow limb observations on Mars by SPICAM IR on Mars-Express and connection to water vapor distribution. *Icarus* 239, 131–140.
25. Hoekzema, N.M., Garcia-Comas, M., Stenzel, O.J., Petrova, E.V., Thomas, N., Markiewicz, W.J., Gwinner, K., Keller, H.U., Delamere, W.A., 2011. Retrieving optical depth from shadows in orbiter images of Mars. *Icarus* 214, 447–461.
26. Izakov, M.N., 2012. On the small-scale turbulence parameters in the atmosphere of Venus and their use in the global circulation models. *Solar System Research* 46, 278–290.
27. Izakov, M.N., 2013. Large-scale quasi-two-dimensional turbulence and a inverse spectral flux of energy in the atmosphere of Venus. *Solar System Research* 47, 170–181.
28. Jacquinet-Husson, N., Crepeau, L., Armante, R., Boutammine, C., Chédin, A., Scott, N.A., Crevoisier, C., Capelle, V., Boone, C., Poulet-Crovisier, N., Barbe, A., Campargue, A., Benner, D.C., Benilan, Y., Bézard, B., Boudon, V., Brown, L.R., Coudert, L.H., Coustenis, A., Dana, V., Devi, V.M., Fally, S., Fayt, A., Flaud, J.-M., Goldman, A., Herman, M., Harris, G.J., Jacquemart, D., Jolly, A., Kleiner, I., Kleinböhl, A., Kwabia-Tchana, F., Lavrentieva, N., Lacombe, N., Xu, L.-H., Lyulin, O.M., Mandin, J.-Y., Maki, A., Mikhailenko, S., Miller, C.E., Mishina, T., Moazzen-Ahmadi, N., Müller, H.S.P., Nikitin, A., Orphal, J., Perevalov, V., Perrin, A., Petkie, D.T., Predoi-Cross, A., Rinsland, C.P., Remedios, J.J., Rotger, M., Smith, M.A.H., Sung, K., Tashkun, S., Tennyson, J., Toth, R.A., Vandaele, A.-C., Vander Auwera, J., 2011. The 2009 edition of the GEISA spectroscopic database. *Journal of Quantitative Spectroscopy and Radiative Transfer* 112, 2395–2445.
29. Karel'skii, K.V., Petrosyan, A.S., Chernyak, A.V., 2013. Nonlinear theory of the compressible gas flows over a nonuniform boundary in the gravitational field in the shallow-water approximation. *Soviet Journal of Experimental and Theoretical Physics* 116, 680–697.

30. Karelsky, K. V., Petrosyan, A. S., 2013. The Riemann problem for shallow-water equations on a step: stationary solutions, the quasi-two-layer model and numerics. *Physica Scripta* Volume T 155, 4043.
31. Karelsky, K. V., Petrosyan, A. S., Chernyak, A. V., 2012. Nonlinear dynamics of flows of a heavy compressible gas in the shallow water approximation. *Soviet Journal of Experimental and Theoretical Physics* 114, 1058–1071.
32. Khatuntsev, I. V., Patsaeva, M. V., Titov, D. V., Ignatiev, N. I., Turin, A. V., Limaye, S. S., Markiewicz, W. J., Almeida, M., Roatsch, T., Moissl, R., 2013. Cloud level winds from the Venus Express Monitoring Camera imaging. *Icarus* 226, 140–158.
33. Kirillov, A. S., 2013. The calculations of quenching rate coefficients of O₂(b1g+, v) in collisions with O₂, N₂, CO, CO₂ molecules. *Chemical Physics* 410, 103–108.
34. Kirillov, A. S., 2014. Calculated vibrational populations of O₂ Herzberg states in the mixture of CO₂, CO, N₂, O₂ gases. *Chemical Physics Letters* 603, 89–94.
35. Kirillov, A. S., 2014. The calculation of quenching rate coefficients of O₂ Herzberg states in collisions with CO₂, CO, N₂, O₂ molecules. *Chemical Physics Letters* 592, 103–108.
36. Kislyakova, K. G., Lammer, H., Holmström, M., Panchenko, M., Odert, P., Erkaev, N. V., Leitzinger, M., Khodachenko, M. L., Kulikov, Y. N., Güdel, M., Hanslmeier, A., 2013. XUV-Exposed, Non-Hydrostatic Hydrogen-Rich Upper Atmospheres of Terrestrial Planets. Part II: Hydrogen Coronae and Ion Escape. *Astrobiology* 13, 1030–1048.
37. Korablev, O., Fedorova, A., Bertaux, J.-L., Stepanov, A. V., Kiselev, A., Kalinnikov, Y. K., Titov, A. Y., Montmessin, F., Dubois, J. P., Villard, E., Sarago, V., Belyaev, D., Reberac, A., Neefs, E., 2012. SPICAV IR acousto-optic spectrometer experiment on Venus Express. *Planetary and Space Science* 65, 38–57.
38. Korablev, O., Fedorova, A., Villard, E., Joly, L., Kiselev, A., Belyaev, D., Bertaux, J.-L., 2013. Characterization of the stray light in a space borne atmospheric AOTF spectrometer. *Optics Express* 21, 18354.
39. Korablev, O., Montmessin, F., Trokhimovsky, A., Fedorova, A. A., Kiselev, A. V., Bertaux, J.-L., Goultail, J.-P., Belyaev, D. A., Stepanov, A. V., Titov, A. Y., Kalinnikov, Y. K., 2013. Compact echelle spectrometer for occultation sounding of the Martian atmosphere: design and performance. *Applied Optics* 52, 1054–1065.
40. Korablev, O., Trokhimovsky, A., Grigoriev, A. V., Shakun, A., Ivanov, Y. S., Moshkin, B., Anufreychik, K., Timonin, D., Dziuban, I., Kalinnikov, Y. K., Montmessin, F., 2014. Three infrared spectrometers, an atmospheric chemistry suite for the ExoMars 2016 trace gas orbiter. *Journal of Applied Remote Sensing* 8, 4983.
41. Korablev, O., Zasova, L., Fedorova, A., Rodin, A., Ignatiev, N., Breus, T., Izakov, M., Maiorov, B., Krivolutsky, A., Petrova, E., Ivanov, A., Trokhimovskii, A., 2009. New in the physics of planetary atmosphere. *Izvestiya Atmospheric and Oceanic Physics* 45, 503–516.
42. Korablev, O. I., Grigor'ev, A. V., Moshkin, B. E., Zasova, L. V., Montmessin, F., Gvozdev, A. B., Shashkin, V. N., Patsaev, D. V., Makarov, V. S., Maksimenko, S. V., Ignatiev, N. I., Fedorova, A. A., Arnold, G., Shakun, A. V., Terentiev, A. I., Zharkov, A. V., Mayorov, B. S., Nikol'sky, Y. V., Khatuntsev, I. V., Bellucci, G., Giuranna, M., Kuz'min,

R. O., Rodin, A. V., 2012. AOST: Fourier spectrometer for studying Mars and Phobos. *Solar System Research* 46, 31–40.

43. Korablev, O. I., Zasova, L. V., Fedorova, A. A., Titov, D. V., Ignatiev, N. I., Rodin, A. V., Shematovich, V. I., Belyaev, D. A., Khatuntsev, I. V., Izakov, M. N., Shakun, A. V., Burlakov, A. V., Mayorov, B. S., 2012. Studies of the planetary atmospheres in Russia (2007–2010). *Izvestiya Atmospheric and Oceanic Physics* 48, 309–331.

44. Krasnopolsky, V., 2012. Search for methane and upper limits to ethane and SO₂ on Mars. *Icarus* 217, 144–152.

45. Krasnopolsky, V. A., 2012. A photochemical model for the Venus atmosphere at 47–112 km. *Icarus* 218, 230–246.

46. Krasnopolsky, V. A., 2013. Night and day airglow of oxygen at 1.27 μm on Mars. *Planetary and Space Science* 85, 243–249.

47. Krasnopolsky, V. A., 2013. Nighttime photochemical model and night airglow on Venus. *Planetary and Space Science* 85, 78–88.

48. Krasnopolsky, V. A., 2013. S₃ and S₄ abundances and improved chemical kinetic model for the lower atmosphere of Venus. *Icarus* 225, 570–580.

49. Krasnopolsky, V. A., 2014. Chemical composition of Titan's atmosphere and ionosphere: Observations and the photochemical model. *Icarus* 236, 83–91.

50. Krasnopolsky, V. A., 2014. Observations of CO dayglow at 4.7 μm , CO mixing ratios, and temperatures at 74 and 104–111 km on Venus. *Icarus* 237, 340–349.

51. Krasnopolsky, V. A., 2014. Observations of the CO dayglow at 4.7 μm on Mars: Variations of temperature and CO mixing ratio at 50 km. *Icarus* 228, 189–196.

52. Krasnopolsky, V. A., Belyaev, D. A., Gordon, I. E., Li, G., Rothman, L. S., 2013. Observations of D/H ratios in H₂O, HCl, and HF on Venus and new DCl and DF line strengths. *Icarus* 224, 57–65

53. Kurgansky, M. V., 2012. Statistical distribution of atmospheric dust devils. *Icarus* 219, 556–560.

54. Kurgansky, M. V., 2014. On the vertical lifting of dust in a convective unstable atmospheric boundary layer. *Izvestiya Atmospheric and Oceanic Physics* 50, 337–342.

55. Lammer H., H. I. M. Lichtenegger, M. Pflieger, O. Dutuit, V. I. Shematovich, Y. N. Kulikov, and H. K. Biernat. Hot oxygen atoms in the Venus nightside exosphere, *Geophys. Res. Lett.*, 2012, 39, L03202, doi:10.1029/2011GL050421

56. Lammer, H., Gudel, M., Kulikov, Y., Ribas, I., Zaqarashvili, T. V., Khodachenko, M. L., Kislyakova, K. G., Groller, H., Odert, P., Leitzinger, M., Fichtinger, B., Krauss, S., Hausleitner, W., Holmstrom, M., Sanz-Forcada, J., Lichtenegger, H. I. M., Hanslmeier, A., Shematovich, V. I., Bisikalo, D., Rauer, H., Fridlund, M., 2012. Variability of solar/stellar activity and magnetic field and its influence on planetary atmosphere evolution. *Earth Planets and Space* 64, 179–199.

57. Lammer, H., Kislyakova, K. G., Odert, P., Leitzinger, M., Schwarz, R., Pilat-Lohinger, E., Kulikov, Y. N., Khodachenko, M. L., Güdel, M., Hanslmeier, A., 2011. Pathways to Earth-Like Atmospheres. Extreme Ultraviolet (EUV)-Powered Escape of Hydrogen-Rich Protoatmospheres. *Origins of Life and Evolution of the Biosphere* 41, 503–522.

58. Lavrentieva, N. N., Voronin, B. A., Fedorova, A. A., 2015. H216O line list for the study of atmospheres of Venus and Mars. *Optics and Spectroscopy* 118, 11–18.
59. Lavrentieva, N. N., Voronin, B. A., Naumenko, O. V., Bykov, A. D., Fedorova, A. A., 2014. Linelist of HD16O for study of atmosphere of terrestrial planets (Earth, Venus and Mars). *Icarus* 236, 38–47.
60. Lee, Y. J., Titov, D. V., Tellmann, S., Piccialli, A., Ignatiev, N., Pätzold, M., Häusler, B., Piccioni, G., Drossart, P., 2012. Vertical structure of the Venus cloud top from the VeRa and VIRTIS observations onboard Venus Express. *Icarus* 217, 599–609.
61. Lyulin O. M., T. M. Petrova, A. M. Solodov, A. A. Solodov, V. I. Perevalov, 2014. Measurements of the broadening and shift parameters of the methane spectral lines in the 5550–6140 cm⁻¹ region induced by pressure of carbon dioxide, *Journal of Quantitative Spectroscopy and Radiative Transfer* 147, 164–170
62. Maltagliati, L., Montmessin, F., Fedorova, A., Korablev, O., Forget, F., Bertaux, J., 2011. Evidence of Water Vapor in Excess of Saturation in the Atmosphere of Mars. *Science* 333, 1868–1871.
63. Maltagliati, L., Montmessin, F., Korablev, O., Fedorova, A., Forget, F., Määttänen, A., Lefèvre, F., Bertaux, J.-L., 2013. Annual survey of water vapor vertical distribution and water-aerosol coupling in the martian atmosphere observed by SPICAM/MEX solar occultations. *Icarus* 223, 942–962.
64. Marcq, E., Belyaev, D., Montmessin, F., Fedorova, A., Bertaux, J.-L., Vandaele, A. C., Neefs, E., 2011. An investigation of the SO₂ content of the venusian mesosphere using SPICAV-UV in nadir mode. *Icarus* 211, 58–69.
65. Marcq, E., Bertaux, J.-L., Montmessin, F., Belyaev, D., 2013. Variations of sulphur dioxide at the cloud top of Venus's dynamic atmosphere. *Nature Geoscience* 6, 25–28.
66. Markiewicz, W. J., Petrova, E., Shalygina, O., Almeida, M., Titov, D. V., Limaye, S. S., Ignatiev, N., Roatsch, T., Matz, K. D., 2014. Glory on Venus cloud tops and the unknown UV absorber. *Icarus* 234, 200–203.
67. Migliorini, A., Altieri, F., Zasova, L., Piccioni, G., Bellucci, G., Cardesin Moineo, A., Drossart, P., D'Aversa, E., Carrozzo, F. G., Gondet, B., Bibring, J.-P., 2011. Oxygen airglow emission on Venus and Mars as seen by VIRTIS/VEX and OMEGA/MEX imaging spectrometers. *Planetary and Space Science* 59, 981–987.
68. Mingalev, I. V., Rodin, A. V., Orlov, K. G., 2012. A nonhydrostatic model of the global circulation of the atmosphere of venus. *Solar System Research* 46, 263–277.
69. Mingalev, I. V., Rodin, A. V., Orlov, K. G., 2015. Numerical simulations of the global circulation of the atmosphere of Venus: Effects of surface relief and solar radiation heating. *Solar System Research* 49, 24–42.
70. Montmessin, F., Bertaux, J. L., Lefèvre, F., Marcq, E., Belyaev, D., Gérard, J. C., Korablev, O., Fedorova, A., Sarago, V., Vandaele, A. C., 2011. A layer of ozone detected in the nightside upper atmosphere of Venus. *Icarus* 216, 82–85.
71. Nikitin, A. V., Thomas, X., Régalia, L., Daumont, L., Rey, M., Tashkun, S. A., Tyuterev, V. G., Brown, L. R., 2014. Measurements and modeling of long-path 12CH₄ spectra in the 4800–5300 cm⁻¹ region. *Journal of Quantitative Spectroscopy and Radiative Transfer* 138, 116–123.

72. Petrosyan, A., Galperin, B., Larsen, S.E., Lewis, S.R., Määttänen, A., Read, P.L., Renno, N., Rogberg, L.P.H.T., Savijärvi, H., Siili, T., Spiga, A., Toigo, A., Vázquez, L., 2011. The Martian Atmospheric Boundary Layer. *Reviews of Geophysics* 49, 3005.
73. Petrova T.M., A. M. Solodov, A.A. Solodov, O.M. Lyulin, S.A. Tashkun, V.I. Perevalov. 2013 Measurements of $^{12}\text{C}^{16}\text{O}_2$ line parameters in the 8790–8860, 9340–9650 and 11430–11505 cm^{-1} wavenumber regions by means of Fourier transform spectroscopy, *Journal of Quantitative Spectroscopy and Radiative Transfer* 124, 21–27
74. Petrova, E. V., Hoekzema, N.M., Markiewicz, W.J., Thomas, N., Stenzel, O.J., 2012. Optical depth of the Martian atmosphere and surface albedo from high-resolution orbiter images. *Planetary and Space Science* 60, 287–296.
75. Piccialli, A., Tellmann, S., Titov, D.V., Limaye, S.S., Khatuntsev, I.V., Pätzold, M., Häusler, B., 2012. Dynamical properties of the Venus mesosphere from the radio-occultation experiment VeRa onboard Venus Express. *Icarus* 217, 669–681.
76. Robert, S., Borkov, Y.G., Vander Auwera, J., Drummond, R., Mahieux, A., Wilquet, V., Vandaele, A.C., Perevalov, V.I., Tashkun, S.A., Bertaux, J.L., 2013. Assignment and rotational analysis of new absorption bands of carbon dioxide isotopologues in Venus spectra. *Journal of Quantitative Spectroscopy and Radiative Transfer* 114, 29–41.
77. Rothman, L.S., Gordon, I.E., Babikov, Y., Barbe, A., Chris Benner, D., Bernath, P.F., Birk, M., Bizzocchi, L., Boudon, V., Brown, L.R., Campargue, A., Chance, K., Cohen, E.A., Coudert, L.H., Devi, V.M., Drouin, B.J., Fayt, A., Flaud, J.-M., Gamache, R.R., Harrison, J.J., Hartmann, J.-M., Hill, C., Hodges, J.T., Jacquemart, D., Jolly, A., Lamouroux, J., Le Roy, R.J., Li, G., Long, D.A., Lyulin, O.M., Mackie, C.J., Massie, S.T., Mikhailenko, S., Müller, H.S.P., Naumenko, O.V., Nikitin, A.V., Orphal, J., Perevalov, V., Perrin, A., Polovtseva, E.R., Richard, C., Smith, M.A.H., Starikova, E., Sung, K., Tashkun, S., Tennyson, J., Toon, G.C., Tyuterev, V.G., Wagner, G., 2013. The HITRAN2012 molecular spectroscopic database. *Journal of Quantitative Spectroscopy and Radiative Transfer* 130, 4–50.
78. Schaufelberger, A., Wurz, P., Lammer, H., Kulikov, Y.N., 2012. Is hydrodynamic escape from Titan possible? *Planetary and Space Science* 61, 79–84.
79. Shematovich, V.I., 2011. Ultraviolet emissions in the planetary atmospheres. *Astrophysics and Space Science* 335, 3–8.
80. Shematovich, V.I., 2013. Suprathermal oxygen and hydrogen atoms in the upper Martian atmosphere. *Solar System Research* 47, 437–445.
81. Shematovich, V.I., Bisikalo, D.V., Barabash, S., Stenberg, G., 2014. Monte Carlo study of interaction between solar wind plasma and Venusian upper atmosphere. *Solar System Research* 48, 317–323.
82. Shematovich, V.I., Bisikalo, D.V., Barabash, S., Stenberg, G., 2014. Monte Carlo study of interaction between solar wind plasma and Venusian upper atmosphere. *Solar System Research* 48, 317–323.
83. Shematovich, V.I., Bisikalo, D.V., Dieval, C., Barabash, S., Stenberg, G., Nilsson, H., Futaana, Y., Holmstrom, M., Gerard, J.C., 2011. Proton and hydrogen atom transport in the Martian upper atmosphere with an induced magnetic field. *Journal of Geophysical Research-Space Physics* 116.

84. Shematovich, V.I., Bisikalo, D.V., Stenberg, G., Barabash, S., DiéVal, C., Gérard, J.-C., 2013. He²⁺ transport in the Martian upper atmosphere with an induced magnetic field. *Journal of Geophysical Research (Space Physics)* 118, 1231–1242.
85. Shematovich, V.I., Ionov, D.E., Lammer, H., 2014. Heating efficiency in hydrogen-dominated upper atmospheres. *Astronomy and Astrophysics* 571, 94.
86. Tashkun S.A., V.I. Perevalov 2013. CDS-296: High resolution carbon dioxide spectroscopic databank. Version 2013. *Journal of Quantitative Spectroscopy and Radiative Transfer* 152, 45–73.
87. Tashkun, S.A., Perevalov, V.I., 2011. CDS-4000: High-resolution, high-temperature carbon dioxide spectroscopic databank. *Journal of Quantitative Spectroscopy and Radiative Transfer* 112, 1403–1410.
88. Tashkun, S.A., Perevalov, V.I., Gamache, R. R., Lamouroux, J., 2015. CDS-296, high resolution carbon dioxide spectroscopic databank: Version for atmospheric applications. *Journal of Quantitative Spectroscopy and Radiative Transfer* 152, 45–73.
89. Titov, D.V., Markiewicz, W.J., Ignatiev, N.I., Song, L., Limaye, S.S., Sanchez-Lavega, A., Hesemann, J., Almeida, M., Roatsch, T., Matz, K.-D., Scholten, F., Crisp, D., Esposito, L.W., Hviid, S.F., Jaumann, R., Keller, H.U., Moissl, R., 2012. Morphology of the cloud tops as observed by the Venus Express Monitoring Camera. *Icarus* 217, 682–701.
90. Trokhimovskiy, A., Fedorova, A., Korablev, O., Montmessin, F., Bertaux, J.-L., Rodin, A., Smith, M.D., 2015. Mars' water vapor mapping by the SPICAM IR spectrometer: Five martian years of observations. *Icarus* 251, 50–64.
91. Vandaele, A.C., Mahieux, A., Robert, S., Berkenbosch, S., Clairquin, R., Drummond, R., Letocart, V., Neefs, E., Ristic, B., Wilquet, V., Colomer, F., Belyaev, D., Bertaux, J.-L., 2013. Improved calibration of SOIR/Venus Express spectra. *Optics Express* 21, 21148.
92. Vorontsov, V.A., Lokhmatova, M.G., Martynov, M.B., Pichkhadze, K.M., Simonov, A.V., Khartov, V.V., Zasova, L.V., Zelenyi, L.M., Korablev, O.I., 2011. Prospective spacecraft for venus research: Venera-D design. *Solar System Research* 45, 710–714.
93. Wilson, C.F., Chassefière, E., Hinglais, E., Baines, K.H., Balint, T.S., Berthelier, J.-J., Blamont, J., Durry, G., Ferencz, C.S., Grimm, R.E., Imamura, T., Josset, J.-L., Leblanc, F., Lebonnois, S., Leitner, J.J., Limaye, S.S., Marty, B., Palomba, E., Pogrebenko, S.V., Rafkin, S.C.R., Talboys, D.L., Wieler, R., Zasova, L.V., Szopa, C., 2012. The 2010 European Venus Explorer (EVE) mission proposal. *Experimental Astronomy* 33, 305–335.
94. Zhang, X., Liang, M.C., Mills, F.P., Belyaev, D.A., Yung, Y.L., 2012. Sulfur chemistry in the middle atmosphere of Venus. *Icarus* 217, 714–739.

Polar Meteorology

A. I. Danilov, V. E. Lagun, A. V. Klepikov
Arctic and Antarctic Research Institute
aid@aari.ru

This section is a review of the results of Russian polar studies performed in 2011–2014. It is based on material prepared by the Commission on Polar Meteorology of the National Geophysical Committee, Russian Academy of Sciences, and included in the National Report on Meteorology and Atmospheric Sciences to the XXIV General Assembly of the International Union of Geodesy and Geophysics, Prague, Czech Republic, June 22 – July 2, 2015.

1. Arctic meteorology investigations

International Polar Year 2007/08 (IPY) provided a unique opportunity for the analysis of meteorological conditions of the polar regions of the Earth in the context of global climate change. Preliminary results of the Russian IPY Science Program are summarized in [1–3].

The peculiarities of the Arctic climate system during the first decade of the XXI century, including IPY period, were considered in [4] based on historic and IPY meteorological data. The development of the warming in 1990–2000s in the Arctic sea and its relation to global climate changes was traced and compared with warming of 1930–40s. Changes in the observed characteristics of the Arctic atmosphere, sea ice and ocean are compared with changes in other areas and with estimates calculated within the Global climate model ensemble CMIP3 [4].

Electronic archives of all available upper-air, standard meteorological and hydrological data obtained at the polar station Tiksi from 1932 to 2007 are created by AARI with participation of Tiksi Branch of Yakutsk Hydrometeorological Service and statistically analyzed in [5].

The total cloud cover (since 1966) and of global short-wave radiation (since 1985) for are reviewed and applied for investigation of Barentsburg region climate variability [6]. Empirical approach is used for estimation of long-term variability of long-wave downward radiation, obtained estimation is compared to cloud characteristic changes, which are supposed to be one of the regional warming [6].

Numerical analysis of different climate regimes and their changes in Polar areas is performed based on simulations with climate models collection to observations and reanalysis in [7].

A review of the modern Arctic stations network development during preparation and implementation of the IPY2007/08 projects is presented in [8]. The

long-term data of air mass transit through three points in Russian Arctic are analyzed for four months (one at each season) for the 20 years period in [9]. Average atmospheric concentrations and average fluxes onto the surface of anthropogenic heavy metals (As, Ni, Pb, Cd) over the Russian Arctic Islands were estimated for two decades 1986–1995 and 1996–2005. Strong seasonal and spatial variations of Arctic air pollutions are found. In the central part of Russian Arctic the concentration of heavy metals in the air as well as annual deposition onto the surface have been decreasing comparable with the decreasing of anthropogenic emissions in Europe and Russia [9].

The model of the solar activity effect on the Earth climatic system is considered taking into account the helio-geophysical disturbance effect on the Earth climatic system parameters in [10]. The long-term troposphere and ocean temperature variation for 1950–2007 is used for showing of continuous increase of the Earth climatic system heat content with local cooling events. The special attention is paid to thermal regime of Northern Hemisphere [10].

Results of the atmosphere — sea ice interaction over the Arctic Ocean based on the direct measurements of heat and momentum turbulent fluxes made in different parts of the Arctic over various surfaces are presented in [11].

Numerical experiments with the atmospheric general circulation model ECHAM5 have been performed in order to simulate the influence of changes in the ocean surface temperature and sea ice concentration on climate characteristics in Northern Eurasia region [12]. The analysis of the sensitivity of the climate in Western Europe to sea ice concentration variations alone in the Arctic is a most important result of the experiments performed in [12].

The calculation results for the wintertime Arctic warming parameters based on ECHAM5 model using the empirical HadISST1.1 data on sea surface temperature are analyzed in [13]. According to the experimental results [13] the mid-20th century warming was accompanied by a significant negative anomaly of the wintertime Arctic sea ice extent comparable to current trends and also point to a considerable contribution of natural variability to the present climate changes. Current amplification of Arctic warming process associated with the increasing of atmosphere and ocean meridional heat transport from the mid-latitudes is demonstrated in [14].

A review of the results of the Arctic Council's recent assessment report "Snow, Water, Ice, and Permafrost in the Arctic" (SWIPA) on the changing of Arctic climate is presented in [15].

The possible consequences of current unprecedented climate change for economical activity in the Russian Arctic (shipping, offshore mineral and marine bioresources exploration) are considered [16–20]. Arctic hydrometeorological network development perspectives for the Northern Sea Route navigation support are presented in [21].

Modern methods of standard upper-air network station measurements data analysis, quality control, proceeding and interpretation are summarized in [22]. The impact of observed and projected changes in meteorological conditions and in the Arctic permafrost layer and the emission of greenhouse gases has been studied in the series of articles [23–38].

Possible Northern Hemisphere land permafrost dynamics due to current climate changes in the 21st century are estimated using the IAP RAS global climate model under the different RCP scenarios [24]. According to model calculations [24] the annual mean northern land temperature during the 21st century amounts to 1,2–5,3 °C depending on the RCP scenario and permanent surface permafrost in the late 21st century persists in several high-latitude parts Siberia and North America.

Based on experimental dataset [31] the total contribution of Western Siberia tundra lakes methane emission into atmospheric budget is estimated as 20 KtCH₄/year. The high spatial and inter-annual variability of the surface methane concentration in the atmosphere over Northern Eurasia area is demonstrated in [32] based on regular station multi-year measurement results. Methane emission over the East Siberian Arctic Shelf under the changing sub-sea permafrost conditions based on detailed ground hydrothermal regime model is estimated in [33].

Projected degradation of subsea permafrost over Russian Arctic shelf impact to methane release from the Late Pleistocene to present time at the West Yamal area shelf is modeled in [34]. Possible release of methane from the seabed mechanism in a present Arctic warming conditions is described. Field high-resolution seismic measurements of subsea permafrost distribution in the South Kara Sea are demonstrated that that local permafrost has degraded more significantly than previously thought [35].

Relationships between summer vegetation phenology parameters for Arctic tundra coastal zone and spring the peculiarity of atmospheric circulation and sea ice distribution are investigated in [36] using satellite data, reanalysis and model statistical modeling results.

Current permafrost degradation dynamics on Svalbard are estimated in [37] based on multi-year meteorological observation, snow and moss distribution and thermodynamic modelling information.

The review of Russian field and model Arctic atmosphere methane studies, including relevant surface methane concentration measurements at the Russian Arctic sites and regional modeling results are presented in [38]. The estimations of both methane emission from the Russian territory and climatic effect of atmospheric methane content are also discussed in [38]. Modern permafrost stability level assessment taking into account current climate change is presented in [39].

Considerable attention during the reporting period was paid to the analysis of the of synoptic climatology parameters as important indicators of the current meteorological conditions, such as climatic variability [40–45].

Handbook [40] presents information about Arctic atmosphere unique natural event: a polar mesoscale cyclone (PMC) or polar low. Polar mesocyclones now attract a lot of attention of many scientists. An interest to PMCs is due to necessity of possible origin strong storm and very strong storm weather events forecasting and their impact on economic objects infrastructure and sea transport tools. This information is useful to support the hydrometeorological service and to increase the quality of forecasting over Arctic sea area of water where mesoscale cyclogenesis processes develop which is necessity for regional Roshydromet branches and oil and natural gas production companies working on Arctic shelf. Polar mesocyclonic vortex weather conditions, duration and drift speed data are presented in this Handbook. Possible polar mesocyclone genesis mechanisms and their annual course and interannual variations peculiarities are described. Possibility of mesoscale cyclone projection estimation and brief description of 20 typical mesoscale cyclogenesis events are collected. The Handbook Annex contents regional PMCs catalogue-calendar with mesoscale cloudy eddies geographical coordinates, size and shape indication for 1981–2006 [40].

The high latitudes atmospheric circulation many-year dynamic study been carried out using a multiscale (global and regional) atmospheric modeling system with horizontal resolutions of 200, 50 and 25 km [41]. The analysis of polar mesocyclones winter season activity has been investigated in [41] depending on the spatial resolution of the model system and compared with that in the reanalyses and satellite-derived analyses [40].

Numerical estimates of the sensitivity of the Northern Hemisphere cyclones number and size to the surface temperature changes are investigated due to multiyear NCEP/NCAR reanalysis data and are compared with model of synoptic eddies activities (MMPKh model) results [42]. According to the reanalysis data number of extratropical cyclones and the density of their packing in extratropical latitudes characterized by decrease during the surface temperature increases period. Important variations in annual mean values in the number and size of mid-latitude cyclones are connected with the troposphere vertical temperature gradient: an increase the vertical temperature gradient in the troposphere corresponds decreases the cyclone size [42].

Arctic region cyclonic climatology parameters (frequency, size, intensity) and their changes have been analyzed with the use of the HIRHAM regional climate model simulations with SRES-A1B anthropogenic scenario for the twenty first century a warmer climate for different seasonal conditions and compared from ERA-40 reanalysis data in [43]. According to the HIRHAM simulations, the frequency of cyclones is increasing in warm seasons and decreasing in cold seasons for a warmer climate era in the twenty first century, but these changes are statistically insignificant [43]. Some increase in the small cyclones number was detected in cold seasons on the contrary to cold seasons, while its frequency decreases in warm seasons [43].

The unique tornado formation event near Khanty-Mansiysk city (12 June 2012) is analyzed in [44]. This case study can demonstrate possible impact of the large-scale circulation changes due to global warming to local weather peculiarities over West Siberia which may contribute to a regular tornado formation in high-latitude areas [44]. Siberian tornado physical mechanism formation is described in [44].

The thunderstorm activity instrumental registrations results near Yakutsk city (Eastern Siberia) are presented in [45]. The seasonal course of thunderstorm number was detected. The number of positive discharges to the ground was estimated and compared with available data. The thunderstorm activity in Yakutsk is three times higher than in the area around Yakutsk with a radius of 400 km, which can be explained by its relative hot island formation over city [45].

Important physical mechanisms of meteorological regime peculiarities formation as well as weather, seasonal and climatic anomalies in the North Polar region are considered in [46–55].

The role of sea surface temperature and sea ice extent variations for modern climate conditions in Russian Arctic is estimated in [46]. Possible increase of extreme weather events such as strong wind and dangerous sea wave height are indicated in [46, 47, 50]. Amplification of the Arctic warming due to sea ice extent reduction is considered in [51] using the atmospheric general circulation with prescribed boundary conditions on the sea surface.

Climate change tendencies of surface air temperature, precipitation and snow cover in the regions of the Arctic to the north of 70° N for the period 1981–2010 are presented in [54].

The polar atmosphere energetic problems are considered in [55, 56]. The total meridional energy flux across 70° N is estimated in [55] based on the Integrated Global Radiosonde Archive (IGRA) for the period 1992–2007. According to diagnostic calculation the mean energy flux in the layer from surface to 30 hPa is 70,6 W m⁻² [55].

The average temperature of the atmospheric vertical column (the temperature of the average energy level) computation method based on the mid-troposphere radiosonde data is proposed in [56]. The annual mean atmospheric energy level temperature values changes are observed with the multi-decadal period with the amplitude of 40C during 1935–2012. Significant decrease in the mean annual values of height-integrated temperature has been registered in recent years over Franz Josef Land archipelago [56] and connected with Barents Sea surface temperature conditions.

Spatial-temporal changes of snow cover parameters in the Northern Polar area considered in [57–67]. The regional and seasonal changes snow cover stability parameters over the Northern Russia for the current warm period (1991–2008) in comparison with the climatic reference period (1961–1990) are described in [66]

based on the 223 meteorological stations routine data. Teteleconnections between snow period duration, snow spatial distribution and the North Atlantic Oscillation and the West Pacific Oscillation indexes are determined.

Daily meteorological data from five North-Eastern Siberia stations (Anadyr, Chokurdakh, Wrangell Island, Verkhoyansk, Markovo) were used in [67] for multi-year dates of formation, occurrence and maximum snow depth changes determination. The snow cover parameters results for the total observation period are compared with long-term changes of the Northern Hemisphere atmospheric circulation form obtained according to Dzerdzeevskii's circulation classification. The circulation types which corresponds to early or late snow cover formation are obtained in [67]. In the Northeastern Siberia during recent years reveal the duration of snow cover reduction connected with the increase of duration of atmospheric blocking processes [67].

Theoretical approaches to the description of microphysical processes and photochemical reactions at polar atmosphere proposed in [68–70]. Applied and methodological aspects of meteorological observations in the Polar Regions and processing the measurement results discussed in [71–81].

2. Antarctic meteorology studies

South Polar area meteorology results obtained during the IPY2007/08 projects are presented and analyzed in [82–85].

The review of three large interdisciplinary IPY cluster projects for the Antarctic is presented in [82]. These three are: COMPASS (Comprehensive Meteorological dataset of archive IPY Antarctic measurement phase for Scientific and applied Studies), CLICOPEN (impact of CLimate induced glacial melting on marine and terrestrial COastal communities on a gradient along the Western Antarctic PENinsula) and ANTPAS (Antarctic Permafrost And Soils). The outcome of the IPY COMPASS Project is the multiuser meteorological and upper-air sounding current data base of all Antarctic stations with long-time observations, which came to be available for Antarctic community for the first time. These data after applying of the quality control procedure are used for Antarctica climate change investigations. The warming impact on local ecosystems over Antarctic Peninsula area for last decades, indicated in decreasing of the sea ice cover, in shortening of the ice period and, as a consequence, in removing of sediments, in changes of salinity exchange and of sea water dissolved oxygen content, in changes of specific structure, of food chains and biota communities structure and so on became a subject of study in the CLICOPEN project.

The outcome of the ANTPASS Project aimed at generalization of historical and current data about the distribution, the thickness, the age, the physical and geochemical properties of Antarctic and sub-Antarctic islands permafrost and

soils is the creation of geocryological polygons National network. The estimations of climate parameters trends for South Polar area for instrumental observation period with account of data obtained during IPY activity are executed. The results of calculations demonstrated that, in spite of remarkable Western Antarctic warming manifestations, the meteorological regime of Antarctic is characterized by atmospheric processes natural variability in whole.

The analysis of the field measurements of the radiation balance components influenced by atmospheric aerosol and the data of the aerosol attenuation of the solar radiation obtained during IPY at the Antarctic stations and on the board of research vessels near the Antarctic shore is presented in [83]. Newly obtained results are compared with the previous long-term measurement results [83].

Surface carbon dioxide and methane concentration measurements were executed at the Russian Antarctic Novolazarevskaya station during IPY2007/08 period [84]. Greenhouse gases concentrations positive trend was estimated and compared with the data from Japan Syowa station in [84].

The results of total ozone content measurements obtained at Antarctic stations and on board of research vessel "Akademik Fedorov" during IPY2007/08 are presented and analyzed in [85]. The quasi-biennial oscillations influence on level and date of total ozone content extreme in the Southern Polar area is analyzed in [86] with reference to quasi-biennial oscillations stages determined by vertical profiles of zonal winds in the equatorial stratosphere taking into account the seasonal regularity of the upper-air jet stream dynamics.

Most progress in the Antarctic meteorological regime parameters study reached when studying the conditions of snow accumulation in the Central Antarctica subglacial lake Vostok area. Brief history of the Soviet/Russian successful deep drilling project in Vostok station is described in [87, 88]. The results of field, laboratory and modeling studies of snow cover in Central Antarctica are shown in [89–98].

According to numerical model experiment results and statistical calculations based on the snow accumulation value changes over the Antarctic ice cover [89], sea ice extent changes, unlike the Arctic, play a secondary role for Southern Hemisphere climate formation after large-scale atmosphere circulation dynamics. Statistical analysis confirmed a not leading impact of changes in the ice cover of the ocean on the nourishment of the Antarctic ice sheet. The relationship between the anomalies of sea ice extent and magnitude of snow accumulation is negative and sufficiently close to the coastal strip, however, for the Central Antarctic inland areas it is positive, because of the prevalence of condensation above the precipitation brought from the ocean [89].

During 1999–2012 the interdisciplinary observations program have been carried out in the Central Antarctica subglacial Lake Vostok and the Ridge B area [90]. Instrumentally obtained snow accumulation data (from 21 to 37 $\text{kgm}^{-2}\text{yr}^{-1}$

depending on ice flow lines direction) as well as data on the stable water isotope concentration ($\delta^{18}\text{O}$) are presented in [90]. The important role the snow re-deposition effect due to air flow — local orography interaction is noted also.

The snow samples from the vicinities of Russian Vostok station chemical analyses results are presented in [91]. High resolution (every 2–3 cm, or about three samples per year) ion measurements allow us to compile a new detailed record of volcanic events for the past 900 years. About 30 low latitude volcanic eruptions were identified during XIII–XX centuries, for instance, Pinatubo (1991), Agung (1963), Krakatau (1883), Tambora (1815), Gamkonora (1673), Huaynaputina (1600), Kuwae (1453) [91].

Antarctic snow chemical composition data obtained along the 1276 km tractor way from coastal Progress station to Vostok station during the 53th Russian Antarctic Expedition are presented in [92]. The time-space features of horizontal and depth distribution of chemical species in snow cover revealed differences in snow cover formation sources (marine, continental and volcanic) and admixture concentration decreases with the distance from the coast [92].

The results on the thermal diffusive properties of the snow cover as well as the snow temperature profile yearly variation on the Central Antarctic plateau obtained in the frame of the Russian-French co-operation during 55th Russian Antarctic Expedition are presented in [93].

Central East Antarctica snow cover micrometeorites composition obtained during the 2010/11 summer season at Vostok station (56th Russian Antarctic Expedition) using electron microscopy is proved that local snow cover is the best spot on the Earth for micrometeorites collecting [94]. This result could be useful in deciphering the origin and evolution of solid matter in Solar System.

The snow-and-firn thickness data in the vicinity of the Lake Vostok during the austral summer season of 2012/2013 (58th Russian Antarctic Expedition) performed using the ground-penetrating geophysical radar are analysed in [95].

The snow mega-dune area located 30 km to the East from Vostok station was investigated during 2013/14 austral summer season (58th and 59th Russian Antarctic Expedition) in [98]. Snow accumulation rate and isotope content are considered in [98], Accumulation rate averaged over the length of a dune wave (25 mm w.e.) corresponds with the value obtained at Vostok station, which suggests no additional wind-driven snow sublimation in the mega-dunes comparing to the surrounding plateau. The snow isotope content is in negative correlation with the snow accumulation, which could be explained by post-depositional snow modification and/or by enhanced winter precipitation redistribution by wind flow [98].

The air temperature and snow accumulation rate reconstruction in the Davis sea sector of East Antarctica over the past 250 years based on the ice core studies are presented in [99]. According to [99] results the climatic characteristics demonstrate cyclic time variability with the periods of 6, 9, 19, 32 and about 120 years.

The air temperature and snow accumulation rate variability near Vostok station vicinity have been obtained for the last 350 years in [100] based on data of interdisciplinary research in snow pits and on snow cores samples. The correlation of these parameter with Southern Hemisphere atmospheric circulation indices has been shown in [100].

The comprehensive Russian Antarctic Mirny Observatory upper-air radiosounding system metadata and assessment of the upper-air soundings time-series homogeneity over the total observation period are presented in [101].

The aerosol optical depth, aerosol Ångström's exponent and actinometrical measurements results obtained after 2000 at the Russian polar stations are presented in [102].

The comparative study of stable-stratified atmospheric surface layer turbulent energy — mass transfer processes parameterizations is executed in [103] based on the calculations of turbulent sensible heat flux with data of profile measurements carried out on the Antarctic ice drifting station "Ice Camp Weddell-1". The surface layer fluxes estimations [103] are demonstrated that the use of different parameterizations give almost identical results. [103]

Simple model describing changes in the total balance of the ice sheet mass due to global climate change is developed in [104]. A nonlinear analytical dependence of the ice sheet thickness on the global near-surface temperature is obtained for estimation of the critical level in global warming, in excess of which the regime of the Antarctic ice sheet gain due to snow accumulation changes to sheet degradation due to more intense growth in ice melting [104].

Regional peculiarities of meteorological conditions of Antarctica on the example of the Schirmacher oasis are considered in [105–108]. Schirmacher oasis (located at the periphery of east Antarctica) experiences impact of the severe katabatic winds flowing from the interior of the continent towards the periphery and the induction of warm, moist air associated with the moving cyclones along the east coast of Antarctica. An unusual atmospheric warming (surface air temperature reached +12 °C) observed at the two closely located stations (Russian Novolazarevskaya station and Indian Maitri station) during February 1996 has been investigated by a number of complementary atmospheric techniques in [106–107]. This unusually high temperature has been investigated as a wide spread warming over the east Antarctic region, which was caused by the induction of warm, humid oceanic air around the Japan Syowa station under a blocking polar high [106].

The Solar wind influence on atmospheric processes in Antarctic winter season is described in [109].

One of the most important science advances of the 2007/08 International Polar Year is that a large amount of new knowledge about the changes in the polar regions has created favorable conditions for the transition from research to

services to improve the different forecasts in the Arctic and Antarctic. As part of the legacy of the IPY2007/08, the World Meteorological Organization has formed an international expert group to develop the concept of the International Polar Partnership Initiative (IPPI) [110]. IPPI proposes a joint plan of activities that unifies observations, research, and services and focuses them on socially important issues. Thus IPI should not be viewed simply as a new research follow-on of IPY2007/08. It is a genuine attempt, using the IPY experience, to maximize the return on investment into polar activities through coordination and cooperation of existing initiatives and proposing new ones only if they are absolutely necessary [110]. Integration of research, observation, services, and governance remains a major task for the future. An observing system would have more chances to be resourced and sustained if there was a clearer understanding how the observations would be used and what would be their value for services and society. IPPI is a new platform for improved polar cooperation and coordination, for agencies and for nations. Focus on planning implies some top-down character of this initiative but it does not preclude bottom-up scientific research, which should comprise a large and important part of IPPI. The balance between top-down and bottom-up approaches can be achieved through proactive participation in IPPI of funding agencies. IPI will help them to issue calls for research proposals that respond to the expressed interests of scientists and at the same time support topics of relevance for their countries and society at large [110].

References

1. Meteorological and geophysical researches. Series: Contribution of Russia to International Polar Year 2007/08. Ed. Alekseev G. V., Paulsen Editions. Moscow – Saint-Petersburg. 2011. 349 p.
2. Dmitriev V. G., Danilov A. I., Klepikov A. V., Kotlyakov V. M., Sarukhanyan E. I., Zaytseva N. A. On the publication of the scientific series “Contribution of Russia to international polar year 2007/08”. *The Arctic: ecology and economy*. 2012. No 3 (7), p. 54–61.
3. Alekseev G. V. Introduction: About «Meteorological and geophysical researches» direction works. In «Meteorological and geophysical researches». 2011, p. 3–5.
4. Alekseev G. V., Ivanov N. E., A. V. Pnyushkov, N. E. Kharlanenkova. Climate change in the marine Arctic in the beginning of 21s century. *Ibid* p. 6–25.
5. Makshtas A. P., Bolshakova I. I., Gunn R. M., Jukova O. L., Ivanov N. E., Shutilin S. V. Climate of Hydrometeorological observatory Tiksi region. *Ibid* p. 49–74.
6. Svyashchennikov P. N., Ivanov B. V., Bocharov P. V., Juravski D. M., Timachev V. F., Semenov A. V., Soldatova T. A., Antsiferova A. R. Investigations of radiation climatic factors and meteorological regime of Spitsbergen archipelago. *Ibid* p. 75–82.

7. Mokhov I. I., Semenov V. A., Eliseev A. V., Khon V. Ch., Arzhanov M. M., Karpenko A. A., Denisov S. N. Climate changes and their consequences in high latitudes: Diagnostics and modeling. *Ibid* p. 96–130.
8. Romantsov V. A., Vasiliev L. Yu., Kozelov D. A. State and development of the observation network of the Arctic in the IPY stage of 2007/08. *Ibid*, p. 150–157.
9. Vinogradova A. A. Trends in sources and sinks of anthropogenic heavy metals in the Arctic atmosphere at the turn of XX and XXI centuries. *Ibid*, p. 215–235.
10. Zherebtsov G. A., Kovalenko V. A., Molodykh S. I., Rubtsova O. A. The effect of the heliophysical disturbance in the polar troposphere on the Earth climatic system. *Ibid*, p. 251–268.
11. Repina I. A., Artamonov A. Yu., Smirnov A. S., Chechin D. G. The investigation of the air-sea interaction in the Polar regions in IPY framework. *Ibid*, p. 236–250.
12. Semenov V. A., Mokhov I. I., Latif M. Influence of the Ocean Surface Temperature and Sea Ice Concentration on Regional Climate Changes in Eurasia in Recent Decades. *Izvestiya, Atmospheric and Oceanic Physics*, 2012, Vol. 48, No. 4, p. 355–372. DOI: 10.1134/S0001433812040135.
13. Semenov V. A. Role of Sea Ice in Formation of Wintertime Arctic Temperature Anomalies. *Izvestiya, Atmospheric and Oceanic Physics*, 2014, Vol. 50, No. 4, p. 343–349. DOI: 10.1134/S0001433814040215.
14. Alekseev G. V. Arctic dimension of global warming. *Ice and Snow*. 2014. No. 2 (126), p. 53–68.
15. Tsaturov Yu. S., A. V. Klepikov. Current Arctic climate change: results of a new assessment reports of the Arctic Council. *Arctic: ecology and economy*. 2012. No. 4 (8), p. 76–81.
16. Alekseev G. V., Danilov A. I., Klepikov A. V. On prediction and evaluation of the sequences of global climatic changes in the Russian Arctic zone under influence of natural and anthropogenic factors. *Russian Polar Studies*. 2013, No. 4 (14), p. 26–28.
17. Danilov A. I., G. V. Alekseev, A. V. Klepikov. The consequences of climate change for maritime activity in the Arctic. *Ice and snow*. 2014. No. 3 (127), p. 91–99.
18. Kovalevskiy D. V., Alekseev G. V., Kuz'mina S. I. Changes of Arctic climate and their sequences for fishery and sea transport. *Proc. International conference*. Tyumen. 2012. Vol. 1, p. 167–170.
19. Matishev G. G., Dzhenyuk S. L. Marine economic activity in Russian Arctic in the conditions of present-day climatic changes. *Arctic: Ecology and Economics*. 2012: No. 1 (3), p. 26–37.
20. Olsen M. S., Callaghan T. V., Reist J. D., Reiersen L. O., Dahl-Jensen D., Granskog M. A., Goodison B., Hovelsrud G. K., Johansson M., Kallenborn R., Key J., Klepikov A., Meier W., Overland J. E., Prowse T. D., Sharp M., Vincent W. F., Walsh J. The Changing Arctic Cryosphere and Likely Consequences: An Overview. *Ambio*. 2011, 40: 111–118. doi: 10.1007/s13280-011-0220-y.
21. Makosko A. A. Hydrometeorological support for navigation on the seaways of the Northern sea route. *The Arctic: ecology and economy*. 2013. No. 3 (11), p. 40–49.

22. Aldukhov O.A., Chernykh I.V. Methods of data analysis and interpretation of radiosonde measurements. — V. 1: Quality control and data proceeding; Vol. 2: Restored cloud layers. — Obninsk: VRIHI-WDC. 2013. 306 p., 151 p.
23. Arzhanov M.M., Mokhov I.I. Temperature trends in permafrost soils of the Northern hemisphere: comparison of model calculations with observations. Transactions (Doklady) of the Russian Academy of Sciences/Earth Science Section. 2013, Vol. 449, No. 1, p. 87–92.
24. Arzhanov M.M., Eliseev A.V., Mokhov I.I. Impact of climate changes over the extratropical land on permafrost dynamics under RCP Scenarios in the 21st century as simulated by the IAP RAS climate model. Russian Meteorology and Hydrology. 2013. No. 7, p. 31–42.
25. Arzhanov M.M., Mokhov I.I. Model estimates of the amount of organic carbon released from permafrost soil under scenarios of global warming in the twenty-first century. Transactions (Doklady) of the Russian Academy of Sciences/Earth Science Section. 2014, Vol. 455, No. 3, p. 328–331.
26. Denisov S.N., Arzhanov M.M., Eliseev A.V., Mokhov I.I. Assessment of the response of subaqueous methane hydrate deposits to possible climate change in the twenty-first century. Transactions (Doklady) of the Russian Academy of Sciences/Earth Science Section. 2011. Vol. 441, No. 5, p. 1706–1709. DOI: 10.1134/S1028334X11120129.
27. Eliseev A.V., Demchenko P.F., Arzhanov M.M., Mokhov I.I. Hysteresis of the Surface Permafrost Area Dependence on the Global Temperature. Transactions (Doklady) of the Russian Academy of Sciences/Earth Science Section. 2012. Vol. 444, No. 4, p. 725–728.
28. Eliseev A.V., Demchenko P.F., Arzhanov M.M., Mokhov I.I. Transient hysteresis of near-surface permafrost response to external forcing. Clim. Dyn., 2014. Vol. 42, No. 5–6, p. 1203–1215.
29. Arzhanov M.M., Eliseev A.V., Mokhov I.I. A global climate model based, Bayesian climate projection for northern extra-tropical land areas. Glob. Planet. Change. 2012. Vol. 86–87, p. 57–65.
30. Stepanenko V.M. Machul'skaya E.E., Glagolev M.V., Lykossov V.N. Numerical modeling of methane emissions from lakes in the permafrost zone Numerical Modeling of Methane Emissions from Lakes in the Permafrost Zone. Izvestiya, Atmospheric and Oceanic Physics. 2011. Vol. 47, No. 2, p. 252–265.
31. Golubyatnikov L.L. Kazantsev V.S. Contribution of Tundra Lakes in Western Siberia to the Atmospheric Methane Budget // Izvestiya, Atmospheric and Oceanic Physics. 2013. V. 49, N 4. P. 395–403. DOI: 10.1134/S000143381304004X.
32. Ginzburg A.S., Vinogradova A.A., Fedorova E.I. Some Features of Seasonal Variations in the Methane Content in the Atmosphere over Northern Eurasia // Izvestiya, Atmospheric and Oceanic Physics 2011. V. 47, N 1. P. 45–63. DOI: 10.1134/S0001433811010087.
33. Anisimov O.A., Borzenkova I.I., Lavrov S.A., Strel'chenko Yu.G. The current dynamics of the submarine permafrost and methane emissions on the shelf of the Eastern Arctic seas // Ice and Snow. 2012. N 2. P. 97–105.

34. Portnov A., Mienert J., Serov P. Modeling the evolution of climate-sensitive Arctic subsea permafrost in regions of extensive gas expulsion at the West Yamal shelf. *Journal of Geophysical Research: Biogeosciences*. 2014. V. 119, N 11. P. 2082–2094. DOI: 10.1002/2014JG002685.
35. Portnov A., Smith A.J., Mienert J., Cherkashov G., Rekant P., Semenov P., Serov P., Vanshtein B. Offshore permafrost decay and massive seabed methane escape in water depths >20 m at the South Kara Sea shelf *Geophysical Research Letters*. 2013. V. 40, N 15. P. 3962–396. DOI: 10.1002/grl.50735.
36. Platonov N.G., Mordvintsev I.N., Alpatsky I.V. Estimate of Relationship between State of Subarctic Vegetation and Climatic Parameters *Izvestiya, Atmospheric and Oceanic Physics* 2013. V. 49, No. 9, 1019–1028. DOI: 10.1134/S0001433813090120.
37. Osokin N.I., Sosnovsky A.V., Nakalov P.R., Chernov R.A., Lavrentiev I.I. Climate change and possible dynamics of the permafrost on Svalbard // *Ice and Snow*. 2012. N 2. P. 115–120.
38. Kiselev A.A., Reshetnikov A.I. Methane in the Russian Arctic: Measurement and model // *Arctic and Antarctic Problems* / 2013. N 2 (96). P. 5–15.
39. Malkova G.V., Pavlov A.V., Skachkov Yu.B. Assessment of permafrost stability under present-day climate change // *Earth Cryosphere*. 2011. 15 (4): 33–36.
40. Lutsenko E., Lagun V. Polar meso-scale cyclonic eddies in the Arctic atmosphere *Handbook, Arctic and Antarctic Research Institute* (in Russian) 2011 (available at www.aari.ru/projects/mesocyclone/mez_ant.html).
41. Shkolnik I.M., Efimov S.V. Cyclonic activity in high latitudes as simulated by a regional atmospheric climate model: added value and uncertainties // *Environmental Research Letters*. 2013. N8. 12 p. Doi:10.1088/1748-9326/8/4/045007.
42. Akperov M.G., Mokhov I.I. Estimates of the sensitivity of cyclonic activity in the troposphere of extratropical latitudes to changes in the temperature regime // *Izvestiya, atmospheric and oceanic physics*. 2013. V 49, N2. P. 113–120. DOI: 10.1134/S0001433813020035.
43. Akperov M., Mokhov I.I., Rinle A., Dethloff K., Matthes H. Cyclones and their possible changes in the Arctic by the end of the twenty first century from regional climate model simulations // *Theor. Appl. Climatol*. 2014. Doi: 10.1007/s00704-014-1272-2.
44. Kurgansky M.V., Chernokulsky A.V., Mokhov I.I. The tornado over Khaty-Mansysk: an exception or a symptom? // *Russian Meteorology and Hydrology*. 2013. N8. P. 40–50.
45. Kozlov V.I., Mullayarov V.A., Grigorev Yu.M., Tarabukina L.D. Parameters of thunderstorm activity and lightning discharges in Central Yakutia from 2009 to 2012 // *Izvestiya, Atmospheric and Oceanic Physics* 2014. V. 50, N. 3. P. 323–329. DOI: 10.1134/S0001433814030086.
46. Mokhov I.I., Semenov V.A., Khon V. Ch., Pogarsky F.A. Change of sea ice extent in the Arctic and the associated climatic effects: detection and simulation // *Ice and Snow*. 2013. N2 (122). P. 53–62.
47. Khon V. Ch., Mokhov I.I., Pogarsky F.A. Evaluation of wind-wave activity in the Arctic basin under possible climate changes in the 21st century on the model

calculations // Transactions (Doklady) of the Russian Academy of Sciences/Earth Science Section. 2013. V. 452. N 4. P. 445–448.

48. Arzhanov M. M., Eliseev A. V., Mokhov I. I. A global climate model based, Bayesian climate projection for northern extra-tropical land areas // *Glob. Planet. Change*. 2012. V. 86–87. P. 57–65. 49. Chernokulsky A. V., Mokhov I. I. Climatology of total cloudiness in the Arctic: An intercomparison of observations and reanalyses // *Advances in Meteorology*. 2012. V. 2012. Article ID542093, 15 pp. doi:10.1155/2012/542093.

49. Khon V., Mokhov I. I., Pogarskiy F., Babanin A., Dethloff K., Rinke A., Matthes H. Wave heights in the 21st century Arctic Ocean simulated with a regional climate model // *Geophysical Research Letters*. 2014. V. 41(8). P. 2956–2961. doi: 10.1002/2014GL059847.

50. Baidin A. V., Meleshko V. P. Response of the atmosphere at high and middle latitudes to the reduction of sea ice area and the rise of sea surface temperature // *Russian Meteorology and Hydrology* 2014. N 6. P. 5–18.

51. Alekseev G. V. Studies of the Ocean and Atmosphere interaction in the North polar area on programs of the large scale field experiments “FEI”, “POLEX-Sever”, “SECTIONS” in 1960–1980s // *Arctic and Antarctic Problems*, 2014. N1 (99). P. 41–52.

52. Karol I. L., Meleshko V. P., Baidin A. V., Kiselev A. A. The radiative and thermodynamic seasonal factors of the Arctic climate warming // *Arctic and Antarctic Problems*. 2014. N3(101). P. 5–15.

53. Radionov V. F., Aleksandrov E. I., Bryazgin N. N., Dementiev A. A. Changes in temperature, precipitation and snow cover in the Arctic Seas region, 1981–2010 // *Ice and Snow*. 2013. N 1 (121). P. 61–68.

54. Sorokina S. A., Esau I. N. Meridional energy flux in the Arctic from data of the radiosonde archive IGRA // *Izvestiya, atmospheric and oceanic physics*. 2011. V. 47, N 5. P. 572–583. DOI: 10.1134/S0001433811050112.

55. Nagurnyi A. P. Variations of Characteristics of the Mean Atmospheric Energy Level in the Area of the Franz Josef Land Archipelago in 1935–2012 // *Russian Meteorology and Hydrology*. 2014. N 1. P. 21–30.

56. Popova V. V., Polyakova I. F. Changes of dates of snow cover lost in the North of Eurasia in 1936–2008: influence of global warming and role of large-scale atmospheric circulation // *Ice and Snow*. 2013. N 2 (122). P. 59–70.

57. Polyakova E. V., Iglovsky S. A. Patterns of snow cover distribution in the subarctic hydrothermal Pymvashor area *Ice and Snow*. 2012. N 2 (118). P. 76–80.

58. Shmakin A. B., Osokin N. I., Sosnovsky A. V., Zazovskaya E. P., Borzenkova A. V. Influence of snow cover on soil freezing and thawing in the West Spitsbergen // *Ice and Snow*. 2013. N 4 (124). P. 52–59.

59. Osokin N. I., Sosnovsky A. V. Spatial and temporal variability of depth and density of the snow cover in Russia // *Ice and Snow*. 2014. N 3. P. 72–80.

60. Osokin N. I., Sosnovsky A. V. Field investigation of efficient thermal conductivity of snow cover on Spitsbergen // *Ice and Snow*/ 2014. N 3. P. 50–58.

61. Osokin N. I., Sosnovsky A. V. Spatial and temporal variability of depth and density of the snow cover in Russia // *Ice and Snow*. 2014. N 4. C. 72–80.

62. Ivanov B. V., Pavlov A. K., Andreev O. M., Zhuravskiy D. M., Svyashchenikov P. N. Investigation of snow and ice cover in Grönfjorden (Spitsbergen): historical data, in situ observations and modelling // *Arctic and Antarctic Problems*. 2012. N 2(92). P. 43–54.
63. Sokratov V. S., Shmakin A. B. Numerical modeling of a snow cover on Hooker Island (Franz Josef Land archipelago) // *Лед и снег*. 2013. N 3 (123). P. 55–62.
64. Popova V. V., Shiryayeva A. V., Morozova P. A. Snow cover onset dates in the north of Eurasia: relations and feedback to the macro-scale atmospheric circulation // *Ice and Snow*. 2014 N 3 (127). P. 39–49.
65. Asmus V. V., Bukharov M. V., Mironova N. S., Sizenova E. A. Properties of the snow-Firn cover of greenlandic glaciers from the satellite measurements of its scattering index // *Russian Meteorology and Hydrology* 2012, N 4. P. 5–16.
66. Krenke A. N., Cherenkova E. A., Chernavskaya M. M. Stability of snow cover on the territory of Russia in relation to climate change // *Ice and Snow*. 2012. N 1 (117). P. 29–37.
67. Kononova N. K. The influence of atmospheric circulation on the formation of snow cover on the north eastern Siberia // *Ice and Snow*. 2012. N 1 (117). P. 38–53.
68. Kolomyts E. G. Evolutionary conception of snow metamorphism based on crystal-morphology and theory of symmetry // *Ice and Snow*. 2012. N3 (119). P. 31–46.
69. Golubev V. N. Nucleation and growth of ice crystals in the atmosphere // *Ice and Snow*. 2013. N 1 (121). P. 53–60.
70. Belikov Yu. E., Nikolaishvili S. Sh Possible Mechanism of Ozone Depletion on Ice Crystals in the Polar Stratosphere // *Russian Meteorology and Hydrology* 2012, N 10. P. 33–43.
71. Andreev O. M. Effect of vertical inhomogeneity of the ridge keel filling on its freezing rate // *Ice and Snow*. 2013. N 2 (122). P. 63–68.
72. Shur G. N., Volkov V. V., Sitnikov N. M., Ulanovskii A. E., Sitnikova V. I. Studying the Mesoscale structure of inhomogeneities within the high-latitude stratosphere during the evolution of the circumpolar vortex on the basis of aircraft measurements // *Izvestiya, atmospheric and oceanic physics* 2014. V. 50, N 2, P. 171–178 DOI: 10.1134/S0001433814020108.
73. Nedashkovsky A. P. Emission and absorption of CO₂ during the sea ice formation and melting in the high Arctic // *Ice and Snow*. 2012. N1 (117). P. 75–84.
74. Polyakov S. P., Andreev O. M., Ivanov B. V., Bezgreshnov A. M. Effect of hummocky masses on the radiation characteristics of sea ice // *Ice and Snow*. 2011. N 4 (116). P. 80–84.
75. Ivanov B. V., Andreev O. M. On the problem of determination of hummocky formation albedo // *Russian Meteorology and Hydrology*. 2011. N 6. P. 78–83.
76. Ivanov B. V., Andreev O. M. On the problem of determination of hummocky formation albedo // *Russian Meteorology and Hydrology* 2011. N 2. P. 58–63.
77. Groisman P. Ya., Bogdanova E. G., Alexeev V. A., Cherry J. E., Bulygina O. N. Impact of snowfall measurement deficiencies on quantification of precipitation and its trends over Northern Eurasia // *Ice and Snow*. 2014. N 2. P. 29–43.

78. Gruza G. V., Ran'kova E. Ya. Dynamic Normals of Surface Air Temperature // Russian Meteorology and Hydrology. 2012. N 12. P. 5–18.
79. Semenov E. K., Sokolikhina N. N., Tudrii K. O. The Warm Winter in the Russian Arctic and Anomalous Cold in Europe // Russian Meteorology and Hydrology. 2013. N 9. P. 43–52.
80. Egorov A. G. Solar activity and spatial variations of the middle troposphere at the middle and high latitudes of the Northern Hemisphere in winter // Russian Meteorology and Hydrology 2014. N 10. P 32–45.
81. Bychkova V. I., Rubinshtein K. G. Preliminary Results of Testing the Snowstorm Short-range Forecast Algorithm // Russian Meteorology and Hydrology. 2013. N 6. P. 30–42.
82. Danilov A. I., Lagun V. E., Klepikov A. V. Antarctic climate current changes. / In «Meteorological and geophysical researches». 2011. P. 26–48.
83. Radionov V. F., Rusina E. N., Sakerin S. M., Sibir E. E., Smirnov A. V. Components of the radiation balance and aerosol — optical parameters in Antarctica during IPY compared with their long-term variability. Ibid. P. 158–169.
84. Kashin F. V., Paramonova N. N., Privalov V. I. The results of monitoring of carbon dioxide and methane concentrations in the air near the surface at the Antarctic station Novolazarevskaya in 2007–2009. Ibid. P. 170–177.
85. Sibir E. E., Radionov V. F. Total ozone content in Antarctica during International Polar Year. Ibid. P. 178–186.
86. Gabis I. P., Troshichev O. A. Changeability of atmospheric circulation and ozone content in the southern polar region: allowance for solar UV variations. Ibid. P. 306–330.
87. Kotlyakov V. M. On the history of the international project of deep ice-core drilling at Vostok station // Ice and Snow. 2012. N 4 (120). P. 5–8.
88. Barkov N. I. The first borehole at Vostok station // Ice and Snow. 2012. N 4 (120). P. 9–11.
89. Ananicheva M. D., Krenke A. N., Semenov A. E., Turkov D. V. Dependence of the snow accumulation in Antarctica from sea ice area // Ice and Snow. 2011. N 4. P. 47–56.
90. Ekaykin A. A., V. Ya. Lipenkov, Yu. A. Shibaev. Spatial distribution of the snow accumulation rate along the ice flow lines between Ridge B and Lake Vostok // Ice and Snow. 2012. N 4 (120). P. 122–128.
91. Hodzher T. V., Golobokova L. P., Osipov E. Yu., Onishchuk N. A., Filippova U. G., Lipenkov V. J., Ekaykin A. A. Volcanic events record over the last 900 years from snow and firn sequence in Vostok station area // Ice and Snow. 2012. № 2. P. 115–121.
92. Golobokova L. P., Hodzher T. V., Shibaev Yu. A., Lipenkov V. Y., Petit J.-R. Chemical composition change of subsurface snow in East Antarctica with distance from the coast // Ice and Snow. 2012. N 2. P. 129–137.
93. Lefebvre E., Arnaud L., Ekaykin A. A., Lipenkov V. Y., Picard G., Petit J.-R. Snow temperature measurements at Vostok station from an autonomous recording system (TAUTO): preliminary results from the first year operation // Ice and Snow. 2012. № 2. P. 138–145.

94. Bulat E. S., Tsel'movich V. A., Petit J.-R., L. M. Gindilis, S. A. Bulat Snow cover of the Central Antarctica (Vostok station) as an ideal natural tablet for cosmic dust collection: preliminary results on the identification of micrometeorites of carbonaceous chondrite type // *Ice and Snow*. 2012. N 2. P. 146–152.
95. Popov S. V., Eberlein L. Investigation of snow-firn thickness and ground in the East Antarctica by means of geophysical radar // *Ice and Snow*. 2012. N 3. P. 95–106.
96. Landais A., Ekaykin A., Barkan E., Winkler R., Luz B. Seasonal variations of ^{17}O -excess and δ -excess in snow precipitation at Vostok Station, East Antarctica. — *J. Glaciology*. 2012. V. 58. N 210. P. 725–733.
97. Richter, A., Fedorov, D. V., Fritsche, M., Popov, S. V., Lipenkov, V. Ya., Ekaykin, A. A., Lukin, V. V., Matveev, A. Yu., Grebnev, V. P., Rosenau, R., Dietrich, R. Ice flow velocities over subglacial Lake Vostok, East Antarctica, determined by 10 years of GNSS observations. — *J. of Glaciology*, 2013, V. 59, N 214, P. 315–326.
98. Winkler R., Landais A., Risi C., Baroni M., Ekaykin A., Jouzel J., Petit J.-R., Prie F., Minster B., Falourd S. Water isotopologues at Vostok (East Antarctica) suggest a stratospheric influence, accounting for mass independent fractionation // *Proceeding of the National Academy of Sciences*, 2013, V. 110, N 44, P. 17674–17679.
99. Ekaykin A. A., Lipenkov V. Ya., Popov S. V., Turkeev A. V., Kozachek A. V., Vladimirova D. O. Spatial variability of Antarctic mega-dunes snow characteristics in the vicinity of the subglacial Lake Vostok // *Arctic and Antarctic Problems* 2014. N 4. P. 71–89.
100. Vladimirova D. O., Ekaykin A. A. Climatic variability in Davis Sea sector (East Antarctica) over the past 250 years based on the 105 km ice core geochemical data // *Arctic and Antarctic Problems* 2014. N 1. (99). P. 102–113.
101. Kozachek A. V., Ekaykin A. A., Lipenkov V. Y., Shibaev Y. A., Vaikmäe R. On the relationship between climatic variability in central Antarctica and the climate of middle and low latitudes of Southern Hemisphere // *Arctic and Antarctic Problems* 2011. N 4(90). P. 5–13.
102. Kazakova N. N., Fridzon M. B. Assessment of uniformity of the data series of temperature-wind sounding of the atmosphere at the Russian Antarctic stations // *Arctic and Antarctic Problems*. 2011. N 1 (87). P. 41–55.
103. Rusina E. N., Radionov V. F., Sibir E. E. Variability of aerosol and optical parameters of the atmosphere in Northern and Southern polar regions after 2000 // *Arctic and Antarctic Problems* 2013. N1(95). P. 51–60.
104. Makshtas A. P., Ivanov B. V., Timachev F. Comparison of universal functions of stability in conditions of strong stable-stratified atmosphere // *Arctic and Antarctic Problems*. 2012. N (93) P. 5–16.
105. Mokhov I. I., Malyshev A. V. Analytical Estimate of the Critical Global-Warming Level for the Antarctic Ice Sheet Mass Gain-to-Loss // *Transition Doklady Earth Sci* Vol. 436, Part 1, 2011 155–158. DOI: 10.1134/S1028334X11010284.
106. Kaur R, Dutta H. N., Deb N. C., Gajananda K., Srivastav M. K., Lagun V. E. Investigation of Unusual Atmospheric Warming over the Schirmacher oasis, East Antarctica // *International Journal of Science and Technology*, 2013. V. 2. N 7. P. 550–559.

-
107. Kaur R, Dutta H. N., Deb N. C., Gajananda K., Srivastav M. K., Lagun V. E. Role of coreless winter in favoring survival of microorganisms over the Schirmacher oasis, east Antarctic // *Journal of Ecophysiology & Occupational Health* (The Academy of Environmental Biology, India). 2013. N 1–2. P. 11–19.
108. Gajananda Kh., Dutta H. N., Lagun V. E. Land-Ie-air-ocean interactions In *The Schirmacher Oasis, East Antarctica / In "Antarctica: The Most Interactive Ice-Air-Ocean Environment"* (Editors: Singh J., Dutta H. N.). Chapter 3. 2011. Nova Science Publishers. P. 39–88.
109. Andersen D. T., McKay C. P., Lagun V. Climate conditions at perennially ice-covered Lake Untersee, East Antarctica // *Journal of Applied Meteorology and Climate*. 2014 (In Press).
110. Troshichev O. A., Vovk V. Ya., Egorova L. V. Solar wind influence on atmospheric processes in winter Antarctica / In *"Antarctica: The Most Interactive Ice-Air-Ocean Environment"* (Editors: Singh J., Dutta H. N.). Chapter 9. 2011. Nova Science Publishers. P. 173–197.
111. Klepikov A. V., V. E. Ryabinin, A. I. Danilov, V. G. Dmitriev. On the preparation of the international polar partnership initiative. *Problems of the Arctic and Antarctic*. 2014. No. 4 (102). P. 104–112.

Atmospheric Radiation

Yu. M. Timofeyev, E. M. Shulgina

St. Petersburg State University
tim@troll.phys.spbu.ru

On the basis of materials presented by L. P. Bass (Keldysh Institute of Applied Mathematics RAS (IAM RAS)); V. P. Budak (Moscow Power-Engineering Institute (MPEI)); A. A. Cheremisin (Siberian Federal University (SFU)); N. E. Chubarova, S. A. Terpygova (Lomonosov Moscow State University (MSU)); G. I. Gorchakov, I. A. Gorchkova, S. A. Sitnov and M. A. Sviridenkov (Obukhov Institute of Atmospheric Physics (IAP RAS)); I. L. Karol (Voeikov Main Geophysical Observatory, MGO); E. N. Kadygrov (Central Aerological Observatory (CAO)), A. F. Neryshev (Scientific and Production Association “Typhoon” (Typhoon)); V. I. Perevalov, Yu. N. Ponomarev, S. M. Sakerin, T. K. Sklyadneva and T. B. Zhuravleva (Zuev Institute of Atmospheric Optics SB RAS (IAO SB RAS)); V. F. Radionov (Arctic and Antarctic Research Institute (AARI)); A. N. Rublev (Russian Research Center “Kurchatov Institute” (Kurchatov Institute)); A. B. Uspensky (Scientific Research Center for Space Hydrometeorology “Planeta” (Planeta)).

During 2011–2014 the Russian Radiation Commission in cooperation with interested departments and institutions hold two International Symposia on Atmospheric Radiation and Dynamics (ISARD-2011, ISARD-2013). At these conferences most actual problems of atmospheric physics (radiation transfer and atmospheric optics, greenhouse gases, clouds and aerosols, climate changes, remote measurement methods, new observation data) were discussed. In this review, 6 directions of studies covering the complete spectrum of investigations in atmospheric radiation are given.

1. Radiation Transfer

Numerous investigations in this line are devoted to the theoretical study of the radiative transfer in different mediums and for different measurement geometries and the development of methods and algorithms for solving the radiation transfer equation as applied to different problem of atmospheric optics.

Different methods of radiation transfer theory have been intensely developed by the MPEI team. The substantiation of the radiative transfer equation (RTE) has been carried out from the standpoint of statistical optics [Budak and Veklenko, 2011]. The essential difference of the method using in this article is the application of the L. V. Keldysh matrix Green’s functions. Traditionally, the approach used here is the Dyson and Bethe-Salpeter equations. Bethe-Salpeter

equation is quadratic, while the matrix Green's function lead to a system of linear equations of the Dyson type. That allows getting much more general results in the derivation of kinetic equations in the approximation of geometrical optics. A solution of the discrete RTE for the planar stratified slab with arbitrary conditions at the boundary is found in the analytical matrix form [Budak et al., 2011]. Numerical solution of the RTE is possible only based on its sampling that demands the replacement of the scattering integral by the finite sum. Since the physical basis of the transfer theory is the geometrical optics approximation, the solution always contains angular singularities. Therefore, to sample RTE it is necessary to eliminate the anisotropic part of the solution, including all of its singularities, even approximately, but analytically, and to formulate the equation for the regular part solution. The anisotropic part elimination in the RTE solution in other geometries and numerical determination of its regular part is considered in papers [Ilyushin and Budak, 2011a, 2011b, 2011c; Budak and Ilyushin, 2011]. The generalization of the small-angle modification of the spherical harmonics method (MSH) is proposed for the refinement of the scattered photon path dispersion. MSH is the most general form of the small-angle approximation, which permits to eliminate the solution anisotropic part and to formulate the equation for the regular part, which solution is possible numerically [Budak and Ilyushin, 2011]. Comparison of different algorithms for solving the RTE for a slab by the efficiency and the estimation of the hardware and software impact has been performed. It is shown that it is based on a unique analytic solution of the discrete RTE. For sampling RTE, the scattering integral should be represented by a finite sum, which is possible only after the angular singularity elimination in the solution. Exist algorithms differ in the way of the solution anisotropic part elimination. It is shown that the most effective method of such elimination is MSH. Because the solution is reduced to a matrix expression, the efficiency of the algorithm is determined by the effectiveness of matrix operations implementation [Budak et al., 2012]. The fact that the basis of all algorithms for solving problems for the slab is one analytical solution of the discrete RTE imposes significant limitations: the speed and accuracy of the solution are inversely related. The calculation difficulties are determined by the dimension of the solution matrix, which in turn depend on the accuracy of the solution regular part representation. It is shown that the number of basis functions in the solution regular part representation is determined by the analog of the Kotelnikov-Shannon theorem: the sampling step should correspond to the smallest angular details of the solutions. This defines a contradiction: the requirements for algorithms of the inverse solution define the direct problem. Today we need an algorithm solving the RTE with a precision of a uniform metric better than 1%, and the computation time is not more than 1 second for one wavelength. It is obvious that satisfy both conditions at once in the framework of the

traditional RTE solution impossible. To overcome this problem it is proposed to use the synthetic iteration that was developed in neutron transport theory. It is shown that it can satisfy the requirements of the inverse solution [Budak and Shagalov, 2013; Budak et al., 2014]. An algorithm for the calculation of the light field in a scene of arbitrary geometry with the multiple reflections from the boundaries has been proposed. It is based on the double local estimation of the Monte Carlo method for the calculation of the decomposition of the desired angular radiance distribution system of spherical functions that eliminates the divergence of the double local estimation. The proposed solution of discrete RTE for a slab is tested for the extreme case of a semi-infinite medium with a single scattering albedo equal 1 by the comparison of other algorithms and in situ measurements. It is shown that, in this case, for an accurate determination of the eigenvalues of the system matrix should use its Jordan form [Sokoletsky et al., 2014]. The effect of coherent scattering impact on the formation of the light field in a turbid medium has been investigated. For this purpose, it was proposed the algorithm of the numerical solution of the Mie theory for a system of one, two and four particles. The calculation of multiple scatterings was based on the Monte Carlo method. It has been shown that coherent scattering does not affect the point spread function of the slab that defines the object visibility through the thickness of a turbid medium [Fokina et al., 2014].

A rigorous approach to the solution of Maxwell equations for a monochromatic field in a homogeneous uniaxial medium has been considered [Marakasov and Troitskii, 2012]. The approach is based on using the tensor Green's function. The general solution satisfying arbitrarily specified boundary conditions is presented. Various models of exponentially correlated random fields associated with Poisson point ensembles, as well as algorithms for simulating radiative transfer in stochastic media of that type, are considered [Mikhailov, 2012].

A number of papers have been devoted to techniques for calculating the radiative transfer in the context of atmospheric and underlying surface remote sensing. The light scattering in water-drop clouds for various distributions of droplet size has been studied. Polarization and angular distributions are simulated by Monte Carlo method for radiation reflected by cloud layers. Computational results make it possible to develop procedures for analyzing the microphysical structure of clouds [Prigarin et al., 2014]. The passive retrieval technique for investigation of the vertical structure of clouds and aerosols from satellites is discussed [Fomin and Falaleeva, 2014]. This technique uses a combination of cross-nadir polarimetry and high-resolution infrared (IR) spectroscopy. The real potential of this technique is demonstrated with the help of a set of numerical experiments, e.g. for the detection of cirrus clouds (Ci). In this regard, new vector versions for the longwave and shortwave in the FLBLM (Fast Line-by-Line Model) radiative transfer model are presented. These new versions are based on

the Line-by-Line (LbL) and “local estimation” Monte Carlo (MC) methods and can calculate the Stokes parameters of the outgoing radiation in vertically inhomogeneous atmospheres with any spectral resolution. The influence of 3D effect on snow reflection function and albedo has been studied in the framework of the stochastic radiative transfer theory [Zhuravleva and Kokhanovsky, 2011]. In particular, the corresponding equations for the averaged intensity of reflected light are solved for the ensemble of realizations of the stochastic field, describing the distribution of 3D elements on the flat semi-infinite snow layer. It is found that the albedo of snow layer is reduced (in particular, in the infrared region), if 3D effects are taken into account. The sea and land surface models used in remote sensing have been developed [Zapevalov and Lebedev, 2014; Matelenok and Melentyev, 2014]. The method of integral distributions is developed for determining the atmospheric aerosol micro-structure from spectral measurements of the aerosol optical depth [Veretennikov and Men’shchikova, 2013].

2. Atmospheric Molecular Spectroscopy

Main directions of investigations in the molecular spectroscopy of atmospheric gases are experimental studies of spectroscopic parameters, the development of methods for calculating the parameters of spectral lines, transmittance functions and the updating of spectroscopic databases.

At the IAO RAS, the analysis and theoretical modeling of experimental spectra of H_2O , CO_2 , O_3 , O_2 , CH_4 , N_2O , NO_2 , C_2H_2 molecules and their isotopic modifications in different spectral ranges and under different conditions are intensively carried on in cooperation with foreign scientists. The investigations are directed to studying the spectroscopic parameters of gases, peculiarities of the spectra obtained by different methods and intermolecular interactions. Results of such studies for atmospheric gases and water vapor are given, for example, in papers [Lyulin et al., 2011, 2013, 2014; Beguier et al., 2011; Liu et al., 2011; Mikhailenko et al., 2011; Lu et al., 2012; Jacquemart et al., 2012; Leshchishina et al., 2011a, 2011b, 2012, 2013; Lukashevskaya et al., 2013; Karlovets et al., 2013, 2014; Oudot et al., 2012; Régalia et al., 2014; Daumont et al., 2012]. Results of these studies contributed greatly to the development of databases and information systems by new and refined information [Rothman et al., 2013; Tashkun et al., 2011; Rey et al., 2014; Lavrentieva et al., 2014; Babikov et al., 2013]. In the frames of the Project IUPAC «A database of water transitions from experiment and theory» jointly with scientists of other countries, a critical expertise of the water vapor rotational-vibrational spectra and transitions has been performed [Tennyson et al., 2013, 2014a, 2014b].

A number of studies have been carried out in context of remote sensing the atmospheric methane and carbon dioxide. The main spectroscopic factors

contributing to the uncertainty in calculations of atmospheric radiative transfer in methane strong absorption bands in near-IR range, which are used to retrieve the methane content in the atmosphere, have been studied. The uncertainties in the parameters of the absorption lines of atmospheric gases in modern databases, as well as the effect of the methane line mixing, are estimated. Methods for enhancing the accuracy of modeling the atmospheric transmittance are proposed. It is shown, that the different spectroscopic databases can give significantly different results for both forward simulations of the atmospheric transmittance and the inverse problem of retrieving the CH₄ total content using spectra measured by ground-based FTIR spectrometer [Chesnokova et al., 2011; Chesnokova, 2013]. On the basis of laboratory measurements of methane absorption spectra, using acoustic and photometric spectrometers based on a tunable diode laser, parameters of overlapping absorption lines of R5 and R9 methane multiplets broadened by nitrogen and neon were defined at pressures of broadening gases of 0.005–0.5 atm. [Osipov et al., 2012; Kapitanov et al., 2012, 2013]. Analysis of laboratory data showed a significant deviation of the line shapes from the Voigt profile, which is typically used in atmospheric modeling. The use of contour Routine-Sobelman profile allowed with an error of less than 1% to describe the experimental spectra.

In paper [Chentsov et al., 2013] the influence of differences in the parameters of CO₂ spectral lines in spectroscopic databases HITRAN-2008 and CDSD on the modeling of atmospheric transmittance has been studied, and it is shown that the difference in the transmissions can reach 10% or more in the strong CO₂ absorption bands.

3. Radiative Climatology

The research work in the frames of this topic has been carried out in several directions: the monitoring of components of radiation budget (RB) and atmospheric constituents effecting the radiation; the study of RB climatic trends near a surface; the analysis of radiative effects caused by atmospheric gases.

Influence of variations of meteorological parameters and distinctions in models of the H₂O continual absorption on calculations of solar and thermal radiation fluxes under conditions realized during various seasons in Western Siberia [Chesnokova et al., 2012, 2013; Zhuravleva et al., 2014] and the Lower Volga Region [Firsov et al., 2013, 2015] have been estimated. Based on calculations of total, direct and diffusion solar radiation fluxes in the 0.2–5 mm range under cloudless atmosphere for various models of the water vapor continual absorption and various total moisture contents characteristic for summer and winter conditions of Western Siberia, it is shown that the CAVIAR model of the continual absorption based on new experimental data provides the higher sensitivity of calculated

solar radiation fluxes to the total moisture content in comparison with the MT_CKD model [Chesnokova et al., 2012, 2013]. For the Lower Volga Region the regression dependence of the CO₂ radiation forcing on the total moisture content is calculated, and the CO₂ radiative forcing is shown to strongly depend on the continuum magnitude. The atmospheric conditions are determined, under which the contribution of the H₂O continuum due to the interaction of water vapor with air molecules to the downward radiative fluxes, is maximal [Firsov et al., 2015].

Team of the IAO SB RAS in 2011–2014 carries on the long-term monitoring of the total and UV radiation in Tomsk and the Tomsk region, and also in certain regions of Western Siberia. On the basis of TOR station (56°28'N of 85°03'E), systematic measurements of total solar radiation and the integrated intensity of UF-V radiation have been conducted since April, 1995, and October, 2002, respectively. Since 2004, IAO SB RAS in cooperation with National institute of Environmental Research (Japan) has carried out the monitoring of the total solar radiation and greenhouse and oxidizing components at the Western Siberian network. Spatial-temporal variability of the total solar radiation in West Siberia during 2004–2011 was jointly analyzed [Arshinov et al., 2013]. Radiation regime in Tomsk during 1995–2010 and the influence of a city on the incoming UV radiation from results of many-year monitoring near Tomsk-city were analyzed in papers [Belan et al., 2012, 2011]. In paper [Ivlev et al., 2013], dynamics of solar UV-B and UV-A radiations in Tomsk during ozone anomaly in spring, 2011 was analyzed and the variability of the UV radiation spectral characteristics depending on the total ozone content was estimated.

At MSU, the influence of different factors on different types on biologically active UV radiation has been estimated [Zhdanova and Chubarova, 2011], new methods were developed for estimating the UV radiation in winter [Zhdanova et al., 2013], the spatial distribution of UV radiation and UV resources over territory of Northern Eurasia and Russia under different conditions were obtained [Chubarova and Zhdanova, 2013]. According to the developed methods and long-term measurements, the UV resources in Moscow were estimated from 1999 till 2013 [Zhdanova, Chubarova, 2014].

Complex studies were fulfilled for estimating the changes in different meteorological and environmental characteristics including the radiative balance and solar radiation in different spectral intervals over 60 years in Moscow [Chubarova et al., 2014]. The resources of solar radiation with accounting the current climate change in the Moscow region are evaluated [Gorbarenko and Shilovtseva, 2013]. Analysis of trends in the long-term variability of total radiation (1955–2012) indicates an increase in solar power resources in Moscow and region in early of the XXI century. The coherence of total radiation change tendencies observable by the Meteorology Observatory MSU with global trend is shown in paper [Samukova et al., 2014]. A dramatic increase in the values of annual sums

of radiation balance has been observed since 1994 [Gorbarenko and Abakumova, 2011]. The tendencies toward the increase in radiation balance, longwave balance, and atmospheric downward radiation have a diurnal course: the maximum variations are observed at nighttime in winter months [Gorbarenko, 2014].

4. Aerosol and Radiation Forcing

Extensive laboratory and ground-based measurements of aerosol parameters, the modeling, and the estimating of the aerosol impact on radiative characteristics of the atmosphere have been carried out at IAO SB RAS, SPbSU, IAP, MGO.

Laboratory studies of aerosol characteristics under the artificial moistening (from 1998) and optical and radiative smoke parameters have been conducted [Rakhimov et al., 2012, 2014] at the IAO SB RAS. Results of multi-year studies of the aerosol condensation activity in Tomsk are integrated [Panchenko et al., 2012a; Terpugova et al., 2012]. A new differential analyzer implementing a technique for studying the hygroscopic properties of filter-precipitated aerosol particles out-performing other similar models has been created [Mikhailov et al., 2011] at the SPbSU. A mass-based hygroscopicity parameter interaction model for efficient description of concentration-dependent water uptake by atmospheric aerosol particles with complex chemical composition is developed [Mikhailov et al., 2013]. Seasonal variations of the ionic composition and the organic and elementary carbon in aerosol probes of Siberian region from 2011 to 2013 and the analysis of aerosol pollution sources in this region have been analyzed. New information on hygroscopic characteristics of atmospheric particles with sizes of 10 nm–10 μ m is obtained for the moisture content of 2–99.6% RH [Sviridenkov et al., 2014].

In 2011–2013 the Planeta together with researchers from Kurchatov Institute, IAO SB RAS and MSU conducted a study of capabilities and limitations of the well-known AERONET network for estimations of optical and microphysical characteristics of coarse aerosol clouds. The quantitative estimates of coarse particle effect on the accuracy of aerosol parameter retrieval from ground-based measurements of spectral fluxes of direct and scattered solar radiation were obtained on the basis of mathematical modeling [Rublev et al., 2011]. The verification of the retrieval algorithm of the well-known AERONET global aerosol network based on special test models has shown the impossibility of using the aerosol parameters retrieved by the algorithm in calculations of integral solar fluxes while dust particles content in the atmosphere is more than two times higher than their content in widespread CONT model of continental aerosol. The same is fair for simulation of space spectroscopic IR measurements. The possibilities for increasing accuracy of the forecast of volcanic aerosol distribution, based on ground actinometrical measurements data, were considered in [Rublev et al., 2013]. The numerical forecast concentrations of volcanic ash from

Grimsvotn volcano in Iceland (May 2011) were adjusted to the results of aerosol optical thickness measurements at the site of the AERONET global network in Hamburg. Comparison of the corrected concentrations with those from the other AERONET sites demonstrated validity of the proposed approach. Actinometrical network of the Russian Meteorological Agency can be used to specify aerosol cloud distribution forecast over Russia's territory. The aerosol properties of the atmosphere in Moscow were estimated using AERONET data [Chubarova et al., 2010] and collocated measurements in Moscow and Zvenigorod. It has been shown that aerosol pollution effects are not very large (about 0.02 in aerosol optical transmittance (AOT) at 500 nm) [Chubarova et al., 2011a]. Using these datasets the cooling effect of urban aerosol was also shown.

Permanent studies of aerosol optical and microphysical characteristics in different Earth regions are carried on. Methodical basis was developed; the apparatus complex was created and combined experiment on studying aerosol characteristics and estimating the input of atmospheric aerosol in the planet radiative balance was performed [Matvienko et al., 2014a, 2014b]. Regular expedition studies of aerosol characteristics have been conducted in marine and high-latitude Earth regions (on Arctic Ocean coast, Antarctic, archipelago Spitsbergen, Atlantic). Latitudinal dependence of aerosol characteristics and its inter-annual trend over Atlantic Ocean and seasonal and in inter-annual variability of parameters at Spitsbergen are determined [Pol'kin et al., 2013; Sakerin et al., 2012a]. Results of aerosol measurements conducted at Russian Antarctic Station "Vostok" and over Caspian Sea were analyzed [Pol'kin et al., 2012, 2014]. Variability of aerosol and optical parameters of the atmosphere in northern and southern polar regions after 2000 is estimated [Rusina et al., 2013]. Combined measurements of aerosol and soot concentrations and size distributions were performed in the near-ground atmospheric layer near Vladivostok and in the near-sea layer in the water area of Japanese sea [Pol'kin et al., 2011]. Speculiarities of spatial-temporal variability of aerosol microphysical characteristics of the atmosphere and the near-ground layers in the transitional zone "continent-ocean" were studied [Shmirko et al., 2014]. Aerosol characteristics were determined during different fire episodes [Trefilova et al., 2013].

Numerous studies were directed to studying the aerosol optical depth (AOD) in different regions. In 2014 the monograph generalizing results of combined aerosol studies in Asian Russia was published [Sakerin S.M. (ed.), 2012]. Regularities of AOD spatial-temporal variability in the Asian Russia atmosphere were studied in papers [Sakerin et al., 2011, 2012b, 2012c, 2014a; Kabanov et al., 2011, 2013, 2014a; Zayakhanov et al., 2012; Poddubnyi et al., 2013]. Similar studies were carried out also for marine and polar regions [Sakerin et al., 2014b, 2014c; Kabanov et al., 2014b] and in the frames of International Programs [Tomasi et al., 2012; Smirnov et al., 2011, 2012].

A number of investigations were devoted to studying thermal effects of smoke aerosol and the radiative forcing during various wildfires. The radiative properties of smoke aerosol in Moscow and Moscow region during extreme conditions of forest fires in 2010 have been studied [Chubarova et al., 2012; Gorchakova and Mokhov, 2012; Shukurov et al., 2014]. Approximation of the smoke aerosol forcing at the atmospheric bottom boundary has been developed [Rublev et al., 2011]. Using the microphysical modeling, the influence assessment of the coarse mode with particle radii greater than 15 μm on the dust aerosol optical properties is obtained. In addition, the comparative analysis has been performed for different fire episodes in Moscow (during 1972, 2002 and 2010 summer periods) and it is shown that the strongest radiative effects are observed in 2010 [Chubarova et al., 2011b]. In June–August 2012, the team of the IAO SB RAS conducted the combined experiment for studying the dynamics of optics-microphysical characteristics of the submicronic aerosol in the near-ground air layer under the smoke haze from Siberian forest fires [Kozlov et al., 2014; Uzhegov et al., 2014; Popovicheva et al., 2014]. Differences in optical and microphysical characteristics of the near-ground aerosol under conditions of the haze smoke and non-smoked atmosphere were estimated.

Methods for the aerosol remote sensing and models for parameterizing the aerosol parameters have been constantly developed and improved. New method (SSMART) for retrieving the aerosol optical and microphysical characteristics is proposed and tested [Bedareva and Zhuravleva, 2011; Bedareva et al., 2013a]. The characteristics are retrieved from data of ground-based AOD spectral measurements and scattered radiation in the solar almucantar. Refined version of the method [Bedareva et al., 2014] has been tested under conditions of moderate and strong aerosol turbidity for Tomsk and Dakar [Bedareva and Zhuravleva, 2012; Bedareva et al., 2013b] and it is shown that retrieved aerosol characteristics fit to AERONET data within total errors. On the basis of data of long-term airborne sounding of vertical profiles of aerosol directed scattering coefficients, the disperse composition and also the maintenance of the absorbing particles, the generalized empirical model of aerosol optical characteristics in the lower 5-kilometer layer of the atmosphere of Western Siberia has been developed [Panchenko et al., 2012b, 2012c]. The model allows retrieving aerosol optical characteristics in visible and near-IR spectral ranges. Spectral dependences of the single-scattering albedo at different altitudes are estimated [Panchenko et al., 2014]. Two-parametric model has been developed for retrieving the aerosol extinction coefficients in visible and near-IR spectral ranges on a long near-ground path from data on the aerosol parameters in a local volume. Spectral dependence of the single-scattering albedo at the 0.45–3.9 μm wavelengths is estimated [Pkhlagov et al., 2013; Pkhlagov and Uzhegov, 2014].

Along with the works estimating the radiation forcing of aerosol and other anthropogenous factors, forming changes of the radiation regime, their impact on climate changes has been studied. The current state of studies on short-lived atmospheric constituents (greenhouse gases and aerosols), sources and destruction mechanisms, estimates of their content, atmospheric emissions, and climate impacts is reviewed [Karol' et al., 2013]. Indices of factors forming multi-scale climate changes, rates of their changes and the input in rates of changing the climatic characteristics are discussed [Karol' et al., 2011, 2012]. Several factors forming the Arctic climate have been considered. Model estimates of contribution of both sea surface temperature and sea ice extent changes during two periods 1980–1989 and 2002–2011 are shown. Also seasonal changes of meridional energy transport into the high northern latitudes (to north of 70°N) are discussed [Karol et al., 2014]. The impact of the size distribution and structure of stratospheric sulphate aerosol on its optical parameters and the radiative forcing are estimated [Frolkis and Kokorin, 2014].

Studies of the photophoretic interaction of aerosol particules illuminated by sunlight in the Earth's rarified atmosphere are carried on at the Siberian Federal University (SFU) and the IAO. A detailed theoretic investigation has been carried out for vacuum chamber conditions [Cheremisin and Kushnarenko, 2013] and for atmospheric conditions [Cheremisin and Kushnarenko, 2014]. Theoretical analysis of the photophoretic motion of soot particles in the field of solar radiation under the conditions of stationary atmosphere is performed [Beresnev et al., 2012]. The hypothesis of photophoretic force sustaining of aerosol layers in the middle atmosphere has been further developed [Cheremisin et al., 2011a]. Systematic lidar observations of aerosol layers in the upper stratosphere and the mesosphere at altitudes of 35–50 and 60–75 km over Kamchatka [Bychkov et al., 2011] can be explained by the occurrence of photophoretic force, resulting in the levitation of aerosol particles at specified altitudes. The transfer of volcanic origin aerosol [Cheremisin et al., 2011b] and polar stratospheric clouds over Tomsk [Cheremisin et al., 2012] is identified. The transfer of aerosol formed in the stratosphere after the falling of Chelyabinsk meteorite on the 15th of February 2013 is traced [Ivanov et al., 2014].

5. Remote Sensing of the Atmosphere

Ground-based studies of the amount of climate-active gases using IR-spectroscopy of direct solar radiation are carried on. Such studies, carried out at Department of Physics SPbSU, using ground-based measurements of IR direct solar spectra with high spectral resolution allowed to receive a new data on total contents of greenhouse, ozone-depleting and toxic gases (H_2O , CH_4 , N_2O , CO , CO_2 , C_2H_6 , CFC-11, O_3 , HCl, HF, HNO_3 , ClONO_2 , NO_2) at Peterhof (59.88 °N,

29.83 °E, 20 m asl.). Many data were obtained for the first time in Russia. These researches have been directed to:

- studying of temporary variations and long-term trends of climate-active atmospheric gases [Yagovkina et al., 2011; Virolainen et al., 2011; Makarova et al., 2011; Polyakov et al., 2011, 2013a, 2014a; Kshevetskaya et al., 2012; Ionov et al., 2013; Rakitin et al., 2013; Semakin et al., 2013; Timofeyev et al., 2013];
- validation of satellite measurements of various devices [Polyakov et al., 2013b; Gavrilov et al., 2014a, 2014b; Gavrilov and Timofeev, 2014; Makarova et al., 2014a];
- comparisons of ground-based measurements with results of numerical modeling [Makarova et al., 2014b; Virolainen et al., 2014a];
- obtaining the new information on elements of vertical distribution of the ozone content [Virolainen et al., 2012, 2014b];
- improvement of techniques for interpreting the remote measurements [Kostsov, 2012, 2013].

Comprehensive program of comparing the different methods for measuring the water vapor content started at SPbSU; the comparison of IR spectroscopic method with data of microwave and radiosonde measurements was performed [Semenov et al., 2014]. Studies of NO₂ and O₃ temporal variations from ground-based measurements of zenith scattered solar radiation in UV and visible spectral ranges are carried on, and the measurements are also used for the validation of different satellite measurements [Makarova et al., 2011b; Ionov and Poberovskii, 2012; Hendrick et al., 2011; Pastel et al., 2013, 2014; Virolainen et al., 2014c]. Measurements of aerosol optical and microphysical characteristics in the frames of AERONET network started. The analysis of the quality of the tropospheric temperature-humidity sounding using the RPG-HATPRO radiometer has shown that the radiometer gives a possibility to obtain real information for Saint-Petersburg up to the 3–4 km altitudes depending on season [Zaitsev et al., 2014].

At the IAP RAS, continuous combined trace gases measurements are carried on over Moscow, Zvenigorod Scientific Station and by a mobile laboratory (the TROICA experiments). Results of the carbon monoxide total content measurements by moderate resolution diffraction spectrometers over Moscow and Zvenigorod for 2005–2008 are compared with the same data sets for Moscow 1986–2005 and Beijing, 1992–2007 [Rakitin et al., 2011]. Results of the 1995–2008 observations of the concentrations of ozone and nitric oxides in the surface air over the Trans-Siberian Railway using a mobile laboratory are analyzed [Pankratova et al., 2011]. The air pollution in the central European part of Russia during the 2010 summer fires has been analyzed. Ground-based (IAP RAS, MSU, and Zvenigorod Scientific Station) and satellite (MOPITT, AIRS, of Terra and Aqua satellites) measurements of the total content and concentration of carbon monoxide (CO), as well as MODIS data on the spatial and temporal

distribution of forest and peat fires obtained from Terra and Aqua satellites, are presented [Fokeeva et al., 2011]. Increase in concentrations of chemically-active (NO , NO_2 , CO , O_3 , SO_2) and greenhouse gases CO_2 , CH_4 , and nonmethane hydrocarbons over Moscow is estimated during the 2010 Fires [Elansky et al., 2011]. The climatic trends and basic features of seasonal variations in and anomalies of the concentration of methane in the atmospheric surface layer have been considered on the basis of the current notion of the processes that form the global field of methane in the Earth's atmosphere. Measurement data on the surface concentration of methane, which were obtained in Moscow and at a number of observation stations in Europe and Siberia in the fall-winter period of the first decade of the 21st century, are analyzed [Ginzburg et al., 2011].

The Ural Atmospheric Fourier Station (UAFS) based on a Bruker IFS-125M Fourier spectrometer and intended for trace gas monitoring in the background atmosphere is now in operation. First results of the retrieval of the heavy water isotopes in the Ural atmosphere are given [Gribanov et al., 2011].

Since 2011 in IAM RAS, algorithms and codes for the hyper-spectral remote sensing of characteristics of the atmosphere, clouds and underlying surface are developed [Bass et al., 2014]. At present the testing of the software package are carried out using the processing of real spectra of atmospheric sounding.

In 2011–2014 the CAO team developed, made and tested a prototype of a ground-based microwave multichannel complex for monitoring the atmospheric thermodynamic parameters [Kadygrov et al., 2013a]. The complex provides continuous measurements of temperature profiles up to the 10 km altitude (under cloudless atmosphere) and to 2–4 km (under cloudiness) and also the total vapor and cloud liquid water content. The complex also provides measurements of temperature profiles in the atmospheric boundary layer practically in any weather conditions. Unique data on phase moisture transitions in clouds, in particular on the cloud liquid water content of thin clouds and a haze, are obtained using the complex [Kadygrov et al., 2014]. Jointly with specialists of Hydrometeorological Center, IAP RAS, MSU and “Mosecomonitoring”, studies of vertical structure of the heat island over Moscow using the microwave temperature profiler of MTR-5 established in the megalopolis and in the suburbs have continued [Kuznetsova et al., 2012]. The analysis of unique data on the heat island and its vertical distribution over Moscow was carried out during the powerful blocking anti-cyclone in the summer of 2010 [Gorchakov et al., 2014a]. The experiment on studying the influence of weather conditions and rainfall on data of the MTR-5 microwave profiler was carried out in cooperation with the Nansen Environmental and Remote Sensing Center (Norway), the Finnish Meteorological Institute (Finland), IPA RAS and Institute of Applied Physics RAS in the valley Bergen (Norway) [Ezau et al., 2013]. Data on the vertical structure variability of the atmospheric boundary layer during solar eclipses are generalized

and published [Kadygrov et al., 2013b]. At present the new generation of Doppler meteorological radars (DMRL-S) is put into operation, and on their basis the observation network covering practically all territory of the Russian Federation is created [Zhukov and Shchukin, 2014]. With the CAO participation the airborne meteo-laboratory of the new generation YaK-42D “Roshydromet” for the environment studies has been created. It is equipped with the most modern contact and remote devices for atmospheric studies and already made a number of research flights to the Arctic regions of the Russian Federation.

6. Interpretation of Satellite Measurements

Studies devoted to the development of methods for determining information products on parameters of the atmosphere and underlying surface on the basis of the analysis of satellite data, and also to problems of the calibration and validation of satellite data and information products are the main part of all studies in this field.

Studies on developing techniques for interpreting and using the data from Russian Polar-orbiting and Geostationary Meteorological Satellites “Meteor-M” and Electro-L and also on creating the operative procedures for the processing of satellite measurements and the retrieval of information products are carried on at SRB “Planeta”. A new method has been developed and tested for the land air temperature retrieval of regional and global covering from microwave imager/sounder MTVZA/Meteor-M N. 1 [Kramchaninova and Uspensky, 2012]. Validation issues of satellite based temperature-humidity profile retrieval are considered. The comparative characteristics of advanced satellite-based microwave radiometers (SSMIS, ATMS, AMSU, AMSR2, and MTVZA) intended to obtain information about the parameters of the atmosphere and the underlying surface are presented. Methodical aspects of determining the atmospheric water vapor, cloud liquid, atmospheric temperature-humidity profiles using ground-based microwave radiometers are considered. The results of the comparison of satellite-based products with upper-air and ground-based microwave radiometric soundings of the atmosphere are reviewed [Karavaev et al, 2014]. The description of the onboard measuring complex, the structure of output products and a ground-based reception complex for processing and distributing the “Meteor-M” N2 data is given in paper [Asmus et al., 2014]. Prospects of receiving products of the remote atmospheric sensing from data of hyper-spectral IR-sounders including IRFS-2 Fourier spectrometer onboard “Meteor-M” N2 have been analyzed [Uspensky and Rublev, 2014]. The Fast Radiative Transfer Model (FRTM) designed for the analysis and validation of the IR-sounder IRFS-2 has been developed jointly with Institute of Computational Mathematics and Mathematical Geophysics. Computational efficiency is estimated and the results of the

verification of developed FRTM are presented. The construction of radiative models, which use the algorithm of the Monte Carlo method and applicable for the analysis and modeling of the data of IR sounders under conditions of cloudiness in the instrument field of view, is considered [Uspensky et al., 2014]. Numerical simulation of the technology for determining the data of temperature-humidity atmospheric sounding from IR and microwave measurements from “Meteor-M” has been performed in cooperation with SPbSU [Polyakov et al., 2013c]. For the preparation for interpreting new space experiments on the Russian “Meteor-M” N2 at St. Petersburg State University, algorithms and codes for retrieving the vertical profiles of temperature, humidity, ozone content, ocean and land temperature, cloud liquid water content, near-surface wind have been developed. Numerical experiments for analyzing the accuracy of the parameters retrieval from data of satellite IR Fourier-spectrometer IRFS-2 and microwave spectrometer MTVZA are carried out by means of various techniques of solving inverse problems (multiple linear regression, iterative method of optimal estimation (statistical regularization) and artificial neural networks) [Polyakov et al., 2013c, 2014b, 2014c].

The description of the measuring complex onboard the Electro-L N1 geostationary weather satellite is provided, and methodical questions of receiving the information products from data of the MSU-GS radiometer-imager are considered [Asmus et al., 2012]. The regression method for retrieving the ozone total content (OTC) from the MSU-GS has been proposed and tested on real satellite data. Validation of the OTC estimates is performed by the comparison with data of ground-based ozonometric network and independent OMI satellite estimates [Kramchaninova and Uspensky, 2013]. The multispectral satellite imaging system (MSIS) aboard the Meteor-M No. 1 spacecraft has surveyed the territory of Russia and neighboring countries for three years. The MSIS data, supplemented by synchronous navigational information, are automatically received, pipeline processed, archived, and cataloged at ground-based receiving stations in Moscow, Novosibirsk, and Khabarovsk. These data are used to solve a wide range of land-use, environmental, and emergency monitoring problems; assess ice situations in seas, rivers, and lakes; etc. [Avanesov et al., 2013].

Many studies have been devoted to retrieving the atmospheric and surface characteristics using data from different foreign satellites and devices (SEVIRI/METEOSAT-9, AVHRR NOAA, MetOp, SSM/I, Terra, Aqua, etc.) or to comparing retrieved results with data of independent measurements. The vertical profiles of the O_3 , CO, CO_2 and CH_4 concentrations measured onboard the Optik Tu-134 aircraft laboratory and retrieved from data obtained with an IASI (MetOp satellite) have been compared [Arshinov et al., 2014]. The improved techniques for the CO_2 and CH_4 retrieval from the AIRS and IASI data have been proposed. A comparison of the satellite data with quasi-synchronous aircraft observations

was performed [Uspensky et al., 2011]. The tropospheric NO_2 content over the Moscow region has been analyzed using OMI data in the period 2004–2009. Possibilities for diagnosing long-term changes in nitrogen oxide emissions in megalopolises are investigated using data from satellite measurements and the modeling of the tropospheric nitrogen dioxide content [Konovalov, 2011]. Using the data from MODIS, MOPITT, MLS, and OMI satellite instruments, the changes in aerosol optical characteristics and in contents of atmospheric trace gases (O_3 , NO_2 , CO , CH_2O , SO_2) and water vapor (H_2O) during the prolonged atmospheric blocking event and wildfires in European Russia (ER) in the summer of 2010 have been analyzed. It is found that among burning products the greatest increase revealed aerosol optical depth (AOD) and CO [Sitnov, 2011a, 2011b], the spatial distribution of total column water vapor over ER during the block is found to be anomalous, with the water vapor excess in the north of ER and its deficit in the south of ER [Sitnov and Mokhov, 2013a]. It is also found that atmospheric moistening was accompanied by warming of the troposphere and cooling of the lower stratosphere [Sitnov and Mokhov, 2013a; Sitnov et al., 2014a]. Using MODIS (Aqua and Terra satellites) and in situ observations, a comparative analysis of two large-scale smoke events caused by the summer wildfires in European Russia (ER) in 2010 and Western Siberia (WS) in 2012 has been performed. Mean aerosol optical depths, radiative forcing effects at the top and the bottom of atmosphere and rates of radiative heating of the smoky atmosphere (AODs) are estimated for both events. Ground-based monitoring air pollution data in Moscow region were also examined [Gorchakov et al., 2014b]. Some aspects of European Russia smoke screening are discussed [Sitnov et al., 2012a, 2012b, 2013]. Preliminary results of Moscow region air pollution studies are outlined [Gorchakov et al., 2011; Golitsyn et al., 2011]. A comparative analysis of vertical temperature and humidity profiles, retrieved from MODIS and test radiosonde data from RAOB inventories has been performed. The analysis results gave a possibility to explore the applicability of meteorological satellite data to radiation calculations and solution of the problem of atmospheric correction of satellite infrared images of the Earth's surface [Afonin, 2011]. Methods and technologies for the automatic classification of scanning radiometers data from polar-orbiting weather satellites to retrieve cloud and precipitation parameters have been developed [Volkova, 2012, 2013]. On the basis of the developed method for retrieving dynamic characteristics of the atmosphere using data geostationary meteorological satellites [Nerushev and Kramchaninova, 2011], the evolution of wind field characteristics under different atmospheric conditions at the cyclone stages has been studied. The construction of maps of atmospheric dynamic characteristics in the zone of the severe cyclone of the moderate latitudes allowed to revealing the peculiarities of these characteristics [Nerushev and Barkhatov, 2012]. The method for retrieving the rainfall characteristics from

frontal cloudy systems has been developed [Nerushev et al., 2013]. Spatial distribution of jet flows in the satellite surveillance zones and the intra-annual variability of their characteristics in the upper troposphere of Northern and Southern hemispheres was studied by the automated method [Ivangorodsky and Nerushev, 2014]. The cycle of studies on developing methods of satellite diagnosis and forecasting of summer squalls and thunderstorms has been fulfilled [Bukharov, 2013].

Some studies devoted to the satellite monitoring of the Black Sea oil pollution [Lavrova and Mityagina, 2013], the total ice concentration [Alekseeva and Frolov, 2013] and blooms of coc-colithophore *E. huxleyi* in Arctic waters [Petrchenko et al., 2013] have been also fulfilled.

Joint studies of Water Problems Institute RAS and SRB “Planeta” directed to using the remote sensing data on surface characteristics in the simulation of components of water and heat balances for a river headwater are carried on. Methods of the AVHRR/NOAA, MODIS/Terra, Aqua, SEVIRI/Meteosat satellite data processing, which provide the retrieval of vegetation characteristics, land-surface temperature, and precipitation, have been developed or refined. The techniques for the assimilation of satellite-based products in the model have been developed. Some major water regime characteristics have been generated such as soil water content, evapotranspiration, and others [Startseva et al., 2014]. In addition the model of the vertical heat-water transfer in the soil-vegetation-atmosphere system (SVAT) utilizing the satellite data on underlying surface and a number of meteorological characteristics has been improved. Using the SVAT model, calculations of the water regime of the vast agricultural areas are carried out [Gelfan et al., 2012].

References

1. Afonin S. V., 2011: Applicability of Space-Derived Meteorological Data to Atmospheric Correction of Satellite Infrared Measurements. *Atm. Oceanic Opt.*, 24, 1, 56–63.
2. Alekseeva T.A. and S.V. Frolov, 2013: Comparative Analysis of Satellite and Shipborne Data on Ice Cover in the Russian Arctic Seas. *Izv., Atm. Oceanic Physics*, 49, 9, 879–885.
3. Arshinov M. Yu., B. D. Belan, D. K. Davydov et al., 2013: Spatial-Temporal Variability of Total Solar Radiation in West Siberia. *Atm. Oceanic Opt.*, 26, 8, 659–664 [in Russian].
4. Arshinov M. Yu., S. V. Afonin, B. D. Belan, et al., 2014: Comparison between Satellite Spectrometric and Aircraft Measurements of the Gaseous Composition of the Troposphere over Siberia during the Forest Fires of 2012. *Izv., Atm. Oceanic Physics*, 50, 9, 916–928.

5. Asmus V.V., V.N. Dyadyuchenko, V.A. Zagrebaev et al., 2012: Space Hydro-meteorological Observational System Development based on Electro-L Geostationary Satellite Series. *Space Journal of Lavochkin Association. Cosmonautics and Rocket Engineering*, 12, 1, 3–14 [in Russian].
6. Asmus V.V., V.A. Zagrebov, L.A. Makridenko, 2014: Complex of polar-orbiting meteorological satellites of the ‘Meteor-M’ series. *Met. and Hydrology*, 12, 5–16 [in Russian].
7. Avanesov G.A., I.V. Polyansky, B.S. Zhukov, 2013: Multispectral Satellite Imaging System Aboard the Meteor-M No. 1 Spacecraft: Three Years in Orbit. *Izv. Atm. Oceanic Physics*, 49, 9, 1057–1068.
8. Babikov Yu. L., S.N. Mikhailenko, A. Barbe, VI.G. Tyuterev, 2014: S&MPO — An Information System for Ozone Spectroscopy on the WEB. *J.Q.S.R.T.*, 145, 169–196.
9. Bass L.P., O.V. Nikolaeva & V.S. Kuznetsov, 2014: Remote Sensing of the Atmosphere and the Small Angle Approximation to the Solution of the Radiative Transfer Equation. *Int. J. Rem. Sensing*, 35, 15, 5830–5844.
10. Bedareva T.V., Zhuravleva T.B., 2011: Retrieval of Aerosol Scattering Phase Function and Single Scattering Albedo According to Data of Radiation Measurements in Solar Almucantar: Numerical Simulation. *Atmos. Ocean Opt.*, 24, 373–384.
11. Bedareva T.V., Zhuravleva T.B., 2012: Estimation of Aerosol Absorption under Summer Conditions of Western Siberia from Sun Photometer Data. *Atmos. Ocean Opt.*, 25, 216–223.
12. Bedareva T.V., Sviridenkov M.A., Zhuravleva T.B., 2013a: Retrieval of Aerosol Optical and Microphysical Characteristics According to Data of Ground-Based Spectral Measurements of Direct and Scattered Solar Radiation. Part 1. Testing of Algorithm. *Atmos. Ocean. Opt.*, 26, 24–34.
13. Bedareva T.V., Sviridenkov M.A., Zhuravleva T.B., 2013b: Retrieval of Aerosol Optical and Microphysical Characteristics According to Data of Ground-Based Spectral Measurements of Direct and Scattered Solar Radiation. Part 2. Approbation of Algorithm. *Atmos. Ocean Opt.*, 26, 107–117.
14. Bedareva T.V., Sviridenkov M.A., Zhuravleva T.B., 2014: Retrieval of Dust Aerosol Optical and Microphysical Properties from Ground-Based Sun-Sky Radiometer Measurements in Approximation of Randomly Oriented Spheroids. *J.Q.S.R.T.*, 146, 140–157.
15. Beguier S., Mikhailenko S., Campargue A., 2011: The Absorption Spectrum of Water between 13540 and 14070 cm^{-1} : ICLAS detection of weak lines and a complete line list. *J. Mol. Spectrosc.*, 265, 106–109.
16. Belan B.D., G.A. Ivlev, T.K. Sklyadneva, 2011: Influence of a City on the Incoming UV Radiation from Results of Many-Year Monitoring near Tomsk-City. *Atm. Oceanic Opt.*, 24, 12, 1113–1119 [in Russian].
17. Belan B.D., G.A. Ivlev, and T.K. Sklyadnev, 2012: Long-Term Monitoring of Total and UV-B Radiation in Tomsk. *Atm. Oceanic Opt.*, 25, 4, 281–285.
18. Beresnev S.A., L.B. Kochneva, T.B. Zhuravleva, and K.M. Firsov, 2012: Photophoretic Motion of Soot Aerosols in Field of Shortwave Solar Radiation. *Atm. Oceanic Opt.*, 25, 4, 286–291.

19. Budak V.P. and Ya.A. Ilyushin, 2011: Isolating the Singularities of a Brightness Field in a Turbid Medium on the Basis of Small-Angle Solutions of Transfer Theory. *Atm. Oceanic Opt.*, 24, 4, 326–334.
20. Budak V.P., Veklenko B.A., 2011: Boson Peak, Flickering Noise, Backscattering Processes and Radiative Transfer in Random Media. *J.Q.S.R.T.*, 112, 864–875.
21. Budak V.P., Klyuykov D.A., Korkin S.V., 2011: Complete Matrix Solution of Radiative Transfer Equation for Pile of Horizontally Slabs. *J.Q.S.R.T.*, 112, 1141–1148.
22. Budak V.P., Efremenko D.S., Shagalov O.V., 2012: Efficiency of Algorithm for Solution of Vector Radiative Transfer Equation in Turbid Medium Slab. *J. Physics: Conference Series*, 369, P. 012021–10.
23. Budak, V.P., Shagalov, O.V., 2013: Solution of the Radiative Transfer Equation by Eliminating the Anisotropic Part within the Method of Synthetic Iteration. *AIP Conf. Proc.*, 1531, 91–94.
24. Budak V.P., Shagalov O.V., Zheltov V.S., 2014: Numerical Radiative Transfer Modeling in Turbid Medium Slab. *Proc. SPIE*, 9292, 92920Y.
25. Bukharov M.V., 2013: Satellite Diagnosis of Thunderstorm Probability. *Rus. Met. Hydrology*, 38, 8, 515–521.
26. Bychkov V.V., A.S. Perezhogin, B.M. Shevtsov et al., 2011: Seasonal Features of the Appearance of Aerosol Scattering in the Stratosphere and Mesosphere of Kamchatka from the Results of Lidar Observations in 2007–2009. *Izv., Atm. Oceanic Physics*, 47, 5, 603–609.
27. Chentsov A.V., Voronina Yu.V., Chesnokova T. Yu., 2013: Atmospheric Transmission Simulation with Different CO₂ Absorption Line Profiles. *Atm. Oceanic Opt.*, 26, 9, 711–715 [in Russian].
28. Cheremisin A.A., I.S. Shnipov, H. Horvath, and H. Rohatschek, 2011a: The Global Picture of Aerosol Layers Formation in the Stratosphere and in the Mesosphere under the Influence of Gravitational-Photophoretic and Magneto-Photophoretic Forces. *J. Geophys. Res.*, 116, D19204, doi:10.1029/2011JD015958.
29. Cheremisin A.A., Marichev V.N., Novikov P.V., 2011b: Lidar Observations of Volcanic Aerosol Content in the Atmosphere over Tomsk. *Rus. Met. Hydrology*, 36, 9, 600–607.
30. Cheremisin A.A., P.V. Novikov, I.S. Shnipov et al., 2012: Lidar Observations and Formation Mechanism of the Structure of Stratospheric and Mesospheric Aerosol Layers over Kamchatka. *Geomagnetism and Aeronomy*, 52, 5, 653–663.
31. Cheremisin A.A., A.V. Kushnarenko, 2013: Photophoretic Interaction of Aerosol Particles and its Effect on Coagulation in Rarefied Gas Medium. *J. Aeros. Sci.*, 62, 26–39.
32. Cheremisin A.A., Marichev V.N., Novikov P.V., 2013: Polar Stratospheric Cloud Transfer from Arctic Regions to Tomsk in January, 2010. *Atm. Ocean Opt.*, 26, 2, 93–99 [in Russian].
33. Cheremisin A.A., Kushnarenko A.V., 2014: Photophoretic Interaction of Aerosol Particles and its Effect on Coagulation in the Atmosphere. *Atm. Oceanic Opt.*, 27, 12, 1090–1098 [in Russian].

34. Chesnokova T. Yu., V. Boudon, T. Gabard et al., 2011: Near-infrared Radiative Transfer Modelling with Different CH₄ Spectroscopic Databases to Retrieve Atmospheric Methane Total Amount. *J.Q.S.R.T.*, 112, 2676–2682.
35. Chesnokova T. Yu., T. B. Zhuravleva, Yu. V. Voronina et al., 2012: Simulation of Solar Radiative Fluxes Using Altitude Profiles of Water Vapor Concentration, Characteristic for Conditions of Western Siberia. *Atm. Oceanic Opt.*, 25, 2, 147–153.
36. Chesnokova T. Yu., 2013: Spectroscopic Factors, Influencing the Accuracy of the Atmospheric Radiative Transfer Simulation in the Methane Absorption Bands in the Near Infrared Region. *Atm. Oceanic Opt.*, 26, 5, 417–426.
37. Chesnokova T. Yu., T. B. Zhuravleva, I. V. Ptashnik, and A. V. Chentsov, 2013: Simulation of Solar Radiative Fluxes in the Atmosphere Using Different Models of Water Vapor Continuum Absorption in Typical Conditions of Western Siberia. *Atm. Oceanic Opt.*, 26, 6, 499–506.
38. Chubarova N., Smirnov A., Holben B. N., 2011a: Aerosol Properties in Moscow According to 10 Years of AERONET Measurements at the Meteorological Observatory of Moscow State University. *Geography, Environment, Sustainability*, 4, 1, 19–32.
39. Chubarova N. E., Gorbarenko E. V., Nezval' E. I., Shilovtseva O. A., 2011b: Aerosol and Radiation Characteristics of the Atmosphere during Forest and Peat Fires in 1972, 2002, and 2010 in the Region of Moscow. *Izv., Atm. Oceanic Physics*, 47, 6, 729–738.
40. Chubarova N., Nezval' Ye, Sviridenkov I. et al., 2012: Smoke Aerosol and its Radiative Effects During Extreme Fire Event Over Central Russia in Summer 2010. *Atm. Meas. Techn.*, 5, 557–568.
41. Chubarova Natalia, Yekaterina Zhdanova, 2013: Ultraviolet Resources over Northern Eurasia. *J. Photochemistry and Photobiology B*, 127, c. 38–51.
42. Chubarova N. E., Nezval' E. I., Belikov I. B. et al., 2014: Climatic and Ecologic Characteristics of Moscow Mega Polis in 60 Years from Data of MSU Meteorological Observatory. *Meteorology and Hydrology*, 9, 49–64 [in Russian].
43. Elansky N. F., I. I. Mokhov, I. B. Belikov, 2011: Gaseous Admixtures in the Atmosphere over Moscow during the 2010 Summer. *Izv., Atm. Oceanic Physics*, 47, 6, 672–681.
44. Ezau I. N., Wolf T., Troitskaya Y. I. et al., 2013: The Analysis of Results of Remote Sensing Monitoring of the Temperature Profile in Lower Atmosphere in Bergen (Norway). *Rus. Met. Hydrology*, 38, 10, 715–722.
45. Firsov K. M., T. Yu. Chesnokova, E. V. Bobrov, and I. I. Klitochenko, 2013: Total Water Vapor Content Retrieval from Sun Photometer Data. *Atm. Oceanic Opt.*, 26, 4, 281–284.
46. Firsov K. M., T. Yu. Chesnokova, and E. V. Bobrov, 2015: The Role of the Water Vapor Continuum Absorption in Near Ground Long-Wave Radiation Processes of the Lower Volga Region. *Atm. Oceanic Opt.*, 28, 1, 1–8.
47. Fokeeva E. V., A. N. Safronov, V. S. Rakitin, et al., 2011: Investigation of the 2010 July–August Fires Impact on Carbon Monoxide Atmospheric Pollution in Moscow and Its Outskirts, Estimating of Emissions. *Izv., Atm. Oceanic Physics*, 47, 6, 682–698.

48. Fokina I.N., Karasik V.E., Orlov V.M., Budak V.P., 2014: Impact of Structure Geometry on Scattering in Partially-Ordered Media. *J.Q.S.R.T.*, 149, 108–116.
49. Fomin B.A. & V.A. Falaleeva, 2014: The Vertical Structure of Aerosols and Clouds Derived from Satellites Equipped with High-Resolution Polarization Sensors. *Int. Journ. Rem. Sensing*, 35, 15, 5800–5811.
50. Frolkis V.A., A.M. Kokorin, 2014: The Influence of Various Variants of both Two-Phase Stratospheric Aerosol Particles and their Size Distribution on Optical Parameters and Radiative Forcing. *Proceedings of MGO*, 571, 88–114 [in Russian].
51. Gavrilov N.M. and Yu.M. Timofeev, 2014: Comparisons of Satellite (GOSAT) and Ground-Based Spectroscopic Measurements of CO₂ Content near St. Petersburg. *Izv., Atm. Oceanic Physics*, 50, 9, 910–915.
52. Gavrilov N.M., M.V. Makarova, A.V. Poberovskii, and Yu.M. Timofeyev, 2014a: Comparisons of CH₄ Ground-Based FTIR Measurements near Saint Petersburg with GOSAT Observations. *Atm. Meas. Tech.*, 7, 1003–1010.
53. Gavrilov Nikolai M., Maria V. Makarova, Yury M. Timofeev, and Anatoly V. Poberovsky, 2014b: Comparisons of Satellite (GOSAT) and Ground-Based Spectroscopic Measurements of CH₄ Content near Saint Petersburg: Influence of Data Collocation. *Int. Journ. Rem. Sensing*, 35, 15, 5628–5636.
54. Gelfan A., Muzylev E., Uspensky A. et al., 2012: Remote Sensing Based Modeling of Water and Heat Regimes in a Vast Agricultural Region. Remote Sensing — Applications. Ed. Boris Escalante-Ramirez. InTech — Open Access Publisher, Rijeka, Croatia. 2012. Chapter 6, 141–176.
55. Ginzburg A.S., A.A. Vinogradova, and E.I. Fedorova, 2011: Some Features of Seasonal Variations in the Methane Content in the Atmosphere over Northern Eurasia. *Izv., Atm. Oceanic Physics*, 47, 1, 45–58.
56. Golitsyn G.S., Gorchakov G.I., Grechko E.I. et al., 2011: Extreme Carbon Monoxide Pollution of the Atmospheric Boundary Layer in Moscow Region in the Summer 2010. *Dokl. Earth Sci.*, 441, 2, 1666–1672.
57. Gorbarenko E.V., 2013: Long-Term Variations of Long-Wave Radiation in Moscow. *Rus. Meteorology and Hydrology*, 38, 10, 669–676.
58. Gorbarenko E.V., Abakumova G.M., 2011: Radiation Balance Variations of Underlying Surface from the Long-Term Observations of the Meteorological Observatory of the Moscow State University. *Rus. Meteorology and Hydrology*, 36, 6, 383–391.
59. Gorbarenko E.V., Shilovtseva O.A., 2013: Solar Power Resources of Moscow. *Int. Sci. J. for Alternative Energy and Ecology*, 6, 2, 28–35.
60. Gorchakov G.I., Sviridenkov M.A., Semoutnikova E.G. et al., 2011: Optical and Microphysical Parameters of the Aerosol in the Smoky Atmosphere of the Moscow Region in 2010. *Dokl. Earth Sci.*, 437, 2, 513–517.
61. Gorchakov G.I., E.N. Kadyrov, V.E. Kunitsyn et al., 2014a: The Moscow Heat Island in the Blocking Anticyclone during Summer 2010. *Dokl. Earth Sci.*, 456, Part 2, 736–740.
62. Gorchakov G.I., Sitnov S.A., Sviridenkov M.A. et al., 2014b: Satellite and Ground-Based Monitoring of Smoke in the Atmosphere during the Summer Wildfires

in European Russia in 2010 and Siberia in 2012. *Int. J. of Remote Sensing*, 35, 15, 5698–5721.

63. Gorchakova I.A., Mokhov I.I., 2012: The radiative and thermal effects of smoke aerosol over the region of Moscow during the summer Fires in 2010. *Izv. Atm. Oceanic Physics*, 48, 5, 496–503.

64. Griбанov K.G., V.I. Zakharov, S.A. Beresnev, 2011: Sensing HDO/H₂O in the Ural's Atmosphere Using Ground-Based Measurements of IR Solar Radiation with a High Spectral Resolution. *Atm. Oceanic Opt.*, 24, 4, 369–372.

65. Hendrick, F., Pommereau, J.-P., Goutail, F. et al., 2011: NDACC/SAOZ UV-Visible Total Ozone Measurements: Improved Retrieval and Comparison with Correlative Ground-Based and Satellite Observations. *Atm. Chem. Physics*, 11, 12, 5975–5995.

66. Ilyushin Ya.A., Budak V.P., 2011: Narrow-Beam Propagation in Two-Dimensional Scattering Medium. *J. Opt. Soc. Am. A*, 28, 2, 76–81.

67. Ilyushin Y.A., Budak V.P., 2011a: Narrow Beams in Scattering Media: The Advanced Small-Angle Approximation. *J. Opt. Soc. Am. A*, 28, 7, 1358–1363.

68. Ilyushin Ya.A., Budak V.P., 2011b: Analysis of the Propagation of the Femtosecond Laser Pulse in the Scattering Medium. *Comp. Phys. Communication*, 2011, 182, 940–945.

69. Ilyushin Ya.A., Budak V.P., 2011c: Calculation of Light Fields of Concentrated Sources in Turbid Media with Strongly Anisotropic Scattering. *Opt. Spectroscopy*, 111, 6, 853–858.

70. Ionov D. V. and A. V. Poberovskii, 2012: Nitrogen Dioxide in the Air Basin of St. Petersburg: Remote Measurements and Numerical Simulation. *Izv. Atm. Oceanic Physics*, 48, 4, 373–383.

71. Ionov D. V., M.A. Kshevetskaya, Yu. M. Timofeev, and A. V. Poberovskii, 2013: Stratospheric NO₂ Content according to Data from Ground-Based Measurements of Solar IR Radiation. *Izv. Atm. Oceanic Physics*, 49, 5, 519–529.

72. Ivangorodsky, A.F. Nerushev, 2014: Characteristics of the Upper Tropospheric Jet Fluxes Inferred from the Data of European Geostationary Meteorological Satellites. *Current Problems in Rem. Sens. Earth from Space*, 11, 1, 45–53 [in Russian].

73. Ivanov V.N., Zubachev D.S., Korshunov V.A. et al., 2014: Lidar Observations of Stratospheric Aerosol Traces of Chelyabinsk Meteorite. *Atm. Ocean Opt.*, 27, 2, 117–122 [in Russian].

74. Ivlev G.A., B.D. Belan, V.M. Dorokhov, 2013: Dynamics of Solar UV-B and UV-A Radiations in Tomsk during Ozone Anomaly in Spring, 2011. *Atm. Oceanic Opt.*, 26, 11, 995–1004 [in Russian].

75. Jacquemart D., Gueye F., Lyulin O. M. et al., 2012: Infrared Spectroscopy of CO₂ Isotopologues from 2200 to 7000 cm⁻¹: I — Characterizing Experimental Uncertainties of Positions and Intensities. *J.Q.S.R.T.*, 113, 11, 961–975.

76. Kabanov D.M., T.R. Kurbangaliev, T.M. Rasskazhikova et al., 2011: The Influence of Synoptic Factors on Variations of Atmospheric Aerosol Optical Depth under Siberian Conditions. *Atm. Oceanic Opt.*, 24, 6, 643–652.

77. Kabanov D. M., Beresnev S. A., Gorda S. Yu. et al., 2013: Diurnal Behavior of the Aerosol Optical Depth of the Atmosphere in Some Regions of Asian Part of Russia. *Atm. Oceanic Opt.*, 26, 4, 291–296 [in Russian].
78. Kabanov D. M., Beresnev S. A., Gorda S. Yu. et al., 2014a: Annual Behavior of the Aerosol Optical Depth in Some Regions of Asian Part of Russia. *Proc. SPIE*, 9292, 929241, doi: 10.1117/12.2074887.
79. Kabanov D. M., Gulev S. K., Holben B. N. et al., 2014b: Latitudinal Distribution of the Aerosol Optical Depth over Oceans in Southern Hemisphere. *Proc. SPIE*, 9292, 929240, doi: 10.1117/12.2074564.
80. Kadygrov E. N., Gorelik A. G., Miller E. A. et al., 2013a: Results of Tropospheric Thermodynamics Monitoring on the Base of Multichannel Microwave System Data. *Atm. Oceanic Opt.*, 26, 6, 459–465 [in Russian].
81. Kadygrov E. N., E. A. Miller, A. V. Troitsky, 2013b: Study of Atmospheric Boundary Layer Thermodynamics during Total Solar Eclipses. *IEEE Trans. Rem. Sens.*, 51, 9, 4672–4677.
82. Kadygrov E. N., A. G. Gorelik, and T. A. Tochilkina, 2014: Study of Liquid Water in Clouds with the “Microradkom” Radiometric System. *Atm. Oceanic Opt.*, 27, 6, 596.
83. Kapitanov V. A., K. Yu. Osipov, A. E. Protasevich, Yu. N. Ponomarev, 2012: Collisional Parameters of N_2 Broadened Methane Lines in the R9 Multiplet of the $2\nu_3$ Band. Multispectrum Fittings of the Overlapping Spectral Lines. *J.Q.S.R.T.*, 113, 16, 1985–1992.
84. Kapitanov V. A., Yu. N. Ponomarev, A. E. Protasevich, K. Yu. Osipov, 2013: Line-shape Models Testing on CH_4 Spectral Line 6105.6257 cm^{-1} (R9F1, R9F2) of $2\nu_3$ Band Broadened by N_2 and Ne. *J. Mol. Spectroscopy*, 291, 57–60.
85. Karavaev D. M., Yu. V. Kuleshov, A. B. Uspensky, G. G. Shchukin, 2014: Validation of Remote Sensing Products Generated from Space-Based Microwave Radiometers Data. *Current Problems in Rem. Sens. Earth from Space*, 11, 3, 259–267 [in Russian].
86. Karlovets E. V., Lu Y., Mondelain D., Kassi S. et al., 2013: High Sensitivity CW-Cavity Ring Down Spectroscopy of N_2O between 6950 and 7653 cm^{-1} (1.44 – 1.31 mm): II. Line intensities. *J.Q.S.R.T.*, 117, 81–87.
87. Karlovets E. V., S. Kassi, S. A. Tashkun et al., 2014: High Sensitivity Cavity Ring Down Spectroscopy of Carbon Dioxide in the 1.19 – 1.26 mm Region. *J.Q.S.R.T.*, 144, 137–153.
88. Karol' I. L., A. A. Kiselev, and V. A. Frol'kis, 2011: Indices of the Factors that Form Climate Changes of Different Scales. *Izv. Atm. Oceanic Physic*, 47, 4, 415–429.
89. Karol' I. L., Kiselev A. A., Frol'kis V. A., 2012: Radiation Indices of Climate-Forming Factors and Their Estimates under Anthropogenic Climate Changes. *Rus. Met. Hydrology*, 37, 5, 298–306.
90. Karol' I. L., A. A. Kiselev, E. L. Genikhovich, and S. S. Chicherin, 2013: Reduction of Short-Lived Atmospheric Pollutant Emissions as an Alternative Strategy for Climate-Change Moderation. *Izv. Atm. Oceanic Physics*, 49, 5, 461–478.
91. Karol I. L., V. P. Meleshko, A. V. Baidin, A. A. Kiselev, 2014: The Radiative and Thermodynamic Seasonal Factors of the Arctic Climate Warming. *Probl. Arctic and Antarctic*, 3, 5–12 [in Russian].

92. Konovalov I.B., 2011: Estimation of Multiyear Changes in Nitrogen Oxide Emissions in Megalopolises from Satellite Measurements. *Izv., Atm. Oceanic Physics*, 47, 2, 201–210.
93. Kostsov V.S., A. V. Poberovsky, S. I. Osipov, Yu. M. Timofeyev, 2012: Multiparameter Technique for Interpreting Ground-Based Microwave Spectral Measurements in the Problem of Ozone Vertical Profile Retrieval. *Atm. Oceanic Opt.* 25, 4, 269–275.
94. Kostsov Vladimir, 2013: General approach to the formulation and solution of the multi-parameter inverse problems of atmospheric remote sensing. *AIP Conference Proceedings*, 1531, 240–243.
95. Kozlov V.S., Yausheva E.P., Terpugova S.A. et al., 2014: Optical-Microphysical Properties of Smoke Haze from Siberian Forest Fires in Summer 2012. *Int. J. Rem. Sensing*, 35, 15, 5722–5741.
96. Kramchaninova E., A. Uspensky, 2012: Land Air Temperature Retrieval from Microwave Meteor-M N. 1 Data. *Current Problems in Rem. Sens. Earth from Space*, 9, 3, 127–136 [in Russian].
97. Kramchaninova E.K., A.B. Uspensky, 2013: Monitoring of the Ozone Total Content in the Atmosphere according Data of Russian Geostationary Satellite Electro-L. *Earth Res. from Space*, 2, 12–18 [in Russian].
98. Kshevetskaya M.A., Poberovsky A.V., Timofeev Yu.M., 2012: Measurements of N₂O total column amount in the vicinity of St. Petersburg. *Atm. Oceanic Opt.*, 25, 1, 75–79 [in Russian].
99. Kuznetsova I.N., Kadyrov E.N., Miller E.A., Nahaev M.I., 2012: Characteristics of Lowest 600 m Atmospheric Layer Temperature on the Basis of MTP-5 Profiler Data. *Atm. Oceanic Opt.*, 25, 10, 877–883 [in Russian].
100. Lavrentieva N.N., B.A. Voronin, O.V. Naumenko et al., 2014: Linelist of HD¹⁶O for Study of Atmosphere of Terrestrial Planets (Earth, Venus and Mars). *Icarus*, 236, 38–47.
101. Lavrova O. Yu. and M.I. Mityagina, 2013: Satellite Monitoring of Oil Slicks on the Black Sea Surface. *Izv., Atm. Oceanic Physics*, 49, 9, 897–912.
102. Leshchishina O.M., Naumenko O.V., Campargue A., 2011a: High Sensitivity ICLAS of H₂¹⁸O in the 12580–13550 cm⁻¹ Transparency Window. *J.Q.S.R.T.*, 112, 913–924.
103. Leshchishina O.M., Naumenko O.V., Campargue A., 2011b: High Sensitivity ICLAS of H₂¹⁸O between 13540 and 14100 cm⁻¹. *J. Mol. Spectrosc.*, 268, 28–36.
104. Leshchishina O., Mikhailenko S., Mondelain D. et al., 2012: CRDS of Water Vapor at 0.1 Torr between 6886 and 7406 cm⁻¹. *J.Q.S.R.T.*, 113, 17, 2155–2166.
105. Leshchishina O., Mikhailenko S., Mondelain D. et al., 2013: An Improved Line List for Water Vapor in the 1.5 μm Transparency Window by Highly Sensitive CRDS between 5852 and 6607 cm⁻¹. *J.Q.S.R.T.*, 130, 69–80.
106. Liu A.W., Kassi S., Perevalov V.I., et al., 2011: High Sensitivity CW-Cavity Ring Down Spectroscopy of N₂O near 1.28 mm. *J. Mol. Spectrosc.*, 267, 191–199.
107. Lu Y., Mondelain D., Liu A.W. et al., 2012: High Sensitivity CW-Cavity Ring Down Spectroscopy of N₂O between 6950 and 7653 cm⁻¹ (1.44–1.31 mm): I. Line Positions. *J.Q.S.R.T.*, 113, 10, 749–762.

-
108. Lukashevskaya A. A., Naumenko O. V., Perrin A. et al., 2013: High Sensitivity Cavity Ring Down Spectroscopy of NO_2 between 7760 and 7917 cm^{-1} . *J.Q.S.R.T.*, 130, 249–259.
109. Lyulin O. M., Perevalov V. I., Morino I. et al., 2011: Measurements of Self-Broadening and Self-Induced Pressure-Shift Parameters of Methane Spectral Lines in the 5556–6166 cm^{-1} *J.Q.S.R.T.*, 112, 531–539.
110. Lyulin O. M., Campargue A., Mondelain D., Kassi S., 2013: The Absorption Spectrum of Acetylene by CRDS between 7244 and 7918 cm^{-1} . *J.Q.S.R.T.*, 130, 327–334.
111. Lyulin O. M., D. Mondelain, S. Beguier et al., 2014: High-Sensitivity CRDS Absorption Spectrum of Acetylene between 5851 and 6341 cm^{-1} . *Molecular Physics*, 112, 2433–2444.
112. Makarova M. V., A. V. Poberovskii, and S. I. Osipov, 2011a: Time Variations of the Total CO Content in the Atmosphere near St. Petersburg. *Izv., Atm. Oceanic Physics*, 47, 6, 739–746.
113. Makarova M. V., A. V. Rakitin, D. V. Ionov & A. V. Poberovskii, 2011b: Analysis of Variability of the CO, NO_2 , and O_3 Contents in the Troposphere near St. Petersburg. *Izv., Atm. Oceanic Physics*, 47, 4, 468–479.
114. Makarova M. V., N. M. Gavrilov, Yu. M. Timofeev, and A. V. Poberovskii, 2014a: Comparisons of Satellite (GOSAT) and Ground-Based Fourier Spectroscopic Measurements of Methane Content near St. Petersburg. *Izv., Atm. Oceanic Physics*, 50, 9, 904–909.
115. Makarova Maria, Oliver Kirner, Anatoliy Poberovskii et al., 2014b: Atmospheric Methane Variability at the Peterhof Station (Russia): Ground-Based Observations and Modeling. *Geoph. Res. Abst.*, 16, EGU2014–7623–2.
116. Marakasov D. A. and V. O. Troitskii, 2012: Propagation of Electromagnetic Radiation in Uniaxial Media. *Atm. Oceanic Opt.*, 25, 6, 387–394.
117. Matelenok I. V., V. V. Melentyev, 2014: Vector-Coordinate Approach to Determination of Viewing Geometry for Accounting the Impact of Large-Scale Roughness of Land Surface on its Microwave Emissivity. *Current Problems in Rem. Sens. Earth from Space*, 11, 4, 300–309 [in Russian].
118. Matvienko G. G., Belan B. D., Panchenko M. V. et al., 2014a: Instrumentation Complex for Comprehensive Study of Atmospheric Parameters. *Int. J. Rem. Sens.*, 35, 15, 5651–5676.
119. Matvienko G. G., Belan B. D., Panchenko M. V. et al., 2014b: Complex Experiment on the Study of Microphysical, Chemical and Optical Properties of Aerosol Particles and Estimation of Atmospheric Aerosol Contribution in the Earth Radiation Budget. *Proc. SPIE*, 9292, doi: 10.1117/12.2075507.
120. Mikhailenko S., Kassi S., Wang Le, Campargue A., 2011: The Absorption Spectrum of Water in the 1.25 mm Transparency Window (7408–7920 cm^{-1}). *J. Mol. Spectrosc.*, 269, 92–103.
121. Mikhailov E. F., V. V. Merkulov, S. S. Vlasenko et al., 2011: Filter-Based Differential Hygroscopicity Analyzer of Aerosol Particles. *Izv., Atm. Oceanic Physics*, 47, 6, 747–759.

122. Mikhailov G. A., 2012: Asymptotic Estimates of the Mean Probability of Radiative Transfer through an Exponentially Correlated Stochastic Medium. *Izv., Atm. Oceanic Physics*, 48, 6, 618–624.
123. Mikhailov E., Vlasenko S., Rose D., Poeschl U., 2013: Mass-Based Hygroscopicity Parameter Interaction Model and Measurement of Atmospheric Aerosol Water Uptake. *Atm. Chem. Physics*, 13, 2, 717–740.
124. Nerushev A. F., and E. K. Kramchaninova, 2011: Method for Determining Atmospheric Motion Characteristics Using Measurements on Geostationary Meteorological Satellites. *Izv., Atm. Oceanic Physics*, 47, 9, 1104–1113.
125. Nerushev A. F., Barkhatov A. E., 2012: Determination of Atmospheric Characteristics in the Zone of Action of Extra-Tropical Cyclone Xynthia (February 2010) Inferred from Satellite Measurement Data. *Proc. 2012 EUMETSAT Meteorological Satellite Conference*, http://www.eumetsat.int/Home/Main/AboutEUMETSAT/Publications/ConferenceandWorkshopProceedings/2012/groups/cps/documents/document/pdf_conf_p61_s7_08_nerushev_p.pdf.
126. Nerushev A. F., Novitskii M. A., Kalinicheva O. Y., 2013: Atmospheric Dynamics in the Center of the European Part of Russia during Intensive Snowfall in April 2012. *Rus. Met. Hydrology*, 38, 2, 61–70.
127. Oudot C., Regalia L., Mikhailenko S. et al., 2012: Fourier Transform Measurements of H_2^{18}O and HD^{18}O in the Spectral Range $1000\text{--}2300\text{ cm}^{-1}$. *J.Q.S.R.T.*, 113, 11, 859–869.
128. Osipov K. Yu., A. E. Protasevich, V. A. Kapitanov, Ya. Ya. Ponurovskii, 2012: Collision Parameters of N_2 -Broadened Methane Lines in R5 multiplet of $2\nu_3$ Band. Multispectrum Fitting of Overlapping Spectral Lines. *Appl. Phys. B*, 106, 3, 725–732.
129. Panchenko M. V., S. A. Terpugova, T. A. Dokukina et al., 2012a: Multiyear Variations in Aerosol Condensation Activity in Tomsk. *Atm. Oceanic Opt.*, 25, 4, 251–255.
130. Panchenko M. V., Zhuravleva T. B., Terpugova S. A. et al., 2012b: An empirical model of optical and radiative characteristics of the tropospheric aerosol over West Siberia in summer. *Atm. Meas. Tech.*, 5, 1513–1527.
131. Panchenko M. V., Kozlov V. S., Pol'kin V. V. et al., 2012c: Retrieval of Optical Characteristics of the Tropospheric Aerosol in West Siberia on the Basis of Generalized Empirical Model Taking into Account Absorption and Hygroscopic Properties of Particles. *Atmos. Ocean Opt.*, 25, 1, 46–54 [in Russian].
132. Panchenko M. V., Kozlov V. S., Polkin V. V., Terpugova S. A., 2014: Model Estimates of the Spectral Dependences of Single Scattering Albedo in the Troposphere in Different Seasons. *Proc. SPIE*, 9292, 9292–125.
133. Pankratova N. V., N. F. Elansky, I. B. Belikov et al., 2011: Ozone and Nitric Oxides in the Surface Air over Northern Eurasia According to Observational Data Obtained in TROICA Experiments. *Izv., Atm. Oceanic Physics*, 47, 3, 333–338.
134. Pastel M., J.-P. Pommereau, F. Goutail et al., 2013: Comparison of Long Term Series of Total Ozone and NO_2 Column Measurements in the Southern Tropics by SAOZ/NDACC UV–Vis Spectrometers and Satellites. *Atm. Meas. Tech. Discuss.*, 6, 4851–4893.

135. Pastel M., J.-P. Pommereau, F. Goutail et al., 2014: Construction of Merged Satellite Total O₃ and NO₂ Time Series in the Tropics for Trend Studies and Evaluation by Comparison to NDACC SAOZ Measurements. *Atm. Meas. Tech.*, 7, 3337–3354.
136. Petrenko D.A., E.V. Zabolotsikh, D.V. Pozdnyakov et al., 2013: Interannual Variations and Trend of the Production of Inorganic Carbon by Coccolithophores in the Arctic in 2002–2010 Based on Satellite Data. *Izv., Atm. Oceanic Physics*, 49, 9, 871–878.
137. Pkhalagov Yu.A., Uzhegov V.N., Kozlov V.S. et al., 2013: Retrieval of the Aerosol Extinction Coefficients on a Long Near-Ground Path from Data on the Aerosol Parameters in a Local Volume. *Atm. Ocean Opt.*, 26, 6, 478–483 [in Russian].
138. Pkhalagov Yuri A., Uzhegov Viktor N., 2014: Diurnal Variability of Aerosol Extinction of Optical Radiation in the Surface Atmosphere West Siberia. *Proc. SPIE*, 9292, 92922S, doi: 10.1117/12.2075135.
139. Poddubnyi V.A., A.P. Luzhetskaya, Yu.I. Markelov et al., 2013: Features of Optical Characteristics of Atmospheric Aerosol in the Middle Urals. *Izv., Atm. Oceanic Physics*, 49, 3, 285–293.
140. Pol'kin V.V., Kozlov V.S., Turchinovich Yu.S., Shmargunov V.P., 2011: Joint Lidar and Sodar Investigations of the Atmospheric Boundary Layers. *Atm. Oceanic Opt.*, 24, 6, 538–546 [in Russian].
141. Pol'kin V.V., Pol'kin Vas.V., Panchenko M.V., 2012: Annual Variations of Microphysical Properties of Aerosol at the Station “Vostok” in 2009 and 2011. *Atm. Oceanic Opt.*, 25, 11, 963–967 [in Russian].
142. Pol'kin V.V., Pol'kin Vas.V., Golobokova L.P. et al., 2013: On the Interannual Variability of the Latitudinal Distribution of Microphysical and Chemical Parameters of Near-Water Aerosol of Eastern Atlantic in 2006–2010. *Atm. Oceanic Opt.*, 26, 6, 519–524 [in Russian].
143. Pol'kin, D.M. Kabanov, S.M. Sakerin, and L.P. Golobokova, 2014: Comparative Studies of Optical and Microphysical Characteristics and Chemical Composition of Aerosol over Water Basin of Caspian Sea in the 29th and 41st cruises of RV Rift. *Atm. Oceanic Opt.*, 27, 1, 16–23.
144. Polyakov A.V., Yu.M. Timofeev, A.V. Poberovskii, I.S. Yagovkina, 2011: Seasonal Variations in the Total Content of Hydrogen Fluoride in the Atmosphere. *Izv., Atm. Oceanic Physics*, 47, 6, 760–765.
145. Polyakov A.V., Yu.M. Timofeev & A.V. Poberovskii, 2013a: Ground-Based Measurements of Total Column of Hydrogen Chloride in the Atmosphere near St. Petersburg. *Izv., Atm. Oceanic Physics*, 49, 4, 411–419.
146. Polyakov A.V., Yu.M. Timofeyev, and K.A. Walker, 2013b: Comparison of the Satellite and Ground-Based Measurements of the Hydrogen Fluoride Content in the Atmosphere. *Izv., Atm. Oceanic Physics*, 49, 9, 1002–1005.
147. Polyakov A., Yu. Timofeyev, V. Kostsov et al., 2013c: The Atmospheric and Surface Sounding from the Meteor Satellite (Numerical Simulation). *AIP Conf. Proc.*, 1531, 224–227.
148. Polyakov A.V., Yu.M. Timofeev, Ya.A. Virolainen, and A.V. Poberovskii, 2014a: Ground-Based Measurements of HF Total Column Abundances in the Stratosphere near St. Petersburg (2009–2013). *Izv., Atm. Oceanic Physics*, 50, 6, 675–682.

149. Polyakov A. V., Yu. M. Timofeev, Ya. A. Virolainen, 2014b: Using Artificial Neural Networks in the Temperature and Humidity Sounding of the Atmosphere. *Izv., Atm. Oceanic Physics*, 50, 3, 330–336.
150. Polyakov A., Yurii M. Timofeyev, and Yana Virolainen, 2014c: Comparison of different techniques in atmospheric temperature-humidity sensing from space. *Int. Journ. Rem. Sensing*, 35, 15, P. 5899–5912.
151. Popovicheva, O.B., Kozlov V.S., Engling, G. et al., 2014: Small-scale study of Siberian biomass burning: I. Smoke microstructure. *Aerosol and Air Quality Research*, 2014.10.4209/aaqr.2014.09.0206.
152. Prigarin Sergei M.; Kim B. Bazarov, Ulrich G. Oppel, 2014: The effect of Multiple Scattering on Polarization and Angular Distributions for Radiation Reflected by Clouds: Results of Monte Carlo Simulation. *Proc. SPIE*, 9292, 92920S, doi:10.1117/12.2074418.
153. Rakhimov R.F., V.S. Kozlov, and V.P. Shmargunov, 2012: On Time Dynamics of the Complex Refractive Index and Particle Microstructure According to Data of Spectronephelometer Measurements in Mixed-Composition Smokes. *Atm. Oceanic Opt.*, 25, 1, 51–60.
154. Rakhimov R.F., V.S. Kozlov, M.V. Panchenko et al., 2014: Properties of Atmospheric Aerosol in Smoke Plumes from Forest Fires according to Spectronephelometer Measurements. *Atm. Oceanic Opt.*, 27, 3, 275–282.
155. Rakitin V.S., E.V. Fokeeva, E.I. Grechko et al., 2011: Variations of the Total Content of Carbon Monoxide over Moscow Megapolis. *Izv., Atm. Oceanic Physics*, 47, 1, 59–66.
156. Rakitin A. V., Poberovskii A. V., Yu. M. Timofeev et al., 2013: Variations in the Column-Average Dry-Air Mole Fractions of CO₂ in the Vicinity of St. Petersburg. *Izv., Atm. Oceanic Physics*, 49, 3, 271–275.
157. Régalia L., C. Oudot, S. Mikhailenko et al., 2014: Water Vapor Line Parameters from 6450 to 9400 cm⁻¹. *J.Q.S.R.T.*, 136, 119–136.
158. Rey M., A.V. Nikitin, V.I.G. Tyuterev, 2014: Theoretical Hot Methane Line Lists up to T = 2000 K for Astrophysical Applications. *Astrophys. Journ.*, 789, 1, 2.
159. Rothman L.S., Gordon I.E., Babikov Y. et al., 2013: The HITRAN2012 Molecular Spectroscopic Database. *J.Q.S.R.T.*, 130, 4–50.
160. Rublev A. N. Gorchakova, I.A., Udalova T.A., 2011: The Effect that Coarse Particles Have on Estimates of Both Optical and Radiation Characteristics of Dust Aerosol. *Izv., Atm. Oceanic Physics*, 47, 2, 190–200.
161. Rublev A. N., Vlasova Y. V., Gorbarenko E. V., 2013: Specifying the Atmospheric Pollutant Distribution Forecast Using the Mathematical Modeling and Measurement Data. *Rus. Meteorology and Hydrology*, 38, 5, 320–328.
162. Rusina E.N., V.F. Radionov, E.E. Sibir, 2013: Variability of Aerosol and Optical Parameters of the Atmosphere in Northern and Southern Polar Regions after 2000. *Probl. Arct. Antarct.* 95, 1, 51–60 [in Russian].
163. Sakerin S.M., Andreev S. Yu., Bedareva T.V. et al., 2011: Atmospheric Aerosol Optical Depth in Far East Primorye According to Data of Satellite and Ground-Based Observations. *Atm. Oceanic Opt.*, 24, 8, 654–660 [in Russian].

164. Sakerin S. M. (ed.), 2012: *Investigations of Aerosol Radiative Characteristics in Asian Part of Russia*. Tomsk, Institute of Atmospheric Opt., 484 p.
165. Sakerin S. M., D. G. Chernov, D. M. Kabanov et al., 2012a: Preliminary Results of Studying the Aerosol Characteristics of the Atmosphere in the Region of Barentsburg, Spitsbergen. *Probl. Arct. Antarct.*, 1(91), 20–31 [in Russian].
166. Sakerin S. M., Andreev S. Yu., Bedareva T. V. et al., 2012b: Spatiotemporal variations in the atmospheric aerosol optical depth on the territory of Povolzhye, Urals, and Western Siberia. *Atm. Oceanic Opt.*, 25, 11, 958–962 [in Russian].
167. Sakerin S. M., Andreev S. Yu., Bedareva T. V., Kabanov D. M., 2012c: Specific features of the spatial distribution of the atmospheric aerosol optical depth in the Asian part of Russia. *Atm. Oceanic Opt.*, 25, 6, 484–490 [in Russian].
168. Sakerin S. M., Beresnev S. A., Kabanov D. M. et al., 2014a: Analysis of Approaches to Modeling the Annual and Spectral Behaviors of the Atmospheric Aerosol Optical Depth in Regions of the Siberia and Primorye. *Atm. Oceanic Opt.*, 27, 12, 1047–1058 [in Russian].
169. Sakerin S. M., N. I. Vlasov, D. M. Kabanov et al., 2014b: Results of Spectral Measurements of Atmospheric Aerosol Optical Depth with Sun Photometers in the 58th Russian Antarctic Expedition. *Atm. Oceanic Opt.*, 27, 5, 393–402.
170. Sakerin S. M., S. Yu. Andreev, D. M. Kabanov et al., 2014c: On Results of Studies of Atmospheric Aerosol Optical Depth in Arctic Regions. *Atm. Oceanic Opt.*, 27, 6, 517–528.
171. Samukova E. A., Gorbarenko E. A., Erokhina A. E., 2014: Multiyear Variations of Solar Radiation at European Territory. *Meteorology and Hydrology*, 8, 15–24 [in Russian].
172. Semakin S. G., A. V. Poberovskii, and Yu. M. Timofeev, 2013: Ground-Based Spectroscopic Measurements of the Total Nitric Acid Content in the Atmosphere. *Izv. Atm. Oceanic Physics*, 49, 3, 294–297.
173. Semenov A. O., Virolainen Ya. A., Timofeyev Yu. M., Poberovsky A. V., 2014: Comparison of Ground-Based IR Spectrometer and Radio Sounding Total Column Water Vapor Measurements. *Atm. Oceanic Opt.*, 27, 11, 976–980 [in Russian].
174. Shmirko K. A., A. N. Pavlov, S. Yu. Stolyarchuk et al., 2014: Variations in Aerosol Microphysical Parameters of the Surface Air Layer in the “Ocean–Continent” Transitional Zone. *Atm. Oceanic Opt.*, 27, 1, 16–23.
175. Shukurov K. A., I. I. Mokhov, and L. M. Shukurova, 2014: Estimate for Radiative Forcing of Smoke Aerosol from 2010 Summer Fires Based on Measurements in the Moscow Region. *Izv. Atm. Oceanic Physics*, 51, 3, 256–265.
176. Sitnov S. A., 2011a: Satellite Monitoring of Atmospheric Gaseous Species and Optical Characteristics of Atmospheric Aerosol over the European Part of Russia in April–September 2010. *Dokl. Earth Sci.*, 437, part 1, 368–373.
177. Sitnov S. A., 2011b: Aerosol Optical Thickness and the Total Carbon Monoxide Content over the European Russia Territory in the 2010 Summer Period of Mass Fires: Interrelation between the Variation in Pollutants and Meteorological Parameters. *Izv. Atm. and Oceanic Physics*, 47, 6, 714–728.

178. Sitnov S.A., Gorchakov G.I., Sviridenkov M.A. et al., 2012a: Aerospace Monitoring of Smoke Aerosol over the European Part of Russia during the period of Massive Forest and Peatbog Fires in July–August 2010. *Atm. Oceanic Opt.*, 26, 4, 265–280.
179. Sitnov S.A., Gorchakov G.I., Sviridenkov M.A., Karpov A.V., 2012b: Evolution and Radiation Effects of the Extreme Smoke Pollution over the European Part of Russia in the Summer of 2010. *Dokl. Earth Sci.*, 446, 2, 1197–1203.
180. Sitnov S.A., Gorchakov G.I., Sviridenkov M.A. et al., 2013: The effect of Atmospheric Circulation on the Evolution and Radiative Forcing of Smoke Aerosol over European Russia During the Summer of 2010. *Izv., Atm. Oceanic Physics*, 49, 9, 1006–1018.
181. Sitnov S.A., I.I. Mokhov, 2013a: Peculiarities of Water Vapor Distribution in the Atmosphere over the European part of Russia in Summer 2010. *Dokl. Earth Sci.*, 448, Part 1, 86–91.
182. Sitnov S.A., I.I. Mokhov, 2013b: Water-Vapor Content in the Atmosphere over European Russia during the Summer 2010 Fires. *Izv., Atm. Oceanic Physics*, 49, 4, 380–394.
183. Sitnov S.A., I.I. Mokhov, A.R. Lupo, 2014: Evolution of Water Vapor Plume over Eastern Europe during Summer 2010 Atmospheric Blocking. *Adv. Meteorology*, 2014, Article ID253953, 11 pages. DOI:10.1080/01431161.2014.945008.
184. Smirnov A., Holben B.N., Giles D.M. et al., 2011: Maritime Aerosol Network as a Component of AERONET — First Results and Comparison with Global Aerosol Models and Satellite Retrievals. *Atm. Meas. Techn.*, 4, 583–597
185. Smirnov A., Sayer A.M., Holben B.N. et al., 2012: Effect of Wind Speed on Aerosol Optical Depth over Remote Oceans, based on Data from the Maritime Aerosol Network. *Atm. Meas. Techn.*, 5, 377–388.
186. Sokoletsky L.G., Budak V.P., Shen F., Kokhanovsky A.A., 2014: Comparative Analysis of Radiative Transfer Approaches for Calculation of Plane Transmittance and Diffuse Attenuation Coefficient of Plane-Parallel Light Scattering Layers. *Applied Optics*, 53, 3, 459–468.
187. Startseva Zoya, Eugene Muzylev, Elena Volkova et al., 2014: Water and Heat Regimes Modelling for a Vast Territory Using Remote-Sensing Data. *Int. J. Rem. Sensing*, 35, 15, 5775–5799.
188. Sviridenkov M.A., K.S. Verichev, S.S. Vlasenko et al., 2014: Retrieval of Atmospheric Aerosol Parameters from Data of a Three-Wavelength Integrating Nephelometer. *Atm. Oceanic Opt.*, 27, 3, 230–236.
189. Tashkun S.A., Perevalov V.I., 2011: CDS-4000: High-Resolution, High-Temperature Carbon Dioxide Spectroscopic Databank. *J.Q.S.R.T.*, 112, 1403–1410.
190. Tennyson J., Bernath P.F., Brown L.R. et al., 2013: IUPAC Critical Evaluation of the Rotational-Vibrational Spectra of Water Vapor. Part III: Energy Levels and Transition Wavenumbers for H₂¹⁶O. *J.Q.S.R.T.*, 117, 29–58.
191. Tennyson J., P.F. Bernath, L.R. Brown et al., 2014a: IUPAC Critical Evaluation of the Rotational-Vibrational Spectra of Water Vapor. Part IV: Energy levels and transition wavenumbers for D₂¹⁶O, D₂¹⁷O, and D₂¹⁸O. *J.Q.S.R.T.*, 142, 93–108.

192. Tennyson J., A. Campargue, P.F. Bernath et al., 2014b: A Database of Water Transitions from Experiment and Theory (IUPAC Technical Report). *Pure & Appl. Chem.*, 86, 71–83.
193. Terpugova S.A., Dokukina T.A., Yausheva E.P., Panchenko M.V., 2012: Seasonal Peculiarities of Manifestation of Different Types of Gyrograms for the Scattering Coefficient. *Atm. Oceanic Opt.*, 25, 11, 952–957 [in Russian].
194. Timofeyev Yu., Dmitry Ionov, Maria Makarova et al., 2013: Measurements of Trace Gases at Saint-Petersburg State University (SPbSU) in the Vicinity of Saint-Petersburg, Russia. In *Disposal of Dangerous Chemicals in Urban Areas and Mega Cities*, NATO Science for Peace and Security Series C: Environmental Security 2013, XV, Barnes, Ian; Rudzinski, Krzysztof J. (Eds.), 346 p., pp. 173–184
195. Tomasi C., Lupi A., Mazzola M. et al., 2012: An Update of the Long-Term Trend of Aerosol Optical Depth in the Polar Regions using POLAR-AOD Measurements Performed during in International Polar Year. *Atm. Environment*, 52, 29–47.
196. Trefilova A.V., M.S. Artamonova, T.M. Kuderina et al., 2013: Chemical Composition and Microphysical Characteristics of Atmospheric Aerosol over Moscow and Its Vicinity in June 2009 and during the Fire Peak of 2010. *Izv., Atm. Oceanic Physics*, 49, 7, 765.
197. Uspensky A.B., A.V. Kukharsky, S.V. Romanov, and A.N. Rublev, 2011: Monitoring the Carbon Dioxide Mixing Ratio in the Troposphere and the Methane Total Column over Siberia According to the Data of the AIRS and IASI IR Sounders. *Izv., Atm. Oceanic Physics*, 47, 9, 1097–1103.
198. Uspensky A.B., A.N. Rublev, 2014: The Current State and Prospects of Satellite Hyperspectral Atmospheric Sounding. *Izv., Atm. Oceanic Physics*, 50, 9, 892–903.
199. Uspensky A.B., A.N. Rublev, E.V. Rusin, V.P. Pyatkin, 2014: A Fast Radiative Transfer Model for the “Meteor-M” Satellite-Based Hyperspectral IR Sounders. *Izv., Atm. Oceanic Physics*, 50, 9, 968–977.
200. Uzhegov Viktor N., Kozlov Valery S., Panchenko Mikhail V. et al., 2014: Comprehensive Study of Optical Properties of Natural Smoke Aerosols in July 2012 in Tomsk. *Proc. SPIE*, 9292, 92923V, doi: 10.1117/12.2075152.
201. Veretennikov V.V. and S.S. Men'shchikova, 2013: Features of Retrieval of Microstructural Parameters of Aerosol from Measurements of Aerosol Optical Depth. Part I. Technique for Solving the Inverse Problem. *Atm. Oceanic Opt.*, 26, 6, 473–479.
202. Virolainen Ya.A., Yu. M. Timofeev, D. V. Ionov et al., 2011: Ground-based Measurements of Total Ozone Content by the Infrared Method. *Izv. Atm. Oceanic Physics*, 47, 4, 480–490.
203. Virolainen Ya.A., Yu. M. Timofeyev, D. V. Ionov et al., 2012: The Ozone Vertical Structure Determining From Ground-Based Fourier Spectrometer Solar IR Radiation Measurements. *Geoph. Res. Abst.*, 14, EGU2012–896.
204. Virolainen Yana, Maria Makarova, Dmitry Ionov et al., 2014a: Comparison of Ground-Based FTIR Measurements and EMAC Model Simulations of Trace-Gases Columns near St. Petersburg (Russia) in 2009–2013. *Geoph. Res. Abst.*, 16, EGU2014–8050–7.

205. Virolainen Yana, Maxim Eremenko, Yury Timofeyev et al., 2014b: Measurements of Ozone Columns in Different Atmospheric Layers over St. Petersburg (Russia) Using Ground-Based FTIR Spectrometer in Comparison with IASI Satellite Data. *Geoph. Res. Abst.*, 16, EGU2014–11353–5.
206. Virolainen Y.A., Yury Timofeyev, Alexander Polyakov et al., 2014c: Intercomparison of Satellite and Ground-Based Measurements of Ozone, NO₂, HF, and HCl near Saint Petersburg, Russia. *Int. Journ. Rem. Sensing*, 35, 15, 5677–5697.
207. Volkova E. V., 2012: Utilization of a Complex Threshold Method's Estimation of Cloud Cover Parameters Obtained by SEVIRI/METEOSAT-9 for Climatic Observations. *Current Problems in Rem. Sens. Earth from Space*, 9, 2, 200–206 [in Russian].
208. Volkova E. V., 2013: Automatic Estimation of Cloud Cover and Precipitation Parameters Obtained by AVHRR NOAA for Day and Night Conditions. *Current Problems in Rem. Sens. Earth from Space*, 10, 3, 66–74 [in Russian].
209. Yagovkina I. S., A. V. Polyakov, A. V. Poberovskii, Yu. M. Timofeev, 2011: Spectroscopic Measurements of Total CFC-11 Freon in the Atmosphere near St. Petersburg. *Izv., Atm. Oceanic Physics*, 47, 2, 186–189.
210. Zaitsev N.A., Yu. M. Timofeyev, and V.S. Kostsov, 2014: Comparison of Radio Sounding and Ground-Based Remote Measurements of Temperature Profiles in the Troposphere. *Atm. Oceanic Opt.*, 27, 5, 386–392.
211. Zapevalov A. S. and N.E. Lebedev, 2014: Simulation of Statistical Characteristics of Sea Surface during Remote Optical Sensing. *Atm. Oceanic Opt.*, 27, 6, 487–482.
212. Zayakhanov A. S., G. S. Zhamsueva, S.A. Naguslaev et al., 2012: Spatiotemporal Characteristics of the Atmospheric AOD in the Gobi Desert according to Data of the Ground-Based Observations. *Atm. Oceanic Opt.*, 25, 5, 346–354.
213. Zhdanova Ye. Yu., N. Ye. Chubarova, 2011: The Assessment of Different Atmospheric Parameters on Biologically-Active UV Radiation according to the Data of Modeling and Measurements. *Atm. Oceanic Opt.*, 24, 9, 775–781.
214. Zhdanova Ye., N. Chubarova, Ye. Nezval, 2013: A Method of Estimating Cloud Transmission in the UV Spectral Range using Data from Different Satellite Measurements and Reanalysis. *AIP Conf. Proc.*, 1531, 911–914.
215. Zhdanova E. Yu, Chubarova N. Ye, Blumthaler M., 2014: Biologically Active UV-Radiation and UV-Resources in Moscow (1999–2013). *Geography. Environment. Sustainability*, 2, 71–85.
216. Zhukov V.Y., Shchukin G.G., 2014: The State and Prospects of the Network of Doppler Weather Radars. *Rus. Met. Hydrology*, 39, 2, 126–131.
217. Zhuravleva T.B., Kokhanovsky A.A., 2011: Influence of Surface Roughness on the Reflective Properties of Snow. *J.Q.S.R.T.*, 112, 1353–1368.
218. Zhuravleva T.B., S.M. Sakerin, T.V. Bedareva et al., 2014: Solar Radiative Fluxes in the Clear-Sky Atmosphere of Western Siberia: A Comparison of Simulations with Field Measurements. *Atm. Oceanic Opt.*, 27, 2, 176–186.

Научное издание

**НАЦИОНАЛЬНЫЙ ОТЧЕТ РОССИИ
ПО МЕТЕОРОЛОГИИ И АТМОСФЕРНЫМ НАУКАМ
В 2011–2014 гг.**

XXVI Генеральная Ассамблея
Международного союза геодезии и геофизики,
Прага, Чехия, 22 июня – 2 июля 2015 г.

На английском языке

Под редакцией:
И.И. Мохова, А.А. Криволицкого

Подготовка оригинал-макета:
Издательство «МАКС Пресс»
Главный редактор: *Е.М. Бугачева*
Компьютерная верстка: *Е.П. Крынина*

Подписано в печать 09.06.2015 г.
Формат 60x90 1/16. Усл.печ.л. 17,0. Тираж 100 экз. Заказ 121.

Издательство ООО “МАКС Пресс”
Лицензия ИД N 00510 от 01.12.99 г.
119992, ГСП-2, Москва, Ленинские горы, МГУ им. М.В. Ломоносова,
2-й учебный корпус, 527 к.
Тел. 8(495)939-3890/91. Тел./Факс 8(495)939-3891.